Evaluation of Protein Tyrosine Phosphatase Receptor Gamma (PTPRG) as a Biomarker in Chronic Myeloid Leukaemia patients in the State of Qatar.

This Thesis is Being Submitted as Partial Fulfillment
of the Requirements for the Degree of
Doctor of Philosophy (PhD)
in Anatomy, Physiology and Pathology
JACS code: B100

By

Mohamed Araby Ismail
BSc, PgD Biochemistry
In collaboration with National Center for Cancer Care and Research (NCCCR)
And Interim Translational Research Institute (iTRI), Hamad Medical Corporation (HMC),
Doha, Qatar

October 2021

Declaration and Statement of Originality

I, Mohamed Araby Ismail, confirm that the work presented in this thesis is my own. The material contained in the thesis has not been presented, nor is currently being Presented, either wholly or in part for any other degree or other qualification. Where information has been derived from other sources, I confirm that this has been indicated in the thesis.

…… ……

Dedication

بِسْمِ اللَّـهِ الرَّحْمَـٰنِ الرَّحِيمِ

وَقُلِ اعْمَلُوا فَسَيَرَى اللَّهُ عَمَلَكُمْ وَرَسُولُهُ وَالْمُؤْمِنُونَ ۖ وَسَتُرَدُّونَ إِلَىٰ عَالِمِ الْغَيْبِ وَالشَّهَادَةِ فَيُنَبِّئُكُمْ بِمَا كُنْتُمْ تَعْمَلُون

صدق اللَّهِ العظيم

In the name of God, Most Gracious, Most Merciful.

And say, `Go on doing (as you like), Allâh will surely keep an eye on your deeds and (so will) His Messenger and the believers, and you will surely be brought back to Him Who knows the hidden and the manifest realities, then He will tell you all that you have been doing.

(Translation from the Holly Qura’an).

Acknowledgments

First of all, I would say “Alhamdulillah” for the support at this critical stage of my life. Secondly, I am grateful for my local supervisor Dr Nader Al-Dewik for accepting me as his first PhD student. His advice and guidance have been precious throughout.

I would also like to thank my overseas supervisor Professor Helmout Modjtahedi along with Dr Richard Cook for giving directions and reviewing my work during this project. Also, I owe thanks for Professor Claudio Sorio and Dr Marzia Vezzalini for all their support of technical training during PhD journey.

I could not have reached this stage without their help.

I am also grateful to the Qatar National Research Fund in the State of Qatar for sponsoring the study. I would also like to thank staff in Interim Translational Research Institute (iTRI) and National Centre for Cancer Care and Research (NCCCR) all of whom helped me with different aspects of this project.

Finally, I would like to express my deepest appreciation to my parents for their prayers, love, guidance, and encouragement throughout my studies, especially my mother, without her I will not be here. Also, my wife Nesma and my kids Rawan, Malak and Adam for encouragement and support.

Contents

List of Chapter Specific Figures

List of Specific Tables

List of abbreviations

ABL1	Abelson Murine Leukaemia
A/E	Emergency Department
AF	Alexa Fluro
ALL	Acute Lymphoblastic Leukaemia
ANOVA	Analysis of variance
AP	Accelerated Phase
APC	Allophycocyanin
ATP	Adenosine Triphosphate
AzaC	5-azacytidine
B-ALL	B-cell Acute Lymphoblastic leukaemia
BC	Blast Crisis Phase
BCR	Breakpoint Cluster Region
BCR-ABL1	Breakpoint cluster region- ABL Proto-Oncogene 1
BD	Becton and Dickinson biosciences company
BV	Brilliant Violet
CBC	Complete Blood Count
CCA	Clonal chromosomal abnormalities
CCyR	Complete Cytogenetic Remission
CDC2	Cell division cycle protein 2 homolog
CDK1	Cyclin-dependent kinase 1
CDH13	Cadherin 13
CDKN2B	Cyclin Dependent Kinase Inhibitor 2B
cDNA	Complementary DNA
CHR	Complete Haematological Remission
CI	Confidence interval
CML	Chronic Myeloid Leukaemia
CMR	Complete Molecular response
CP	Chronic Phase
CpG	Cytosine Phosphate Guanine
c-MYC	The Myc family

CN	Copy Numbers
CRKL	CRK-oncogene-like protein
Ct	Cycle threshold
CyR	Cytogenetic Response
D	Domain
DAS	Dasatinib
DMR	Deep Molecular Response
DMSO	Dimethyl sulfoxide
DNA	Deoxyribonucleic acid
DPYS	Dihydropyrimidinase
dsDNA	double-stranded DNA
ECD	The extracellular domain
EDTA	Ethylenediaminetetraacetic acid
EFS	Event-Free Survival
ELN	European LeukaemiaNet
EMR	Early Molecular Response
ESME	Epigenetic Sequencing Methylation
EtBr	Ethidium bromide
EUTOS	European Treatment and Outcome Study
F	Failed Treatment
FACs	Fluorescence-activated cell sorting
FDA	Food and Drug Administration
FEM1B	Fem-1 Homolog
FGFRs	Fibroblast growth factors receptors
FISH	Fluorescence in situ hybridization
FU	Follow up
G	Gram
GAP	Guanosine triphosphates-activating protein
GEF	Guanidine Exchange Factor
GDP	Guanosine diphosphate
GEF	Guanidine Exchange Factor

GRB-2	Growth factor Receptor-bound protein 2
GTP	Guanosine-5'-triphosphate
H	Healthy individuals
HMC	Hamad Medical corporation
HSCs	Hematopoietic stem cells
ICD 10	The International Classification of Diseases
IgG	Immunoglobulin
IM	Imatinib Mesylate
IMDM	RPMI-1640 w L-glutamine
IFN-α	Interferon-α
IRIS	The International Randomized Study of Interferon and STI571
IS	International scale
ISP	Ion Sphere™ Particles
iTRI	Interim Translational Research Institute
JAK-STAT	Janus kinase-Signal transducer, an activator of transcription
JMML	Juvenile Myelomonocytic leukaemia
KD	Kinase domain
KB	Kilobases
kDa	Kilodalton
Km2	Kilometre
L	Lymphocytes
LSCs	Leukemic stem cells
LMN	Lymphocytes, Monocytes, and Neutrophils (LMN)
M	Monocytes
M-bcr	The major breakpoint cluster region
m-bcr	The minor breakpoint cluster region
mAb	Monoclonal antibody
mC	Methylated Cytosine
MDS	Myelodysplastic Syndrome
MFI	Mean Fluorescent Intensity
Mg	Milligram

MLH1	MutL homolog 1
MMR	Major Molecular response
MOPH	Ministry of Public Health
MRD	Monitoring minimal residual disease
mRNA	Messenger RNA
N	Neutrophils
NC	Negative Control
NCBI	The National Centre for Biotechnology Information website
NCN	Normalized Copy Number
NCCCR	The National Centre for Cancer Care and Research
ND	New Diagnosis
Ng	Nanogram
NFW	Nuclease-free Water
NGS	Next generation sequencing
NIH	National Institutes of Health
Nm	Nanometre
NTC	Non-template control
NIL	Nilotinib
NPM2	Nucleoplasmin 2
NT	non-trans membrane
OR	Odds ratio
OSCP1	Organic Solute Carrier Partner 1
P13K	The phosphatidylinositol 3-kinase
PADs	PP2A activating drugs
PBc	Peripheral blood cells
PBPC	Peripheral blood progenitor cell
PBS	Phosphate-buffered saline
PCR	Polymerase Chain Reaction
PCyR	Partial Cytogenetic Response
PDLIM4	PDPDZ And LIM Domain 4
PE-CY7	A tandem fluorochrome consisting of R-phyco erythrin

PGM	PGM Personal Genome Machine
PGP	Protein Glycoprotein
PGR-A:	Progesterone Receptor-A
PGR-B:	Progesterone Receptor-B
Ph+	Philadelphia chromosome
PHCC	Primary Health Care Corporation
PON	Ponatinib
PTP	Protein tyrosine phosphatase
PTPN	Non-receptor-type PTPs
PTPR	Receptor-type PTPs
(R)	
PTPRG	Protein Tyrosine Phosphatase Receptor Gamma
PXXP	Proline-rich stretches
QC	Quality Control
QGP	Qatar genome program
QNCR	Qatar National Cancer Registry
R	Radius
RACS	The Regulatory, Accreditation, and Compliance
RAS-MAPK	The Rat Sarcoma-Mitogen-activated protein kinase
RNA	Ribonucleic acid
RBMS	Referral and booking management system
Rpm	Revolutions Per Minute
RPRM	Reprimo TP53 Dependent G2 Arrest Mediator Homolog
RT	Room Temperature
RT-qPCR	Reverse transcription PCR
RR	Risk Ratio
SCs	Standard Curves
SD	Standard deviation
SEER	The Surveillance, Epidemiology, and End Results
SHC	SRC homology 2-containing protein
SNP	Single nucleotide polymorphisms

SOX30	Sry-related high-motility group box 30
SPSS	Statistical Package for the Social Sciences
SOS	Son of Sevenless protein
SRC	The Src homology (SH) domains
SSC	Side scatter
STAT5	Signal Transducer and Activator of Transcription 5
T	Thymidine
TAE	tris base, acetic acid, and EDTA
THAP2	THAP domain containing 2
TFAP2E	Transcription Factor AP-2 Epsilon
TKAs	External regulators to regulate the ABL1 tyrosine kinase activities
TKIs	Tyrosine Kinase Inhibitors
TPγ B9-2	A monoclonal antibody of PTPRG
TSA	Trichostatin A
W	Shapiro-wilk
WHO	World Health Organization
WSRT	Wilcoxon Signed-Ranks Test
U	Uracil
µ-bcr	The micro-breakpoint cluster region
Uc	Unmethylated Cytosine
UCSC	The University of California, Santa Cruz
UV	Ultraviolet
UK	United Kingdom
Ml	microliter
USA	United States of America
β –ME	β-mercaptoethanol
7-AAD	7-aminoactinomycin D
°C	Celsius

Abstract

Chronic Myeloid Leukaemia (CML) is a clonal myeloproliferative disorder characterized by a shortened chromosome 22 known as the Philadelphia chromosome (Ph). As the main transforming property of the Breakpoint Cluster Region- Abelson Murine Leukaemia 1 (BCR-ABL1) oncoprotein is mediated by its constitutive tyrosine kinase activity, direct inhibition of such activity seems to be the most straightforward means of silencing the oncoprotein. Indeed, Tyrosine Kinase Inhibitors (TKIs) has dramatically improved the outcomes in CML patients. However, a percentage of patients are treatment resistance. Internationally, over 25% of CML patients have resistance to treatments with the TKIs and this is around 54% in Qatar. It is therefore essential to identify biomarkers of prognostic significance, predictive value for the response to therapy and as targets for therapy.

Dysregulation phosphorylation and dephosphorylation of protein by kinases and phosphatases are important in cancer. Of these, Protein Tyrosine Phosphatases (PTPs) are a group of enzymes that remove the phosphate groups derived from the Tyrosine kinase. One of these, Protein Tyrosine Phosphates Receptor Gamma (PTPRG) is known as tumour suppressor gene and found to be down regulated in CML.

The aim of this PhD project was to examine expression level and predictive value of PTPRG as biomarker for the response to therapy with the small molecules tyrosine kinase inhibitors (TKIs) in CML patients in Qatar. The findings are consistent with the mainstream findings that the PTPRG has a natural inhibitory mechanism and it was found to be down regulated in CML patients. In addition, using anti-PTPRG monoclonal antibody TPγ B9-2, a unique flow cytometry technique was developed. It was able to record changes in the expression level of PTPRG at diagnosis and in particular its restoration following treatment with one of the BCR/ABL TKIs. Interestingly, the aberrant DNA methylation of PTPRG was found be one of the possible mechanisms of its under expression in CML patients. Furthermore, 7 PTPRG variants (4 annotated and 3 Novel) were found in this study and their expression was found to be significantly different between the TKI resistant cases compared to responders as well as healthy individuals. Finally, towards the end of this PhD project, CML biobanking was successfully

established at Interim Translational Research Institute (iTRI) Doha-Qatar and this should open new spectrum in support of health care research strategies. All these findings and their importance will be discussed in this thesis.

1 Chapter 1 Introduction on CML

1.1 Background and a Brief History of CML

Chronic Myeloid Leukaemia (CML) is a haematopoietic stem cell disorder that transforms normal stem cells to hyper-proliferated abnormal stem cells. The term "chronic" specifies that this kind of malignancy tend to progress more slowly than acute forms of leukaemia while, the term "myelogenous" (my-uh-LOHJ-uh-nus) refers to the type of cells affected by this tumour. These abnormal stem cells gradually substitute the normal stem cells and ultimately lead to the expansion of total myeloid cells in peripheral blood (Goldman, 2003a, Jabbour and Kantarjian, 2020a). It can affect all age groups, however; it is predominantly a disease of an adult with slightly male predominance and no association with race or ethnicity (Cancer, 2015, Radivoyevitch et al., 2014).

1.2 Incidence and Mortality Rates of CML

The CML accounts for 15 to 20 % of leukaemia cases in adults (Arber et al., 2016). The annual incidence rate in the United States of America (USA) is roughly up to 1.9 per 100.000 adults. However, the mortality rate significantly reduced from 0.9 to 0.3 per 100.000 adults in the last two (2) decades (Figure1. 1A) (Siegel et al., 2020, Huang et al., 2012, Hao et al., 2019, The Surveillance, 2020). In the UK, the annual incidence rate for the same period was reduced from 1.8 to 1.3 per 100,000 adults and so did the mortality rate of CML (Figure1. 1B, Bhayat et al., 2009). In general, the annual incidence rate of European CML registries dropped from 11.25 to 0.7 per 100,000 adults, with slight male predominance (Bhayat et al., 2009, Hoglund et al., 2015, Research(UK), 2020). The worldwide CML incidence is expected to be over 100,000 patients every year that represent a substantial health burden (Dong et al., 2020). On the other hand, over the last ten decades, there were only two studies reported the incidences rate of CML in the Middle East region. The rate of incidence was 0.5 and 1.2 in Kuwait and the Kingdom of Saudi Arabia, respectively (Al-Bahar et al., 1994, Bawazir et al., 2019), while there was no audited data in the literature available at Qatar.

Due to a lag in cases captured and reported, most of the CML patients are diagnosed at outpatient clinics, which can cause delay-adjustment in data collection/correction.

In the same context, recent data from The Surveillance, Epidemiology, and End Results (SEER) registries showed that the adjusted incidence rate of leukaemia was 10% higher than reported in the previous registries (Howlader, 2016, The Surveillance, 2019). The 5-year overall survival for CML patients was 78.9%,100% for the UK and USA, respectively, while there is no audited data for third world counties in the literature yet (Siegel et al., 2020, Smith et al., 2014).

1.3 Aetiology of CML

CML is characterizing by various types of genetic alterations, including mutation, deletion, and translocation. Out of these, a fusion gene termed *BCR-ABL1* has been identified in most patients with CML, which is the result of translocation of the Abelson murine leukaemia viral oncogene homolog 1 (*ABL1*) gene from chromosome 9 to the breakpoint cluster region (*BCR*) gene on chromosome 22 (Vinhas et al., 2017). The first CML case was described in 1845 by Hughes Bennett and was assessed as an infectious disease. Later in 1973, Rowley identified the translocation of the Philadelphia chromosome (Ph+) as a minute of the disease (Deininger et al., 2000, Groffen et al., 1984). As a result of translocation, the resulting oncoprotein tyrosine kinase leads to activation/ alteration in many pathways, including, but not limited to, RAS, MAPK, JAK and STAT pathways and was an important target for therapy with the small molecule tyrosine kinase inhibitors in patients with CML (Eden and Coviello, 2019, Faderl et al., 1999). Recent studies documented presence one or more genetic alterations during the transition from CP to BC phase, this includes but not limited to the RUNX1-ETS2 fusion and NBEAL2 mutations (Branford et al., 2019, Ochi et al., 2021, Wu et al., 2020).

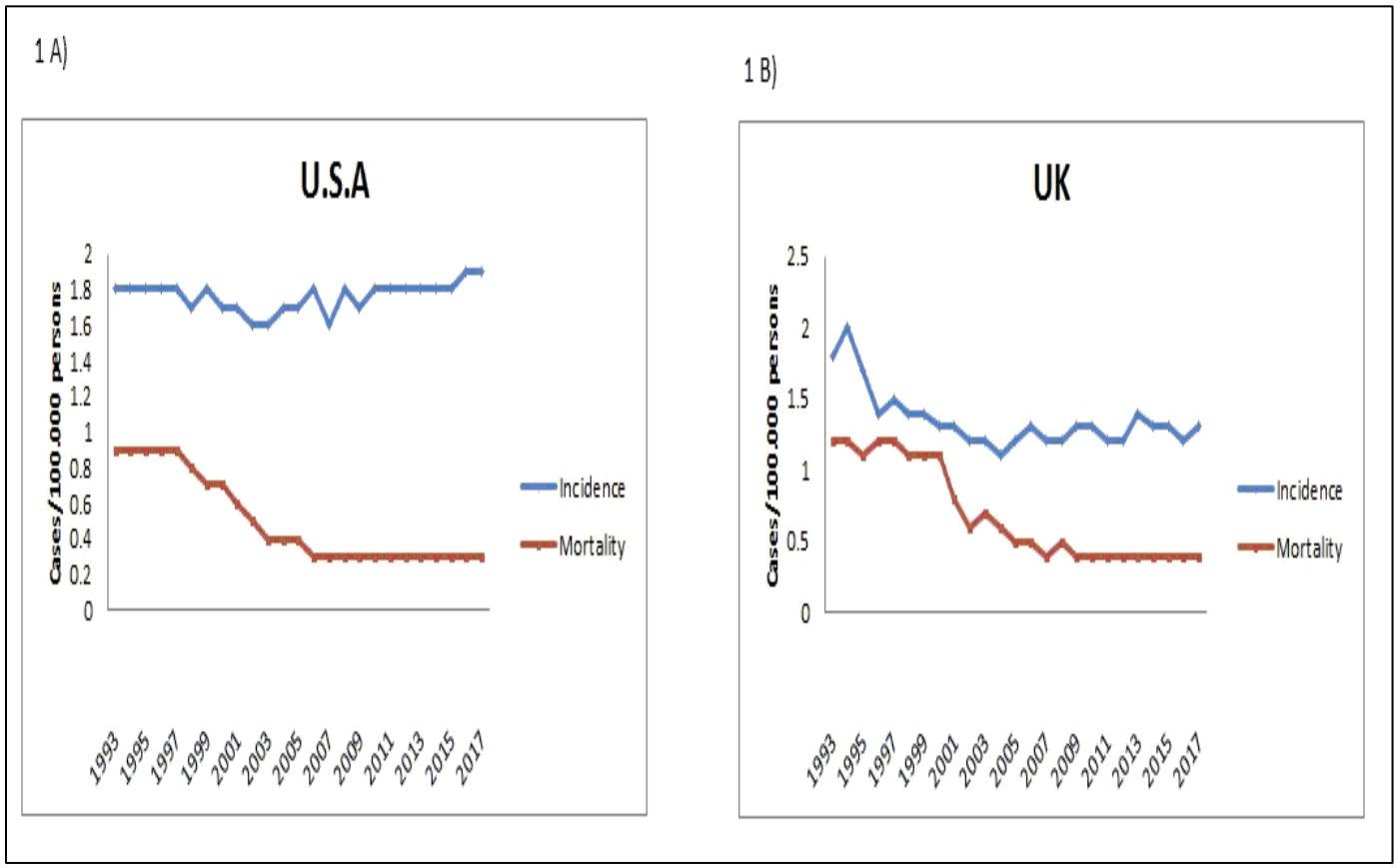

Figure1. 1 Trends in Cancer Incidence/ Mortality Rates in USA and UK for the period between 1993-2017.

1A) The annual incidence rate of CML in the United States of America (USA) was an average of 1.76 and the mortality average was 0.5 cases /100,000 adults. 1B) the annual incidence rate of CML in the UK was an average of 1.35 and the mortality average was 0.7 cases /100,000 persons.

1.4 Classification of CML

Based on the revised 2016 World Health Organization (WHO) classification of tumours of the hematopoietic and lymphoid tissues, CML is divided into the Chronic phase (CP), Accelerated phase (AP) or Blast phase (BC) (Table1 1).

Table1 1 WHO criteria of CML phases.

The revised 2016 World Health Organization (WHO) classification of tumours of the hematopoietic and lymphoid tissues were employed and divided the CML patients into Chronic phase (CP), Accelerated phase (AP) or Blast phase (BC) (Arber et al., 2016).

phase	Chronic Phase (CP)	Accelerated Phase (AP)	Blast Phase (BP)
Definition	Not meeting WHO criteria for accelerated and Blast Phases.	**One or more of the following hematologic/cytogenetic criteria or response –to-TKI criteria:** • Persistent or increasing WBC (>10 X 10^9/L), unresponsive to therapy • Persistent or increasing splenomegaly, unresponsive to therapy • Persistent thrombocytosis (>1000 X 10^9/L), unresponsive to therapy • Persistent thrombocytopenia (<100 X 10^9/L), unresponsive to therapy • 20% or more basophils in the peripheral blood (PB) • 10%-19% blasts in the PB and/or BM • Additional clonal chromosomal abnormalities in Ph^+ cells at diagnosis that include “major route” abnormalities (second Ph, trisomy 8, isochromosome 17q, trisomy 19), complex karyotype, or abnormalities of 3q36.2 Any new clonal chromosomal abnormality in Ph+ cells that occurs during therapy. Provisional” response-to-TKI-criteria.	One or more of the following features →Blasts > 20% of peripheral blood leucocytes or of nucleated bone marrow cells →Extra medullary blast proliferation Large foci or clusters of blasts in the bone marrow biopsy

1.5 The role of oncogenes in CML pathogenesis

The *BCR-ABL1* alteration is the key in the CML pathogenesis and leads to activation of different pathways and ultimately promotion of cell proliferation and survival and inhibition of apoptosis (Minciacchi et al., 2021). In addition to that the *BCR-ABL1*-independent mechanism, due to an alternative signalling pathway, can also affect the survival of leukaemia cells. Of these, chromosomal abnormalities and additional mutation represent 30 to 50% of the *BCR-ABL1*-independent mechanisms (Medina et al., 2003). For instance, the presence of trisomy 8 Ph+ CML patients leads to overexpression of c-MYC and overexpression of LYN kinase which in turn may lead to resistance to treatment (Donato et al., 2003, Jennings and Mills, 1998, Wang et al., 2016, Wang et al., 2015).

Another important independent a molecular pathway in CML is Musashi2-Numb axis that plays a vital role in signalling pathways such as Hedgehog and Notch that are essential for self-renewal of hematopoietic stem cell as well as CML leukemic stem cell pathways. Recent studies suggested a controlled Musashi2-Numb signalling pathways will possibly pave the way for treatment free strategy (Ito et al., 2010, Mojtahedi et al., 2021, Moradi et al., 2019).

In the same context, recent studies documented that the translocation of *BCR-ABL1* is not only the main reason of CML disease but also the activation of an additional pathway or loss its function/ expression of other genes. Of these, cyclin-dependent kinase 1 (CDK1) or cell division cycle protein 2 homolog (CDC2) mutations cause alterations in many cell signalling pathways. The resulting mutation leads to loss of regulation of DNA damage response and apoptosis of cells. Since not all individuals with *BCR-ABL1* translocations develop CML disease, the involvement of secondary pathogenic mechanisms, such as epigenetic/genetic aberration has also been hypothesized (Chohan et al., 2018, Fan et al., 2020).

Also in that context, Ross and his *et al., 2014* reported that mice expressed *BCR/ABL* transcript didn't develop CML phenotype (Ross and Mgbemena, 2014). In addition to

that, Ismail and his *et al., 2014* documented presence of BCR/ABL transcripts in the blood of a significant proportion of healthy individuals (Ismail et al., 2014).

1.6 The structural and functional domains of *ABL1* and *BCR* in CML

The main domains of CML disease are *ABL1* and *BCR* that will be discussed briefly in the following paragraphs.

1.6.1 Structure of *ABL1*.

The *ABL1* gene is a homologue human cellular proto oncogene, (Abelson and Rabstein, 1970). The *ABL1* gene is over 230kb and is located on chromosome 9. It has 11 exons and two isoforms 1a and 1b, with 1a shorter than 1b (Chissoe et al., 1995, Ren, 2005, Wang, 2014) (Figure1. 2).

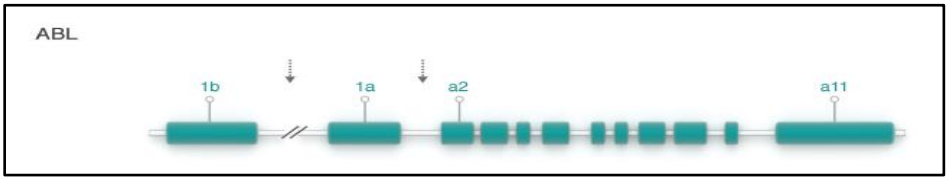

Figure1. 2 Schematic diagram of the *ABL1* gene.
Arrows point to the location of breakpoints in ABL gene [Adopted from (Mughal et al., 2016)].

The *ABL1* gene is transcribed into 6 or 7 kb mRNA and then translated into two spliced forms of round 145-KDa 1a and 1b, where the 1b form is longer than 1a by 19 residues (Laneuville, 1995). SRC homology of ABL1 protein has three domains (SH1-SH3) that are located towards the NH_2 terminus. SH1 domain contains the tyrosine kinase function, while SH2 and SH3 domains allow interaction with other proteins (Cohen et al., 1995, Hazlehurst et al., 2009) (Figure1. 3). In contrast, the C terminal consists of proline-rich stretches (PXXP) with three nuclear location signals (NLS), DNA–binding (Kipreos and Wang, 1992), actin-binding motifs (McWhirter and Wang, 1993), and nuclear localization signals (Van Etten, 1999).

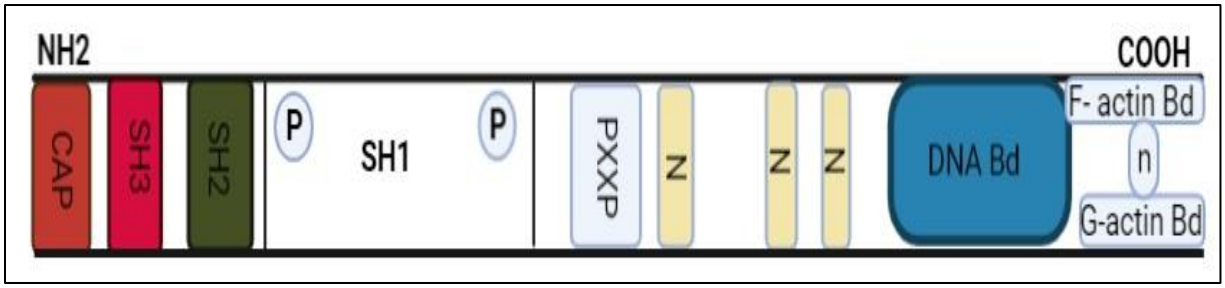

Figure1. 3 Schematic diagram of the Abl1 protein SRC.
Homology of ABL1 protein has three domains (SH1-SH3). Y412 and Y245 are the active site of ATP binding PXXP: motifs to mediate protein-protein interaction. N: 3 nuclear localization signal (NLS). DNA Bd: DNA-binding domain. F-actin Bd: filamentous actin-binding domain G-actin Bd: globular actin-binding domain.

Regulation of ABL1 protein takes place via the tyrosine kinase domain, which acts as an enzyme via transferring a phosphate group to activate substrate proteins in terms of phosphorylation process; tyrosine kinase has both internal and external regulators. The activation loop is the key element that acts as an internal regulator of the tyrosine kinase domain. It exists at the interface of N and C lobes of SH1. It activates through a cascade of interactions of different proteins which has catalytic property leading to the transfer phosphorus atom of ATP to the substrate tyrosine kinase domain (Knighton et al., 1991, Nagar et al., 2002, Nagar et al., 2003, Roskoski, 2003, Schindler et al., 2000). The activation loop exists at the SH1 domain; other subdomains such as the SH2 kinase domain as well as the SH2-SH3 connector also play an important role in the regulation of the activation loop. This will maintain an equilibrium status in normal cell growth (Gonfloni, 2014, Hantschel et al., 2003, Hantschel and Superti-Furga, 2004, Nagar et al., 2003, Roskoski, 2003) (Figure1. 4).

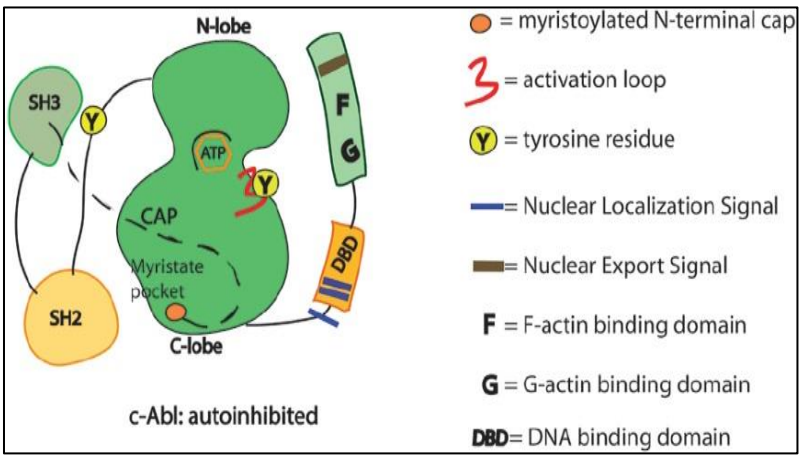

Figure1. 4 Intramolecular regulation of c-Abl activity.
The activation loop of tyrosine kinase (in red) occurs at the interface of N and C lobes of SH1. In contrast, regulation tyrosine residue is done through coordination of SH2 and SH3 domains [Adopted from (Gonfloni, 2014)].

Reverse external inhibitory proteins play an essential role as external regulators to regulate the ABL1 tyrosine kinase activities (TKAs) through binding to different locations of ABL1 domains (Dai and Pendergast, 1995, Natarajan et al., 2019, Sawyers et al., 1994, Welch and Wang, 1993, Woodring et al., 2001).

1.6.2 Structure and function of *BCR*.

The *BCR* is a cellular gene and located on chromosome 22. It has 23 exons, and it spans over 130 Kilobases (kb) (Figure1. 5) (Laurent et al., 2001, Ren, 2005).

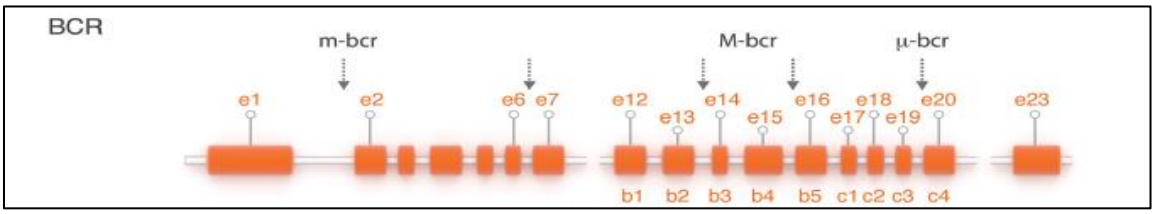

Figure1. 5 Schematic diagram of the *BCR* gene *BCR* gene has 23 exons.
Arrow points suggest the breakpoints in the BCR-ABL1 fusion gene [Adopted from (Mughal et al., 2016)].

BCR gene is transcribed into 4.5 or 6.7 kb mRNA and then translated to 160-kd and $p160^{BCR}$ proteins. The protein has three functional segments, the N terminal segment, the central segment, and the C segment as shown in (Figure1. 6). In addition, the Bcr protein has been found to complex with several proteins (Chissoe et al., 1995, Deininger et al., 2000, Laneuville, 1995, Laurent et al., 2001, Wetzler et al., 1993).

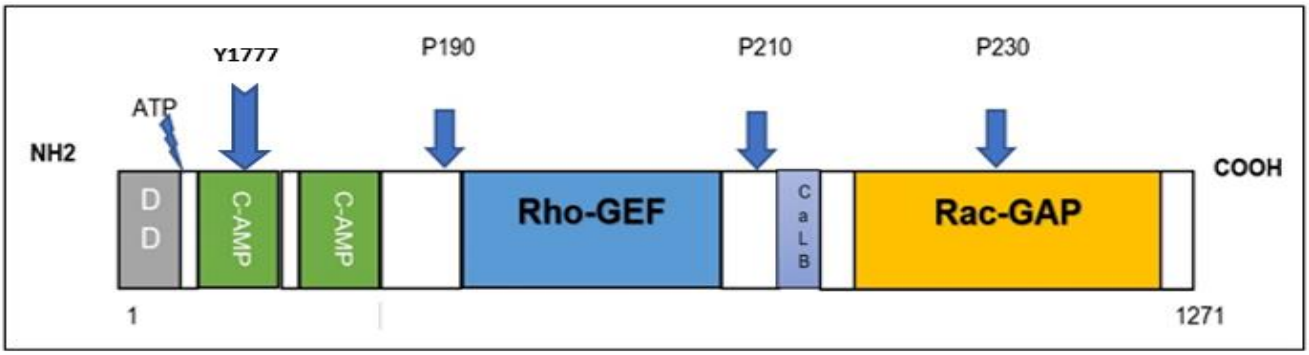

Figure1. 6 Schematic diagram of the Bcr protein.
The Bcr protein consists of several domains 1-The dimerization domain, 2-Two cyclic AMP kinase homologous domains C-AMP which has Y177 position for auto phosphorylation site of ATP; Rho-GEF: Rho guanidine nucleotide exchange factors. CaLB: a site for calcium-dependent lipid binding. Rac-GAP: GTPase. Blue arrows indicate different level of cleavage during different Bcr-Abl1 fusion.

N-terminal segment encodes a serine-threonine kinase that plays a vital role by phosphorylating Bap-1 substrates, which is a parcel of the 14-3-3 family of proteins and has the ability to attach to the SH2 domain of Abl protein (Arlinghaus, 1998, Deininger et al., 2000, Laurent et al., 2001, Reuther et al., 1994). The central segment includes Guanidine Exchange Factor (GEF) related domain, which activates G protein via exchanging GDP for GTP in RAS-like G proteins, plays an essential role in polarity, as well as DNA repair and cell cycle regulation (Denhardt, 1996, Laurent et al., 2001, Ron et al., 1991). Guanosine triphosphates-activating protein (GAP) is a part of the C-terminal segment, which has a negative regulatory function when it binds to the SH3 region of Abl protein (Diekmann et al., 1991, Voncken et al., 1995).

1.6.3 The structural and function of the translocated *BCR-ABL1 oncogene*

The BCR-ABL1 translocation is common in patients with CML. It results from juxtaposing the 5’ part of the BCR gene along with the 3’ part of the ABL1 gene. Due to the changeability of the sites of distraction in the BCR gene, three chimeric proteins p210Bcr-Abl, P190 Bcr-Abl and p230 Bcr-Abl may emerge as a result of translocation (Kurzrock et al., 2003, Morris and Benjes, 2008, Randolph, 2020, Tim, 2020). Alternatively, the breakpoints in ABL1 occur in the first and second introns only. The resulting fusion mRNA have the names upon exon links in ABL1 to BCR cluster region, called b2a2 transcripts if ABL1 gene exon b2 links to BCR breakpoint cluster region (M-

bcr), b3a2 transcripts if ABL gene exon b3 links to BCR breakpoint cluster region (M-bcr),e1a2 transcripts if ABL1 gene exon a2 links to exon e1 of BCR or e19a2 transcripts if ABL1 gene exon a2 links to exon e19 BCR breakpoint cluster regions at m-bcr and µ-bcr (Baccarani et al., 2019a, Hermans et al., 1987). The resulting chimeric proteins depend on the mRNA transcripts mentioned earlier; the majority of CML patients (95%) expressed as p210kDa fusion protein if mRNAs were b2a2 or b3a2. A minority of CML patients expressed fusion proteins 190kDa and 230kDa if mRNAs were e1a2 and e19a2, respectively (Dasgupta et al., 2017, Westbrook et al., 1992). The expression of BCR-ABL1 oncoprotein is the cause of continuous activation of the tyrosine kinase domain in patients with CML disease (Chen et al., 2000, Druker et al., 1996, Flis and Chojnacki, 2019) (Figure1. 8 & Figure1. 9).

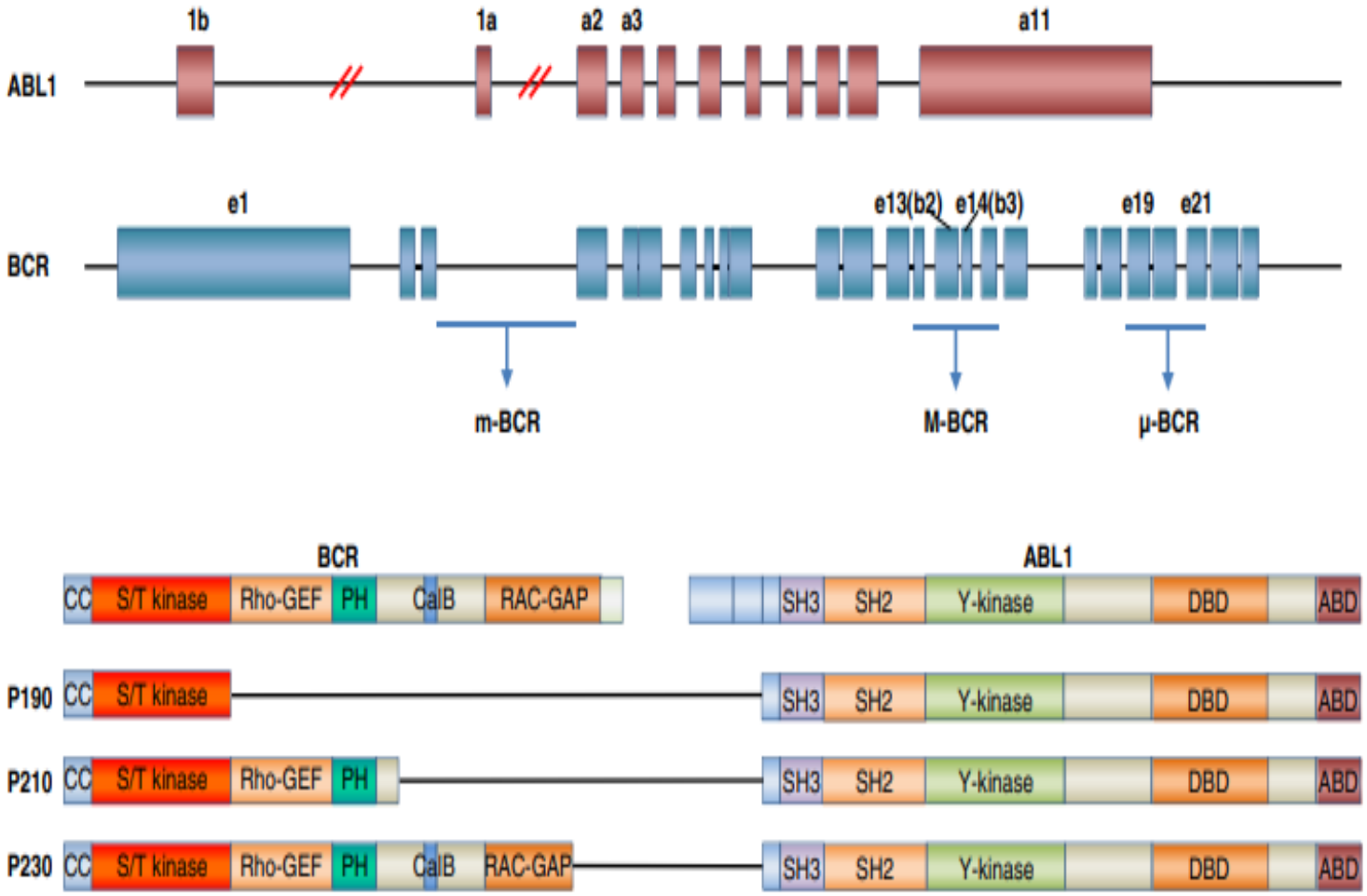

Figure1. 7 Schematic diagram of *BCR-ABL1* translocation.

Three different proteins are the results of translocation of BCR with ABL1, ABL1 breakpoints designated by parallel oblique lines, where the major breakpoint cluster region is (M-bcr). The breakpoint P210 is noticed in over 95% of CML incidents. While other breakpoints are associated with different Leukaemia. The resulting three fusion proteins shared same common ABL1 domains, that including the SRC homology domains SH2 and SH3, tyrosine kinase (Y-kinase) domain SH1, and DNA- and actin-binding domains (DBD and ABD). [Adopted from (Zhou et al., 2018).

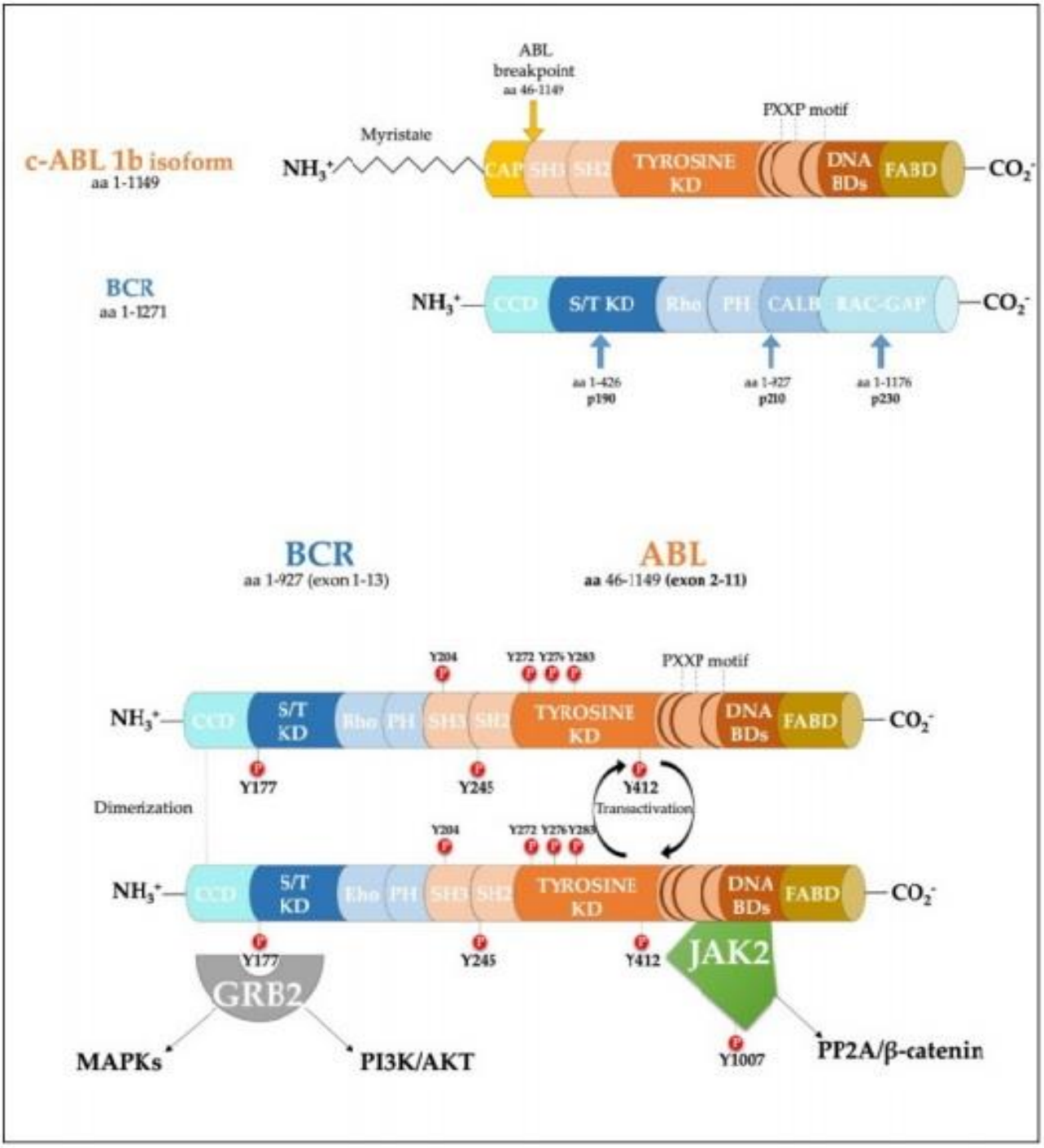

Figure1. 8 Schematic diagram of BCR-ABL1 kinase.

The formation of modularity shows the structural of SRC, ABL1b and BCR-ABL1 kinase. SRC is the key element of regulation of BCR-ABL1 kinase, and ABL1 kinase represents 42% overall homology as a result of myristoryl moiety group presence β-catenin acting as one of the BCR-ABL1-independent checkpoints, through the interactions of JAK2 and PP2A. Growth Factor Receptor Bound Protein-2 (GRB2) plays avital role in fundamental Y177 binding site on the BCR domain that's promotes CML [Adopted from (Boni and Sorio, 2021)].

1.6.4 Downstream cell signalling pathways activated by BCR-ABL Oncoprotein.

Although BCR-ABL translocation is the hallmark for CML, additional activation of secondary pathways is required for full neoplastic transformation. Between 20-30% of the healthy population carries traces of *BCR-ABL1* transcripts in their circulating blood (Biernaux et al., 1995, Bose et al., 1998). This was evidenced by data published from a knock-in model of BCR-ABL1 p210 expressed from the Bcr locus, which expressed BCR-ABL1 p210, that *BCR/ABL* transcript alone is not sufficient to induce CML.(Foley et al., 2013). These secondary pathways included the Rat Sarcoma-Mitogen-activated protein kinase (RAS-MAPK), Janus kinase-Signal transducer, an activator of transcription (JAK-STAT), the phosphatidylinositol 3-kinase (P13K), and c-MYC pathway, as shown in (Figure1. 9, (Deininger et al., 2000). More details of these pathways will be discussed briefly in the following sections.

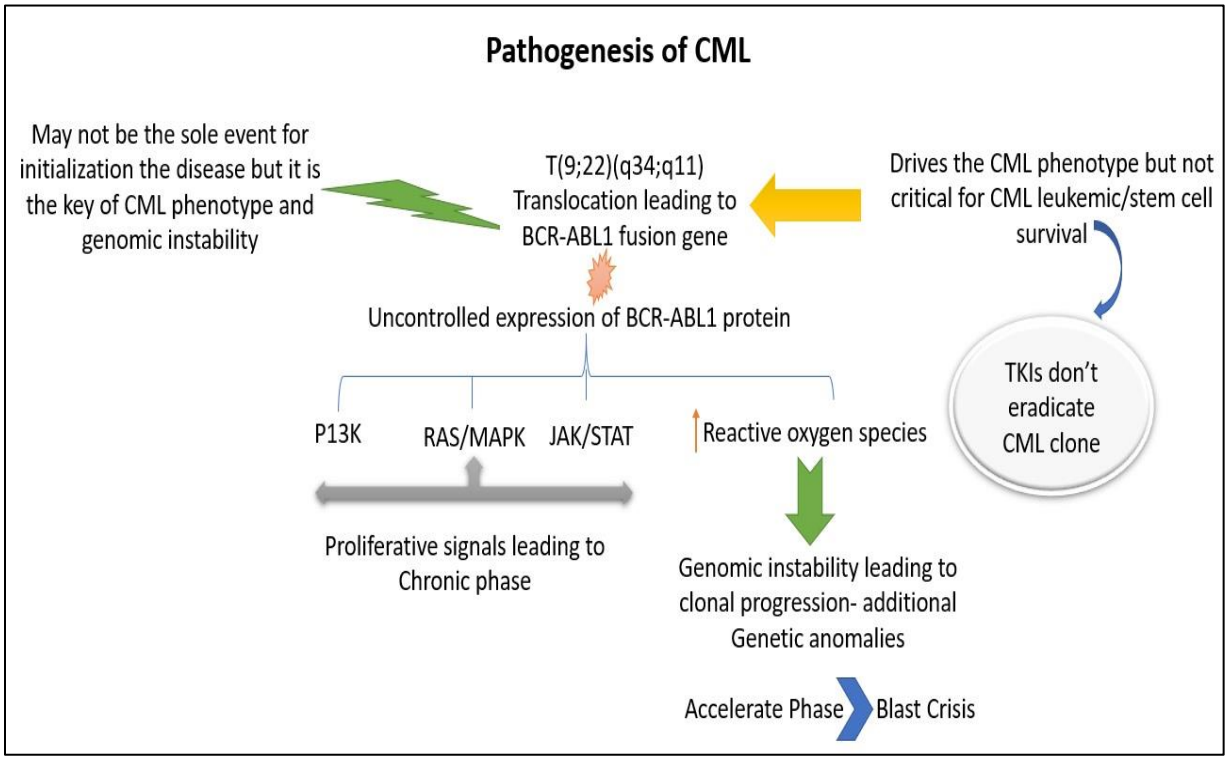

Figure1. 9 Signalling pathways in *BCR-ABL*-transformed cells.
As a result of the formation of BCR-ABL1; many pathways are being activated, such as P13K, RAS/MAPK, and JAK/STAT leading to cell proliferation and decrease apoptosis, which could be responsible for the chronic phase of the CML. Recent studies reported another pathway, which is reactive oxygen species, which belief to be the main reason to transform to accelerate/ blast phases of CML.

1.6.4.1 RAS and MAPK pathways

Several studies supported the link between Ras and Bcr-ABL1. Indeed, auto phosphorylation of tyrosine 177 of BCR offers a binding spot for the adaptor molecule, Growth factor Receptor-Bound protein 2 (GRB-2) (Pendergast et al., 1993), which associates with the Son of Sevenless protein (SOS). As a result of this binding, the inactive GDP-bound RAS changes to active GTP-bound RAS (Puil et al., 1994). At the same time, RAS has another two adaptor molecules, CRK-oncogene-like protein (CRKL) (Oda et al., 1994) and SRC homology 2-containing protein (SHC) (Pelicci et al., 1995) that work as substrates of BCR-ABL1 via SH3 and SH2 domains of ABL1 accordingly (Guo et al., 2020).

1.6.4.2 Phosphatidylinositol 3 kinase (PI3K) Pathway

PI-3K pathway is another important pathway which has been shown to be activated in BCR-ABL–positive cells (Skorski et al., 1995). Activation of this pathway takes place via the formation of a multimeric complex with P120Cbl along with adaptor molecules CRK and CRKL. The Activation of PI-3K has the ability to stimulate the other related substrate in this cascade, which is the serine-threonine kinase Akt (Skorski et al., 1997), which plays an important role in cell survival and apoptotic signalling (Franke et al., 1997, Yang et al., 2019).

1.6.4.3 JAK-STAT pathway

Interestingly, these pathways do not require adaptor protein for activation, as it is directly activated by the chimeric BCR-ABL1 protein (Barnes and Melo, 2002). It is important for leukaemogenesis by inactivating of the pro-apoptotic BAD and up-regulation of the anti-apoptotic molecule Bcl-xL (Cilloni and Saglio, 2009, del Peso et al., 1997, Owen et al., 2019).

1.6.4.4 c-MYC pathway

This pathway, similar to the JAK-STAT path, does not require adaptor protein for activation, as it directly interacts with the SH2 domain of *ABL1,* which enhances the

transformation of BCR-ABL1 positive cells (Cilloni and Saglio, 2009, Gómez-Casares et al., 2013, Xie et al., 2002).

In conclusion, the output signalling of *BCR-ABL1* pathways is utilized through connections with numerous proteins that transduce the oncogenic signals. This leads to a reduction of the apoptotic process, response to cytokine withdrawal, mutagenic stimuli, deregulate cellular proliferation, and decrease adherence of leukaemia to bone marrow stroma (Gonfloni, 2014). However, the mechanisms of progression of the disease from chronic to accelerate and blast phases of CML remain poorly understood (Quintas-Cardama and Cortes, 2009). In this context, the holistic view is the aberrant expression and activation of genes and their protein products in the cell signalling pathway, resulting in the continuous activation of tyrosine kinase, which is a significant contributing factor. The silencing of tyrosine kinase activities is mediated by protein tyrosine phosphatases (PTP) (Lee et al., 2015, Tonks, 2006). In the following section, advances, and challenges in the treatment of patients will be discussed followed by the role potential of PTP and PTP- receptor gamma (PTPRG) in cancer.

1.7 Advances and challenges in the treatment of patients with CML

The uncontrolled BCR-ABL1 oncoprotein has become an important target for therapeutic interventions with small-molecule tyrosine kinase inhibitors (TKIs) that can compete with the ATP binding site of the catalytic domain of several oncogenic tyrosine kinases (Baccarani et al., 2019b, Biernaux et al., 1995, Bose et al., 1998, Soverini et al., 2019).

1.7.1 Treatment of CML patients with cytotoxic drugs

Interferon-α (IFN-α) was the first human historical treatment of CML disease along with Hydroxyurea that is used to reduce leukocytosis at time of diagnosis (Hochhaus et al., 1997, Kujawski and Talpaz, 2007, Talpaz et al., 2015). Other chemotherapy such busulfan, cyclophosphamide (Cytoxan®), and vincristine (Oncovin®) are used as well in treatment CML patients. On the other hand, as TKIs were introduced to CML. Several

studies proved superiority of TKIs in all outcome measures when compared to the cytotoxic drugs (Druker et al., 2006, Mu et al., 2021). From another perspective, CML patients on chemotherapy are likely to develop Adverse Effects (AEs) of different grades, many of which lead to cardiovascular/ toxicity events. However, these AEs are significantly higher when compared to AEs of TKIs. It is worth mentioning that median survival of CML patients on chemotherapy was improved but not as same as TKIs.

1.7.2 Treatment of CML patients with tyrosine kinases inhibitors

Over the past decade, and following the introduction of TKIs, there have been significant changes in the management and survival of CML patients. At present, five TKIs, namely Imatinib Mesylate (IM), Nilotinib, Dasatinib, Ponatinib and Bosutinib, are approved by the United States Food and Drug Administration (FDA) for treating patients with CML disease (Akard et al., 2016, Druker et al., 1996, Gover-Proaktor et al., 2019). The most common approved treatments in Qatar are Imatinib (400 mg), Nilotinib (300 mg), and Dasatinib (100 mg). Imatinib Mesylate (IM), previously known as ST1571, was introduced in 2001 as the standard treatment of Philadelphia positive (Ph+), which had significant improvement in the life span of CML patients. After several clinical trials, the dose was adjusted to 400 mg daily for patients in the chronic phase and raised to 600 mg and 800 mg if patients were in the accelerated phase (AP) or blast crisis (BC), respectively (Cohen et al., 2005, Zhang et al., 2019).

Nilotinib, previously known as (formerly AMN107), is the second generation of TKIs. However, it got recently approved as the first line treatment due to achieving superior molecular response compared to IM. The approved dosage is 300 mg bid (Castagnetti et al., 2016, Liu et al., 2019). Dasatinib has a wider effect by suppressing the Src family of kinases. It was also found to be superior in patients who had developed resistance to IM treatment (Aladag and Haznedaroglu, 2019, Cannell, 2007, Ottmann et al., 2007), at the approved dose of 70mg bid or 100mg daily. A summary of TKIs available for CML treatment is presented in (Table1. 2) (NIH, 2007, Rossari et al., 2018, Shiotsu et al., 2009, Tokarski et al., 2006, Zhang et al., 2010, Zhang et al., 2013).

Table1. 2 List of TKIs available for CML treatment.

Name	Abl	BCR-ABL	c-Abl	v-Abl	IC50 / Ki	Description
1-Naphthyl PP1(1-NA-PP1)	+		+		c-Abl, IC50: 0.6 μM	1-Naphthyl PP1(1-NA-PP 1) is a highly selective and potent pan-PKD inhibitor with IC50 of 154.6 nM,133.4 nM and 109.4 nM for PKD1, PKD2 and PKD3, respectively. 1-Naphthyl PP1 is a selective inhibitor of Src family kinases (v-Src, c-Fyn) and the tyrosine kinase c-Abl with IC50 of 1.0 μM, 0.6 μM, 0.6 μM, 18 μM and 22 μM for v-Src, c-Fyn, c-Abl, CDK2 and CAMK II, respectively.
1-NM-PP1	++					1-NM-PP1 (PP1 Analog II, 1NM-PP1, analogue 9) is a potent inhibitor of Src family kinases with IC50 of 4.3 nM and 3.2 nM for v-Src-as1 and c-Fyn-as1, respectively. 1-NM-PP1 also inhibits CDK2-as1, CAMKII-as1 and c-Abl-as2 with IC50 of 5.0 nM, 8.0 nM and 120 nM, respectively.
Asciminib (ABL001)	++++				Abl1, IC50: 0.45 nM	Asciminib (ABL001) is a potent and selective allosteric ABL1 inhibitor with dissociation constant (Kd) of 0.5-0.8 nM and selectivity to the myristoyl pocket of ABL1.
AST-487 (NVP-AST487)	√					AST-487 (NVP-AST487), a N,N'-diphenyl urea,is an ATP competitive inhibitor of Flt3 with ki of 0.12 μM.Besides FLT3, AST487 also inhibits RET,KDR,c-KIT,and c-ABL kinase with IC50 values below 1 μM.
AT9283	+++				Abl (Q252H), IC50: 10 nM-30 nM; Abl1 (T315I), IC50: 4 nM	AT9283 is a potent JAK2/3 inhibitor with IC50 of 1.2 nM/1.1 nM in cell-free assays: also potent to Aurora A/B, Abl1(T315I). Phase 2.
Bafetinib (INNO-406)	+++				Abl, IC50: 5.8 nM	Bafetinib (INNO-406, NS-187) is a potent and selective dual BCR-ABL/Lyn inhibitor with IC50 of 5.8 nM/19 nM in cell-free assays,

						does not inhibit the phosphorylation of the T315I mutant and is less potent to PDGFR and c-Kit. Phase 2.
Berbamine		√				Berbamine (BA), a traditional Chinese medicines extracted from Berberis amurensis (xiaoboan), is a novel inhibitor of bcr/abl fusion gene with potent anti-leukemia activity and also an inhibitor of NF-κB. Berbamine (BA) induces apoptosis in human myeloma cells and inhibits the growth of cancer cells by targeting Ca^{2+}/calmodulin-dependent protein kinase II (CaMKII).
Berbamine dihydrochloride		√				Berbamine (BA, BBM) dihydrochloride, a traditional Chinese medicines extracted from Berberis amurensis (xiaoboan), is a novel inhibitor of bcr/abl fusion gene with potent anti-leukemia activity and also an inhibitor of NF-κB. Berbamine (BA, BBM) dihydrochloride induces apoptosis in human myeloma cells and inhibits the growth of cancer cells by targeting Ca^{2+}/calmodulin-dependent protein kinase II (CaMKII).
Bosutinib (SKI-606) *	++++				Abl, IC50: 1 nM	Bosutinib (SKI-606) is a novel, dual Src/Abl inhibitor with IC50 of 1.2 nM and 1 nM in cell-free assays, respectively. Bosutinib also effectively decreases the activity of PI3K/AKT/mTOR, MAPK/ERK and JAK/STAT3 signaling pathways by blocking the phosphorylation levels of p-ERK, p-S6, and p-STAT3. Bosutinib promotes autophagy.
CZC-8004						CZC-8004 (CZC-00008004) is a pan-kinase inhibitor that binds a range of tyrosine kinases including ABL kinase.
Danusertib (PHA-739358)	+++				Abl, IC50: 25 nM	Danusertib (PHA-739358) is an Aurora kinase inhibitor for Aurora A/B/C with IC50 of 13 nM/79 nM/61 nM in cell-free assays, modestly potent to Abl, TrkA, c-RET and FGFR1, and less potent to Lck, VEGFR2/3, c-Kit, CDK2, etc. Danusertib induces apoptosis, cell cycle arrest, and autophagy. Phase 2.

Dasatinib (BMS-354825) *	++++				Abl, IC50: 0.6 nM	Dasatinib (BMS-354825) is a novel, potent and multi-targeted inhibitor that targets Abl, Src and c-Kit, with IC50 of <1 nM, 0.8 nM and 79 nM in cell-free assays, respectively. Dasatinib induces autophagy and apoptosis with anti-tumor activity.
Dasatinib hydrochloride	++++				Abl, IC50: 0.6 nM	Dasatinib hydrochloride (BMS-354825) is the hydrochloride salt form of dasatinib, an inhibitor that targets Abl, Src and c-Kit, with IC50 of <1 nM, 0.8 nM and 79 nM in cell-free assays, respectively.
Dasatinib Monohydrate	++++				Abl, IC50: 0.6 nM	Dasatinib Monohydrate (BMS-354825) is a novel, potent and multi-targeted inhibitor that targets Abl, Src and c-Kit, with IC50 of <1 nM, 0.8 nM and 79 nM, respectively.
Degrasyn (WP1130)		+				Degrasyn (WP1130) is a selective deubiquitinase (DUB: USP5, UCH-L1, USP9x, USP14, and UCH37) inhibitor and also suppresses Bcr/Abl, also a JAK2 transducer (without affecting 20S proteasome) and activator of transcription (STAT). Degrasyn (WP1130) induces apoptosis and blocks autophagy.
GMB-475		√				GMB-475 is a proteolysis-targeting chimera (PROTAC) that allosterically targets BCR-ABL1 protein and recruit the E3 ligase Von Hippel-Lindau (VHL), resulting in ubiquitination and subsequent degradation of the oncogenic fusion protein.
GNF-2		++				GNF-2 is a highly selective non-ATP competitive inhibitor of BCR-ABL, shows no activity to Flt3-ITD, Tel-PDGFR, TPR-MET and Tel-JAK1 transformed tumor cells.
GNF-5		++				GNF-5 is a selective and allosteric BCR-ABL inhibitor with IC50 of 220 nM.
GNF-7	+++		++		c-Abl, IC50: 133 nM; G250E, IC50: 136 nM; E255V, IC50: 122 nM;	GNF-7 is a potent type-II kinase BCR-ABL inhibitor with IC50 of <5 nM, 61 nM, 122 nM, 136 nM, and 133 nM for M351T, T315I, E255V, G250E, and c-Abl, respectively.

					T315I, IC50: 61 nM; M351T, IC50: <5 nM	
Imatinib (STI571)	+			+	v-Abl, IC50: 600 nM	Imatinib (STI571, CGP057148B, Gleevec) is a multi-target inhibitor of tyrosine kinase with inhibition for v-Abl, c-Kit and PDGFR, IC50 values are 0.6 μM, 0.1 μM and 0.1 μM in cell-free or cell-based assays, respectively. Imatinib (STI571) induces autophagy.
Imatinib (STI571) Mesylate*	+			+	v-Abl, IC50: 600 nM	Imatinib (STI571, CGP057148B, Gleevec) Mesylate is an orally bioavailability mesylate salt of Imatinib, which is a multi-target inhibitor of v-Abl, c-Kit and PDGFR with IC50 of 0.6 μM, 0.1 μM and 0.1 μM in cell-free or cell-based assays, respectively. Imatinib Mesylate (STI571) induces autophagy.
KW-2449	+++				Abl, IC50: 14 nM; Abl (T315I), IC50: 4 nM	KW-2449 is a multiple-targeted inhibitor, mostly for Flt3 with IC50 of 6.6 nM, modestly potent to FGFR1, BCR-ABL and Aurora A; little effect on PDGFRβ, IGF-1R, EGFR. Phase 1.
Nilotinib (AMN-107)*		+++				Nilotinib (AMN-107) is a selective BCR-ABL inhibitor with IC50 less than 30 nM in Murine myeloid progenitor cells. Nilotinib induces autophagy through AMPK activition.
Nilotinib hydrochloride*		+++				Nilotinib hydrochloride (AMN-107) is the hydrochloride salt form of nilotinib, an orally bioavailable BCR-ABL tyrosine kinase inhibitor with antineoplastic activity.
Nilotinib hydrochloride monohydrate*		+++				Nilotinib (AMN-107, Tasigna) hydrochloride monohydrate is a selective and orally bioavailable inhibitor of BCR-ABL with IC50 < 30 nM in Murine myeloid progenitor cells. Nilotinib induces autophagy through AMPK activition.
Nocodazole (R17934)	++				Abl (T315I), IC50: 0.64 μM; Abl (E255K), IC50:	Nocodazole (R17934, Oncodazole, NSC238159) is a rapidly reversible inhibitor of microtubule polymerization, also inhibits Abl, Abl(E255K) and Abl(T315I) with IC50 of 0.21 μM, 0.53 μM and

					0.53 μM; Abl, IC50: 0.21 μM	0.64 μM in cell-free assays, respectively. Nocodazole induces apoptosis.
NVP-BHG712	+		+		c-Abl, IC50: 1.667 μM	NVP-BHG712 is a specific EphB4 inhibitor with ED50 of 25 nM that discriminates between VEGFR and EphB4 inhibition; also shows activity against c-Raf, c-Src and c-Abl with IC50 of 0.395 μM, 1.266 μM and 1.667 μM, respectively.
Olverembatinib dimesylate (HQP1351)	++++				Abl (M351T), IC50: 0.29 nM; Abl (Y253F), IC50: 0.35 nM; Abl (H396P), IC50: 0.35 nM; Abl (Q252H), IC50: 0.15 nM; Abl (G250E), IC50: 0.71 nM; Abl (E255K), IC50: 0.27 nM; Abl (T315I), IC50: 0.68 nM; Abl, IC50: 0.34 nM	Olverembatinib dimesylate (HQP1351, GZD824) is a novel orally bioavailable BCR-ABL inhibitor for BCR-ABL (WT) and BCR-ABL (T315I) with IC50 of 0.34 nM and 0.68 nM, respectively.
PD173955		+++				PD173955 is a potent Bcr-Abl inhibitor with IC50 of 1-2 nM, also inhibiting Src activity with IC50 of 22 nM.
Ponatinib (AP24534) *	++++				Abl, IC50: 0.37 nM	Ponatinib (AP24534) is a novel, potent multi-target inhibitor of Abl, PDGFRα, VEGFR2, FGFR1 and Src with IC50 of 0.37 nM, 1.1 nM, 1.5 nM, 2.2 nM and 5.4 nM in cell-free assays, respectively. Ponatinib (AP24534) inhibits autophagy.

PP-121	+++					PP-121 is a multi-targeted inhibitor of PDGFR, Hck, mTOR, VEGFR2, Src and Abl with IC50 of 2 nM, 8 nM, 10 nM, 12 nM, 14 nM and 18 nM, also inhibits DNA-PK with IC50 of 60 nM.
Radotinib		++				Radotinib (IY-5511) is a selective BCR-ABL1 tyrosine kinase inhibitor with IC50 of 34 nM, used to treat Chronic Myeloid Leukemia.
Rebastinib (DCC-2036)	++++				p-Abl1 (T315I), IC50: 4 nM; u-Abl1 (T315I), IC50: 5 nM; Abl1 (H396P), IC50: 1.4 nM; p-Abl1 (native), IC50: 2 nM; u-Abl1 (native), IC50: 0.75 nM	Rebastinib (DCC-2036) is a conformational control Bcr-Abl inhibitor for Abl1(WT) and Abl1(T315I) with IC50 of 0.8 nM and 4 nM, also inhibits SRC, LYN, FGR, HCK, KDR, FLT3, and Tie-2, and low activity to seen towards c-Kit. Phase 1.
Tozasertib (VX-680, MK-0457)		+++				Tozasertib (VX-680, MK-0457) is a pan-Aurora inhibitor, mostly against Aurora A with Kiapp of 0.6 nM in a cell-free assay, less potent towards Aurora B/Aurora C and 100-fold more selective for Aurora A than 55 other kinases. The only exceptions are Fms-related tyrosine kinase-3 (FLT-3) and BCR-ABL tyrosine kinase, which are inhibited by the Tozasertib with both Ki of 30 nM. Tozasertib induces apoptosis and autophagy. Phase 2.
URMC-099	+++				Abl1, IC50: 6.5 nM	URMC-099 is an orally bioavailable, brain penetrant mixed lineage kinase (MLK) inhibitor with IC50 of 19 nM, 42 nM, 14 nM, and 150 nM, for MLK1, MLK2, MLK3, and DLK, respectively, and also inhibits LRRK2 activity with IC50 of 11 nM. URMC-099 also inhibits ABL1 with IC50 of 6.8 nM. URMC-099 induces autophagy.

XL228	++++				ABL T315I, IC50: 1.4 nM; wild-type ABL kinase, IC50: 5 nM	XL228 is a protein kinase inhibitor with IC50 of 5 nM, 1.4 nM, 3.1 nM, 1.6 nM, 6.1 nM and 2 nM for wild-type ABL kinase, ABL T315I, Aurora A, IGF-1R, SRC and LYN, respectively.

+ Inhibitory effect, multiple "+" signs indicate increased inhibition.

√ Inhibitory chemicals have an impact on the associated isoform, but without a specified value.

* FDA approved TKIs

1.7.2.1 Side effect of Tyrosine kinase inhibitors

As CML patients remain on TKIs treatment indefinitely, some degree of toxicities can occur. The treating physicians usually alert patients with the toxicities of TKIs which have distinct safety profiles. However, comorbidities, expectations of patients, and progression of disease lead to intolerance of treatments. In general, the most common side effects of TKIs treatment are cytopenia, headache, vomiting, nausea, muscle pain, liver damage, diarrhoea, fatigue, and rash (Apperley, 2015, Cortes et al., 2016, Cortes et al., 2018, Garcia-Gutierrez and Hernandez-Boluda, 2019, Gugliotta et al., 2015, Kantarjian et al., 2012).

Currently, around 95% of CML patients represented in the chronic phase, and the rest 5% represents advanced Phases (accelerate and blast crisis). All TKIs are approved in newly diagnosed, and as the first line of treatment; however, advanced phases are the dilemma of TKIs as it requires management with TKI alone or with a combination of TKI together and conventional chemotherapy regimens (Bonifacio et al., 2019).
Even though most of the mentioned side effects are common between different TKIs, the percentages of patients who discontinue treatments are varying from one TKI to another. Recently, publications documented that around 4% of patients on Imatinib Mesylate (Gugliotta et al., 2015) had discontinued the treatment, while the percentage increased to 20% for patients on Nilotinib (Cortes et al., 2016, Garcia-Gutierrez and Hernandez-Boluda, 2019).

1.7.3 Resistance to TKIs

Despite the dramatic effect of TKIs, however, a percentage of patients are resistance to treatments. Internationally, over 25% of CML patients have a kind of resistant to treatments. In the state of Qatar, it is around 54% (Al-Dewik et al., 2014, Apperley, 2007a, Apperley, 2007b, Branford et al., 2019, Chandrasekhar et al., 2019). Resistance to TKIs was classified into primary resistance if CML patients failed to achieve haematological or molecular, or cytogenetic responses according to the time-dependent endpoints of European LeukaemiaNet (ELN) guidelines. Secondary resistance was

categorized if CML patients had lost one of the achieved haematological, molecular, and cytogenetic responses. At this mechanistic level, the resistance to TKIs was identified as *BCR-ABL1* -dependent or *BCR-ABL1* independent (Hochhaus, 2006, Patel et al., 2017).

The main concept of the *BCR-ABL1*-dependent resistance mechanism arises due to the blocking site of the Kinase domain (KD) against TKIs; this is due to several factors which included but not limited to *BCR-ABL1* KD Mutations. In 2005, reports were published on the evidence of molecular heterogeneity at the chronic phase (CP). However, genes of clinical relevance were not defined, and the patients progressed to the accelerated phase (AP) after one year (Corm et al., 2005). In addition to that, there are more than 50 kinase domain mutation sites and more than 70 different BCR-ABL1 mutations, which can contribute to resistance to treatment with Imatinib (Apperley, 2007a, Apperley, 2007b, Baccarani et al., 2019b). The point of mutations within the kinase domain is being the most common and frequent mechanism of resistance. Later in 2010, Al-Dewik *et al*., reported that 54% of CML patients in Qatar showed a resistance phenotype when treated with Imatinib (Al-Dewik et al., 2015). Most recently, 45% of CML patients who participated in the International Randomized Study of Interferon and STI571 (IRIS) failed to continue on Imatinib therapy by the 8-year follow-up time (Jabbour and Kantarjian, 2016). Therefore, not all patients with CML would gain long term benefit from therapy with TKIs, and it is essential to uncover the underlying mechanisms of resistance to treatment with the *BCR-ABL1* TKIs. Overall, 15 to 20% of CML patients show some degree of resistance to current TKIs in the long term, especially those who have achieved molecular responses. This may occur due to the persistence of positive *BCR-ABL1* cells at the stem cell level, which can't be detected by current technology (Mahon, 2015). Other types of mutations such as insertions and deletions have been reported; recent studies evidenced insertion of 35 bases –pairs between exons 8 and 9 while deletions of exons 4 and 7 at BCR-*ABL1*. Deletions or insertions affect directly or indirectly on BCR-ABL1 fusion protein, which consequently has significance on pharmacokinetic or changing cellular response to TKIs (Meggyesi et al., 2012). On the other hand, overexpression of BCR-ABL1 or/ and Protein

Glycoprotein (PGP) may directly affect the efficiency of TKIs, which lead to escaping leukemic cells to achieve molecular response within the timeframe (Mahon et al., 2003). Therefore, there is an urgent need not only for more detailed studies of factors contributing to resistance therapy with the TKIs but also development of novel and more effective therapeutic agents.

1.8 Protein Tyrosine phosphatases (PTP).

Under normal circumstances, there is a balance between the rate of hematopoietic cell division and cell death in haematopoiesis. This mechanism is tightly regulated by the activation and inactivation of various cell signalling molecules and proteins, namely proteins kinases and protein phosphatases. Cancer is typified by dysregulation between protein tyrosine kinase and phosphatases levels in cell signalling pathways.

PTPs are a superfamily of enzymes that have the ability to remove the phosphate groups from target proteins to maintain the equilibrium status in cell activities (Tonks, 2006). Human genomes have more than 103 genes that encode PTPs (Andersen et al., 2004, Alonso et al., 2004). PTPs are also known as holoenzymes and share cascades (HCX_5R motif, where X is every amino acid), located at the active site of the enzyme (Andersen et al., 2001). They are classified based on their cellular location, specificity, and function. Based on cellular location, the classical phosphotyrosine distinguishes into receptor-type PTPs (PTPR) located at the plasma membrane and non-receptor-type PTPs (PTPN), which is located in the cytosol (Figure1. 10) ((Andersen et al., 2001, Lee et al., 2015, Ooms et al., 2015).

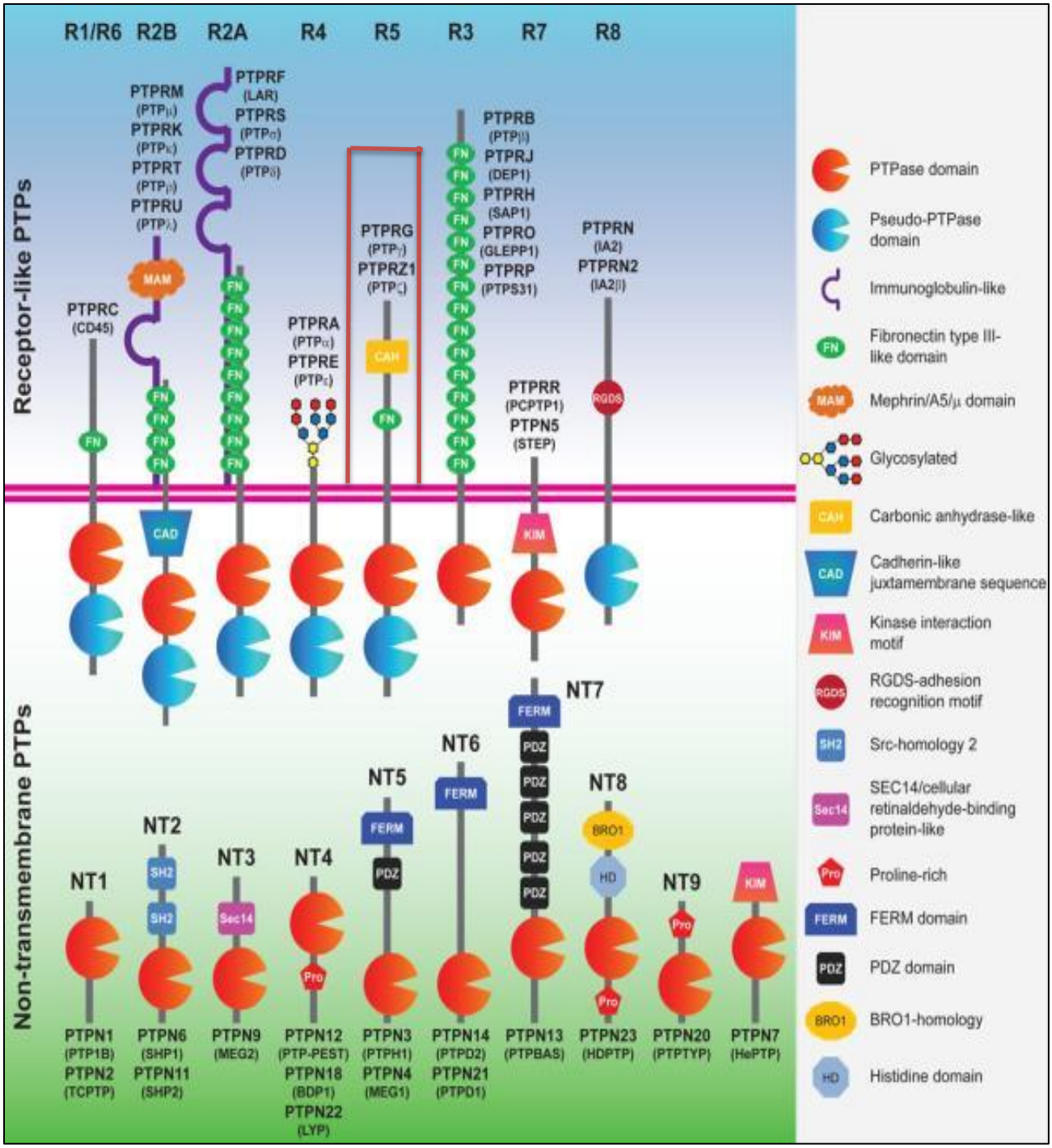

Figure1. 10 The schematic classical PTPs.

The classical protein tyrosine phosphatases (PTPs) can be categorized as receptor-like (R) or non-trans membrane (NT) proteins. In each case, the PTPs have been designated by a name that is commonly used in the literature. Where the former differs from the gene symbol, the latter is included in parentheses for clarification. In each case, the various subdivisions are based upon sequence similarity. [Adopted from (Lee et al., 2015)].

1.9 Receptor-type PTPs (PTPRs).

PTPRs consist of multiple extracellular domains, a transmembrane domain, and an intracellular catalytic domain (Du and Grandis, 2015). RPTP has a potential role in signalling regulation through ligand-controlled protein dephosphorylating. To date, 21 RPTPs have been identified. Recent studies showed that the core site of RPTP is in the membrane-proximal name (D1) domain. The cascade starts by the soluble cytokine pleiotrophin, which acts as a ligand for RPTPs. The binding of pleiotrophin blocks the activity of RPTPs and thus promotes the tyrosine phosphorylation of the protein, which in turn regulates cell adhesion.

PTPRs are firmly regulated in cell signalling by mechanisms such as dimerization, post-translational or reversible oxidation mechanisms (Lee et al., 2015, Tonks, 2006). Another type of regulation is named the “zipper model,” where the dimeric state is tightly controlled by interactions of many components of the PTP (Jiang et al., 2000). In this framework, the ligand binding can disturb dimer formation, thus stimulating PTP initiation. A further level of regulation is reversible oxidation. The cysteine residue is in the active location of PTPRs, which has low pKα and makes the active site of PTPRs subject to oxidation (Salmeen and Barford, 2005). The result of oxidation supports a reversible mechanism of PTPR activation (Du and Grandis, 2015).

Even though PTPRs share a similar basic structure, distinct PTPRs have specific targets and may thus play altered roles in cell regulation. Indeed, as will be highlighted later, the primary aim of this study is to investigate the role of protein tyrosine phosphatase receptor type γ (PTPRG) in CML in the state of Qatar. *PTPRG* is located on chromosome 3 short arm (3p14.2) (Kastury et al., 1996, LaForgia et al., 1993). *PTPRG* has 30 exons in the region of 780 kb in size. *PTPRG* has four isoforms (Shintani et al., 1997). However, their distribution and function are not fully understood (Lorenzetto et al., 2014). Like most RPTPs, *PTPRG* has an extracellular domain, a transmembrane domain, and an intracellular catalytic domain. A transmembrane protein results from the encoding of 5787 bp of mRNA (Moratti et al., 2015). In addition to that, *PTPRG* has a carbonic anhydrase-homologous amino terminus followed by a

fibronectin III domain and a cysteine-free domain (Barnea et al., 1993). *PTPRG* is essentially expressed in many tissues such as the human kidney, stomach, colon, lung, oesophagus, and spleen. Its regulation is controlled by ligand-binding capability, modulating activity (Tsukamoto et al., 1992).

1.10 Role of receptor tyrosine phosphatases in cancer

The importance of phosphatases in the physiological process, genetic and epigenetic alterations have also been reported in several human cancers (Du and Grandis, 2015). Genetic and epigenetic alterations occur but are not limited to change in copy number or promoter methylation or mutation. These alterations have a direct influence on the expression level or function of PTPR (Julien et al., 2011). The genetic alteration has two sub-sequences: either by increasing the activity of an oncogene due to mutation by gain-of-function or loss/deletion copy number, or by silencing a tumour suppressor gene by loss-of the function. Recent data from the Cancer Genome Atlas (TCGA) showed that 20 out of the 21 PTPR are mutated in several kinds of cancer (Figure1. 11). The ratio of mutation in *PTPRG* is higher than the deletion and amplification ratios.

1.11 Role of tyrosine phosphatase and PTPRG cell signalling in cancer

Over the past decades, the role of emerging phosphatases in the pathogenesis of hematologic malignancies had been documented. There is a related notion which strongly suggested that the decreased expression levels of the tyrosine phosphatase PTPN6 (SHP-1) are affected by aberrant promoter hypermethylation, which may play a vital role in the progression of CML by dysregulating *BCR-ABL1*, MAPK, MYC and JAK2/STATS5 signalling (Amin et al., 2007, Li et al., 2014). In study reports, the ability of PTPRG to act as a tumour suppressor by inhibition breast tumour formation in vivo, where PTPRG was shown to up-regulate p21cip and p27kip proteins via the ERK1/2 pathway (Shu et al., 2010). The same model applies in nasopharyngeal carcinoma, where the overexpression of *PTPRG* is shown to enhance the suppression of tumour growth in vivo. Moreover, *PTPRG* was found to have the competency to inhibit cell growth and accumulate the cells in G0 and G1 phases through the down-regulation of cyclin D1 (Cheung et al., 2008). On the other hand, several studies reported mutations

in tyrosine phosphatases in different kinds of leukaemia such as Acute Myeloid leukaemia (AML), Juvenile Myelomonocytic leukaemia (JMML), Myelodysplastic Syndrome (MDS), B-cell Acute Lymphoblastic leukaemia (B-ALL) and in patients of colorectal cancer, lung cancer, melanoma, neuroblastoma, head and neck cancer (Labbe et al., 2012, Lui et al., 2014, Paez et al., 2004, Tartaglia et al., 2003, Wang et al., 2004). Hyper cellular proliferation, disease progression, and poor outcomes are associated with mutated PTPs (Lui et al., 2014, Ostman et al., 2006).

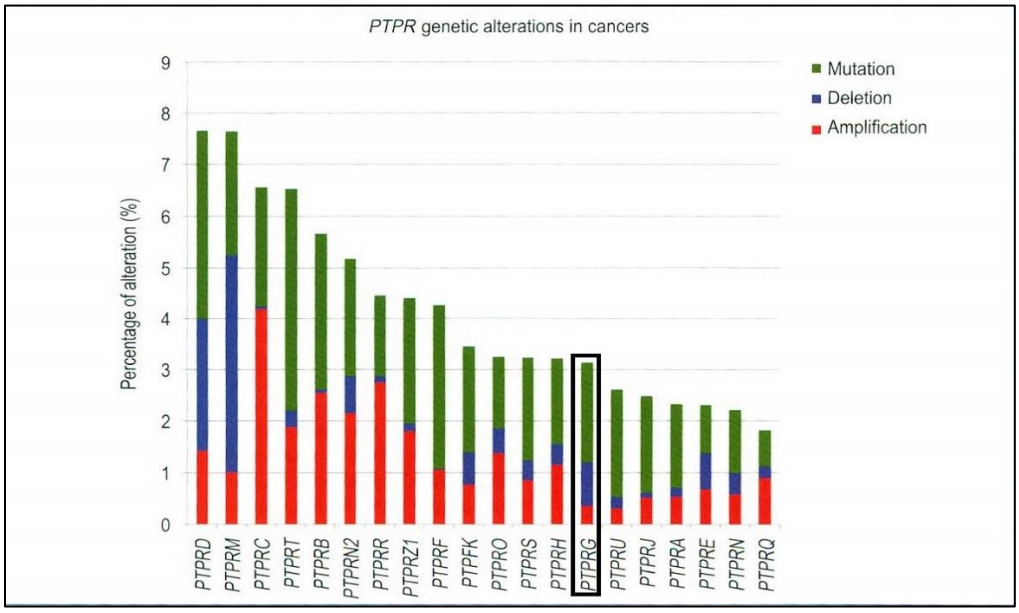

Figure1. 11 Genetic alterations in receptor-type protein tyrosine phosphatase (PTPs) in cancer.

Mutation, deletion, and amplification are the three genetic mechanisms reported in the Cancer Genome Atlas (TCGA) in Green, blue, and red colours accordingly. 20 PTPRs have genetic alternations across 25 human cancers (TCGA, provisional). The figure also shows the ratio of mutation in PTPRG, which is high compared to deletion and amplification that has been reported to date. [Adopted from (Du and Grandis, 2015)]

In terms of epigenetic changes, promoter methylation is a fundamental mechanism for *PTPRG* activation in different neoplasms. Wang and Dai in 2007, suggested that *PTPRG* is hyper methylated in many cancers such as gastric cancer (Wang and Dai, 2007), as well as Su *et al*. documented hyper methylation of *PTPRG* in breast cancer (Shu et al., 2010). Xiao reported the same condition in childhood acute lymphoblastic leukaemia (Xiao et al., 2014), and finally, similar status was reported in cutaneous T-cell lymphoma (van Doorn et al., 2005). PTPRG expression is in reverse correlation with

methylation, and its expression can be improved if treated with methylation-suppressive agents such as 5-aza-2,-deoxycytidine (van Doorn et al., 2005, Wang and Dai, 2007). However, relatively little is known about *PTPRG* mutations and its role in response to therapy in patients with CML disease.

On the other hand, *PTPRG* is reported to have strong relation with fibroblast growth factors receptors (FGFRs), which have remarkable significance on inhibition of tumour progression. FGFRs are a family of receptor tyrosine kinase which plays a vital role in physiological processes such as cell migration, differentiation, proliferation, and survival. FGFR family consist of four members (FGFR-1 to FGFR-4) (Dai et al., 2019), out of which FGFR-3 had documented its overexpression in CD34+ BCR-ABL+ cells in CML disease (Dvorak et al., 2003) while the disturbance role of FGFR1 was observed in CML patients with an additional chromosomal abnormality (Demiroglu et al., 2001).

Additionally, *PTPRG* had the ability to inhibit tumour progression by interacting with Human Epidermal Growth Factor Receptor (EGFR) which leads to the dephosphorylating of EGFR at different sites (Cheung et al., 2015). In a different scenario Luisa *et al*, had evidenced that β-catenin, which is a key for the transcriptional regulator in stem cell renewal, has a role in developing of *BCR-ABL1. PTPRG* controls it through the dephosphorylating process (Tomasello, 2016). *PTPRG* plays a vital role as an oncosuppressor gene in CML, suggesting a complex which is not yet fully explained (Figure1. 12).

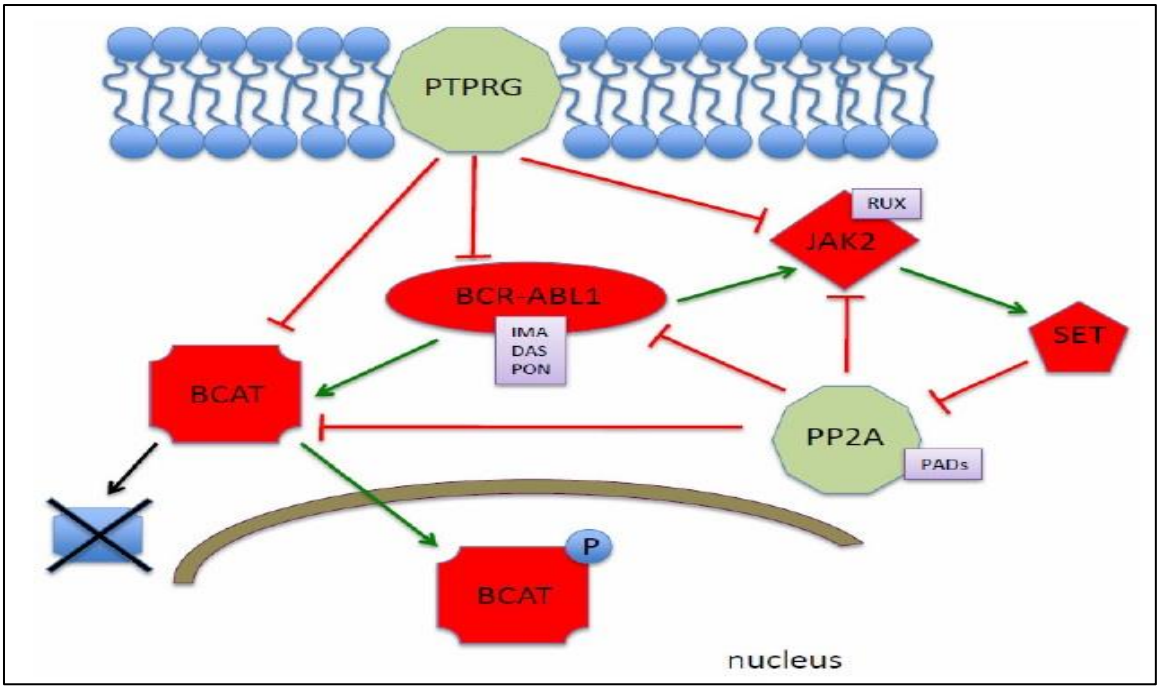

Figure1. 12 Shortened network of PTPRG interaction in CML cells.
Colour coding of PTPRG signalling pathway: In red are inhibitory pathways and in green activator pathways. Drugs modulating the specific targets are RUX (Ruxolitinib), IMA (Imatinib Mesylate), NIL (Nilotinib), DAS (Dasatinib), PON (Ponatinib), PADs (PP2A activating drugs) [Adopted from (Bonifacio, 2018)].

1.12 CML and Its management in Qatar

The State of Qatar is in the Middle East, and its capital is Doha, where most of the population lives. The total area of Qatar is 11.437 Km^2. Qatar's population is rapidly growing, with an average annual increase in population up to 40% during the last decade. This is due to the country's strong economic performances and rapid infrastructure development for hosting the World cup 2022. The country's population has been split between 50-55% for non-Arab expatriates, and 20% native Qatari, and the rest are Arab expatriates. The gender breakdown from the 2019 census showed that men represented 73.5% of the total population, while women make up 26.5%. The incidence percentage of CML patients in Qatar was less than the international statistics according to the National cancer strategy of Qatar 2015* (QNCR). CML disease encodes C921 in the International Classification of Diseases (ICD 10) of QNCR coding. The recorded numbers of CML patients were 5, 12, and 9 patients for 2013, 2014 and

2015 years respectively, while the population was almost 2.0, 2.24, and 2.5 million for those years (psa.gov.qa) though, there was no audited recorded data up to date. This information was not available online and an official request had been submitted to Cancer Registry Manager to release such information. Of note, the majority of clinical trials had assessed ELN classification for the efficacy of TKIs and is recommended as a basis for treatment judgments (Hochhaus et al., 2017). However, the National Centre for Cancer Care and Research (NCCCR) facility utilized WHO classification for new diagnosis cases and no tools for monitoring the efficiency of TKIs until October 2018. Moving forward, NCCCR had adopted a policy to use both classifications since then.

Hamad Medical Corporation (HMC) is the governmental health provider in Qatar and manages 13 hospitals under its umbrella for different specialties (hamad.qa) The NCCCR, established in April 2004 as the tertiary oncology centre. It incorporates all necessary oncology services, cancer registry, haematology services, including in-patients and out-patients and nutritional and social services. Qatar National Cancer Registry was established in January 2014 and operated under the National Cancer Program in the Ministry of public health (MoPH).

QNCR's concept is to collect all cancer information from all healthcare providers and sectors through a home-made online application. QNCR has three database domains: cancer incidence, cancer screening, and cancer waiting times. The primary health care centres including but not limited to military, police, and Medical private sectors, are the first line for evaluating all patients. Alternatively, most patients access the accident and emergency department (A/E) which is a branch of the main hospital of Hamad Medical Corporation in Doha, or other (A/E), departments under the HMC umbrella, if they live nearby, due to free/ subsidized cost of visits as the health care system is freely available to all citizens and residents. It is free of charge for all Qatari patients, and nominal fees are applied for residents compared to the private health sector. This creates huge traffic to most of the A/E departments of HMC due to the low socioeconomic labour force; otherwise, they struggled to afford costs for health care management. TKIs that are available at NCCCR are Imatinib (400mg), Nilotinib

(300mg), and Dasatinib (70mg), while Bosutinib and Ponatinib are non-formulary at HMC.

CML patients may present with signs and symptoms at presentation that may include fatigue, weight loss, abdominal fullness, bleeding, purpura and splenomegaly, however; a peripheral blood examination is incidentally or routinely requested and shows abnormal white blood counts (WBC) and/ or low platelets counts with the shift to lift in the WBC subpopulation. This would be the first indicator of CML disease. Later, patients are referred to NCCCR for further specialized management. Once the patient is confirmed with CML disease, hospital policy" Clinical Practice Guideline" is applied. CML referral and triage pathways for new haematology patients were established by the Regulatory, Accreditation, and Compliance (RACS) department at HMC, which classifies CML patients into urgent and routine referrals. This classification was based on standardized rules or tests applied to patients' groups based on a preliminary judgment that applies further evaluation, such as in–depth pain assessment. Based on the results of screening, it determines the patients' needs for urgent or regular referral as described in (Figure1. 13).

RBMS* forwards referral to Haematology triage physician

1

Triage physician reviews appropriateness of Referral

Referral appropriate for Hematology

Yes

No

Complete

Urgent Referral

Triage physician identifies clinic, subspecialty & assigns priority

No

No

Yes

Slot available

Back to RBMS

Trigger urgent referral process if necessary

Appointment booked

2

Philadelphia Chr.

Clinical work up

Lab follow up

3

Patients Stratification

Optimal

Warning

Failure

RBMS* Referral and booking management system

Figure1. 13 The referral pathway of CML patients to NCCCR, clinical and laboratory management

Suspected CML patient's referral electronic form is initially evaluated by triage physicians who can classify patient's urgent or routine referral according to clinical symptoms available electronically in the Cerner system. Upon initial evaluation, a haematologist appointment is placed. Slot availability is operated by referral and booking management staff, which usually takes up to 6 months. There is no written protocol for the timeline of visits; however, a new approach was implemented to see new suspected malignancies cases within 48 hours by introducing clinics for new cases.

Clinics work to evaluate phases of CML patients through laboratory investigation (Haematology, cytogenetic, and molecular). Once the stage of CML disease is identified, treatment according to hospital policy will be applied. Treatment decisions for patients with CML are complex due to the variety of available options, many of which are conflicting. Firstly, cytoreductive treatment Hydroxyurea (HU) is initiated to reduce the white blood count to normal range. A period of two weeks was recommended prior to starting TKIs to wash out the effect of HU, and then one of the TKIs is prescribed according to clinical decision. Factors influencing the choice of therapy include, but are not limited to, patient age, presence of medical co-morbidities affecting patient's suitability such as mutation should be given due consideration along with laboratory results to optimize the usefulness of TKIs.*

Laboratory tests, along with follow-ups clinical slots, are booked according to the availability of physicians, which may be different than the timeline recommended by ELN. Upon the availability of laboratory results, patient's stratification is done. The main aim of treatment is to achieve complete Haematological Remission (CHR) by three (3) months, complete Cytogenetic Remission (CCyR) by six (6) months, and Major Molecular Remission (MMR) by 12 months of therapy. Failure of one or more of these remissions may risk the progression of the disease.

**Increase in normal white blood cells "leucocytosis" in CML usually associates with an increase in neutrophilic series count from myeloblasts to mature neutrophils with peaks in the percentage of myelocytes and segmented neutrophils. Although morphologically seems normal, the neutrophils in CML are cytochemical abnormal, and a cytochemical reaction called leukocytes alkaline phosphatase (LAP) is recommended.*

1.13 Aims and objective of the prospective study

This Ph.D. aims to evaluate the role of protein tyrosine phosphatase receptor Gamma (*PTPRG*) in tumour progression as a biomarker in patients with CML in the State of Qatar.

The objectives of the proposed study are:

To evaluate the potential use of PTPRG as a biomarker in CML via:

- Studying PTPRG expression at hematopoietic, progenitor cells, and mature white blood populations (from fresh, fixed, and cryopreserved samples) by flow cytometry utilizing a new monoclonal antibody that targets the extracellular domain (ECD) of PTPRG.
- Studying PTPRG expression level by RT-qPCR and correlate PTPRG expression with patients' response /resistance to treatment with TKIs.
- Determining whether there is any correlation between the PTPRG expression levels is determined by flow cytometry and RT-qPCR techniques.
- Screening and assessing whether the PTPRG is genetically altered in CML using NGS and associated resistance.
- Screening and evaluating whether the PTPRG is epigenetically altered in CML using NGS and associated resistance.
- To establish a hospital–based database & cryopreservation for patients with CML at the state of Qatar as such information and facilities are not available there.
- To establish a hospital-based database to record the results of PTPRG monitoring for CML patients.

2 Chapter 2 Material and Methods

2.1 Patients cohort

CML patients have no universal symptoms; most patients are diagnosed upon a visit to one of the following clinics in Qatar: outpatients, Primary Health Care Corporation (PHCC), military, police clinics, or Accident and Emergency (A/E) department. A resident, specialist, or family physician checks the family history of the patients during the visit and request check-up blood tests such as blood chemistry and complete blood count (CBC) tests. Patients are then referred to the specialist hospital if the results of blood tests were abnormal (e.g., High WBC count with the shift to the left). The National Centre for Cancer Care and Research (NCCCR) is the prime cancer hospital in the state of Qatar for further diagnosis and treatments. As a result, suspected CML patients are referred to NCCCR to confirm the diagnosis. The presence of Philadelphia chromosome t (9; 22) translocation and further examination of peripheral blood smears for white blood cells will assist the physicians in confirming the diagnosis and in determining the status and progression of the disease. Once CML diagnosis confirmed, the principal investigator (PI) or treating physician would invite the patients to the research clinic at NCCCR, if Patient's criteria were met Inclusion and exclusion criteria for this study are summarised in (Table 2. 1). Further information, including the purpose and nature of this research, the study timeline and the number of samples required, and the eligibility criteria will be briefly explained. A period would be given to patients to decide participation in the research project and to answer any inquiry/doubt that may arise. Once the patients signed the consent form, necessary blood samples for research purposes would be withdrawn along with routine blood tests by a phlebotomist at outpatient lab NCCCR. The institutional review board approved the study of Hamad Medical Corporation (Project No. SCH-HMC-020-2015) and the study was also approved by the Kingston University London Ethical Committee. This study adhered to the World Medical Association's Declaration of Helsinki (1964–2008) for Ethical Human Research, including confidentiality, privacy, and data management. Appendix A copy ethical approval (10.1).

Table 2. 1 *Patient's inclusion and exclusion criteria for this study.*
The presence of the Philadelphia chromosome is the sole mark for participating in the study, while elderly patients over 70 years old and women with pregnancy conditions were excluded from the study. Due to intolerance to therapy, this may lead to reduce the dose, which to some degree effects molecular response or significant risk of fetal abnormalities and miscarriage.

Inclusion criteria	Exclusion criteria
Positive Philadelphia chromosome of (Ph^+) t (9; 22) translocation Age: ≥ 18 and< 70 years.	Age < 18 ≥70 years. Pregnancy or lactation.

2.1.1 Prognostic scoring system

For patients in the chronic phase, it is common to utilize one of the accessible risk stratification scores, such as Sokal or the more recently developed European Treatment and Outcome Study (EUTOS) score. There was no suggestion to employ one method over another. The Sokal score was the first scale to calculate the CML Risk level. In the TKI era, it has been known to correlate with response to Imatinib, with event-free survival (EFS), and even with the probability of maintaining a durable CMR after treatment discontinuation. Introducing a TKI other than Imatinib, such as Nilotinib and Dasatinib, has become a dilemma to utilize another tool, the EUTOS score. The EUTOS score has the magnificence of simplicity as it includes only two factors: spleen size and basophils. Sokal score is the most used clinical score.

EUTOS and Sokal scores were employed in our study. EUTOS was collaboration between the European LeukaemiaNet ELN and Novartis, which was started to improve the understanding of CML to promote the best practice and enhance treatment outcomes. Using the EUTOS score, patients were stratified into two risk groups: high risk if the score ≥ 87 and low risk if the score < 87. Patients with high risk scores are likely to progress to accelerate and blast phases. On the other hand, Sokal score was also used to stratify patients into three risks groups: high-risk patients have a RR >1.2, intermediate-risk patients have between 0.8 – 1.2, and low-risk patients have an RR<0.8 with a median survival of 32, 45, and 60 months respectively (LeukemiaNet, 2015b, Sokal et al., 1984, LeukemiaNet, 2015a).

2.2 Monitoring protocol and response evaluation

Peripheral blood samples were collected at day zero and every three months to monitor the *PTPRG* and *BCR-ABL1* expressions as summarized in (Table 2. 2).

Table 2. 2 Monitoring of CML patients treated with one of tyrosine kinases inhibitors (TKIs).

Complete Blood picture (CBC) is the first line to monitor Morphology changes. If refer to count of white blood cells was enough for this experiment and the research plan needs. Collecting blood samples at 9 months were subject to availably of clinic of treating physician.*

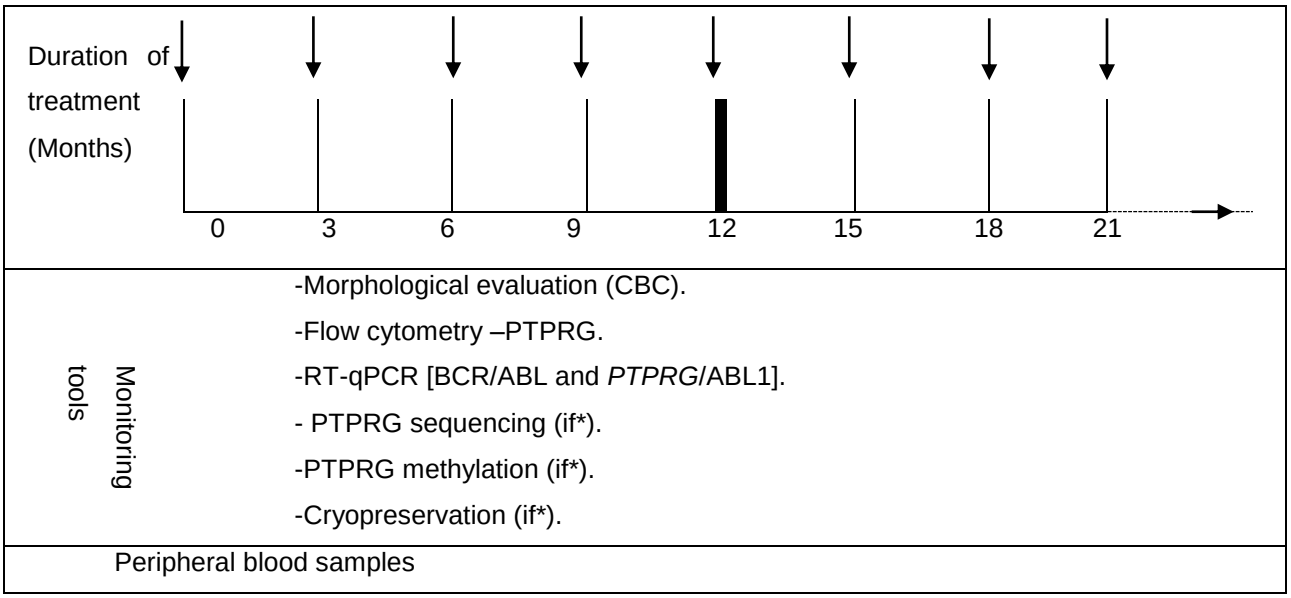

The 2013 European LeukaemiaNet (ELN) recommendations for the management of Chronic Myeloid Leukaemia (CML) were adopted and employed in this study to assess the response or resistance to treatment in CML patients (Baccarani et al., 2013). Patients' responses were determined at the haematological, cytogenetic, and molecular levels (Table 2. 3).

Management of hematologic malignancies generally, and chronic myeloid leukaemia has been assessed via regular laboratory tests to assess residual disease on an on-going basis. Monitoring minimal residual disease (MRD) has many goals which could be summarized as follows:

- To give a practical exhibition and explanation of the effectiveness of initial therapy.

- To pay attention to patients who may develop resistance or relapse if blood tests did not achieve the target with a timeline, which identifies the mechanism of treatment failure to help the physician to catch up and allow time to select alternative therapy.
- The purpose of ELN guidelines is to assess the response/ resistance of patients to treatment according to the diagnosis phase and follow up findings. Three levels of response were identified at Haematological, cytogenetic, and molecular levels and response classified into optimal, warning failure as described briefly below.

Table 2. 3 ELN 2013 guidelines for CML patients' response.

Anyfirst-line therapy (left) or second line (right) therapy with BCR-ABL TKIs. N/A: Not applicable, CCA: Clonal chromosomal abnormalities, CyR: Cytogenetic Response, PCyR: Partial Cytogenetic Response (1-35% of Ph positive metaphases), CCyR: Complete Cytogenetic Response (0% of Ph positive metaphases), Major route CCA/Ph+(trisomy 8,2 [d]Ph+[+der(22)t(9;22)(q34;q11)],is chromo some 17[i(17)(q10)],trisomy19, and ider (22)(q10)t(9;22)(q34;q11);MMR: Major Molecular Response (≤ 0.1%BCR-ABL1) IS: BCR-ABL on international scale; Mutation (BCR-ABL kinase domain point mutation).For haematological response was defined as Normalization of blood picture such as White blood cell < 10x109/L, platelets counts< 450x109/L and normal differential blood count without any immature stage, Schedule for monitoring hematologic response should be at diagnosis and every 15 days until complete hematologic Response (CHR) achieved, then every 3 months or as required.

Time	Optimal Response	Warning	Failure
Baseline	N. A	High Risk Major route CCA/Ph+	N. A
3 mos.	BCR-ABL^{IS}≤ 10%* Ph+ ≤ 35% (PCyR)	BCR-ABL^{IS}>10%* Ph+36-95%	No CHR* Ph+ >95%
6 mos.	BCR-ABL^{IS} <1%* Ph+0% (CCyR)	BCR-ABL^{IS} 1-10%* Ph+1-35%	BCR-ABL^{IS} >10%* Ph+>35%
12 mos.	BCR-ABL^{IS} ≤0.1%* (MMR)	BCR-ABL^{IS} 0.1-1%*	BCR-ABL^{IS} >1%* Ph+>0%
Then and at any time	MMR or better	CCA/Ph- (-7, or 7q-)	Loss of CHR Loss of CCyR Loss of MMR, confirmed** CCA/Ph+

Time	Optimal Response	Warning	Failure
Baseline	N. A	No CHR Loss of CHR on Imatinib Lack of CyR to 1st line TKI High Risk	N. A
3 mos.	BCR-ABL^{IS}≤ 10%* Ph+ <65%	BCR-ABL^{IS} > 10%* Ph+65-95%	No CHR* Ph+ >95%, or New mutations
6 mos.	BCR-ABL^{IS} <10%* PH+ >35% (PCyR)	BCR-ABL^{IS} ≤10%* Ph+35-65%	BCR-ABL^{IS} >10%* Ph+65%* New mutations
12 mos.	BCR-ABL^{IS} >1%* Ph+ 0 (CCyR)	BCR-ABL^{IS} 1-10%* Ph+1-35%	BCR-ABL^{IS} >10%* Ph+>35%* New mutations
Then and at any time	MMR or better	CCA/Ph- (-7, or 7q-) or BCR- ABL^{IS} >0.1%	Loss of CHR, or Loss of CCyR or PCyR New mutations Loss of MMR** CCA/Ph+

2.2.1.1 Optimal response

No suggestion to change treatment.

2.2.1.2 Warning response

Close monitoring is required to identify the response to treatment and permit a timely change in the therapy.

2.2.1.3 Failure response

The patient should receive different treatment to minimize the risk of disease progression as well as death. Response criteria to further TKIs treatment were illustrated below and highlighted the difference between first and second-line therapy treatment criteria and eligibility for both.

CML patients with MMR (≤ 0.1%*BCR-ABL1*), in other words, 3-log re-education in BCR-ABL, are associated with improved progression-free survival (PFS). PFS is defined as the duration from the time treatment starts until disease progression is achieved or death (regardless of the cause of death), whichever comes first. However, prognostic values are still debated (Press et al., 2006). “Molecularly undetectable leukaemia” is recommended by the ELN as Complete Molecular Response (CMR), which is not clinically recommended at present, with importance to specify the number copy of gene at reporting (Baccarani et al., 2013). Recently Deep Molecular response is a dilemma for optimal CML patient management, as the level of *BCR-ABL1* beyond MMR remains unknown due to lack of standardization and technology that are able to catch the very low number of copies for *BCR-ABL1* (Hasford et al., 2011). In addition, a recent study suggests further developments which are obligatory to assess the leukemic burden for *BCR-ABL1* quantifications (Marum and Branford, 2016). Later studies reported that some in-depth molecular responses could achieve treatment–free remission (TFR); therefore, CML patients can’t be cured without allogeneic bone marrow that has become a doubt (Mahon, 2015). However, it is subjected to available technology as well as the outcome of studies for CML patient’s progression in the long term to achieve

deep Molecular Response. The progression of disease was monitored by counting the number of leukaemia cells in peripheral blood. For this purpose, international scales were employed for a molecular response, as explained in (Figure 2. 1).

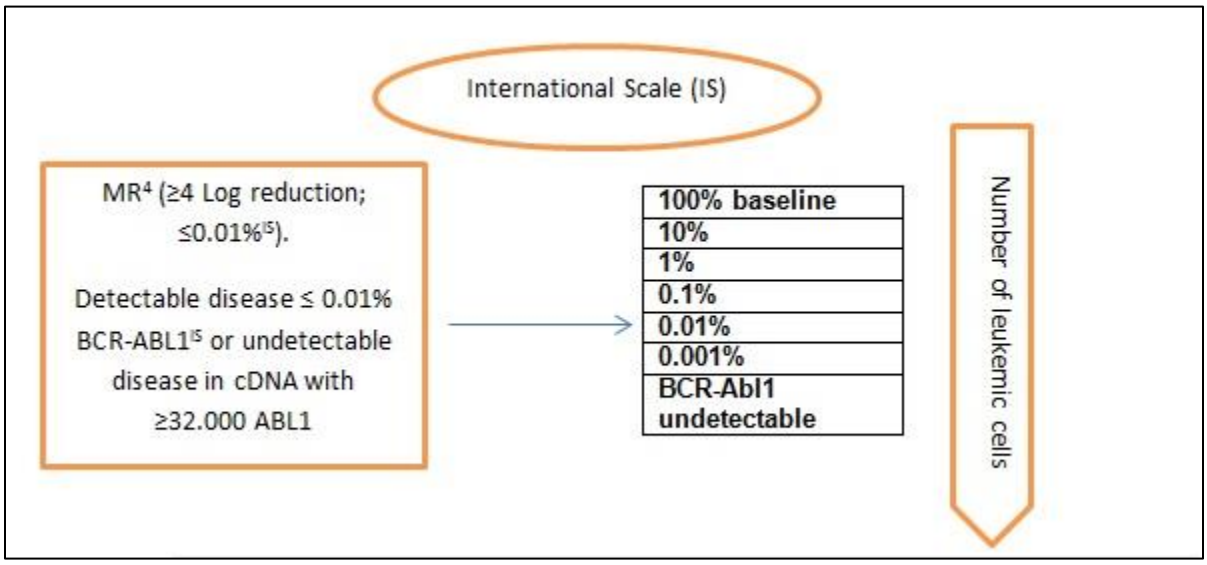

Figure 2. 1 International Scale and corresponding copy numbers of leukemic cells in peripheral blood.
MR, referred to molecular response, while Major Molecular Response (MMR) was defined as 0.1% IS.

2.3 List of Materials

The following table summarized all materials has been utilized in all experiments during Ph.D.

List of Materials		
Product	**Supplier**	**Catalogue no:**
Agarose powder	APS LABS	MAGSPIN-69
Alexa Fluro 488IgG	BD Bioscience	557782
BCR-ABL Mbcr IS-MMR	Qiagen	670823
BCR-ABL1 Mbcr Dx Fusion Quant® Kit	Qiagen	670125
BigDye™ Terminator v3.1 Cycle Sequencing Kit	Thermo Fisher Scientific	4337454
CD3	Thermo Fisher Scientific	14-0037-82
CD14	Thermo Fisher Scientific	14-0149-82

CD19	Thermo Fisher Scientific	MA1-81724
CD34	BD Bioscience	562577
CD38	BD Bioscience	555462
CD45	BD Bioscience	557748
CD293	Thermo Fisher Scientific	11913019
Dimethyl sulfoxide (DMSO)	Sigma	RNBC8297
DNA ladder	Thermo Fisher Scientific	SM0102
DNA Purification Kits	The Maxwell® 16	AS1010
DNase I (Deoxyribonuclease I)	Thermo Fisher Scientific	90083
Ethidium bromide	Sisco Research Laboratories PvT.Ltd (SRL)	27094
Ethidium Bromide (EtBr) Dye	Thermo Fisher Scientific	15585011
EZ DNA Methylation™ Kit	ZYMO RESEARCH	D5003
Fetal Bovin Serum	GIBCO	809533A
High-Capacity cDNA Reverse transcription Kits	Qiagen	4387406
High Sensitivity DNA Kit	Agilent Technologies	5067-4626
Ion Ampliseq library kit 2.0	Thermo Fisher Scientific	4480441
Ion PGM™ Hi-Q™ Sequencing Kit	Thermo Fisher Scientific	A25592
Ion PGM TM OT2 supplies	Thermo Fisher Scientific	179149
Ion Xpress™ Barcode Adapters 1-16 Kit	Thermo Fisher Scientific	4471250
Lysis buffer	Qiagen	79217
Methylation Primers for Promotor and Intron	Bioserve India Pvt.ltd.	IAD 69908
MicroAmp® Optical 96-Well Reaction Plate with Barcode	Thermo Fisher Scientific	4306737
M β- mercaptoethanol	Sigma-Aldrich	M6250-100ML
NucleoSpin® Gel and PCR Clean-up	MACHEREY-NAGEL	740609.50

PTPRG Probe	life technologies	HS00892788
QIAamp RNA blood Mini kit	Qiagen	52304
Qubit™ dsDNA HS Assay Kit	Thermo Fisher Scientific	Q32851
RPMI-1640 w L-glutamine	Thermo Fisher Scientific	11875085
TaqMan™ Universal PCR Master Mix	Thermo Fisher Scientific	4304437
7-AAD (7-Aminoactinomycin D)	Thermo Fisher Scientific	559925
50 X TAE	Thermo Fisher Scientific	B49
316™ Chip Kit v2 BC- 4 pack	Thermo Fisher Scientific	4488145

2.4 Total white blood cell isolation protocol.

Between 5-10mls of peripheral blood samples were collected in EDTA tube at day zero and during patients' follow up visits. Samples were processed within 1-3 hours to maintain high viability for flow cytometry analysis as well as to avoid RNA degradation for q-PCR. Then, 5 volume of erythrocytes Lysis buffer was added to samples and incubated on ice for 10 minutes before the centrifugation at 300g (Heraeurs Megafuge 16.0 r) at 4°C. This step was repeated until a colourless pellet was obtained. Cells were then washed twice with phosphate-buffered saline (PBS) at 200g (Heraeurs Megafuge 16.0- r) for 5 Minutes to eliminate the effect of erythrocytes Lysis buffer. The final cell pellet was dissolved in an appropriate volume of PBS and kept in ice for further analysis.

2.5 Flow cytometry for PTPRG.

Flow cytometry is robust technique that offers rapid quantification of multidimensional characteristics for millions of cells in shorter time. A monoclonal antibody named (TPγ B9-2) has the capacity to detect down-regulation of protein tyrosine phosphatase receptor gamma (PTPRG) expression and re-expression while patients are optimally responsive to treatment. The antibody was adopted from Italian collaborators (Vezzalini et al., 2017).

2.5.1 PTPRG flow cytometry protocol.

The gating and staining strategy for the PTPRG flow cytometry experiment utilized the following antibodies, CD45 antibody to target monocytes and neutrophils populations. Granulocytes were characterized by intermediate CD45 and high side-scattered light (SSC) while the monocyte population has intermediate SSC and a slightly higher CD45 expression. CD38 the antibody was utilized to identify the lymphocyte population.
On the other way, to target PTPRG expression on myeloid lineage for this purpose, we targeted the level of PTPRG against the CD34 antibody and its sub-populations, where [CD34+/CD38-(Dim) targeted Leukemic stem cells] (the "circulating" CML LSCs CD26+ found in the majority of peripheral blood of CML patients). While [CD34+/CD38+ (bright)] targeted hematopoietic stem cell (HSC). Notably, Minor Fluorescent compensation was done due to differences in fluorophores and correct for the spectral overlap.
Briefly, about $2x10^6$ of cells prepared in section 2.3 were transferred into 200µls PBS1x to FACs tubes (two tubes for isotope and PTPRG expression). Then the FAC tubes are placed on ice, followed by adding the necessary volume of CD45, CD34, and CD38, according to the manufactory recommendations. Then the required volume of mouse IgG1-AF 488 and 1µl TPγ B9-2 has added to the isotope and PTPRG tubes accordingly. In addition, another FAC tube about 1µl 7-AAD was added to $1x10^6$ of cells are prepared in section 2.3 to check the viability of cells. The FAC tubes were incubated at dark for 40 minutes, after which the cells are washed twice with cold PBS1x at 200 g for 5 minutes 4°C. The expression of PTPRG was recorded by the flow cytometry machine (BD LSR Fortessa™ cell analyser available at Interim Translational Research Institute (iTRI-HMC). Events number of 500.000 to 1.000.000 was targeted at acquisition records. The gating strategy of the flow cytometry experiment aimed at monitoring PTPRG expression in the major populations represented by neutrophils, monocytes, and lymphocytes at diagnosis and during the follow up phase of TKIs treatment (Figure 2. 2).

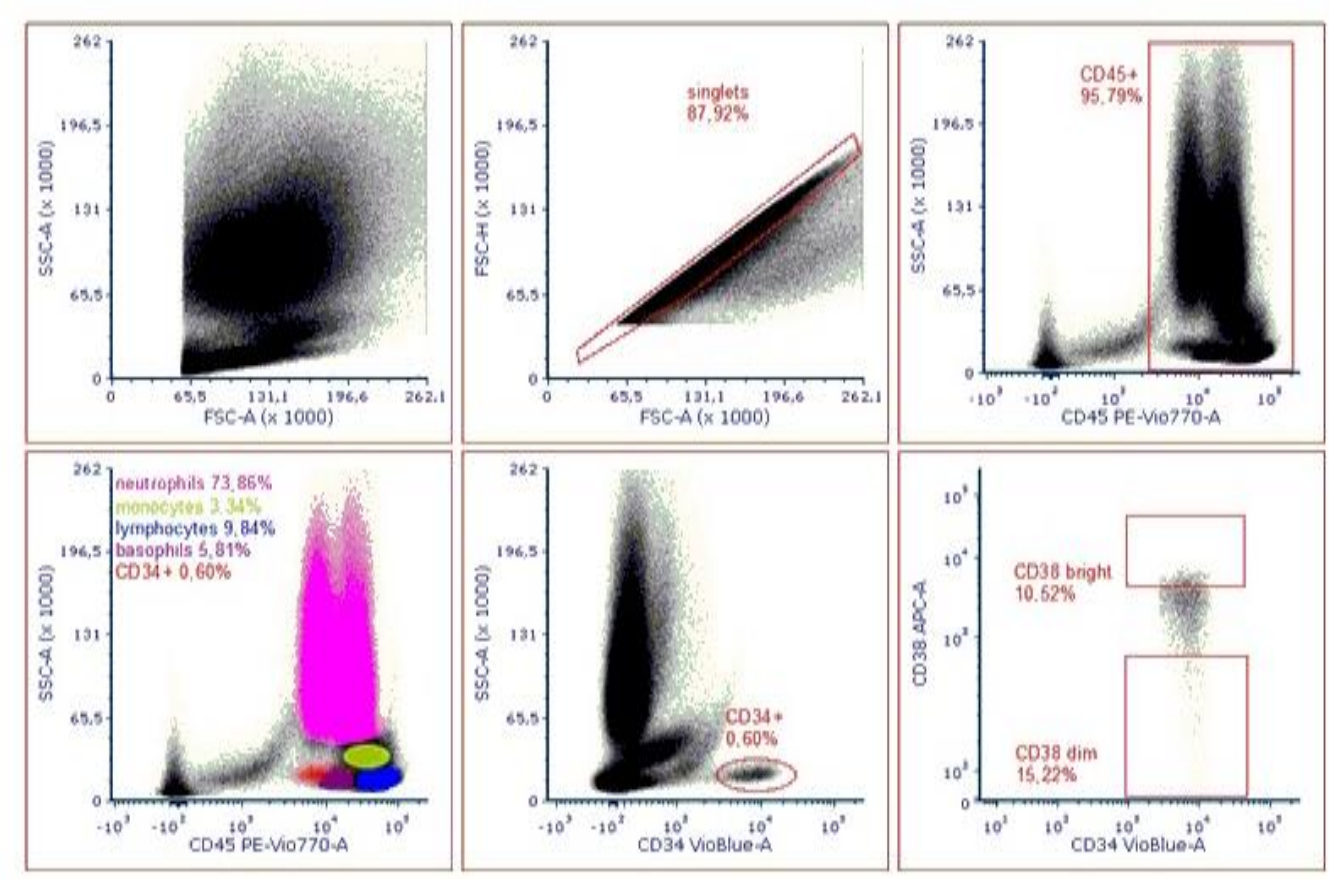

Figure 2. 2 Gating strategies of flow cytometric analysis of PTPRG protein and its expression during the treatment plan.

Gating strategies of PTPRG expression on the sub-population of white blood cells. Neutrophils have an intermediate level of CD45 expression and a high side-scattered light (SSC); Monocytes have a slightly higher level of CD45 expression and intermediate SSC while lymphocytes have the highest level of expression of CD45 but the lowest level of SSC. Gating strategy to identify leukemic CD34+CD38−stem cells. For myeloid progenitors and its sub-population, we targeted 15-20% upper and lower population of CD34 (red colour) with CD38, where the upper population was the target of interest of hematopoietic stem cells. In comparison the lower population was the target of part of the leukemic stem cell.

2.5.2 PTPRG flow cytometry analysis

The analysis was performed using FCS Express 4 plus Research Edition (De Novo Software), where the expression of PTPRG measuring in CD34, CD45, CD38 against isotope, and results in value reported in Mean fluorescence intensity (MFI). MFI was checked for the gates mentioned above at diagnosis and followed to check the expression change values. Moreover, the lymphocytes population was the negative control compared to other population monocytes and neutrophils. There was no

restriction or limitation to do flow cytometry technique as this stage aimed to have a picture of PTPRG expression at diagnosis and during follow-ups.

2.6 Molecular Monitoring of *PTPRG and BCR-ABL1*

As the main transforming property of CML is the BCR-ABL1 protein, so monitoring BCR-ABL1 is the main tool of disease progression and treatment response. In addition, currently, lacking flow cytometry test of *BCR-ABL1*, make real-time quantitative (RQ-PCR) of the fusion transcript is the golden tool of CML monitoring. RQ-PCR is a reliable, high-throughput method to assess mRNA levels accurately using specific probes to quantitate specific nucleic acid sequences. The analyser monitors an increase in fluorescence during the PCR cycle, which is proportional to the amount of accumulated product

2.6.1 RNA Purification Protocol

RNA purification was performed using the QIAamp RNA Blood Mini Kit according to the manufacturer's instruction. About $1x10^7$ of isolated cells, as mentioned in (Section 2.4), were added to 1.5ml Eppendorf tubes and then mixed with 600µl of a mixture of β-mercaptoethanol (β –ME) with RLT buffer (contains guanidine thiocyanate) to inactive RNases. The lysate was stored overnight at -20°C. Then 750µl of lysate was transferred to QIAshredder, ion-exchange chromatography spin-column, to homogenize the RNA. After centrifugation for 2 mins at the maximum speed (Sigma 1-14), 600µl of 70% ethanol was added to the homogenized lysate to capture the RNA followed by centrifugation for 15 seconds at (10.000 rpm) [using QIAamp spin column (Sigma 1-14)]. QIAamp spin column was then washed up with 700µl of RW1 buffer (guanidine Thiocyanate with ethanol) to eliminate and minimize contamination of DNA and then centrifuged for a further 15 seconds at (10.000 rpm) (Sigma 1-14). About 500 µl of RPE buffer (the composition of Buffer RPE is not available online) was added to the QIAamp spin column then centrifuged for 15 seconds at (10.000 rpm). This step was repeated once more to eliminate the RPE buffer carryover. Finally, RNA was released from the QIAamp spin column by adding 40µl of RNase free water (elution buffer) and

centrifugation at 10.000 rpm for 1 minute (Sigma 1-14). RNA was stored at -80°C for further processing.

2.6.2 Quantification and Purity of Total RNA

The purpose of this protocol was to measure RNA concentration in 1 microliter of sample volume by Nanodrop spectrophotometer_2000. Optical path formation was the concept of measurement resulting from placing the sample directly on the top of the detection surface and via the surface tension to generate a column between the ends of optical fibres. The measurement resulted from the output of wavelength vs. absorbance at 260 nm and 280 nm (260/280), where a ratio of 1.8 was accepted as “pure” RNA. A low ratio may be caused due to a low concentration of RNA or residual reagent with the extraction protocols, while a high ratio has no significance. RNA reading was reported in ng/µL. There were some features to be considered prior to the run, such as a blank test run done by the same elution used during the extraction of RNA, and a Kim wipe was used to clean the sensor after each run.

2.6.3 Complementary DNA (cDNA) Synthesis

cDNA synthesis was performed using the Applied Biosystems High-Capacity cDNA Reverse transcription Kits. All necessary components of the kit were thawed and then centrifuged for 10 seconds at 10.000rpm (Sigma 1-14). The concentration of RNA samples was adjusted to 1µg with nuclease-free water. Then the RNA was linearized by incubation at 65°C for 5 minutes and transferred immediately on ice for 5 minutes to prevent RNA degradation. After this, 10µl of 2 X RT master mixtures was prepared according to the manufacturer method kit, transferred into the individual tube, and mixed gently with 10µl of RNA sample. The tubes were centrifuged (10s at 10,000rpm) to settle down cDNA at the bottom of tubes and eliminate any air bubbles. The tubes were then placed in a thermal cycler, and the reverse transcription program run. cDNA aliquots were stored at -20°C for the subsequent *PTPRG* and *BCR-ABL1* quantifications.

2.6.4 Quantitative Real-Time PCR for *PTPRG*

In-house PTPRG plasmid preparation was carried out to build standards. A stock of PTPRG plasmid with a concentration = 4,5e106/µl was adopted from the Italian collaborators where 'e' refers to PTPRG-Pcr3.1 (cDNA was cloned in EcoR1 site of PCR3.1 plasmid). Stock solution of $2.0e10^6$/ul was serially diluted in order to prepare the following dilutions:

100ul 2.0^e10^5/ul PTPRG Standard A

100ul 2.0^e10^4/ul PTPRG Standard B

100ul 2.0^e10^3/ul PTPRG Standard C

100ul 2.0^e10^2/ul PTPRG Standard D

2.6.4.1 PTPRG Absolute Quantification

For *PTPRG* and *ABL1* detection, labelled probes FAM-MGB and FAM-TAMRA were employed, respectively. The *PTPRG* and *ABL1* standards run independently and in duplicate, leaving the place for nine (9) patients and non-template control (NTC) to be also run in duplicate in the 96 wells (Figure 2. 3), *PTPRG* along with ABL1 run in the same track at the same RT-qPCR. The Master Mix for PTRPG and ABL1 were prepared, as shown in (Table 2. 4).

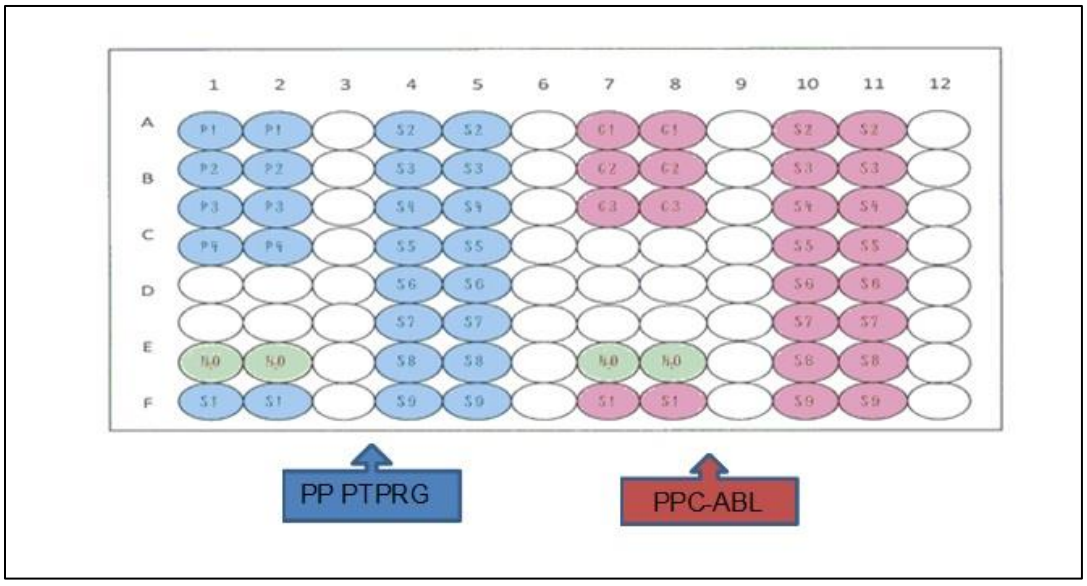

Figure 2. 3 Suggested Plate setup for PTPRG experiment.
P1 to P4 known concentration plasmids of PTPRG while C1 to C3 Control gene standards, H_2O: water control. Negative control and blanks were included in the run as part of controls.

The resulting cDNA prepared in (Section 2.6.3) was divided into two separate tubes in duplicate. The proposed amount of Master Mix was added, tube 1 for *PTPRG* detection and tube 2 for housekeeping gene ABL1 detection (Table 2.4). The wells were sealed and transferred to The QuantStudio™ 12K Flex instrument, and the Quantification program was set in place. The quantification program had three steps, firstly denaturation and enzyme activation; secondly, Amplitaq Gold activation and finally amplification as summarized in (Table 2. 5).

Table 2. 4 Master Mix Preparation.

*Master Mix was *prepared n+1, where n is the number of RNA samples.*

PTPRG Master Mix		Per Sample
1	TagMan® Gene Expression Assay, SM PTPRG 20X	1.25µl
2	TagMan® Universal Master Mix II, with UNG 2X	12.5µl
3	H2O	6.25µl
Total		20µl

ABL1 Master Mix		Per Sample
1	Primers and probe mix, 25X	1.0µl
2	TagMan® Universal Master Mix II, with UNG 2X	12.5µl
3	H2O	6.5µl
Total		20µl

Table 2. 5 Absolute Quantification program the amplification.

Step is the core step of the absolute quantification program, which has two (2) segments at 95°C and 60°C intervals and repeated 50 times.

Absolute Quantification Protocol				
Step	Segment	Temperature	Time	Cycle
Step 1 Pre-PCR		50° C	2 Minutes	1
Step 2 Enzyme deactivation	Denaturation	95° C	10 Minutes	1
Step 3 PCR amplification and quantification	Denaturation	95° C	15 Seconds	50
	Annealing and fluorescence emission	60° C	1 Minute	
Cooling		4° C	60 Seconds	1

2.6.4.2 Standard Curves (SCs) and calculation of PTPRG

Four sequential dilutions of PTPRG plasmid were carried out to create the *PTPRG* standard curve (SC) ($2x10^2$, $2x10^3$, and $2x10^4$), and three sequential dilutions for *ABL1* SC (Ipsogen $1x10^1$, $1x0^2$ and $1x10^3$). The intercept values for both *PTPRG* and *ABL1* were similar, and the slopes were between -3.20 and -3.60. A manual threshold was performed to define the cycle threshold (Ct), which was customarily set in the log-linear phase against the amplification curve and persisted constant overtime at 0.02. The concept to calculate the absolute quantity of *PTPRG* was to transform raw CT values obtained with PPC- *PTPRG* and *ABL1,* respectively, for the unknown samples into Copy Numbers (CN). The Ratio of these CN values gives the Normalized Copy Number (NCN). To calculate its absolute quantity, *PTPRG* transcripts were calculated as a ratio between *PTPRG* and the concentration of the housekeeping *ABL1* multiplied by 100, as shown in the equation below:

$$\text{NCN (sample)} = \frac{\text{PTPRG}}{\text{ABLCN}} * 100$$

2.6.5 Quantitative Real-Time PCR for *BCR-ABL1*

The absolute *BCR-ABL1* was initially reported against ABL. Later, the technique upgraded to report absolute BCR-ABL in the International Scale (IS).

2.6.5.1 BCR-ABL1 Mbcr Dx Fusion Quant® Kit (Simplex Absolute Quantification)

The kit was designed according to Europe Against Cancer (EAC) studies (Gabert et al., 2003) and updated internationally accordingly (Branford S et al., 2006). The kit concept uses qPCR double-dye oligonucleotide hydrolysis principle, where (FAM-TAMRA) dual-labelled probe was carried out for *BCR-ABL1* and ABL1 detection. The *BCR-ABL1* was quantified using material from (Section 2.6.3). For *BCR-ABL1* and *ABL1* detections, the labelled probe FAM-TAMRA was used. The *BCR-ABL1* and *ABL1* standards were run independently and in duplicate, leaving the place for nine (9) patients, Non-template

control (NTC) in duplicate in the 96 wells (Figure 2. 4), and the *BCR-ABL1* and ABL1 were done at the same time of qPCR run.

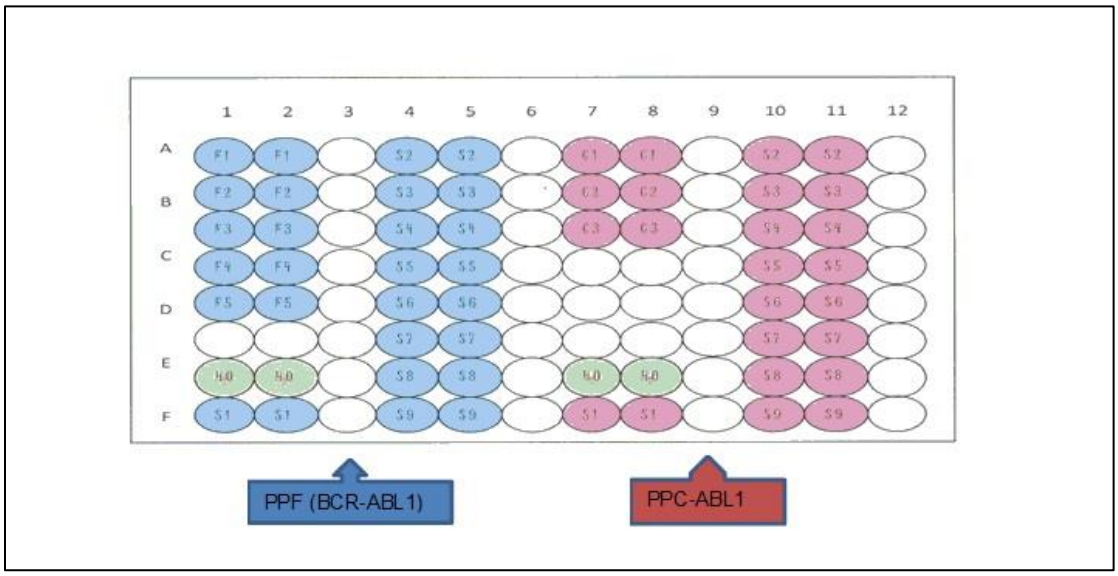

Figure 2. 4 Suggested Plate setup for *BCR-ABL1* experiment.
F1 to F5: fusion gene standards while C1 to C3 Control gene standards, H2O: water control. Negative control and blanks were included in the run as part of controls.

Master Mix for *BCR-ABL1* and *ABL1* were prepared according to manufacturer's guidelines, and the wells were sealed and transferred to the QuantStudio™ 12K Flex system. The quantification program carried out, as described previously.

2.6.5.1.1 Standard Curves (SCs) and calculation of BCR-ABL1

The same concept of calculation was adopted, as explained in the calculation of absolute PTPRG and the following equation to report the result BCR-ABL /ABL.

$$NCN(Sample) = \frac{BCR - ABL\ 1\ M\ bcr\ CN}{ABL\ CN} * 100$$

2.6.5.2 BCR-ABL Mbcr IS-MMR.

Different real-time technologies, assay designs, or instrument platforms lead to un-harmonized results across other laboratories, which affect directly or indirectly on patients' progression. These reasons highlight the need for harmonization of

quantification reports of BCR-ABL1 across the world. In October 2005, the National Institutes of Health (NIH) in Bethesda proposed to implement the preliminary guidelines for the establishment of an international scale (IS) (Branford et al., 2006). (IS) standards that were available as a Reference Panel for quantitation of BCR-ABL1 in 2010 (White et al., 2010). The kit was designed, as mentioned in section 2.6.5.1. However, the only difference was that high cDNA positive control, as well as IS-MMR calibrator, was added to suggest plate setup, which validates the results reading with IS (Figure 2. 5).

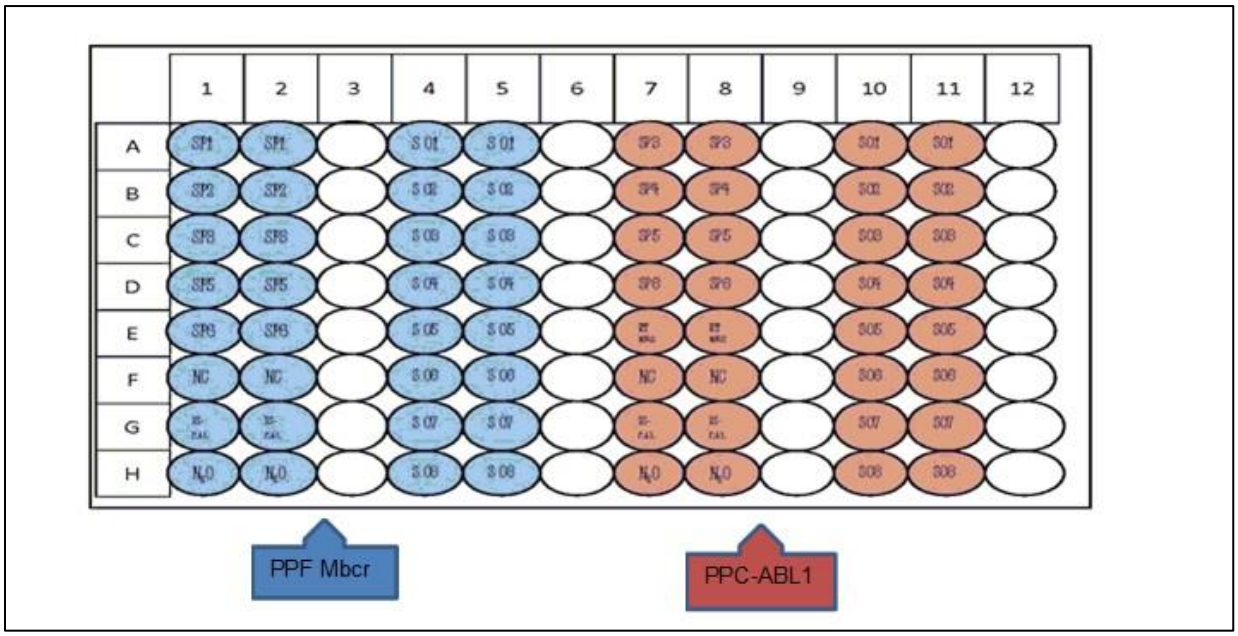

Figure 2. 5 Suggested Plate setup for *BCR-ABL1*^{IS} experiment.
SP1-SP6: BCR-ABL Mbcr and ABL standards; HC: High cDNA positive Control; IS-Cal: IS-MMR calibrator; RT negative control; S: cDNA; H2O: water control.

The resulting RNA prepared in (Section 2.6.2) was thawed and used for preparing cDNA using SuperScript Ⅲ Reverse transcriptase using the kit protocol (Cat No. 670823). The cDNA was then mixed with Master Mix qPCR reagent. The wells were sealed and transferred to the QuantStudio™ 12K Flex system. The quantification program was carried out as described previously.

2.6.5.2.1 Standard Curves (SCs) Molecular Analysis of BCR-ABL1 by International scale (IS).

Five sequential dilutions of *BCR-ABL1* plasmid were carried out to create the *BCR-ABL1* SC (Ipsogen $1x10^1$,$1x10^2$,$1x10^3$,$1x10^4$ and $1x10^5$), and four consecutive dilutions for ABL1 SC (Ipsogen $1x10^3$,$1x10^4$,$1x10^5$ and $1x10^6$), both SC run in duplicate along

with high RNA positive control and IS-MMR calibrator. The intercept values for both *BCR-ABL1* and *ABL1* were analogous, and the slopes were between -3.0 and -3.9.
The normalized copy number (NCN) results in High positive RNA control (NCNHC) and IS-MMR calibrator (NCNcal), which were calculated along with each sample (NCNsample). The following equation was applied, which reports the result in IS.

$$\text{IS-NCNsample} = \frac{\text{NCNsample x IS-Cal value*}}{\text{NCNcal}}$$

*Value supported by company on calibrator label

2.7 PTPRG mutation by Ion torrent (NGS)

The first proposed mechanism to investigate the reason of *PTPRG* down regulation is mutation. The mutation mechanism may affect the structure of gene and occurs in DNA sequence of *PTPRG* and consequences affect function. Ion Torrent PGM is a reliable and cost-effective tool when compared to other platforms (I.e. Illumina).

2.7.1 DNA extraction and purification

DNA purification was done via transferred 400mls of EDTA blood to The Maxwell® 16 DNA Purification Kits. The Maxwell® 16 Instrument is supplied with pre-programmed purification procedures designed to carry out predisposed reagent cartridges and processes within 30-40 minutes.

2.7.2 NanoDrop, Qubit, and gel electrophoresis results.

The concept was the same for Nanodrop results, as mentioned in section 2.6.2. On the other hand, Qubit's vision was to evaluate DNA quantitation accurately where Fluorometer v2.0 (Invitrogen, U.K) and Qubit™ dsDNA HS Assay Kit were utilized for this purpose. The kit was very selective for double-stranded DNA (dsDNA). The primary sample with concentrations between 0.1ng/µl and 100 ng/ µl was accepted. The DNA sample was intact by the gel method, or otherwise, much deviation would be recorded between readings of Nanodrop and Qubit. Firstly, the components of the kit were in

Room Temperature (RT), and the working station was in the dark to secure the optimal performance. Secondly, 198 µL of a buffer solution with 1 µL of QubitTM ds DNA HS reagent (reaction dye) was added to 1µl of the target sample in 0.5mL PCR tubes. The sample was mixed by vortex 2–3 seconds and incubated in the dark for 2 minutes. The sample was loaded to Qubit® 2.0 Fluorometer, and the cursor arrow was pressed to select the sample volume added to the assay tube (1µl), the dropdown menu sets the units for the output sample concentration, and then the Read tube was pressed. Quality assurance was applied, as described in (Table 2. 6.2). Finally, the DNA Yield (µg) was calculated as DNA Concentration × Total Sample Volume (ml).

Table 2. 6 Quality of DNA.
DNA quality was identified as optimal if the reading of Nanodrop was >1.5, while suitable if reading between >1 and <1.5 and low quality if the task is < 1.

QC Purity	Optimal: 260/230 and 260/280 >1.5
	Suitable: 260/230 and / or 260/280 >1 and <1.5
	Low: 260/230 and 260/280 < 1

If samples passed QC for Nanodrop and Qubit, they were preceded for gel electrophoresis to check DNA intensity. The purpose was to evaluate DNA according to size fragments, or in other words separating DNA fragments according to their size due to the enzyme's digestion effect. The casting of 0.8 % Agarose gel was done: Firstly, 1X TAE buffer (tris base, acetic acid, and EDTA) was prepared by adding 20 ml of 50 X TAE to 980 ml distilled water with the cap firmly, shaken well, and stored at RT. Secondly, a solution of Ethidium bromide was prepared by adding 5 mg of Ethidium bromide to 1 ml of milli Q water, mixed well, and stored at 4°C. Finally, the gel casting tray was sealed from both ends with cellophane tape. The casting of 0.8 % Agarose gel was started by adding 0.8 g of agarose powder to 100 ml of 1X TAE buffer in a conical flask. It was heated in the oven for 3- 5 minutes, which was sufficient to melt all agarose particles. The agarose solution was cooled down to about 45 °C (should be able to hold the flask), then 2-3µls of Ethidium bromide solution was added and mixed well. The molten agarose was poured into the sealed casting, and the combs were inserted. Forty-five minutes could solidify the gel before carrying out the run. Running the gel was

prompted by removing the comb carefully to avoid the wells from damaging. Cellophane tape was later removed from both ends, and the gel was placed into the negative end of the gel tank (The MUPID-exU). An adequate amount of 1X TAE buffer was placed into the gel tank until the gel was covered.

A piece of Parafilm was spotted on the upper portion of the gel tank, and 2-3µls of DNA samples (~50-100ng) were mixed with 1-2µl of loading dye (EtBr) starting from the second upper left well of the tank while 1µl of standard DNA ladder (Figure 2. 6) loaded to the first well. The power pack was connected to the electrodes after the buffer tank was covered and run was on-going at 120-V for approximately 45- 60 minutes or till the samples reached ¾ gel. Gel documentation was done by transferring the gel to Geneflash Gel DOC to visualize the bands, the gel placed on the glass surface, and the transilluminator and camera were switched on, the clear image recorded and saved. Quality Control (QC) was done by comparing bands of DNA samples intensity with standard ladder, samples which showed a single band and were considered as QC passed (DNA intact). In contrast, samples with multiples or streaky bands were reported as QC failed.

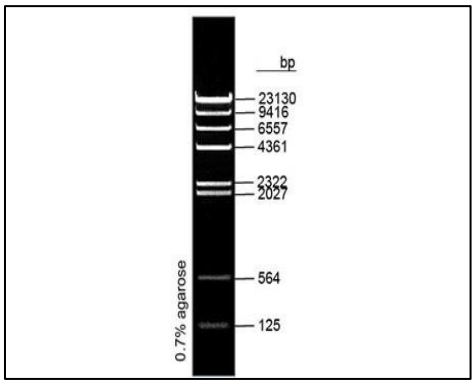

Figure 2. 6 Lambda DNA HindIII.
Lambda DNA HindIII consists of 8 purified individual DNA fragments (in base pairs): 23130, 9416, 6557, 4361*, 2322, 2027, 564 and 125.*

2.7.3 Amplicon Primer design

In our methodology, the Ion Ampliseq primer design tool was employed to identify primers for the full exonic regions of the *PTPRG* gene utilizing custom Ion Ampliseq Designer v4.0 (ampliseq.com) The following 33 Primer Pairs were received in 2 pools (Table 2. 7) and covered almost 94% of all targeted exonic regions of the *PTPRG*

Genes with five (5) bp Intron-Exon Padding to detect splice mutations (total base pair was 4638 while covered base 4362).

Amplicon ID	Ion Ampliseq (Forward Primer*)	Ion Ampliseq (Reverse Primer*)	Amplicon starts	Insert Start	Insert Stop	Amplicon Stop
AMPL7155182860	AGTATGCAGGGAGTGATCCCAA	TACGACTATTCACAGGAGCAGGAA	62189520	62189542	62189651	62189675
AMPL7155225306	GGGACATGTTGAGAGATGCAGT	CTATTTAAGGAGCAAGTCATGGTTAAGGA	61975199	61975221	61975544	61975573
AMPL7155225339	GCTCTATTTAGTTGTTCTGCCAAAAGTT	GAAGACCAGTCAATAATTCAAATGCCTTC	62252940	62252968	62253285	62253314
AMPL7155225393	CCTGTGTCTTAAAAGGTTCTTTGTGG	GGACATTTTCAAAACCTTCTACCATACG	62261410	62261436	62261756	62261784
AMPL7155225414	GGGTTTAGATTGGAATTTTTCGAATCCA	GCCCTAAAAGAATGAATCTGTCTCTTCATT	62258538	62258566	62258824	62258854
AMPL7155225418	GCAGTTAAACTCACGTATTCCTTTTTCA	CAAGTTGGTTATGAGATTTGGCCTT	62254569	62254597	62254914	62254939
AMPL7155225438	CATTTATGCTATTGCTGTTTCTCTAGTGTG	GGTTATTGTATAACCTAGAGTCTGGCAA	62278713	62278743	62279048	62279076
AMPL7155225451	GATATAAACAAACATAAGGCTTGCGATGT	ACAAATTCCTTAGTGGTATACTCTAGCCA	62142620	62142649	62142964	62142993
AMPL7155225455	AGTTAGCAAAGGAAAAATATGAACAGGTGA	GAAATATCTTTCATTTGGACAGGTGTGAAC	62063690	62063720	62064029	62064059
AMPL7155225471	CGCACGGAGGCAAGAACTTATT	CGGAGCAATCCTTTTCTCCTATCC	61547891	61547913	61548176	61548200
AMPL7155225508	TGCATAAGCATCCTCT	TCAGGTAAAGCAGGTG	62216742	62216770	62217092	62217116

	TTTGAAAATGTC	AGTTTCAG				
AMPL7155225514	GCTCTCCGCATGTTTTTGTAGG	TTTTTCTCTACTATAACCGCTTTACACTGA	62186987	62187009	62187328	62187358
AMPL7155225520	ACAACATTGTTGAGAGTTACCTATAACACA	ACAAGCTGAGGTTGTTGATAGGTTTTA	62268285	62268315	62268631	62268658
AMPL7155225525	CTGCCTCTTCAGCCGACAT	CGCTTTTCTCATCCTTCTCTCCTTC	62188860	62188879	62189203	62189228
AMPL7155225528	GACTTTTCTTCAGGACATCTATTTTGTGTG	TGAAAAGAAAAACTCCACTTTCCGTAGT	62240647	62240677	62240993	62241021
AMPL7155225537	ACAATGTTAAGAGGACCCAGGAGAA	CTCTGCAGCATGTACCCTGAAT	62176998	62177023	62177346	62177368
AMPL7155225540	CCAAATGTACCGAATGCCTTTCTC	CCCTCCCTAGCATATATGGATACTATAGC	62263087	62263111	62263432	62263461
AMPL7155204402	TGGTGATTCGTCACCAACCAAG	TCCTTCTTTTCGGAGTCCTTCTCT	62189164	62189186	62189265	62189289
AMPL7155225318	CTTATGAATTCAGTTTAAACGATGGCTTGA	CCTGGCTTGAGGGTGGTAAATT	62267115	62267145	62267457	62267479
AMPL7155225325	GTGAATGTGATCAGTGGTCATGTG	CAGCTTCTAAGTGAAAGCAGTAGCA	62256956	62256980	62257305	62257330
AMPL7155225346	TTAGAAAGGGAAGCCAGGAGGATA	ACCAGCACTGATTAGGTATCTTTTGTTAAA	62262533	62262557	62262869	62262899
AMPL7155225350	TGTACAGAGCTTTCACTAAAAACAAAGC	AGAGAACACTTTTCATTTCCGTAACTCTTT	62253246	62253274	62253588	62253618

AMPL7155225407	TAAGTTGGTTCTAGTCAGTCATCCTCA	ACTTTTAGTGAACTACGAAAGATTTGAGCA	61734421	61734448	61734757	61734787
AMPL7155225411	CCGAAGTTGGGATTGAGAAGGT	GCTAATGAGAGGTTAGCTTGCAAGAA	62248344	62248366	62248676	62248702
AMPL7155225423	CATTTGGTGAGAGCCATGGTGTA	CATCATATAATGGCTCTAATGCCCTTCA	62118129	62118152	62118461	62118489
AMPL7155225434	GAGTTTACCCTCAGTGCTGTGT	AAGAGAATTTCTTATACTGGGCAAGCTT	62229358	62229380	62229671	62229699
AMPL7155225460	CACCTGCTTTGGACCAAATAGC	CAATTCCTGGCTGGCTTTGAAT	62153554	62153576	62153905	62153927
AMPL7155225475	AATCACTGGGAGGTCCCTGTTA	TCCATTTCGGTGTATACATTAATGCAAAGA	62259263	62259285	62259594	62259624
AMPL7155225503	GTTCGCCAGAAACCACACAAAA	CTACCTCACCTTCCTGAATGCA	62204423	62204445	62204741	62204763
AMPL7155225506	CCCACCAGCATTTCATTCAGTC	CCCAATTGAGAACTACTGCTCTAAACT	62277948	62277970	62278288	62278315
AMPL7155225524	TTTTTGGCACCTAGCCTCATCT	AGAGGACGTCCAGGTAGAAGAC	62188557	62188579	62188896	62188918
AMPL7155225535	GCGGTCTTTCCTTCCAAAGTGA	TGATTCTTCTGCCAGGCTTGTT	62180587	62180609	62180939	62180961
AMPL7155225549	ACAGAAAAACTCCATTTGGTTTTGAAACT	ACAGCATCTGATTAACATAAAGACCGA	61988957	61988986	61989208	61989235

Table 2. 7 PTPRG primers (forward and reverse)

Primers in two pools (the first pool contained 17 amplicons while the second pool contained 16 amplicons).

2.7.4 PTPRG Ion Ampliseq library Preparation and amplification reactions.

Ion Ampliseq library kit 2.0 was utilized for the rapid preparation of Ion Ampliseq Library using the designed Ampliseq primer pools from 300-30,000 copies of DNA (1-100ng) or cDNA. The kit contained all the reagents except the Ion barcodes and Agincourt magnetic beads for library purifications. As per the kit instructions, a mixture of 10uL of each standard and 2 ul of DNA sample combined with the Qubit® working solution by diluting the Qubit® dsDNA BR Reagent 1:200 in Qubit® dsDNA BR Buffer respectively. The samples were mixed and incubated at room temperature for 2 minutes and measured on the Qubit® 2.0 Fluorometer. Based on the Fluorometer DNA concentration readings, DNA samples were diluted to the final Ion Ampliseq Library with the working concentration of 10ng/ul for each Primer pool.

$$\frac{\text{Qubit reading (ng/ml)}}{10} - 1 = \text{1X TE Buffer (Recommended volume)} + \text{1 ul DNA (sample) 10 ng/ul}$$

Later, Ampliseq PCR mix preparation required PCR enzymes to be thawed on ice while all other components such as primer pool and nuclease-free water had to be thawed at room temperature. All the PCR master mix preparations were carried under the PCR hood for contamination-free of the amplicon. Briefly, Master mix was centrifuged, and only 9.0 ul was added into each well or each PCR tube, and finally, 1.0µl of DNA separately was added for each sample (Table 2.8). The plate of PCR tubes was sealed or capped and loaded on the Thermal Cycler to run the below PCR program as per the manufacture's protocol (Table 2.9) The resulting target amplification reactions of the two pools were combined to a total volume of 20µl and preceded to the partially digest amplicon step.

Table 2.8 Master Mix preparations.
Target amplification reactions of 2 primer pools were prepared for amplification purposes and added finally into each PCR tube or well on the PCR plate.

Reaction Components for each Primer Pool	Volume
5X Ion Ampliseq™ HiFi Mix (red cap)	2 µL
2X primer pool	5 µL
Nuclease-free Water (NFW)	2 µL
p10 ng/ul DNA (sample)*	1 µL
Total volume	10 µL

Table 2.9 PCR program of DNA amplification.
*Starts with activation followed by denaturation, ends with annealing, and extend. * No of Cycles to be modified according to the number of primer pairs per pool.*

Stage	Step	Temperature	Time	Cycles
Hold	Activate the enzyme	99°C	2 minutes	22 cycles
Cycling	Denature	99°C	15 seconds	
	Anneal and extend	60°C	4 minutes*	
Hold	-	10°C	∞	Hold

2.7.5 Partially digest amplicons, Adapters Ligation to the amplicons and perform the ligation reaction.

About 2.0µl of thawed FuPa reagent (brown cap) on ice was added slowly to the 20µl amplified samples, pipetted up and down to mix well. The tubes were sealed and loaded on to the thermal cycler, and the partially digested amplicons program was run as the following (Table 2. 10).

Table 2. 10 The thermal temperature of partially digested amplicons program.

Temperature	Times
50°C	10 minutes
55°C	10 minutes
60°C	20 minutes
10°C	Hold (for up to 1 hour)

As a result of sequencing multiple libraries on a single chip, a different Ion barcode adapter to each library was required to identify each sample in the final data. For each barcode X selected, a mix of Ion P1 Adapter and Ion Xpress™ barcode X at a final dilution of 1:4 for each adapter was prepared as per the below (Table 2. 11). The resulting product was ready for the adaptor's ligation step.

Table 2. 11 Adapter preparation set up.

Component	Volume
Ion P1 Adapter	1µL
Nuclease-free Water	2µL
Total	3µL*

** referred to a single sample.*

Subsequently, 1µL of distinct Ion Xpress™ Barcode X (1-16) was added to each amplified sample, and then 2µL of this mixture was utilized for the ligation set up a process that was performed as per the Ligation setup protocol; Ligation reaction mixes with the barcodes vortex gently, spun briefly and immediately loaded on to thermal cycler and ligation program was set up as per the following (Table 2. 12).

Table 2. 12 Ligation set up protocol.
Along with the thermal temperature of the ligation program.

Component	Volume
Switch Solution (yellow cap)	4µL
Diluted Ion Xpress™ barcode adapter mix	2µL
DNA Ligase (blue cap)	2µL
Total volume (including ~22 µL of digested amplicon)	30µL

Temperature	Times
22°C	40 minutes
68°C	5 minutes
72°C	5 minutes
10°C	Hold

2.7.6 Library Purification

The ligation clean-up process was done by adding SPRI magnetic beads to remove the free adapters. After the Ligation reaction, the centrifuged samples briefly collect the contents at the bottom of the wells. Agencourt™ AMPure™ XP Reagent was adjusted to room temperature and vortex to disperse the beads before use. Carefully, the seal

was removed, and 45 µL of AMPure™ XP Reagent (Beckman Coulter, USA) to each well was added to the resulting product of ligation reaction. The reaction mix was pipetted up and down five (5) times to mix the bead suspension thoroughly. The plates incubated for 5 minutes at room temperature were then transferred on to a Magnetic rack - DynaMag™-96 Side Magnet (Ambion, USA) and incubated for 2 minutes until the solution became clear, while the plate on the magnetic rack, the supernatant was carefully pipetted and discarded without disturbing the pellet. The pellet was washed two times with 150µl of 70% freshly prepared ethanol (prepared in Nuclease Free water). All ethanol droplets were removed from the wells; the plate was kept in the magnet, and beads were air-dried at room temperature for 5 minutes. The plates were removed with purified libraries from the plate magnet, and then 50µl of Platinum™ PCR SuperMix HiFi and 2µl of Library Amplification Primer Mix was added to each bead pellet. The plate sealed vortexes were centrifuged briefly. The plate was placed back on the magnet for at least 2 minutes, then carefully ~50µl of supernatant were transferred from each well to a new well or a new plate without disturbing the pellet. The pellet eluted in 52µl PCR mix [50µl of Platinum™ PCR SuperMix HiFi and 2µl of Library Amplification Primer Mix (white cap)] was thoroughly vortexed and briefly centrifuged to collect droplets. The plate was sealed, and the PCR enrichment program run on a thermal cycler as per the following (Table 2. 13). At this stage, the library was ready for emulsion PCR and enrichment.

Table 2. 13 PCR enrichment program

Stage	Temperature	Time	Cycles
Hold	98°C	2 minutes	
Cycling	98°C	15 seconds	6 cycles
	64°C	1minutes	
Hold	10°C*	∞	Hold

** Stopping point where samples can be stored at –20°C.*

2.7.7 The amplified library purification and Library QC.

A two-round purification process was performed with the Agencourt™ AMPure™ XP Reagent. First-round at 0.5X bead-to-sample-volume ratio: High molecular weight DNA was bound to beads, while amplicons and primers remained in solution, the supernatant was saved. The second round at 1.2X bead-to-original-sample-volume ratio: Amplicons were bound to beads, and primers remained in solution. The bead pellet was saved, and the amplicons were eluted then, followed by centrifugation of the plate to collect the contents at the bottom of the wells, and then seal was removed. About 25µl (0.5X sample volume) of Agencourt™ AMPure™ XP Reagent was added to each plate well containing ~50µl of the sample, which was pipetted up and down five (5) times to mix the bead suspension with the DNA thoroughly.

The mixture was incubated for 5 minutes at room temperature and placed in a magnet such as the DynaMag™ Side Magnet for at least 5 minutes or until the solution is clear. Carefully the supernatant was removed from each well to a new well of the 96 well PCR plate without disturbing the pellet. Second round purification was done by adding 60µls (1.2X original sample volume) of Agencourt™ AMPure™ XP reagent to the supernatant from the above step, pipetted up and down five (5) times to mix the bead suspension with the DNA thoroughly and the mixture was incubated for 5 minutes at room temperature. The plate was then placed in the magnet for 3 minutes or until the solution cleared. Carefully removed, the supernatant was discarded without disturbing the pellet. The pellet was washed two times with 150µl of 70% freshly prepared ethanol to each well by moving the plate side to side on the 96 well plate magnets. The supernatant was removed and discarded without disturbing the pellet. Likewise, the second wash with 70% ethanol was performed, and the pellet was allowed to air dry for 5 mins at room temperature. The plate was then removed from the magnet and dispersed by adding 50µl of Low TE and mixed well. Briefly centrifuged, incubated for 2 minutes at room temperature, and finally placed on the PCR plate magnet for another 2 minutes to recover the purified Amplified library. At this point, Amplified library was ready for Quality checks its concentration and size determination.

The library quantification was performed using the Qubit TM 2.0 and library size determination using the Bioanalyzer - Agilent 2200 Tape Station instrument (Agilent Technologies, USA).

2.7.8 Library Quantitation, Size Estimation, normalization, and pooling

About 10µl of each amplified library was analysed using the Qubit™ 2.0 or 3.0 Fluorometer and the Qubit™ dsDNA HS Assay Kit, as mentioned in section 2.6.2. The concentration was calculated by multiplying the undiluted library by 24. Based on the calculated library concentration, the dilution determined that results in a concentration of ~100 pM as per (Table 2. 14).

Table 2. 14 Amplicon size of PTPRG.
The dilution factor depended on the average size of the amplicon of the gene. In our study average amplicon size of PTPRG was 375 bp: hence the Library was diluted by multiplying the undiluted library by 24 to reach ~100 pM, then proceed to template preparation.

Average amplicon size	Concentration in ng/mL (~100 pM)
140 bp	9
175 bp	11
225 bp	15
275 bp	18
375 bp	24

Later, around 1µl of the amplified library was analysed on the Agilent™2200 Tape Station instrument with the Agilent™ High Sensitivity DNA Kit. Multiple peaks were observed in the 120–400 bp size range, while typically amplified libraries had concentrations of 2000–10,000 pM. If the library concentration was over 20,000 pM, the library was diluted to 1:10, and the quantification was repeated to obtain a more accurate measurement. The molar concentration of the amplified library was determined using the Bioanalyzer™ software.

Library concentration from Qubit was reported in ng/µL (mass); however, the final concentration for Ion Sequencing must be ~100 pM, so appropriate dilution was performed to adjust the concentration according to average amplicons size. The

average amplicon size of PTPRG is 375 bp; hence the concentration of the library sample would divide by 24 (as per the recommendation of the Ion Ampliseq library kit 2.0 user guide). At this step, the concentration of the library was in 1 nanomolar, and dilution was carried out to reach the final concentration ~100 pM. About 5µl of each diluted sample was transferred and collected as a single pool in one 1.5mL Low bind tube and mixed with other combined libraries and proceeded to templating and sequencing.

2.7.9 Emulsion PCR and Library Enrichment

The Ion One Touch 2 system was set up as per the Ion PGM™ Hi-Q™ OT2 Kit user guide (Publication Number MAN0010902). Appropriate Oil and recovery solutions were installed in the respective tubes on the One Touch 2 system. New Ion One Touch Amplification plate, recovery tubes, and router were installed. Around 150µl Ion OneTouch™ Breaking Solution was dispensed into each of two recovery Tubes. The Amplification reaction mix was prepared with a library and was filled into a new Ion One Touch reaction filter to a 2mL tube (violet cap) containing 800µls of Ion PGM™ Hi-Q™ Reagent Mix. The following components were added in the designated order (Table 2. 15).

Table 2. 15 The Amplification reaction mix.
Amplification reaction mix was added to the library in orders and pipetted solution up and down to mix the solution prior to adding the next component.

S.No	Reagent	Cap colour	Volume
1	Nuclease-free Water (NFW)	-	25 µl
2	Ion PGM™ HiQ™ Enzyme Mix	Brown	50 µl
3	Diluted library (not stock library)	-	25 µl
4	Ion PGM™ HiQ™ ISPs	Black	100 µl
	TOTAL	-	1,000 µl

From the barcode pooled 100uM library, 2µl of the library was added into a 1.5mL tube, diluted with 23µl of NFW, so the final volume was 25µl. The listed components were added as per the above table in the same order into a new 2.0ml tube (supplied with Ion PGM TM OT2 supplies). The entire 1000µl of the OT2 reaction mix was carefully pipetted vertically through the sample port of the Ion OneTouch™ reaction filter, and the

pipette tip was removed without aspiration. Later, 850µl of Ion OneTouch™ reaction oil (25ml size bottle) was pipetted through the same sample port, another 850µl was added with a new tip. The filter was inverted as described in the OT2 user guide and installed on the Ion One Touch 2 system. The run wizard was employed with the right selection of kits and sequencing methods to perform the One Touch2 run.

At the end of the OT2 run, the final spin was performed on the OT2 system before removing the two recovery tubes. The screen prompt on the OT2 screen was followed to remove the tubes and clean the system for the next use. New Pipettor was developed for each recovery tube to remove all recovery solution but left 100µl in each tube without disturbing the pellet. Around 500µl of Ion OneTouch™ Wash Solution (OT2 Reagent kit) was added to each recovery Tube; the ISP was pipetted in solutions up and down and combined the washing from two tubes a single 1.5ml Eppendorf low BindTM tube. The ISP was centrifuged for 2.5 minutes @ 15.5000 x g at room temperature (Centrifuge 5415 R, Eppendorf). The supernatant was removed, but 100µl of the wash solution was not used from the tube without disturbing the pellet. ISP immediately proceeded to the enrichment step using the Ion Touch ES system from the recovered 100µl of ISPs.
Later, to enrich the template library from OT2, the Ion One Touch ES system was prepared as per the Ion PGM™ Hi-Q™ OT2 Kit user guide (Publication Number MAN0010902). The melt-Off solution was prepared by combining 280µl between TM solution with 40µl 1M NaOH. Dynabeads TM Moyne TM streptavidin C1 beads solution (Invitrogen, UK) was ready for the enrichment step. Around 13µl of Dynabeads TM Moyne TM streptavidin C1 beads were Vortexed and pipetted to a new 1.5mls Eppendorf loBindTM tube placed on the DynaMag™ 2 Magnet for 2 minutes. The supernatant was removed without disturbing the pellet, and 130µl of Moyne TM beads wash solution was added. An 8-well strip was obtained from the Ion OneTouch™ ES Supplies Kit and ensured that the square-shaped tab of an 8-well strip is on the left. The ISP was pipetted up and down ten times to mix then, the suspension was transferred into Well 1 of the 8-well strips, and the remaining wells in the eight (8) well strip was filled. A new Tip was attached to a 0.2mls PCR tube and placed on the appropriate

position with the cap opened filled with 10µl of Neutralization Solution. Once the strips were loaded, the Enrichment run started with 40 minutes as time out (Figure 2. 7).

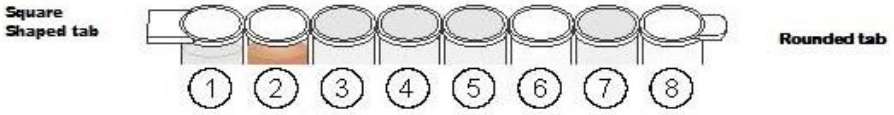

Well Number	Reagent to dispense in well
Well 1	100 µL of prepared template- positive ISP sample
Well 2	130 µL Dynabeads ™ Myone ™ beads wash solution
Wells 3,4 and 5	300 µL Ion one touch ™ solution
Well 6 and 8	Empty
Well 7	320 µL freshly Melt-off solution

Figure 2. 7 Suggested 8- Well strip for library enrichment.
Dynabeads with brown colour in well number 2, and other components.

The resulting product (enriched, template –positive ISPs) was collected automatically in a 0.2mL PCR collection tube containing Neutralization Solution. After the run, the PCR tube cap was sealed and removed from the Ion One Touch ES System containing the enriched ISPs. The contents of the PCR tube were mixed gently by inverting the tube five (5) times. Sequencing was performed on the template-positive ISPs using the Ion PGM™ Hi-Q™ Sequencing Kit on Ion PGMTM Sequencer.

2.7.10 Chip loading and sequencing protocol on Ion PGM™.

2.7.10.1 PGM system Initialization.

PTPRG Ion sequencing performed on Ion Personal Genome Machine™ (PGM™) using the Ion PGM™ Hi-Q™ Sequencing Kit, which contains all the necessary components such as sequencing reagents, buffers, Ion PGM system disposables. Based on the Total read output for the combined sample libraries, an appropriate Ion Chip kit should be used. In our study, we employed 316™ Chip Kit v2 BC- 4 pack with capacity 300 Mb – 600 Mb as output.

The first step was to create the planned run that contained all settings used in a sequencing run, including the number of flows, kit types, barcodes, sample information,

and reference files using the Torrent Suite™ Software. Then, it was essential t to clean the PGM system using the 18 MΩ water as per the instructions in the kit user guide. Once the cleaning procedure was completed, using the PGM screen prompt precede to the Buffer Initialization step to auto adjust the appropriate pH for the sequencing run. Appropriate Wash buffers were prepared by adding 350µl of freshly prepared 100 mM NaOH, to thoroughly cleaned wash bottle #1 and 40ml of Ion PGM™ HiQ™ Sequencing W3 Solution to wash bottle #3. The entire bottle of Ion PGM™ HiQ™ Sequencing W2 Solution and using a P100 pipette, around 70µl of 100 mM NaOH was added to the Wash #2 Bottle. The three wash bottles were connected to the PGM system using a new sipper in the PGM sequencing accessories kit. The initialization started using the touch screen menu on the PGM system. Once the pH of Wash #2 buffer passed, it proceeded immediately to install the four dNTP reagent tubes and continue the rest of the initialization procedure using the screen prompt. If every reagent was in the target pH range, a green passed screen will be displayed, and “next” was to be pressed to continue the initialization.

After successful initialization of the PGM system, about 5µl of control ISPs was added to the entire volume of enriched, template –positive ISPs (prepared in Emulsion PCR and Enrichment section) and placed on a micro centrifuge with a suitable adaptor where the tube lid was pointed away from the centre of the centrifuge (to indicate pellet formation). Then the ISPs centrifuged for 2 minutes at 15.500 x g. The supernatant was removed, but 15µl was left, and 12µl of sequencing primer was added, so the total volume was 27µl. The Tube was loaded to thermal cycler and programmed for 95°C for 2 minutes to denature then for 37°C for 2 minutes for annealing the primer. Following this, 3µl of Ion PGM Hi-Q Sequencing polymerase was added after completing the program, and the total volume was 30µl.

The new Ion 316 Chip was loaded on the PGM system, and Chip Check was performed to ensure that the new chip was functioning properly before loading the sample. After annealing the Sequencing Primer, the ISPs were removed from the thermal cycler, and then 3µl of Ion PGM™ HiQ™ Sequencing Polymerase was added to the ISP's final total

volume of 30µl. The sample was pipetted up and down and then incubated at room temperature for 5 minutes. The chip was removed, and the liquid was aspirated from the chip using the pipette from the sample port. The Ion 316 chip was placed on a flat Chip loading bucket and loaded the entire 30µl volume of the sample through loading port using dial down pipette technique (~ 1µl per second) to avoid inserting bubbles to the chip. On the other hand, the extra liquid was removed from the different ports of the chip; it was centrifuged two times in minifuge for 30 seconds. The chip was pointing towards the centre of the minifuge while the second round, the chip was pointing out.

Pipettor was adjusted to 25µl (as per user guide). The chip was tilted at a 45° angle so the loading port would be in lower port, and the extra solution was removed carefully without removing the tip. The sample was slowly pipetted out and back to the chip for one time, and the excess liquid is discarded by dialling the pipette out. Finally, the chip was turned upside-down in the bucket of minifuge and centrifuged for 5 seconds to ensure the dryness of the chip. The sample filled chip was loaded on to the PGM sequencer, using the prompted screen, select the planned run and perform the run. The PGM system performed a leak test for the first few minutes, a Chip check procedure, and then the run started automatically after passing all the calibrations. The run performance was monitored using Torrent software.

2.7.11 Variants Analysis

We employed GeneGrid (Genomatix, GmbH) cloud variant analysis software for variants annotation from the sample. Vcf files to list the variants classifying for dbSNP, allele frequency. Positions of variants and variant effect predictor data were verified by data mining using the Ensembl project utilizing version browser 99 (GRCh37, 2021) . Single nucleotide polymorphisms of similar positions and base change from different patients in the study were annotated from sequence data across to identity polymorphic sites. Genotype and allele frequencies for annotated SNPs in the PTPRG in CML patients were compared to 1000 Genomes Project (Auton et al., 2015) as well as The Qatar genome program (QGP) as reference (Al Thani et al., 2019).

2.8 Direct Bisulfite Sequencing of PTPRG Promoter and Intronic CPG Island.

Other possible mechanism of down regulation of *PTPRG* is bisulfite sequencing. Bisulfite sequencing is main technique to detect DNA methylation patterns. This process was done by PCR (polymerase chain reaction) amplification.

2.8.1 Primer Designing

Initially, the CpG islands of PTPRG are located through the National Centre for Biotechnology Information website (NCBI) via genome (hg19), and workflow was DNA (Figure 2. 8). The initial search showed that the PTPRG gene had two CpG islands sites, one in the Promoter region and the other located at the first Intronic region, which could also regulate the gene expression with CpG counts 25 and 26 accordingly. By clicking on the target CpG Island, the CpG island info was showed, and DNA for this feature was clicked to get all DNA sequencing. The sequencing was copied and pasted to Methyl primer software v1.0.

CpG islands were presumed thorough the sequence of one base at a time, scoring each dinucleotide (+17 for CG and -1 for others) and classifying outstandingly counting segments. Each segment was then evaluated for the subsequent criteria: GC content of 50% or greater (the ratio was ≥0.5) and length between 150 and 250 bases. Later, in silico pogrom primer design and search tool (Enzymology, 2020) was employed to ensure the sole product of PCR (Table 2. 16).

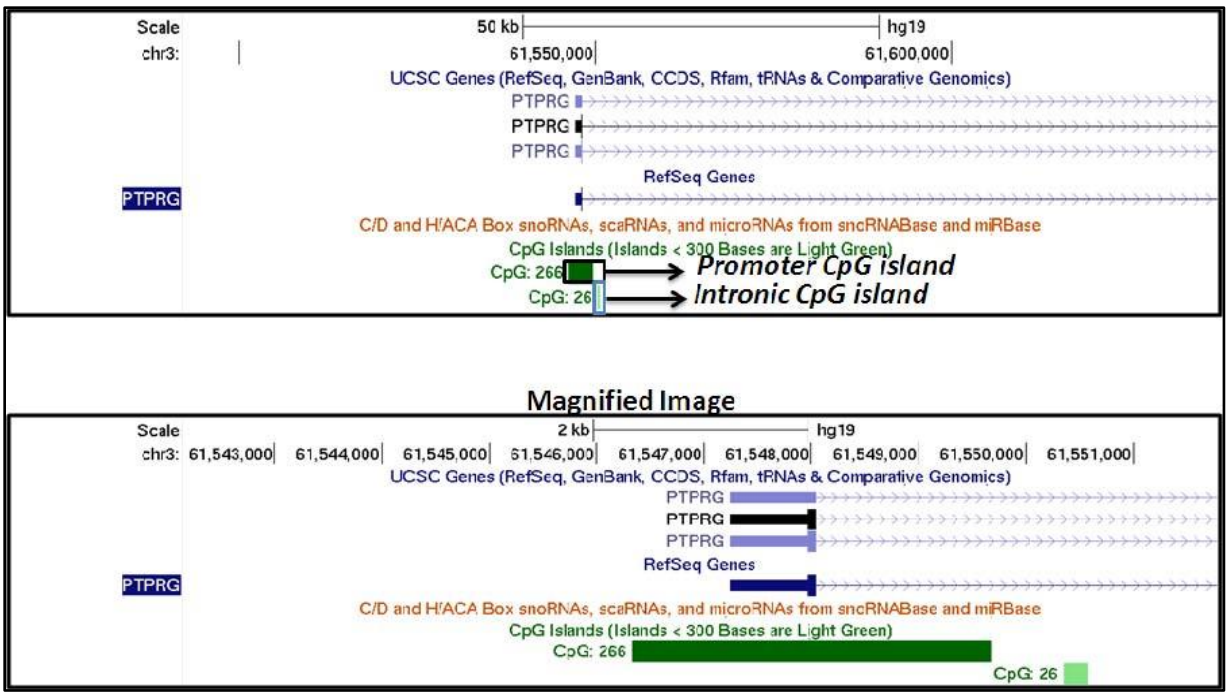

Figure 2. 8 Genomic Representation of CpG Islands present in the PTPRG gene.
PTPRG gene has two CPF islands in prompter and intronic respectively which may has potential role in regulating the gene [adopted from(NCBI, 2020)].

2.8.1.1 Bisulfite Sequencing of PTPRG Promoter CpG Island

INITIAL NUCLEOTIDE SEQUENCE

CGG**AGAGAGCAGAGCCGAGGGACCC**AGCGCAAGGCGGGAGCCAAGCGCGGCT
GCTTTAAGAACGCGGAGAGCGCGCGCCCGCCGCCAGCTGGCCCGGGCTGCGCG
CCCCCGCCGCCACCGCGCGCCCCCTGTTCGCTCGCTCCTTCGCTCGCCGGCTTT
AAAGTCTCTGCCAGGATCCATGCTCACATGTTACTTCC**TGTATGGAGGCATGGCCA**
GTTTCCAGCCCCGCGCTCTTCGTTCCTTCCCAGCCTGCGCCGGAGCCACAACTTT
CAGGAGCATGGACTGAAGGCGCCCTCGCCCCAGCGCCCCTCTGA

BISULFITE MODIFICATION OF DNA

CGG**AGAGAGTAGAGTCGAGGGATTT**AGCGTAAGGCGGGAGTTAAGCGCGGTTGT
TTTAAGAACGCGGAGAGCGCGCGTTCGTCGTTAGTTGGTTCGGGTTGCGCGTTTT
CGTCGTTATCGCGCGTTTTTTGTTCGTTCGTTTTTTCGTTCGTCGGTTTTAAAGTTTT
TGTTAGGATTTATGTTTATATGTTATTTT**TTGTATGGAGGTATGGTTAGTTTT**TAGTT
TCGCGTTTTTCGTTTTTTTTTAGTTTGCGTCGGAGTTATAATTTTTAGGAGTATGGAT
TGAAGGCGTTTTCGTTTTAGCGTTTTTTTGA

2.8.1.2 Bisulfite Sequencing of PTPRG Intronic CpG Island.

INITIAL NUCLEOTIDE SEQUENCE

GGCGCAGGGAAGAGGGCGGTTTGGTTTGGAAAAGTGCAGCCC**GAGAGGGAGCA**
GCAGGCTTTGGAGCAAGGTAAAGTTAAAATATCAGAGCTCTGGGAGACGCTGGCT
TTTCGTTTTCCGAGGTTGCCGCGACGCCGCTGGACCTCAGGGGGCGCCCCCGAG
CCACTGGTGGGGCTCCTGCCACCTCCACACTGGTCGGCCTCGGCCACCTCCACG
CCTCAGGGATGGGGCGCGCGTGCCCGGGTTCCCAGGCTCTGGGGCTGCAGACG
CGCCTTGGCGCGAGGCGGCGGCCTCGGCCTGGCGATGCTGCTCCTGGCTTTCTC
GAAACCCGCTGGGGGC**TGGAGTTAGCCTTGGGACCCCTAC**TTCTTGCCTGCTATG
ACCTCGAAAGCGCTTATCTGTTTGACATGAGGGATAAAAATGCTTCTGTTTTG

BISULFITE MODIFICATION OF DNA

GGCGTAGGGAAGAGGGCGGTTTGGTTTGGAAAAGTGTAGTTC**GAGAGGGAGTAG**
TAGGTTTTGGAGTAAGGTAAAGTTAAAATATTAGAGTTTTGGGAGACGTTGGTTTTT
CGTTTTTCGAGGTTGTCGCGACGTCGTTGGATTTTAGGGGGCGTTTTCGAGTTATT
GGTGGGGTTTTTGTTATTTTTATATTGGTCGGTTTCGGTTATTTTTACGTTTTAGGGA
TGGGGCGCGCGTGTTCGGGTTTTTAGGTTTTGGGGTTGTAGACGCGTTTTGGCGC
GAGGCGGCGGTTTCGGTTTGGCGATGTTGTTTTTGGTTTTTTCGAAATTCGTTGGG
GGT**TGGAGTTAGTTTTGGGATTTTTAT**TTTTTGTTTGTTATGATTTCGAAAGCGTTTATTTGTT
TGATATGAGGGATAAAAATGTTT

Table 2. 16 Suggested primers (Forward and Reverse) of PTPRG.

Promotor and Intron Islands of PTPRG with expected product The Promoter region is the expected to investigate methylation status in 25 CpG sites, while 26 CpG sites for Intron region.

PTPRG Promoter CpG island		**PCR product**
Forward primer	Length: 22bp. 5' AGAGAGTAGAGTYGAGGGATTT 3' Tm=58.94; CpG=1; C=5	Length: 218 bp. 5' AGAGAGTAGAGTYGAGGGATTTAGYGTAAGGYGGGAGTTAAGYGYGGTTGTTTT AAGAAYGYGGAGAGYGYGYGTTYGTYGTTAGTTGGTTYGGGTTGYGYGTTTTYGT YGTTATYGYGYGTTTTTTGTTYGTTYGTTTTTTYGTTYGTYGGTTTTAAAGTTTTTG TTAGGATTTATGTTTATATGTTATTTTTTGTATGGAGGTATGGTTAGTTTTT 3' %CGs=42.66 25 CpG sites
Reverse primer	Length: 24 bp. 5' AAAACTAACCATACCTCCATACAA 3' Tm=58.96; CpG=0; C=5	
PTPRG Intron CpG island		**PCR product**
Forward primer	Length: 22bp. 5' GAGAGGGAGTAGTAGGTTTTGG 3' Tm=59.54; CpG=0; C=3	Length: 321 bp. 5' GAGAGGGAGTAGTAGGTTTTGGAGTAAGGTAAAGTTAAAATATTAGAGTTTTGGG AGAYGTTGGTTTTTYGTTTTTYGAGGTTGTYGYGAYGTYGTTGGATTTTAGGGGG YGTTTTYGAGTTATTGGTGGGGTTTTTGTTATTTTTATATTGGTYGGTTTYGGTTAT TTTTAYGTTTTAGGGATGGGGYGYGYGTGTTYGGGTTTTTAGGTTTTGGGGTTGT AGAYGYGTTTTGGYGYGAGGYGGYGGTTTYGGTTTGGYGATGTTGTTTTTGGTTT TTTYGAAATTYGTTGGGGGTTGGAGTTAGTTTTGGGATTTTTAT 3' %CGs=43.61 26 CpG sites
Reverse primer	Length: 24 bp. 5' ATAAAAATCCCAAAACTAACTCCA 3' Tm=60.09; CpG=0; C=7	

2.8.2 Bisulfite Conversion

The Bisulfite treatment catalyses the deamination of all the unmethylated cytosine (uC), nucleotides to uracil (U) and leaves the methylated cytosine (mC) unchanged. About 1.2-1.5 ug of DNA from the stock extracted, as mentioned previously (in section 2.6.1), was made up to 45 ul with miliQ water in a microfuge. About 5 ul of M-Dilution Buffer was pipetted into the DNA sample, which mainly favours the denaturation of DNA at 37-40C. It was mixed by flicking. The sample was then incubated in a water bath at 37C for 30 minutes. The provided CT Conversion reagent was received in its powdered form and prepared in the dark by dissolving the solid reagent in 750ul of fresh milliQ water and 210ul of M-Dilution buffer. After half-an-hour incubation, 100ul of the prepared CT Conversion reagent was added to each sample and mixed gently until the contents of the tube formed a single- phase, vortexes completely were avoided. The samples were incubated in a water bath at 50C for 16 hours, after which they were removed from the water bath and immediately placed ice for 10 minutes. A 400ul of M-Binding Buffer was pipetted into a labelled ZymoSpin™ IC Column placed in the Collection Tube. The samples from ice were loaded into their respective Zymo-Spin™ IC Columns. The caps were closed, and the contents were mixed by inversion for three minutes. The ZymoSpin™ IC Columns in the Collection Tubes were centrifuged at 13000 rpm for 30 seconds. The flow-through was discarded.

M-Wash Buffer was prepared by decanting 96mL of 100% ethanol into the 24mL MWash Buffer concentrate. Around 100ul of the prepared M-Wash Buffer was pipetted into the column, the columns were centrifuged at 13000 rpm for 30 seconds, and the flow-through got discarded. About 200ul of M-Desulfonation Buffer was added to the Zymo-Spin™ IC Column and was left at room temperature for exactly 20 minutes. The columns were centrifuged at 13000 rpm for 30 seconds, and the flow-through discarded. A 200ul of MWash Buffer was pipetted into the column. The contents were centrifuged at 12000 rpm for 30 seconds. The step was repeated. The Zymo-Spin™ IC Column was placed in a labelled 1.5mL microfuge tube. A 30ul of M-Elution Buffer was added directly to the column matrix. Centrifugation was carried out at 13000 rpm for 30

seconds to elude the DNA into the microfuge tube. The microfuge tubes containing the bisulfite converted the DNA samples, which were stored at -20^{0}C. About 2-3 ul of the bisulfite -converted DNA was utilized to carry out each PCR reaction. The bisulfite conversion and bisulfite specific primer design is carefully performed by using previously published research paper by Hernández HG et al. (Hernandez et al., 2013).

2.8.3 Agarose Gel Electrophoresis and Amplicon Purification

Firstly, 5X TBE, 0.5X TBE solutions were prepared as 54 grams of Tris Base and 27.5 grams of Boric Acid, which are accurately weighed and 20 mL of 0.5 M EDTA 800mL of distilled water and all components were decanted into the beaker. The contents were stirred using a magnetic bead stirrer until the solution became clear. To prepare 5X TBE, the solution was made up to 1000mL using distilled water, which is added to the beaker after removing the bead. The solution was diluted in a 1:10 ratio using distilled water. Secondly, 6X Bromophenol blue and 30% Glycerol solutions were prepared as 30mL of 100% glycerol, made up to100mL with distilled water in a volumetric flask to prepare 30% glycerol and autoclaved. Then 25 milligrams of Bromophenol Blue were accurately weighed out with the aid of a beam balance and dissolved in 10mL of 30% glycerol in a falcon tube. Later 1mL aliquots were prepared for use. The agarose gel casting tray, conical flask, and comb were cleaned well with detergent and then washed with tap water to altogether remove any residual detergent. The apparatus was allowed to dry and later wiped with 100% ethanol.

For the preparation of 100mL of 1.2% Agarose Gel, 1.2 grams of Agarose were weighed out using a weighing boat and poured into the cleaned conical flask. About 100 mL of prepared 0.5X TBE was measured using a graduated measuring cylinder and poured into the conical flask. The contents of the Erlenmeyer flask were heated in a microwave and continually monitored to ensure that boiling does not take place. The molten gel was gently swirled to avoid spillage. It was cooled under tap water until its temperature was just bearable to the hand. Around 2µl of Ethidium Bromide was carefully pipette into the flask and swirled to achieve uniform distribution of the dye.

The comb was placed in the notches of the gel casting tray, and a pair of chilled metal slabs were used to block the open sides of the casting tray. The molten gel was decanted into the tray and allowed to solidify. The metal slabs were removed, and the gel was placed into an electrophoresis tank, ensuring that it was completely immersed in buffer. The comb was removed. Samples to be electro-separated were loaded into the wells using 6X ESB in 30% glycerol to run at 100V. The agarose gel image was captured under UV using the MultiDocIT Digital Imaging Unit.

A thick welled 1.2% Agarose Gel was prepared and completely submerged in 0.5X TBE Buffer in a gel electrophoresis tank. About 5ul of 1X ESB was pipetted into the remaining 27µl of the PCR mix in the PCR Tube. Then the contents were properly mixed and loaded into the wells of the gel. Electrophoresis was carried out for 90 minutes at 100V. The surface of the UV Trans illuminator was wiped with cotton soaked in 100% ethanol and left to dry. The gel was placed onto the UV Transilluminator and exposed to Ultraviolet light in the range of 360-365nm. Using a sterile blade, the gel slice containing the amplified DNA fragment was carefully excised as close to the DNA band as possible to minimize the gel volume. Then the gel slice was placed onto a glass plate, cleaned by washing the surface with detergent, and sterilized by wiping with 100% ethanol. The slice was then finely chopped with a sterile blade, and its remnants are transferred into a labelled microfuge tube. The Amplicons from agarose gel was purified using NucleoSpin® Gel, and PCR Clean-up and the methodology adopted from manufacture protocol

2.8.4 Gradient Polymerase Chain Reactions (PCR)

Gradient PCR was employed to determine the appropriate annealing temperature experimentally, and specificity of the designed primers to bisulfite converted DNA in a single trial. PCR Master Mix for Gradient PCR was prepared in a sterile, autoclaved 1.5mL microfuge tube. Notably, the run was done over two days for Promoter and Intron, as shown (Table 2. 17) respectively.

Table 2. 17 PCR Master Mix preparation for PTPRG Promoter/Intron CpG islands.

Gradient PCR The Master Mix was prepared for four bisulfite converted DNA samples; four genomic DNA samples, and one Negative Control. ~ refereed to adjusted volume for CpG Island associated with the PTPRG-Intron region

.

Component	Volume	
10X PCR Buffer	30µl	
4m M dNTP	30µl	
50Mm $MgCL_2$	5µl	2.5µl~
MiliQ water	135 µl	137.5 µl~
10pmol/ ul Forward Primer	20µl	
10pmol/ ul Reverse Primer	20µl	

The run described in (Figure 2. 9) was paused at 2 minutes 30 seconds during Initial denaturation to add 2µl L of Epi-Taq Polymerase (Takara Bio Inc, Japan) (0.5U/ul) to each PCR tube. The contents of each tube were mixed well upon enzyme addition; then, the run was resumed and allowed to complete. Later, about 3µl of the PCR products from each tube were loaded into the wells of a 1.5% Agarose gel with the aid of 6X ESB in 30% glycerol and let to run 100V. The agarose gel image was captured under UV using the MultiDocIT Digital Imaging Unit.

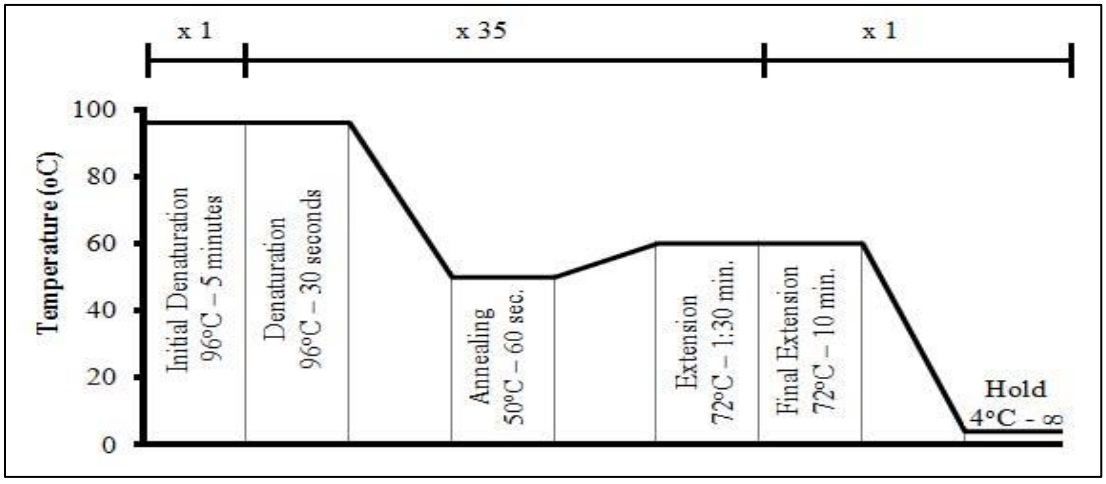

Figure 2. 9 Gradient Polymerase Chain Reactions (PCR).

The PCR tubes were prepared and placed in the Eppendorf Master cycler Gradient after setting an Annealing Temperature (Tann50^0, 52^0, 55^0, 58^0, 60^0 and 62^0 C) gradient.

2.8.5 Bisulfite Specific PCR

As a result of the gradient polymerase chain reaction, the specific product was observed at 60^0C for the promoter and intern CpG islands. The inference specific product was 321 bp and 218 bp for intronic and promoter, respectively. The PCR Master Mix was prepared in a sterile, autoclaved 1.5mL microfuge tube (Table 2. 18).

The Negative Control for PCR was prepared by adding 25µl of the Master Mix into a thin-walled PCR tube and labelled as Negative Control (NC); in addition to that, no DNA was added to the negative control. For the amplification of the bisulfite converted DNA samples, 25µl of the Master Mix and 3µl of bisulfite converted DNA was pipetted into a thin-walled PCR tube, the tubes are placed in the Agilent Sure Cycler (Agilent Technologies, USA), and the program started. PCR programs were employed (Figure 2. 10).

Table 2. 18 PCR Master Mix preparation.

For the amplification of the differentially methylated region of CpG Island associated with PTPRG (Promoter-Intron) in "N" bisulfite converted DNA samples one Negative control. ~ refereed to adjusted volume for CpG Island associated with the PTPRG-Intron region.

Component		Volume	
10X PCR Buffer		(N+2) *3.0µl	
4m M dNTP		(N+2) *3.0µl	
50Mm $MgCL_2$		(N+2) *0.5µl	(N+2) *0.25µl ~
MiliQ water		(N+2) *13.5µl	(N+2) *13.75 µl ~
100ng/ ul PTPRG-Promoter Forward Primer	10pmol/ul PTPRG-Intron Forward Primer~	(N+2) *2.0µl	
100ng/ ul PTPRG-Promoter Reverse Primer	10pmol/ul PTPRG-Intron Reverse Primer~	(N+2) *2.0µl	

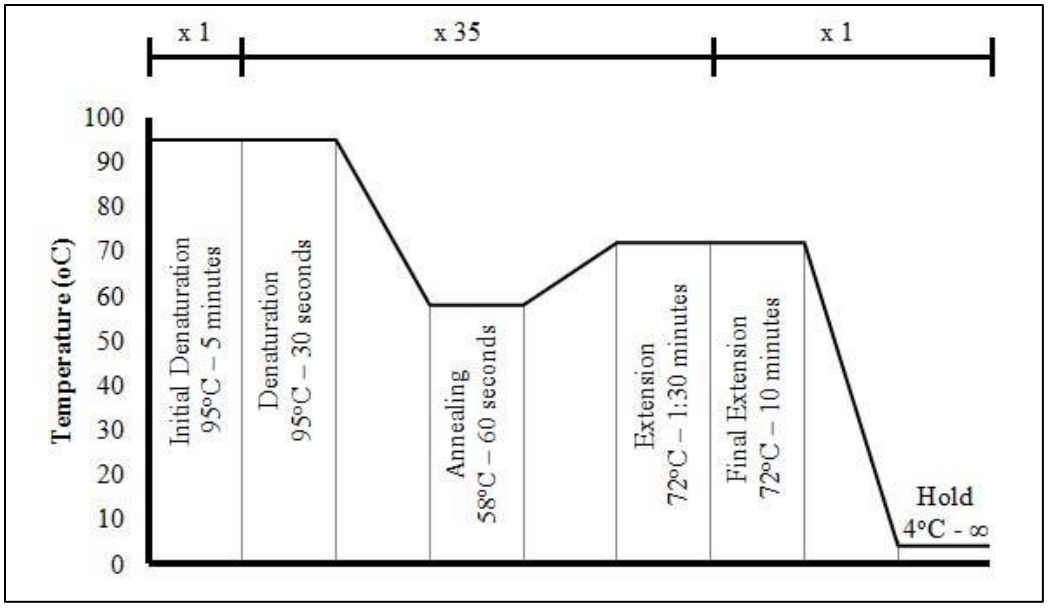

Figure 2. 10 PTPRG-Promoter and Intron Bisulfite PCR program

The run was paused at 2 minutes 30 seconds during Initial denaturation, and then 2µl of Epi-Taq Polymerase (0.5U/ul) was added to each PCR tube. The contents of each tube were mixed well upon enzyme addition, and the run was resumed and allowed to complete. Around 3µl of the PCR products from each tube were loaded into the wells of a 1.5% Agarose gel aid 6X ESB 30% glycerol. Finally, the agarose gel image was captured under UV using the MultiDocIT Digital Imaging Unit.

2.8.6 DNA Sequencing by Sanger Method

Due to small size of region of interest, Sanger method was employed for DNA sequencing, which was fast, cost-effective when compared to other platforms (I.e. QPCR). To 3µl of the diluted sequencing primer with a concentration of 100ng/ul in a labelled, sterile, thin-walled PCR tube, 2µl of Big Dye ready® reaction termination mix was added. Then 1µl of the sequencing buffer and 3µl of freshly distilled MilliQ water was carefully pipetted into each PCR tube. Finally, 3µl of the eluted PCR product was pipetted into a PCR Tube that was labelled accordingly. The contents of the tube were well mixed by pipetting up and down and then were placed in a Thermal Cycler, and the PCR program was run, as shown below (Figure 2. 11).

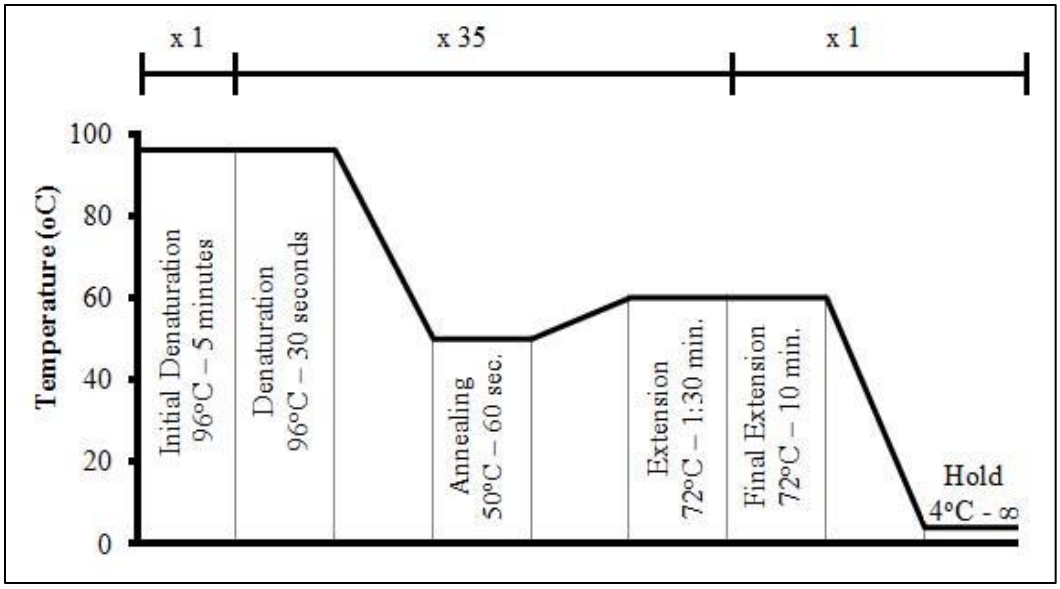

Figure 2. 11 DNA Sequencing PCR Program for Sanger technique

After the program is completed, the PCR tubes got removed from the instrument, and 10µl of autoclaved MilliQ water was added to each tube to prevent dye blobs. Around 2µl of 3M Sodium Acetate (pH 5.2) was well mixed with 50µl of 100% chilled ethanol in a labelled 1.5mL microfuge tube. Around 20µl of the reaction volume of the PCR, the tube was pipetted into the appropriate Tarsons tube and mixed well. Then the contents of the tube were vortexed vigorously and incubated at room temperature for 20 minutes. Finally, the tubes were spun at 12,000rpm for 20 minutes at 4^{o}C. The supernatant was discarded, and the pellet was saved. Later, 200µl of 70% ethanol was added to each pellet for washing, and then the tubes were spun again for 20 minutes 12,000rpm at 4^{o}C. Finally, Ethanol was decanted, and the pellet vacuum dried.

The dried pellet was re-suspended in 4µl of formamide, followed by a denaturation process carried out at 95^{o}C for 3 minutes, following which; the microfuge tube was immediately placed on ice. The contents of the tube were loaded onto a sequencer plate. The sequence of nucleotides composing the PCR fragment was determined by an Applied Biosystems® 3130 Genetic Analyser. The results were analysed by the sequencing software Gene Mapper® Software 5, Applied Biosystems®. The Results were viewed using Chroma's Lite.

2.8.7 Methylation Analysis

The analysis of the methylation status of CG sites in the region amplified by PCR was performed using the ESME (Epigenetic Sequencing Methylation) Analysis Software (Lewin et al., 2004). The software uses a genomic sequence as a reference and four-dye trace sequencing data as tests; it determines the ratio of C to T at CG sites after correction for incomplete conversion to determine methylation. Further, the percentage of methylation was calculated as the peak height of C vs. the peak height of C plus the peak height of T for each CpG site, as shown in the computer-generated sequencing chromatogram extracted from the Chroma's program (Version 2.32, Technelysium). A single C at the corresponding CpG site was considered, 100% methylation, a single T as no methylation, and overlapping C and T as partial methylation (0–100%) (Jiang et al., 2010). CpG sites of Promoter and Intronic regions of PTPRG were plotted using Methylation plotter where the methylation levels (0–100%) were converted (0-1) for plotting purposes (Mallona et al., 2014).

2.9 Cryopreservation and thawing of CML patients' cells.

The primary purpose of cryopreservation is to reserve vital biological signs of cells in good condition for an experimental purpose later of time, which usually does occur in a living state of suspended cellular medium (Bakhach, 2009). The process was done by halting the cell's metabolism either by controlled rate freezers or step-down freezing. Previously, the cells were frozen in their growth media or high serum media. However, since the introducing of the Cryoprotective agent, a significant improvement was documented to cell viability after thawing (Mazur, 1984). Currently, there are six applications of cryopreservation that include preservation of cells or organs, cryosurgery, biochemistry or molecular biology, food sciences, ecology or plant physiology, and medical applications (Jang et al., 2017).

In the same context, several studies documented the importance of cryopreservation of leukocytes from hematopoietic cells. As its help in several approaches in the clinical research field as well as clinical trials. For the last decade, recovery of thawed

leukocytes was the dilemma of the Cryopreservation process due to several reasons which include but not limited to. Firstly, the type of cryovials materials which effects on the period of storage, the efficacy of the recovered cells (Stroncek et al., 2011) and technical issues. Secondly, the content of freezing cells that includes intracellular and extracellular complex procedures that are not fully understood to date. Finally, freezing media components was another dilemma that affects the viability of cryopreserved Peripheral blood progenitor cell (PBPC), which depends on the Dimethyl sulfoxide (DMSO) concentration. Some studies documented that 2% or 4% or 5 % of DMSO were suitable freezing media, depends on the subpopulation of white blood cells aiming to preserve. For instance, 2% DMSO was significant for CD34+ cell recovery while, 5% DMSO was perfect for (PBPC) cryopreserving (Liseth et al., 2005). However, recent studies reported increasing DMSO a concentration of up to 10% was ideal concentration of freezing media (Hunt, 2019).
The freezing media concept was flowing into the cell component freely and swapping water, lowering the amount of ice formed, and acting as a secondary solvent for salts (Pegg, 2007). Not only that but freezing media should contain another component that preserves cell membrane in good condition (Meryman, 1971).

By the end of 2015, Government regulations of cells for medical had documented cell handling processes that accounts for regulations and protocols of cryopreservation process and should be adhered by all researchers (Baust et al., 2015).

The high rate of resistance to treatment in the state of Qatar (Al-Dewik et al., 2016) was one of the reasons to establish cryopreservation (Bio banking) for CML patients in this study. The isolated cells in section 2.3 were employed for this purpose. The cells were counted and checked for viability by the 7-AAD dye. The total amount of alive cells was recorded by flow cytometry. The freezing media, which contains 90% RPMI-1640 w L-glutamine, and 10% DMSO, were added. The total number of Cryovials was decided, such that every 1 ml of cryopreservation tube would contain 10-20 million cells. The Cryovials were transferred to Nalgene cryo1°C Freezing container (Mr. Frosty) for 24hrs - 48hrs at (-80°C). Latter cells were transferred to cryobox in -156°C or Liquid nitrogen.

2.9.1 Thawing of cryopreserved cells of CML patients

In general, cells thawed quickly but diluted slowly to remove DMSO. Several attempts were conducted to finalize the thawing protocol. Firstly, about 10mls of medium IMDM (RPMI-1640 w L-glutamine) containing 20% FBS was warmed in a 37°C water bath. Secondly, the vial was thawed for approximately 2 minutes in a 37°C water bath; then, the vial was cleaned from outside with 70% alcohol. Later, to avoid clumping of cells, 4µl of DNase I (~2500/vial) was added to the bottom of a 50ml conical tube. The cryovials were rinsed with 1ml of 37°C medium IMDM containing 20%FBS, slowly and drop by drop (5 seconds per drop) to the cells while gently shaking the tube. The rest of the 9ml was added with the same technique above. The cell suspension was centrifuged at 200xg at room temperature for 15 minutes (acceleration 6, deceleration 6).

The supernatant was removed and left with few millilitres of the supernatant behind to dissolve the pellet. Then the cells were checked for viability via 7-AAD dye and count by flow cytometry machine. The thawed cells at this stage are ready for cell culture or functional assay.

2.10 Statistical Analysis

All statistical tests were performed using SPSS v24 and GraphPad Prism version 8.0. All *P* values presented will be two-tailed, and *P* values <0.05 will be considered statistically significant.

2.10.1 Flow cytometry experiment

The distribution of the data was tested for normality with the Shapiro-Wilk test (W), and Skewness and normally distributed data was tested by the one-way analysis of variance (ANOVA) and Dunnett's multiple comparison tests. Non-normally distributed data was tested by Friedman and Dunnett's multiple comparison tests. On the other hand, the Mann Whitney test was performed to analyse the difference between normally and non-normally distributed data. Changes in expression of PTPRG in CML patients over timeline were analysed with Friedman and Wilcoxon signed ranks (WSRT) tests and a pairwise comparison with Hodges–Lehmann estimator. Finally, Kruskal-Wallis, along

with Mann Whitney tests, were employed to examine the changes of PTPRG among healthy (H), optimally (R), and failed (F) groups.

2.10.2 Quantitative Real-Time PCR experiment

Changes in mRNA levels of (BCR-ABL1 & PTPRG) over timeline were analysed with the Wilcoxon matched pairs signed ranks test (WSRT). The effect size of TKIs was reported and assessed on both genes (BCR-ABL1 & PTPRG) via the Cohen's d coefficient for which d=0.2 was considered a 'small' effect size, 0.5 a 'medium' effect size, 0.8 a 'large' effect size and 2.0 “huge” effect size. Additionally, a Spearman’s rank-order correlation was run to determine the relationship between the two genes.

2.10.3 Genetic variants experiment

For comparison of the allele and genotype frequencies between patients and reference, to generate odds ratios (ORs), 95 percent confidence intervals (CIs), and *P*-values, Fisher exact tests and multiple logistic regression models (co-dominant, dominant, and recessive) were conducted.

2.10.4 Methylation experiment

Descriptive statistics in the forms of median range and frequency and percentages were calculated. For continuous outcomes and categorical independent variables, the T-test for independent samples was used to test the mean differences for two groups. One-way ANOVA with Bonferroni post hoc analysis was employed to test the mean differences for three groups.

3 Application of flow cytometry for monitoring Tyrosine Phosphatase Receptor Gamma Protein level in Chronic Myeloid Leukaemia patients and predicting the treatment response

This chapter will discuss level of the expression of PTPRG at diagnosis and followed introduced TKIs and its importance as biomarker for monitoring treatment response by flow cytometry technique along with RT q-PCR.

3.1 Introduction

Background: Protein tyrosine phosphatase receptor gamma (*PTPRG*) is a member of the receptor-like family protein tyrosine phosphatases and acts as a tumour suppressor gene in different neoplasms (Zhao et al., 2015). Recent studies reported the down regulation of *PTPRG* levels in Chronic Myeloid Leukaemia disease (CML) (Della Peruta et al., 2010). In addition, the *BCR-ABL1* transcript level is currently a key predictive biomarker of CML response to treatment with Tyrosine Kinase Inhibitors (TKIs) (Hughes et al., 2003).

Aim: In this chapter, the aim was to employ flow cytometry to monitor the changes in the expression level of PTPRG in the white blood cells (WBCs) of CML patients at the time of diagnosis and following treatment with TKIs.

Methods: WBCs from peripheral blood of 21 adult CML patients who were regularly followed up and treated with Tyrosine Kinase Inhibitors (Imatinib and Nilotinib) were recruited into this study. Peripheral blood samples were collected in EDTA tubes, where 63 subsequent samples were collected according to the ELN treatment timepoints. Seven matched healthy individuals (H) with normal complete blood count (CBC) and who were negative for *BCR-ABL1* translocation were included in this study. The PTPRG expression level was determined at protein and mRNA levels by both flow cytometry with monoclonal antibody (TPγ B9-2) and RT-qPCR, and *BCR-ABL1* transcript by RT-qPCR respectively.

Results: PTPRG expression was found to be lower in the neutrophils and monocytes of CML patients at time of diagnosis compared to healthy individuals. Treatment with TKIs nilotinib and Imatinib Mesylate restored the expression of PTPRG in the WBCs of CML patients to levels observed in healthy controls. Moreover, restoration levels were greatest in optimal responders and occurred earlier with nilotinib compared to imatinib.

Conclusion: The results presented in this chapter support the measurement of PTPRG expression level in the WBCs of CML patients by flow cytometry as a monitoring tool for the response to treatment with TKIs in CML patients.

3.2 Quality assurance for TPγ B9-2 antibody.

The mAb TPγ B9-2 was tested against the following antibodies CD14, CD3, and CD19 targets monocytes, lymphocytes, and neutrophil population respectively and CD34 for hematopoietic stem (Figure 3. 1) this step was done prior running to peripheral blood of CML patients as quality indicator. On the other hand, the full characterisation of the mAb TPγ B9-2 has already been published in the literature (Vezzalini et al., 2017).

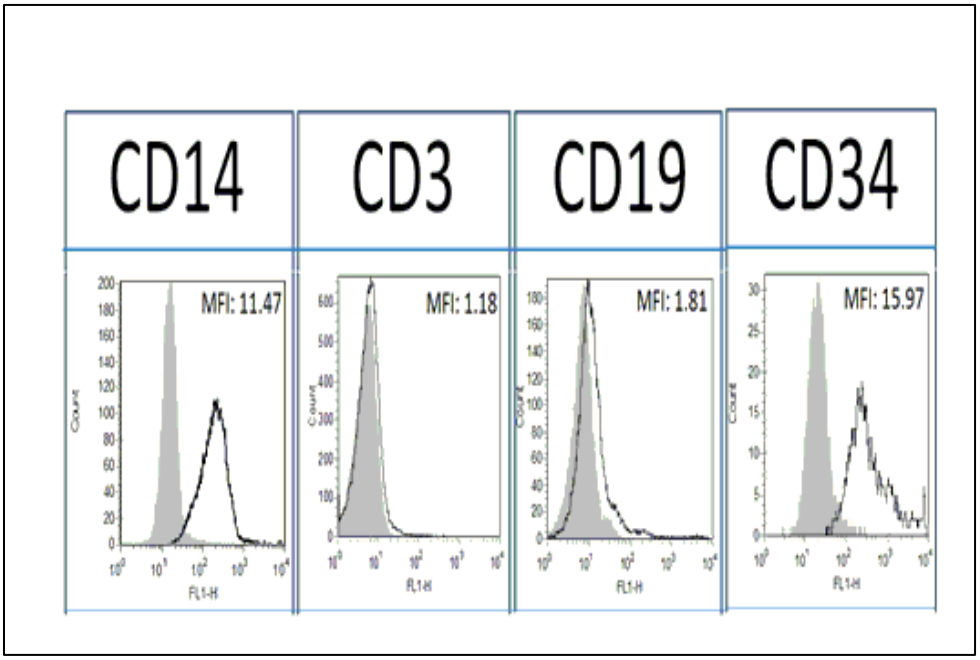

Figure 3. 1 Flow cytometry analyses of human leukocytes subpopulations against *TPγ B9-2 antibody.*

TPγ B9-2 antibody showed expression with CD14, CD19 and CD 34 antibodies which target monocytes, neutrophil and haematopoiesis precursor cells while no expression was observed with CD 3 antibody which target lymphocytes as negative control in human peripheral blood.

3.3 Results

To my knowledge, mAb TPγ B9-2 is currently the only mAb for use in the detection of PTPRG protein by flow cytometry. Therefore, in this study, the changes in the expression level of PTPRG protein were determined in the WBCs of 7 healthy individuals and 21 CML patients at the time of diagnosis and following treatment with BCR-ABL TKIs, using flow cytometry.

Out of the 21 CML patients examined in this study, 18 (86%) were diagnosed at chronic phase (CP) and 3 (14%) at accelerated phase (AP). The mean ages of the 21 CML patients were 38.21 years and those of 7 healthy controls 35.2 years respectively. Eleven patients were treated with Imatinib (400mg) and of these only two patients had optimal responses. Optimal response has also been developed in one patient following treatment with 600mg of Imatinib. Out of the remaining nine CML patients who treated with Nilotinib (300mg), 7 patients had optimal responses and the remaining 2 patients failed responses (Table 3. 1).

Presentation of results:

Figure 3. 2 show the sequence of results and analysis that were performed using two techniques at different time points (diagnosis and follow up) for different comparisons.

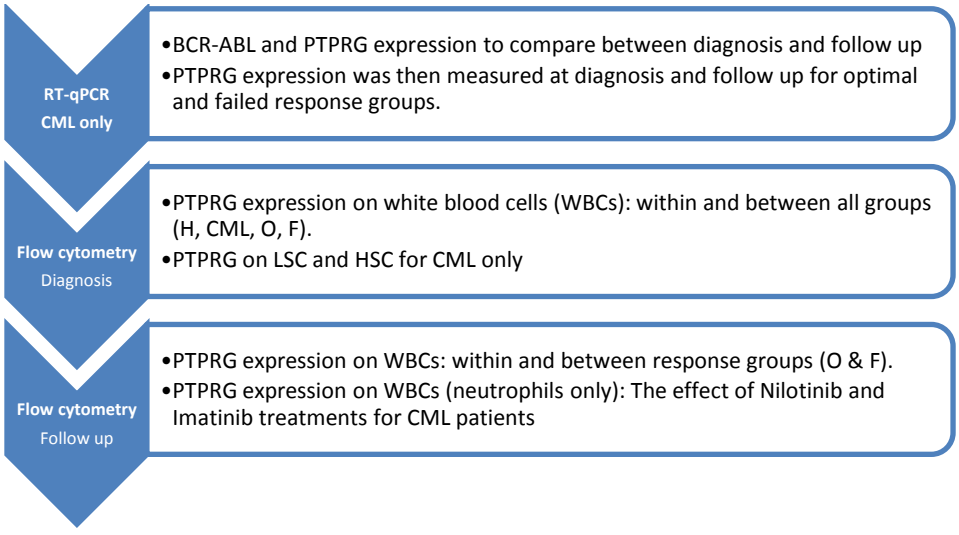

Figure 3. 2 Presentation of results.

Table 3. 1 CML patient's characteristics for flow cytometry experiment.

*Gender, age, clinical phase, TKIs (BCR/ABL1 and PTPRG) at diagnosis stage and response to treatment*CML04 AP with additional chromosomal (9:22) (q34, q11.2) T (11; 14) (q23, q32) (30). **CML13 CP with Tuberculosis. ***CML20 AP with double Ph+. ˜CML14 patient lost to record myeloid lineage events at time of relapsed.IS international scale.*

Patients	Age (years)	Diagnosis	BCR-ABL1/ABL (IS%)	PTPRG/*ABL (%)	Treatment	Final Response
CML 01.	61	CP	37%	0.02%	Imatinib (400mg)	Failed
CML 02.	61	CP	100%	0.03%	Imatinib (400mg)	Optimal
CML 03.	33	CP	100%	0.02%	Nilotinib (300mg)	Optimal
CML 04.	46	AP *	100%	0.01%	Nilotinib (300mg)	Optimal
CML 05.	23	CP	100%	0.01%	Imatinib (400mg)	Failed
CML 06.	48	CP	100%	0.02%	Imatinib (400mg)	Optimal
CML 07.	43	CP	100%	0.02%	Imatinib (400mg)	Failed
CML 08.	36	CP	100%	0.01%	Imatinib (400mg)	Failed
CML 09.	48	CP	100%	0.02%	Imatinib (400mg)	Failed
CML 10.	45	CP	100%	0.02%	Imatinib (400mg)	Failed
CML 11.	26	CP	100%	0.01%	Imatinib (400mg)	Failed
CML 12.	28	CP	100%	0.01%	Nilotinib (300mg)	Optimal
CML 13.	40	CP **	100%	0.01%	Imatinib (600mg)	Optimal
CML 14.˜	45	CP	100%	0.01%	Nilotinib (300mg)	Failed
CML 15.	26	CP	100%	0.01%	Imatinib (400mg)	Failed

CML 16.	40	CP	100%	0.01%	Imatinib (400mg)	Failed
CML 17.	33	CP	89%	0.02%	Nilotinib (300mg)	Optimal
CML 18.	34	CP	100%	0.02%	Nilotinib (300mg)	Optimal
CML 19.	32	AP	100%	0.01%	Nilotinib (300mg)	Optimal
CML 20˜.	65	AP ***	100%	0.01%	Nilotinib (300mg)	Failed
CML 21.	40	CP	100%	0.01%	Nilotinib (300mg)	Optimal

Overall, out of 21 CML treated patients with TKIs, 11 patients had optimal responses (52%), and 10 patients had failed treatment (48%).

3.3.1 Expression of BCR-ABL1 and PTPRG mRNA in whole white blood cells using RT-qPCR

The expression levels of *BCR-ABL1* and *PTPRG* mRNA levels in CML patients at diagnosis and follow up were determined by RT-qPCR and the results are presented in (Figure 3. 3). As the results of Cohn's d coefficient analysis show that there was a "huge" and "large" size effect on *BCR-ABL1* (Cohen's d = 5.05) and *PTPRG* transcripts (Cohen's d = 0.81) following treatment with TKIs. A significant difference was found in the mean levels of *BCR-ABL1* mRNA at diagnosis and at follow up (WSRT p <0.001, Figure 3. 3A) and *PTPRG* mRNA at diagnosis and follow up (WSRT p <0.001, Figure 3. 3B).

In contrast to *BCR-ABL1* mRNA which had significantly higher levels at diagnosis compared to follow up, *PTPRG* mRNA expression levels were found to be at lower at diagnosis compared to follow up. There was also a moderate negative correlation between *BCR-ABL1* at diagnosis and *PTPRG* at follow up (rs (21) = -0.422, p = 0.028). Moreover, the PTPRG transcript was also assessed to compare between optimal and failed CML groups. The results showed that the optimal response group had significantly higher *PTPRG* expression during follow up (WSRT p < 0.0005) compared to diagnosis time point, while no significant difference was found amongst the failed group at diagnosis and during follow up (WSRT p = 0.312, Figure 3. 3C).

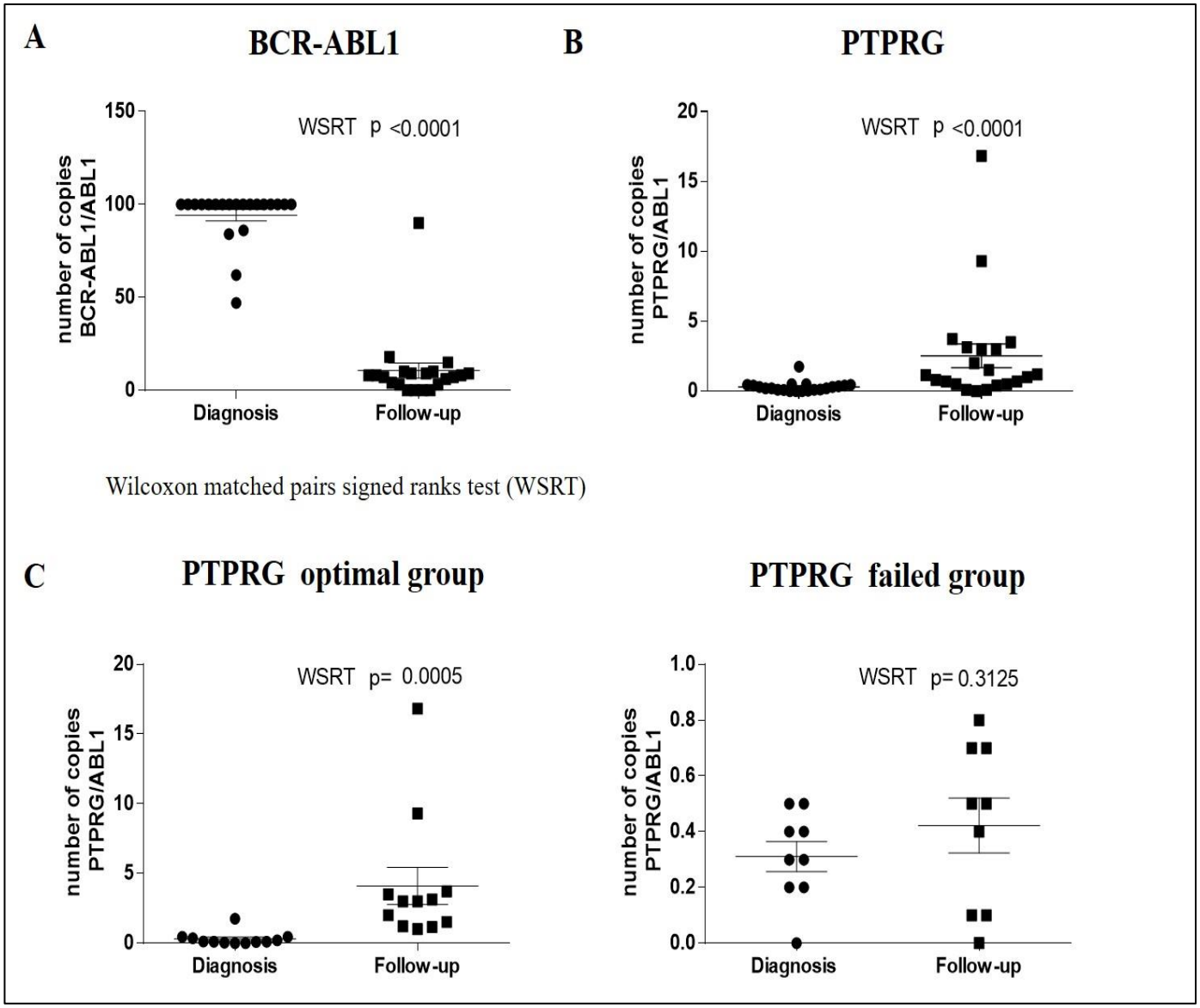

Figure 3. 3 mRNA levels of PTPRG in CML patients at diagnosis and follow up.

A) *BCR-ABL1 transcript levels at diagnosis and follow up (mean of post-test ranks = 10 and mean of pre-test ranks = 94.24, Z= -4.018, p <0.001).* ***B)*** *PTPRG transcript levels at diagnosis and follow up (mean of post-test ranks = 2.53 and mean of pre-test ranks = 0.3, Z= -3.50, p <0.001).* ***C)*** *mRNA transcripts level of PTPRG in the optimal response and failed treatment groups. The mRNA level of PTPRG in the optimal response group was significantly higher when compared with diagnosis, while this significance was lost in the CML group. The (X-axis) represents numbers of mRNA of PTPRG/ABL1, while (Y-axis) represented timelines at diagnosis and mean of follow up. P values were derived from the WSRT test.*

3.3.2 PTPRG expression levels on white blood sub-populations (WBCs) of Healthy individuals and CML patients at diagnosis using Flow cytometry

Next, the expression levels of PTPRG protein were determined in the WBCs sub-populations of healthy and CML patients using flow cytometry and the results are presented in (Figure 3. 4A). A significant difference was found in the of expression levels of PTPRG between different WBC sub-population (neutrophils, monocytes, and lymphocytes) [$F (3, 5) = 19.15$, $p < 0.0001$]. PTPRG protein expression levels were found to be higher on neutrophils and monocytes when compared to lymphocytes in both healthy individuals (Figure 3. 4B) and CML patients at diagnosis (Figure 3. 4C).

When comparing healthy individuals against CML patients, PTPRG protein expression levels were significantly higher on neutrophils ($U= 30$, $p < 0.002$) and monocytes ($U= 24$, $p < 0.007$) amongst healthy individuals in comparison to CML patients at diagnosis (Figure 3. 4D). A significant difference was also found in the expression level of PTPRG on neutrophils between the healthy, optimal and failed groups ($H= 14.94$, $df = 3$, $p =0.001$). The optimal response group had higher expression PTPRG in their neutrophils compared to the healthy group ($U= 3$, $p =0.004$), and the failed groups had higher expression of PTPRG than the healthy group ($U= 7$, $p =0.004$).

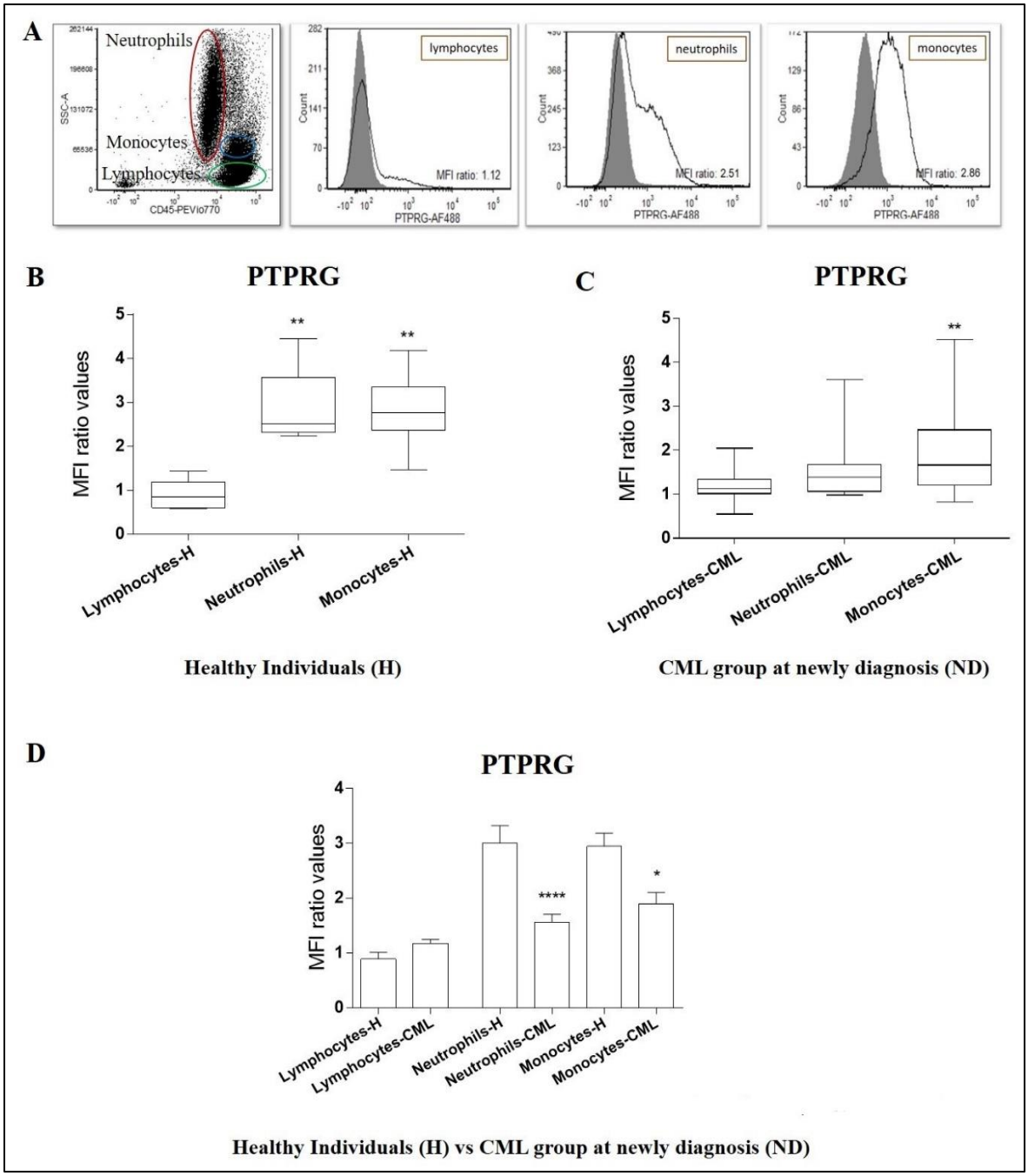

Figure 3. 4 PTPRG expressions on sub-population of white blood cells of healthy individuals (H) and CML patients (ND).

A) *Level of PTPRG expression on sub-population of white blood cells of Healthy Individuals (H). (Y-axis) refers to count numbers of peripheral blood cells recorded in each sub-population at flow cytometry acquisition. The expression of PTPRG was reported in Mean Fluorescent Intensity (MFI).* ***B)*** *The mean of PTPRG expression of healthy donors (H) on both neutrophils (mean= 3.0) and monocytes (mean= 2.8) was significantly higher when compared with lymphocytes (mean= 0.89).* ***C)*** *The mean of PTPRG expression of CML patients at diagnosis (ND) was significantly higher only on monocytes (median = 1.7) but not on neutrophils (mean = 1.5) when compared with lymphocytes (mean= 1.14).* ***D)*** *PTPRG expression on neutrophils and monocytes was significantly lower in CML (ND) patients in comparison with healthy individuals (H).*

3.3.3 Expression levels of PTPRG protein on neutrophils and monocytes in optimal and failed groups at follow up determined by Flow cytometry

The PTPRG expression level on WBCs was also re-assessed during the follow up for both optimal and failed CML groups (Figure 3. 5).There was a significant difference between the expression of PTPRG on the neutrophils (χ^2 (2, 11) = 13.82, *p* =0.001) and monocytes (χ^2 (2, 11) = 10.09, *p* =0.006) during the follow-up time points in the optimal response group. For the neutrophils, there were significant differences between 1st follow up (median: 3.68) and 2nd follow up (median: 4.8, Z= -2.93, *p* <0.001) and 1st follow up and 3rd (median: 4.9) (Z= -2.67, *p* <0.001), but no significant differences between the 2nd and 3rd follow up (Z= -0.89, *p* =0.37, Figure 3. 6A). However, for the monocytes there were only significant differences in its expression levels between 1st follow up (median: 3.5) and 3rd follow up (median: 4.5, Z= -2.05, *p* =0.004, Figure 3. 6D). There were no significant differences between the follow up time-points in relation to the expression of PTPRG on the lymphocytes in the optimal response group (χ^2 (2, 11) = 2, *p* =0.6).

In the failed response group, there were significant differences in the PTPRG expression levels between 1st follow up (median: 3.1) and 2nd follow up (median: 4.0) (Z= -2.8, *p* <0.005) and 1st and 3rd follow up (median: 4.5, Z= -2.6, *p* =0.009), but no significant difference between 2nd and 3rd follow up (Z= -1.33, *p* =0.19, Figure 3. 6B). For the monocytes, there were significant differences between only the 1st follow up (median: 3.8) and 3rd follow up (median: 4.6), (Z= -2.7, *p* =0.027, Figure 3. 6E). In contrast, there were no significant differences in the expression levels of PTPRG protein between the follow up time-points in failed response group (χ^2 (2, 10) = 2, *p* =0.8).

When the PTPRG expression was compared on neutrophils of optimal and failed group, there was no significant difference in the 1st follow up (U= 39, *p* =0.26). On the hand, there were significant differences between the two response groups at the 2nd follow up (U= 25.5, *p* =0.036) and the 3rd follow up (U= 28.0, *p* =0.05) (Figure 3. 6C). No

significant differences in the monocytes of the optimal and failed group were found between the follow up time points (1st follow up (U= 46.0, *p* =0.53), 2nd follow up (U= 49.5, *p* =0.7) and 3rd follow up (U= 48.0, *p* =0.62) (Figure 3. 6F).

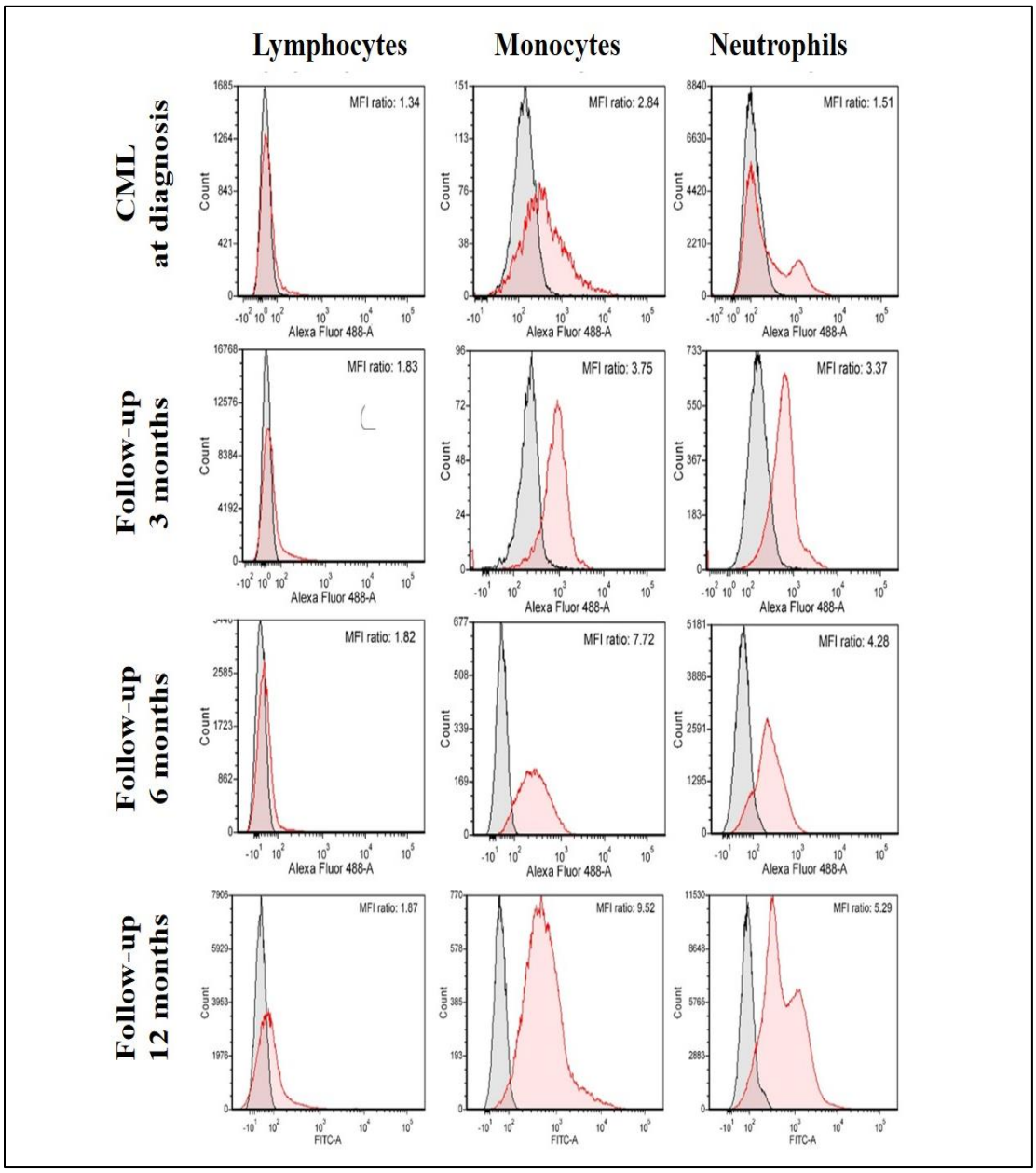

Figure 3. 5 PTPRG protein and its expression during the treatment plan.

Neutrophils and Monocytes showed a low level of PTPRG expression at the time of diagnosis. PTPRG restored its expression, at least in part of the sub-population of white blood cells followed by TKIs therapy. Of note, lymphocytes remained at a low level acting as an internal control. Follow up time points were 3, 6, and 12 months of successful TKIs as per ELN timelines. The MFI values were obtained by calculating the ratio differences between the signals derived from the signal of PTPRG monoclonal antibody TPγ B9-2 and irrelevant mouse IgG1.

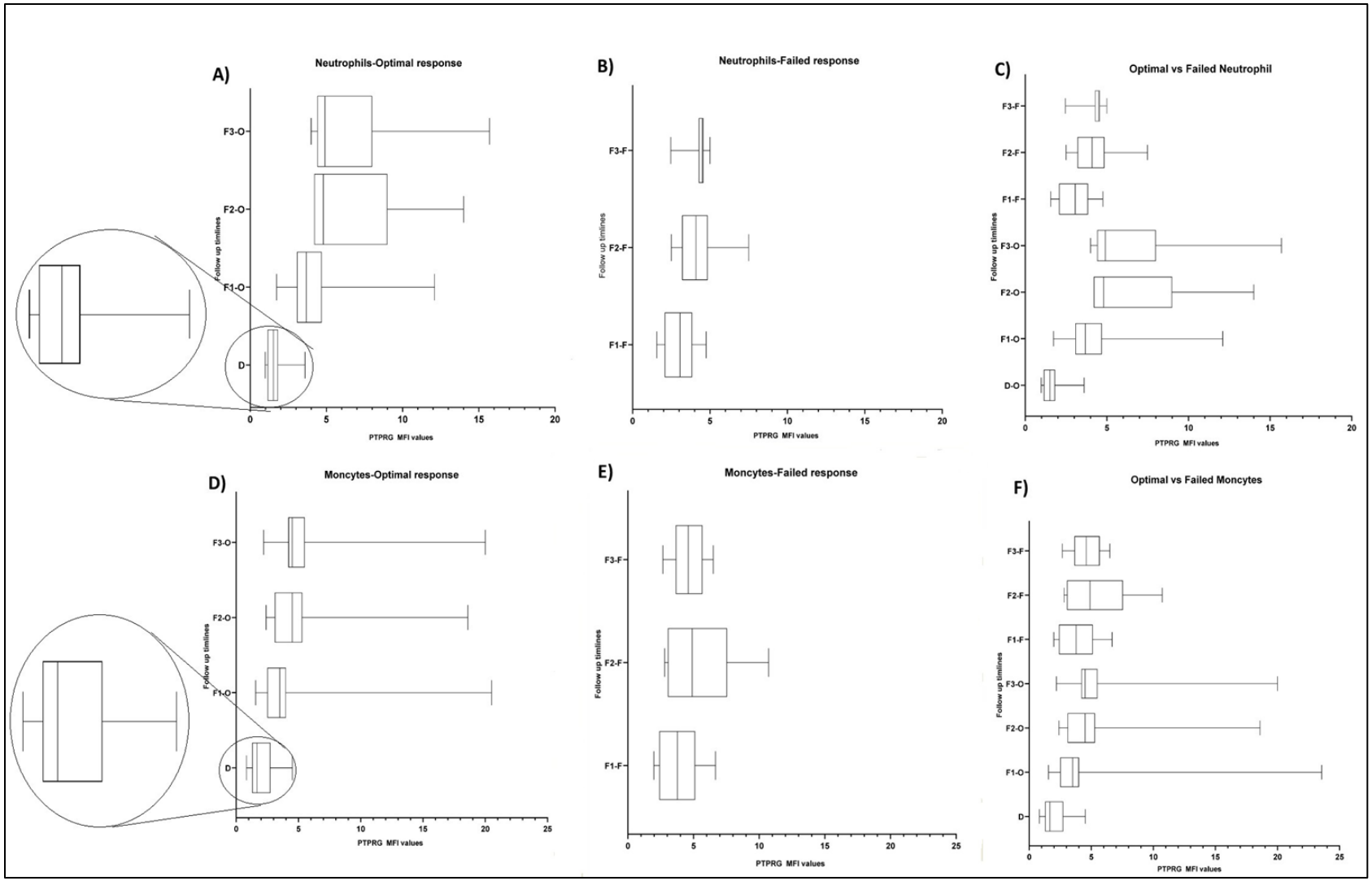

Figure 3. 6 PTPRG expressions upon stratification of CML patients' response in white blood cells and its sub-population.

A) *The level of PTPRG on neutrophils at diagnosis showed a median of 1.50 with negative skewness, the restoration level of PTPRG on neutrophils of the optimal response group was greater in follow up periods compared to diagnosis phase, median Follow-up 1 = 3.68; median Follow-up 2 =4.8; median of Follow-up 3 =4.9. Histogram showed positive skewness for later follow up periods.* ***B)*** *The PTPRG expression on neutrophils of failed response increased significantly by the first follow up compared to the time of diagnosis; median of Follow-up 1 = 3.065; median of Follow-up 2 =4.0; median of Follow-up 3 =4.5. Histogram of 1st and 2nd follow-ups showed a normal distribution (Shapiro-Wilk test, W), while the 3rd follow up showed negative skewness.* ***C)*** *Hodges–Lehmann estimator between optimally and failed groups on neutrophils; 1st follow up: -0.78, 2nd follow up: -1.35 and 3rd follow up: -0.9.* ***D)*** *The level of PTPRG on monocytes at diagnosis showed a median of 1.7 with positive skewness, the restoration level of PTPRG on monocytes of optimal response was greater in follow up periods when compared to diagnosis phase, median Follow-up 1 = 3.5; median Follow-up 2 =4.5; median Follow-up 3 =4.5. Histogram of 1st and 2nd follow-up periods showed negative skewness, while the 3rd follow-up showed positive skewness.* ***E)*** *The restoration level of PTPRG on monocytes in the failed response group showed a similar scenario as the optimal response group with a median Follow-up 1 = 3.8; median Follow-up 2 =4.9; median Follow-up 3 =4.6. The histogram of follow up periods showed a normal distribution (Shapiro-Wilk test, W).* ***F)*** *Hodges–Lehmann estimator between optimally and failed groups on monocytes 1st follow up: -0.34, 2nd follow up: -0.35 and 3rd follow up: -0.35. * Referred p-value was statistically significant. O: optimal response; F: failed group; D = diagnosis (optimal and failed); F1: 1st follow up; F2: 2nd follow up; F3: 3rd follow up.*

In CML patients, the impact of treatment (Nilotinib vs. Imatinib) on neutrophils' PTPRG expression significantly differed over time (Nilotinib: χ^2 (3, 8) =18.45, *p* =0.001; Imatinib: (χ^2(3, 12) = 32.9, p =0.001). There was a significant treatment effect between diagnosis and 1st follow up (only for Nilotinib treatment) (U= 22, *p* =0.047), diagnosis and 2nd follow up (both treatments), and diagnosis and 3rd follow up (both treatments). On the other hand, only Imatinib treatment was significantly more effective at 3rd follow up compared to 1st follow up (Table 3. 2A). In addition, the results of Fisher's Exact Test revealed that treatment with Nilotinib (300mg) was more likely to lead to optimal response compared to treatment with Imatinib (400mg) (Odds Ratio: 15.75, 95% CI: 1.75-141.41, Z: 2.46, $p<0.05$) (Table 3. 2B).

Table 3. 2 Contingency Table.

A) *Contingency table of TKIs therapy with outcome response. *CML patients with IM 600 mg excluded from fisher exact estimation.* ***B)*** *Test Statistics of effect of Nilotinib and Imatinib Mesylate on neutrophils.*

A) Time points	**Difference in mean rank**	***P* value**	**Difference in mean rank**	***P* value**
	Nilotinib (300 mg)		Imatinib Mesylate (400mg)	
Diagnosis- 1st follow up	-1.25	*P* = 0.03	-0.83	*P* = 0.69
Diagnosis- 2nd follow up	-2.38	*P* < 0.001	-2.083	*P* < 0.001
Diagnosis- 3rd follow up	-2.38	*P* < 0.001	-2.75	*P* < 0.001
1st follow up-2nd follow up	-1.13	*P* = 0.49	-1.25	*P* =1.06
1st follow up - 3rd follow up	-1.13	*P* =0.488	-1.91	*P* < 0.002
2nd follow up- 3rd follow up	0.00	*P* = 1.0	-0.667	*P* = 1.0

B) TKI therapy	**Optimal response**	**Failure response**	**Total**
Imatinib Mesylate (400 mg)	2	9	11
Nilotinib (300 mg)	7	2	9
Total	9	11	20

3.3.4 PTPRG expression on myeloid progenitors within the optimal and failed groups

After analysis of mature population (WBCs), we studied PTPRG expression in two subpopulations of progenitors' cells, leukemic stem cell (LSCs) and hematopoietic stem cells (HSCs). The results showed, there was no a significant difference in PTPRG expression at the time of diagnosis (U= 31, p=0.183) although the mean of PTPRG expression level on (LSC) (medium Glass' Delta effect size: 0.52) was higher than HSC (small Glass' Delta effect size: 0.17) (Table 3. 3) Furthermore, the mean rank of PTPRG expression on LSC at the time of diagnosis in the failed group was significantly higher than the optimal group (U= 12, $p < 0.004$).

Table 3. 3 The expression level of PTPRG in the sub-population of myeloid progenitor cells.

$CD34^+$ population	Mean± SD MFI	Glass' Δ
MFI $CD34^+CD38^{bright}$	1.97±0.88	0.17
MFI $CD34^+CD38^{dim}$	3.30±4.15	0.52

3.4 Discussion

For the first time, the study reported the changes in the PTPRG protein level in CML patients at the State of Qatar was determined by flow cytometry using a unique monoclonal antibody against the external domain of PRPRG. It was confirmed that restoration levels of PTPRG were significantly greater during the follow-up period following treatment with BCR-ABL1 TKIs compared to the time of diagnosis (Figure 3. 3)(Figure 3. 5). Moreover, stratification of CML patients' response into optimal and failed treatment groups showed that the expression level of PTPRG to be significantly higher in the optimal response group when compared to the failed group, utilizing both q-PCR and flow cytometry techniques. The results also confirmed the earlier findings using RQ PCR, in which 33 CML patients had been studied and the mRNA level of PTPRG was found to be significantly increased in patient achieving Major Molecular Response (MMR), while this was not the case in non-responsive cases (Vezzalini et al., 2017).

There are currently no clear associations between the expression of a biomarker at mRNA level and its translation at protein level and the link between the two parameters ranged from 40% up to 90% (Nagaraj et al., 2011, Zur and Tuller, 2012). On the contrary, other publications had been reported the low correlation between levels of mRNA and protein expression due to many factors but not limited to steady state, degradation, proteomics, and transcriptomics factors (Karbownik et al., 2016, Kumar et al., 2016, Perl et al., 2017). In the current study, the expression levels of PTPRG at both the mRNA and protein levels were investigated in parallel. While there were not any significant differences in the

expression of *PTPRG* at the mRNA level in the failed group (WSRT p = 0.312) (Figure 3. 3C), there were significant differences in the PTPRG expression level on neutrophils population in CML of the optimally treated group (Figure 3.4A). The results presented in this chapter showed therefore the absence of clear correlation between the expression of various biomarkers at mRNA and protein levels and the importance of studying the expression levels of various biomarkers at both mRNA and protein levels.

In this study, we found that the restoration of the PTPRG level to be significantly higher on the neutrophils population in the optimal response group, when compared to the failed group at two follow up points (2^{nd} and 3^{rd} follow up) (Figure 3. 6C). On the other hand, there wasn't a significant difference in the expression of PTPRG on the monocyte's population between the optimal and the failed groups at any follow up point (Figure 3. 6F). The data also showed that the restoration of PTPRG expression on neutrophils was drug dependent as the expression of PTPRG was restored earlier with Nilotinib when compared to Imatinib Mesylate. This observation might reflect the superior potency of Nilotinib as BCR-ABL1 TKI, which was reported to be 20–50 times more potent than Imatinib, and its ability to achieve complete superior response compared to Imatinib Mesylate (Lipp and Hartmann, 2008).

In another study, Naoto and his colleagues developed a fluorescence in situ hybridization (FISH) technique named "Neutrophil-FISH "that has ability to classify CML cohort to responder and non-responder to Imatinib Mesylate (Takahashi et al., 2005). Here, we have shown the ability of mAB-TPγ -B9-2 to record changes in expression of PTPRG on neutrophils by flow cytometry technique and consequently classify the CML patients in the same manner.

From another perspective, Skewness had ability to capture the degree of asymmetry in data distribution; many studies recommended running the Skewness and kurtosis along with Shapiro wilk test if the data didn't pass the normality assumption. In the same context, recent study showed that Skewness

histogram could reveal new approach into transcription based on asymmetric behaviour in patient's groups (Church et al., 2019).

In the study presented in this chapter, the skewness histogram at diagnosis of neutrophils were negatively skewed suggesting that too many low values to the left of the mean (Figure 3. 6A). On the other hand, skewness histogram at diagnosis of monocytes showed positively skewness (Figure 3. 6D). This will conclude that neutrophils are the most sub-populations of white blood cells affected during disease burden. Furthermore, positively skewed remained constant during follow up of later time points suggesting that to many high values towards the right of the mean (Figure 3. 6A). While the distribution of PTPRG expression showed symmetrical distribution for 1st and 2nd follow up time points of failed treatment (i.e. passed Shapiro-Wilk normality test), and then showed negatively skewed at 3rd follow up time point (Figure 3. 6B). These results suggest that non-normality of PTPRG expression (i.e. over-expression) was required during optimal response to over-compensate the uncontrolled kinase activity during treatment timeline. While PTPRG expression of failed response group showed normality distribution during 1st and 2nd follow up time point that suggest of early indicator of failed treatment prior shifting to negatively skewed (as diagnosis phase). The same finding was observed on monocytes of failed group, the only difference that normality distribution remained constant during follow up periods (Figure 3. 6E).

The restoration of PTPRG expression reached to a level seen at healthy individuals and this may due to that TKIs having a large impact on the PTPRG gene (Cohen's d = 0.81). On the other hand, there was still a significant difference between levels of PTPRG in healthy, optimally, and failed groups. This may be explained by overexpression of PTPRG to overcome the uncontrolled BCR-ABL1 kinase activity.

In relation to expression of PTPRG on myeloid lineage, the previous study by the collaborative team has shown a low level of PTPRG expression on myeloid lineage at diagnosis of CML (Vezzalini et al., 2017). Interestingly, in this study,

the mean PTPRG expression level was found to be higher in hematopoietic stem cells when compared to leukemic stem cells. The Glass' Delta effect size equation showed a small effect size of level of PTPRG at HSCs, while the medium affect size of the level of PTPRG on LSCs (Table 3. 3). Additionally, the expression of PTPRG on LSCs was significantly higher in the failed group when compared to the optimal response. The result was matched with the fact that leukemic stem cells have a unique profile of cell surface, which is different than hematopoietic cells (Thielen et al., 2016). Furthermore, LSCs had the ability to self-renewal (Heidel et al., 2011), and LSCs had a signatory high expression of a gene which independently associated with adverse outcomes of treatment (Andrew J. Gentles, 2010) and could predict the prognosis of the disease (Woolthuis et al., 2010). Additionally, a recent study documented that BCR-ABL1 transcript maybe not transcribed by LSC of CML patients (Houshmand et al., 2019).

Finally, primary resistance and acquired resistance to treatment with BCR-ABL1 TKIs can occur in some patients with CML (Al-Dewik et al., 2015, Apperley, 2007a, Baccarani et al., 2019b). In Qatar, a significantly higher percentage of CML patients develop resistance to TKIs compared to the other parts of the world (Al-Dewik et al., 2014, Ismail et al., 2020). This may be due to most studies in CML management were focused on one component (tyrosine kinases), while the other arm (tyrosine phosphatases) hasn’t yet received equivalent attention.

3.5 Conclusion

In summary, in this study, expression of PTPRG, a tumour suppressor gene, was shown to be suppressed in CML patients at diagnosis and that this can be restored following treatment with BCR-ABL1 TKIs to levels observed in healthy controls. The restoration levels were found to be greatest in optimal responders and occurred earlier with nilotinib compared with Imatinib. Taken together, the results presented in this chapter provide support for the potential use of PTPRG expression determined by flow cytometry as a new biomarker of response to treatment with BCR-ABL1 TKIs and the clinical management of CML patients.

4 Identification of PTPRG genetic variants in a cohort of Chronic Myeloid Leukaemia patients and their ability to influence the response to Tyrosine kinase Inhibitors

This chapter will discuss possible alteration in *PTPRG* gene, and its potential to influence response to treatment with TKIs.

4.1 Introduction

Background: Tyrosine kinase inhibitors (TKIs) have remarkably transformed Ph+ chronic myeloid leukaemia (CML) management; however, TKI resistance remains a major clinical challenge. Mutations in *BCR-ABL1* are well studied but fail to explain 20–40% of resistant cases, suggesting the activation of alternative, BCR-ABL1-independent pathways (Braun et al., 2020). Protein Tyrosine Phosphatase Receptor Gamma (PTPRG), a tumour suppressor, was found to be well expressed in CML patients responsive to TKIs and down regulated in resistant patients (Ismail et al., 2021).

Aim: In this chapter, the aim to identify genetic variants in *PTPRG* that could potentially modulate TKIs response in CML patients.

Methods: DNA was extracted from peripheral blood samples from two CML cohorts (Qatar and Italy) and targeted exome sequencing was performed. Custom primers were used to target specific region of *PTPRG* gene. The DNA were amplified using Ion AmpliSeq Library kit 2.0. The amplicons were ligated with Ion Xpress barcode adapters after partially digesting with FuPa reagent. Next, the amplicons were cleaned up using HighPrep reagent and enriched with adapter specific primers using a limited cycle PCR. The final libraries were quantified on Qubit Fluorometer and samples were pooled and loaded on Ion 318TM Chip kit V2 to be sequenced on Ion Personal Genome Machine (PGM) system. Finally, data were collected directly from software tools then analysed with excel sheet. Thirty-one CML samples (six were TKI-responders and 25 were TKI-resistant) were collected from CML patients at different intervals during the treatment plan, at day one of diagnosis, and at the time of achieving response or failed/relapsed treatments, as described previously. The CML patients' response to treatment was evaluated according to the cytogenetic, hematologic, and molecular responses, as described in the materials and methods chapter. The responder cohort had the ability to

achieve haematological, molecular, and cytogenetic responses, regardless of the time frame. Patients with resistance to treatment (failure cohort) were defined as group showing a lack of any response following a maximum of 36 months follow-up.

Result: Sequencing identified ten variants, seven were annotated and three were novel SNPs (c.1602_1603insC, c.85+14412delC, and c.2289-129delA). Among them, five variants were identified in 15 resistant cases. Of these, one novel exon variant (c.1602_1603insC), c.841-29C>T (rs199917960) and c.1378-224A>G (rs2063204) were found to be significantly different between the resistant cases compared to responders.

Conclusion: Taken together, these findings suggest that *PTPRG* variants may act as an indirect mechanism of resistance to treatment with the BCR-ABL1 TKIs.

4.2 Results

Patient demographic and disease characteristics are presented in (Table 4. 1). In total, 31 CML patients (24 males and 7 females) were included in the study; 17 from Qatar and 14 from Italy. The mean age was 44.4 years. Regarding the clinical phase at diagnosis, 29 (93.5%) patients were in the chronic phase (CP) and 2 (6.5%) patients were in accelerated phase (AP) (CML cases 20 and 23). Out of 29 patients in CP, 28 were treated with imatinib 400 mg/day and the remaining were on nilotinib 300 mg/day (CML case 30), while patients in AP were treated with imatinib 600 mg/day (CML cases 20 and 23). The patients' median follow-up was 24.5 months (range: 6 to 36 months). Out of the 31 CML patients treated with TKIs, 6 patients achieved response (BCR-ABL <1 %) (19%), and 25 patients failed treatment (81%). PTPRG expression of 11 out of 17 CML patients from Qatar was assisted as described in previous chapter. None of the patients had additional chromosomal anomalies (ACA) during the study.

Table 4. 1 CML patient's characterization for sequencing experiment.

*TKIs and overall response timeline. * indicates CML patients from the Italian cohort. CML case 31- achieved molecular response at 1st follow up (3 months), while PTPRG protein expression restored its expression on 2nd follow up (6 months).*

Patients	BCR-ABL1(IS)	PTPRG	Response	follow up Timeline (Months)	Remarks

CML case 01.	100	0.01	Failed	12	
CML case 02.	42.2	1.2	Failed	36	4 subsequent samples
CML case 03.	100	0.01	Failed	15	
CML case 04.	63.4	0.01	Failed	36	2 subsequent samples
CML case 05.	8.2	0.04	Failed	36	2 subsequent samples
CML case 06.	100	N/A	Failed	36	
CML case 07.	100	0.01	Failed	36	
CML case 08.	100	0.1	Failed	24	
CML case 09.	87.1	0.01	Failed	18	
CML case 10.	100	0.1	Failed	20	
CML case 11.	100	0.01	Failed	36	
CML case 12.	100	0.01	Failed	24	2 subsequent samples
CML case 13.	100	0.02	Failed	12	
CML case 14.	73.4	0.01	Failed	36	
CML case 15.	60	0.01	Failed	36	
CML case 16	100	0.01	Failed	–	Single time point
CML case 17*.	100	0.37	Failed	36	
CML case 18*.	86	1.78	Failed	36	
CML case 19*.	100	0.37	Failed	36	
CML case 20*.	91	N/A	Failed	12	
CML case 21*.	101	0.04	Failed	36	
CML case 22*.	113	1.52	Failed	12	
CML case 23*.	19	0.15	Failed	36	
CML case 24*.	100	0.05	Failed	36	1 subsequent sample
CML case 25*.	84	0.03	Failed	24	
CML case 26*.	100	0.13	Responder	24	1 subsequent sample
CML case 27*.	100	4.15	Responder	24	
CML case 28*.	34	0.46	Responder	15	
CML case 29*.	62	0.001	Responder	36	1 subsequent

					sample
CML case 30*.	65	0.01	Responder	6	
CML case 31*.	89	0.01	Responder	12	

4.2.1 Molecular genetic findings

Forty-four samples were sequenced using good quality metrics, with a mean depth of 2,000x from the samples. We detected two missense, one synonymous substitution, one in-frameshift indel and substitution, and six variants in the intronic region.

PTPRG sequencing identified five variants that were distinctive for resistant CML cases only at the time of diagnosis and during follow up. Of the five homozygous variants, c.841-29C>T was identified in three patients, and c.1720G>A; p. Gly574Ser was identified in two patients. The variant c.274T>C; p.Tyr92His was found in homozygous and heterozygous forms in six resistant cases (one homozygous and five heterozygous from the Italian and Qatari cohorts, respectively), while, c.1034-46C>T, was identified as homozygous and heterozygous forms in 2 resistant cases from Qatar cohort. In addition to the above, one novel heterozygous variant was identified in the TKI-resistant CML patient group (c.1602_1603insC; Thr536HisfsTer15), which was identified in two CML patients from the Italian cohort (Table 4. 2).

Apart from above variants, two homozygous variants (2448C>T and c.86-13T>C) were identified in 31 and eight CML cases, respectively. Furthermore, five heterozygous variants (c.1378-224A>G, c.86-13T>C c.841-29C>T, c.1720G>A, c.85+14412delC, and c.2289-129delA) were identified in CML patient (s) number, ten, twelve, seventeen, twenty one, twenty five and thirty one respectively (Table 4. 1). These variants were identified at the time of diagnosis and during follow-up.

Table 4. 2 PTPRG Genetic variants identified in CML patients.

RefSeq no.	Location	Nucleic Acid Position	Amino Acid Change	Zygosity	No patients
rs199917960*	Intron 7	c.841-29C>T	NA	Homo Hetro	3* 10

rs62620047*	Exon 3	c.274T>C	p. Tyr92His	Homo Hetro	1* 5*
rs2292245*	Exon 12	c.1720G>A	p. Gly574Ser	Homo* Hetro	2* 12
rs57829866*	Intron11	c.1034-46C>T	NA	Homo Hetro	1* 1*
Novel1*	Exon 12	c.1602_1603insC	p. Thr536HisfsTer15	Hetro	2*
rs1352882	Exon15	2448C>T	p. Ile816 Ile	Homo	31
rs2063204	Intron 11	c.1378-224A>G	NA	Hetro Homo	29 2
rs3821880	Intron 1	c.86-13T>C	NA	Hetro Homo	17 8
Novel 2	Intron 1	c.85+14412delC	NA	Hetro	25
Novel 3	Intron 13	c.2289-129delA	NA	Hetro	21

4.2.2 Association of PTPRG variants with CML disease

Genotyping and alleles analysis showed that two out of seven *PTPRG* variants were significantly associated with CML disease (Table 4. 3). The rs199917960 variant had three genotypes as C/C, C/T and T/T with frequencies 58%, 32.3% and 9.7%, respectively among the CML patients' group, whereas in the 1000 Genomes Project control the frequencies were C/C: 99.96%, C/T: 0.04% and T/T: 0%, respectively (P <0.0001) as well as QGP C/C: 100%, C/T and T/T: 0%. On the other hand, the three genotypes of rs2063204 were A/A, A/G and G/G with frequencies of 0%, 93.4 % and 6.5%, respectively, among CML patients, and frequencies of 0.08%, 2.8% and 97.12%, respectively in the 1000 Genomes Project control (P <0.0001), while in QGP was 0.03%, 0.9% and 99.07% (P <0.0001). The frequency of the major (C) allele in rs199917960 variant was 74.2% and 99.9% for the CML patients and control group (1000 Genome project) respectively, while the minor (T) allele frequency was 25.8% and 0.01% for CML patients and control group respectively. Notably the distribution of allele frequency was statistically significant between the indicated groups (Table 4. 3). Further, the frequencies of the major (A) and the minor (G) alleles in rs2063204 variant were 46.8% and 53.2% vs. 1.5% and 98.5% among the CML patients' and control groups, respectively.

Genotyping and alleles analysis of QGP showed similar findings of variants when compared to the 1000 Genomes Project control; in addition, rs62620047 and rs57829866 were statistically significant. Rs62620047 variant showed three genotypes as T/T, T/C and C/C with frequencies 80.6%, 16.2% and 3.2%. While the genotypes frequencies of QGP controls were 58.2%, 34.9% and 6.9% respectively. Then again, three genotypes of rs57829866 variant as C/C, C/T T/T with frequencies 93.6%, 3.2 % and 3.2 % which corresponding to 96.8%, 3.0% and 0.2% in QGP controls. The frequency of the major (T) allele in rs62620047 variant was 88.7% and 75.7% for the CML patients and control group respectively. While the minor (C) allele frequency was 11.3% and 24.3% as well for CML patients and control group respectively. Notably the distribution of allele frequency was statistically significant between mentioned groups (Table 4. 3). The variant rs57829866 major (C) allele frequency was 95.2% (CML patients) vs. 98.4% (control group), and the minor (T) allele frequency was 4.8% (CML patients) vs. 1.6% (control group). However, statistical significance was lost between allele frequency distribution (Table 4. 3).

In comparison to the 1000 Genomes Project, rs199917960 was significantly associated with CML disease in all models: co-dominant (C/T vs C/C: OR = 1390.6, 95% CI: 169.0–218 11438.7), *P* <0.0001; T/T vs. C/C: OR = 947.3, 95% CI: 47.2–18994.7), *P* < 0.0001), dominant (OR = 1807.7, 95% CI: 224.5–14559.3, *P* <0.0001); recessive (OR = 615.1, 95% CI: 31.05–12185.6), *P* < 0.0001), and over–dominant (OR = 1191.9, 95% CI: 145.9–9733.8), *P* < 0.0001) (Table 4. 4). On the other hand, rs2063204 was significantly associated with CML disease in the recessive and over-dominant models only (G/G vs. A/A-A/G: OR = 0.002, 95% CI: 0.0005–0.0086, *P* <0.0001; A/G vs. A/A–G/G: OR = 511.7, 95% CI: 119.7–2187.5, *P* <0.0001) (Table 4. 4).

In comparison to QGP, rs199917960 was significantly associated with CML disease in all models: co-dominant (C/T vs C/C: OR =16651.9, 95% CI: 940.8–294717.9, *P* <0.0001; T/T vs. C/C: OR = 5550.6, 95% CI: 276.9–111277.7, *P* < 0.0001), dominant (OR = 21409.5, 95% CI: 1226.9- 373587.0534, *P* < 0.0001); recessive (OR =3603.0, 95% CI:181.9–71358.7, *P* < 0.0001), and over–dominant (OR =14328.3, 95% CI:

813.7–252318.0, *P* < 0.0001) (Table 4. 4). Again, rs2063204 was significant in the co-dominant, recessive, and over-dominant models only (G/G vs. A/A: OR = 0.0012, 95% CI: 0.0000–0.0299, *P* < 0.0001, A/A-A/G vs. G/G: OR = 0.0006, 95% CI: 0.0002–0.0027, *P* < 0.0001; A/A–G/G vs. A/G: OR = 1584.8, 95% CI: 374.3–6709.2436, *P* <0.0001) (Table 4. 4). The variant rs62620047 was significantly associated with CML in the co-dominant (T/C vs T/T: 0.33, 95% CI: 0.13-0.87, *P* =0.025), dominant (T/C–C/C vs. T/T: OR = 0.33, 95% CI: 0.14-0.82, *P*= 0.016) and over-dominant models (T/C vs. T/T-C-C: OR = 0.36, 95% CI: 0.14-0.93, *P* =0.036 (Table 4. 5). In contrast, rs57829866 was significantly associated with CML disease in the co-dominant model only (T/T vs. C/C: OR =28.82, 95% CI: 3.71-223.72, *P*< 0.001). Notably, rs62620047 and rs57829866 variants were exclusive only with QGP (Table 4. 5).

Table 4. 3 Genotype and allele frequencies of variants of PTPRG in CML patients in comparison to 1000 Genomes Project and QGP.

referred to total number for rs1352882 was 14649.* ***Bold* *value denotes statistically significant differences between CML group and reference group (1000 Genomes Project).*

Genetic variants	Genotype	CML patients N=31	1000 Genomes Project Reference N=2504	*P* value	QGP Reference N=14669	*P* value	Allele	CML	Reference	*P* value	QGP Reference	*P* value
rs199917960	C/C	18 (58%)	2503 (99.96%)	**<0.0001**	14669 (100%)	**<0.001**	C	46 (74.2%)	5007 (99.9%)	**<0.0001**	29338 (100%)	**<0.0001**
	C/T	10 (32.3%)	1 (0.04%)		0 (0%)		T	16 (25.8%)	1 (0.01%)		0 (0%)	
	T/T	3 (9.7%)	0 (0%)		0 (0%)							
rs62620047	T/T	25 (80.6%)	2092 (83.54%)	0.5400	8538 (58.2%)	**0.04**	T	55 (88.7%)	4568 (91.2%)	0.4949	22196 (75.7%)	**0.0168**
	T/C	5 (16.2%)	384 (15.34%)		5120 (34.9%)		C	7 (11.3%)	440 (8.8%)		7142 (24.3%)	
	C/C	1 (3.2%)	28 (1.12%)		1011 (6.9%)							
rs2292245	G/G	17 (54.8%)	1565 (62.5%)	0.6699	7616 (51.9%)	0.840	G	46 (74.2%)	3919 (78.3%)	0.4399	20995 (71.6%)	0.7781
	G/A	12 (38.7%)	789 (31.5%)		5763 (39.3%)		A	16 (25.8%)	1089 (21.7%)		8343 (28.4%)	
	A/A	2 (6.5%)	150 (6.0%)		1290 (8.8%)							

rs57829866	C/C	29 (93.6)	2245 (89.7%)	0.2654	14206 (96.8%)	**<0.0001**	C	59 (95.2%)	4723 (94.3%)	>0.9999	28858 (98.4%)	0.0820
	C/T	1 (3.2%)	33 (9.3%)		446 (3.0%)		T	3 (4.8%)	285 (5.7%)		480 (1.6%)	
	T/T	1 (3.2%)	26 (1.0%)		17 (0.2%)							
rs1352882*	C/C	0	9 (0.3%)	0.5214	4 (0.03%)	0.8264	C	0	101 (2.2%)	0.6457	182 (0.6%)	>0.9999
	C/T	0	92 (3.7%)		174 (1.19%)		T	62 (100%)	4898 (97.8%)		29116 (99.4%)	
	T/T	31 (100%)	2403 (96%)		14471 (98.78%)							
rs2063204	A/A	0	2 (0.08%)	**<0.0001**	3 (0.03%)	**<0.0001**	A	29 (46.8%)	73 (1.5%)	**<0.0001**	139 (0.5%)	**<0.0001**
	A/G	29 (93.4%)	69 (2.8%)		133 (0.9%)		G	33 (53.2%)	4935 (98.5%)		29199 (99.5%)	
	G/G	2 (6.5%)	2433 (97.12%)		14533 (99.07%)							
rs3821880	T/T	6 (19.4%)	415 (16.6%)	0.5144	2757 (18.8%)	0.5	T	29 (47.8%)	2023 (40.4%)	0.3622	12214 (41.6%)	0.4403
	T/C	17 (54.8%)	1193 (47.6%)		6700 (45.7%)		C	33 (53.2%)	2985 (59.6%)		17124 (58.4%)	
	C/C	8 (25.8%)	896 (35.8%)		5212 (35.5%)							

Table 4. 4 Logistic regression analysis of the association amongst PTPRG variants (rs199917960 and rs2063204) in CML patients with 1000 Genome and QGP projects.

N.R: Not reported. ***Bold*** *value denotes statistically significant*

Model	Genotype	*1000 Genomes Project Reference N=2504	**QGP Reference N=14669	CML patients N=31	*OR (95% CI)	*P* value	**OR (95% CI)	*P* value
rs199917960								
Co-dominant	C/C	2503 (99.96%)	14669 (100%)	18 (58%)	R			
	C/T	1 (0.04%)	0 (0%)	10 (32.3%)	1390 (169.0-11438.7)	**<0.0001**	16651.9 (940.8-294717.9)	**<0.0001**
	T/T	0 (0%)	0 (0%)	3 (9.7%)	947.3 (74.1–18994.7))	**<0.0001**	5550.6 (276.9-111277.7)	**<0.0001**
Dominant	C/C	2503 (99.96%)	14669 (100%)	18 (58.06%)	R			
	C/T-T/T	1 (0.04%)	0 (0%)	13 (41.94%)	1807.7 (224.5-14559.3)	**<0.0001**	21409.5 (1226.9- 73587.1)	**<0.0001**
Recessive	C/C- C/T	2504 (100%)	14669 (100%)	28 (90.32%)	R			
	T/T	0 (0%)	0 (0%)	3 (9.68%)	N/A (47.60–NA)	**<0.0001**	3603.0 (181.9-71358.7)	**<0.0001**

Over- dominant	C/C-T/T	2503 (99.96%	14669 (100%)	21	R	**<0.0001**	14328 (813.7-252318.1	
	C/T	1 (0.04%)	0 (0%)	10	1192 (145.9-9733.8)			
rs2063204								
Co-dominant	A/A	2 (0.08%)	3 (0.03%)	0 (0%)	R			
	A/G	69 (2.8%)	133 (0.9%)	29 (93.5%)	N/A (0.1884-NA)	>0.9999	N/A (0.1833–NA)	>0.9999
	G/G	2433 (97.12%)	14533 (99.07%)	2 (6.5%)	N/A (0.0003054–NA)	>0.9999	N/A (0.000836–NA)	>0.9999
Dominant	A/A	2	3	0	R			
	A/G-G/G	2502	14666	31	N/A (0.005663–NA)	>0.9999	N/A (0.001799 –NA)	>0.9999
Recessive	A/A–A/G	71	136	29	R			
	G/G	2433	14533	2	0.002013 (0.00047–0.0074)	**<0.0001**	0.0006454 (0.0001512–0.002526)	**<0.0001**
Over-dominant	A/A-G/G	2435	14536	2	R			
	A/G	69	133	29	511.7 (138.7–2734)	**<0.0001**	1585 (404.6–10902)	**<0.0001**

Table 4. 5 Logistic regression analysis of the association between PTPRG variants gene rs62620047, rs57829866 and CML disease.

Model	Genotype	QGP Reference Reference N=14669	CML patients N=31	OR (95% CI)	*P* value
rs62620047					
Co-dominant	T/T	8538 (58.2%)	25 (80.6%)	R	
	T/C	5120 (34.9%)	5 (16.2%)	0.3335 (0.1384-0.8300)	**0.04**
	C/C	1011 (0%)	1 (3.2%)	0.3378 (0.05029-2.024)	
Dominant	T/T	8538	25	R	**0.01**
	T/C-C/C	6131	6	0.3342 (0.1432-0.7644)	
Recessive	T/T-T/C	13.658	30	R	0.72
	C/C	1011	1	0.4503 (0.2558-2.545)	
Over-dominant	T/T-C-C	9549	26	R	**0.036**
	T/C	5120	5	0.3587 (0.1492-0.8842)	
rs57829866					
Co-dominant	C/C	14206(96.8%)	29 (93.6%)	R	**<0.0001**
	C/T	446 (3.0%)	1 (3.2%)	1.098 (0.1496-6.265)	
	T/T	17 (0.2%)	1 (3.2%)	28.82 (3.712-187.2)	
Dominant	C/C	14206	29	R	0.26
	C/T-C/C	463	2	2.116 (1.310-8.060)	
Recessive	C/C-C/T	14652	30	R	0.3671
	T/T	217	1	2.251(0.3056-12.88)	
Over-dominant	C/C-T/T	14223	30	R	0.61
	C/T	446	1	1.063(0.1446-6.034)	

Bold *value denotes statistically significant.*

4.2.3 Correlation of PTPRG SNPS with overall outcome of CML patients

Finally, the models for rs199917960 and rs2063204 were investigated amongst the responsive and non-responsive groups. Rs199917960 was significantly associated with non-responders in the co-dominant (T/T vs. C/C: OR = 259.0 (4.3655 -15366.1, *P* = 0.0076), dominant (C/T-T/T vs. C/C: OR = 32.01 (1.5981 - 643.4, *P*= 0.0234), and recessive (T/T vs. C/C- C/T: OR = 51.0 (2.2 - 1210.4, *P* = 0.015) models when compared to the responders group. However, no significant association was observed in the over-dominant model (Table 4. 6). The variant rs2063204 was significantly associated with non-responsive in the recessive and over-dominant models (G/G vs. A/A–A/G: OR = 28.3 (1.2 - 693.4 *P* = 0.0404) and (A/G vs. A/A–G/G: OR = 0.0353 (0.0014 - 0.87 *P* = 0.0404) correspondingly. However, this significance was lost in the co-dominant and dominant models in comparison to responsive group (Table 4. 6).

Table 4. 6 Logistic regression analysis of the association between PTPRG variants (rs199917960 and rs2063204) and overall response.

Bold *value denotes statistically significant.*

Model	Genotype	Non-responders N =25	Responders N=6	OR (95% CI)	*P* value
rs199917960					
Co-dominant	C/C	18 (72%)	0 (%)	R	
	C/T	7(28%)	3(50%)	17.2667 (0.79–376.6)	0.0701
	T/T	0 (0%)	3 (50%)	259(4.4–15366.1)	**0.0076**
Dominant	C/C	18(72%)	0	R	**0.0234**
	C/T-T/T	7 (28%)	6 (100%)	32.0667 (1.6–643.4)	
Recessive	C/C- C/T	25 (100%)	3 (50%)	R	**0.015**
	T/T	0 (0%)	3 (50%)	51.0 (2.1–1210.4)	
Over-dominant	C/C-T/T	18 (72%)	3 (50%)	R	0.3099
	C/T	7 (28%)	3 (50%)	2.5714(0.42–15.91)	
rs2063204					
Co-dominant	A/A	0 (0%)	0 (0%)	R	
	A/G	25 (100%)	4 (66.7%)	0.1765 (0.42–15.92)	0.4008
	G/G	0(%)	2 (33.3%)	5.000 (0.04–711.9)	0.5247
Dominant	A/A	0 (0%)	0	R	0.5044
	A/G-G/G	25 (100%)	6 (100%)	0.2549 (0.005–14.1)	
Recessive	A/A-A/G	25 (100%)	4(66.7%)	R	**0.0404**
	G/G	0 (0%)	2 (33.3%)	28.3 (1.16–14.10)	
Over-dominant	A/A-G/G	0 (0%)	2 (33.3%)	R	**0.0404**
	A/G	25 (100%)	4 (66.7%)	0.035 (0.01–0.87)	

4.3 Discussion

Despite the great progress that has been made in the treatment of many CML patient with the BCR-ABL1 TKIs in the past years, drug resistance continues to be a major issue for CML patients, suggesting that the activation of alternative, BCR-ABL1-independent survival pathways may be linked to TKI efficacy and disease progression (Boni and Sorio, 2021, Chaitanya et al., 2017, Harrington et al., 2017). While *BCR-ABL1* mutations have been extensively studied, studies on BCR-ABL1-independent mechanisms are not yet received equivalent attention.

In this study, the aim was to identify possible genetic variants in *PTPRG* that could potentially modulate response to TKIs in CML patients. To my knowledge, the present study is the first to identify homozygous variants in *PTPRG* in association with Imatinib and Nilotinib response among CML patients. Of the 31 CML patients; 6 were TKI-responders; and 25 were TKI-resistant. The study identified ten variants in *PTPRG*, of which seven were previously annotated and three were novel variants (Table 4. 2). Of the ten identified *PTPRG* variants, five were distinctive for the TKI-resistant CML patient's group, and six were found to be shared among responders and resistant CML patients. None of the identified variants were previously reported in ClinVar database (ncbi.nlm.nih.gov/clinvar).

Variants in the intronic region do not encode proteins. However, intronic variants were reported to influence gene and protein expression (Deng et al., 2017, Do et al., 2010, Tran et al., 2005). In the present study, six intronic variants were identified and a statistically significant difference was observed for the intronic variants rs199917960 and rs2063204 between CML patients in comparison to 1000 Genomes Project as well as the Qatar genome program (control) (Table 4. 3). These findings were further confirmed when the responders were compared against the non-responders' groups (Table 4. 6), suggesting that both rs199917960 and rs2063204 might be linked to TKI response in CML patients.

In the present study, the major allele (C allele) of rs199917960 predominated in the reference group with a frequency of 99.9% in comparison to 74.2% in CML patients'

group (<0.0001), whereas the minor allele (T allele) frequency was 25.8% in the CML group which was significantly higher compared to the reference group (0.01%) (*P* <0.0005). The percentage of dominant homozygous (C/C) was higher in reference group (99.96%), while the percentage of heterozygous (C/T) and recessive allele (T/T) was significantly higher in CML group (C/C: 32.3% and T/T: 9.7%) in comparison to reference group (C/C: 0.04% and T/T: 0%). The variant was significantly correlated with CML disease risk in all models (Table 4. 4). While regarding QGP, the major allele (C allele) was 100% and absence of minor allele (T allele) frequency.

The major allele (A allele) of rs2063204 variant was found to be significantly predominates in the CML patients' group with an allelic frequency of 46.8% compared to 1.5% in the reference group (Table 4. 3). In contrast, the minor allele (G allele) frequency was significantly higher in the reference group (98.5%) in comparison to the CML group (53.2%) (*P* <0.0001). The percentage of dominant homozygous (A/A) and heterozygous (A/G) was almost same in reference and CML groups, while the percentage of recessive allele (G/G) was higher in reference group 97.2% in comparison to CML group 6.5 % (*P* <0.0005). The variant was significantly correlated with CML disease risk in the recessive and over-dominant models; however this significance was lost in the co-dominant and dominant models (Table 4. 4). These findings are in concordance with the data base from QGP and may explain the presence of rs2063204 in the responder and non-responder patient groups. Interestingly, the same findings were confirmed when the responders and non-responder groups were compared, the only difference being that significance was lost in over-dominant models for rs199917960 (Table 4. 6).

Interestingly, two variants (rs62620047 and rs57829866) with statistically significant differences were found when compared to QGP but this significance was lost when compared to 1000 Genomes Project reference. The variant rs62620047 was found to be associated with CML disease in the co-dominant and dominant models; nevertheless, this association was lost in the recessive and over-dominant models (Table 4. 5). In addition, a significant association was observed between rs57829866 and CML disease in the co-dominant only (Table 4. 5). Notably, this variant was

reported in resistance case only (Table 4. 2). Therefore, it is reasonable to suggest that carriers of rs57829866 are more likely to acquire resistance towards TKI therapy in CML.

This study identified three novel variants, among which one was a frameshift (c.1602_1603insC) that was identified in two patients from the Italian cohort, located in the coding region of *PTPRG*. The remaining two variants (c.85+14412delC and c.2289-129delA) are in intronic regions, and both are deletion variants. The identified *PTPRG* variants in both cohort groups (Qatar and Italy). Of these, one coding sequence homozygous variant (rs1352882; 2448C>T) was found in the promoter region of *PTPRG* which was identified in all 31 CML patients. In addition, two missense variants (1720G>A and c.274T>C) were found in the coding region of *PTPRG*. Interestingly, c.274T>C was identified in homozygous alleles in the Italian group, but present in heterozygosity in Qatari group. However, no significant differences were observed, when compared to the 1000 Genomes Project reference (control).

A limitation of this study was the small sample size. However, this is one of the few studies on BCR-ABL1-independent mechanisms and the first study to identify homozygous mutations in *PTPRG* that are associated with Imatinib and Nilotinib response in patients with CML disease.

In-silico investigations on the structural changes in the PTPRG protein due to the mutation are warranted and will pave the way for understanding molecular mechanisms involved. In addition, further investigations of genetic variants in *PTPRG* gene in a larger group of CML patients are warranted and could lead to design of better therapeutic modalities such as dose elevation or earlier consideration of second and third generation drugs and these can ultimately help to improve the treatment outcomes and long-term prognosis in CML patients. The homozygous variants could affect the PTPRG structure causing protein loss of function. However, the pathogenicity of these variants in the *PTPRG* gene is uncertain and requires detailed characterization for functional consequences in appropriate disease models.

These findings suggest that *PTPRG* variants could be an indirect mechanism that affects the efficacy of the treatment plan. It may cause delay in patients' response to treatment as significant numbers of CML patients on imatinib treatment have not achieved response within 12 months.

4.4 Summary and Conclusions

CML is one the most common type of adult leukaemia in the world. In the present study, the aim was to identify genetic variants in the *PTPRG* gene in CML patients from two independent cohorts based on potential related clinical outcomes. The findings addressed possible variants associated with *PTPRG* and how it may affect the efficacy of the treatments plan, particularly in Imatinib Mesylate treatment and act as an indirect resistance mechanism of BCR-ABL1. While, other studies showed that PTPRG restoration was achieved earlier with nilotinib treatment and more likely with PTPRG-WT, while this observation lost with mutant *PTPRG* (Drube et al., 2018, Ismail et al., 2021).

Thus, these findings suggest that *PTPRG* could serve as an independent prognostic tool for CML. The identified variants could influence drug efficacy and disease progression and thus might help provide a better understanding of mechanisms of resistance. However, further investigations of genetic variants in *PTPRG* gene in a larger group of CML patients are warranted and could lead to design of better therapeutic modalities such as dose elevation or earlier consideration of second, third, and fourth generation drugs and these can ultimately help to improve the treatment outcomes and long-term prognosis in CML patients. Moreover, While the homozygous variants could affect the *PTPRG* structure causing protein loss of function, the pathogenicity of these variants in the *PTPRG* gene is uncertain and requires detailed characterization for functional consequences in appropriate disease models. These findings, together with numerous functional data available in the literature, provide further support on the importance of *PTPRG* and its variants for in optimizing the therapeutic strategies for CML patients.

5 Aberrant DNA methylation of PTPRG as one possible mechanism of its under-expression in CML patients in the State of Qatar

This chapter will discuss and provide data on DNA methylation as possible mechanism of down regulation of *PTPRG* gene.

5.1 Introduction

Background: Several studies showed that aberrant DNA methylation is involved in leukaemia and cancer pathogenesis (Jelinek et al., 2011). Protein Tyrosine Phosphatase Receptor Gamma (*PTPRG*) expression is a natural inhibitory mechanism that is down regulated in Chronic Myeloid Leukaemia (CML) disease (Della Peruta et al., 2010). However, the mechanism behind its down-regulation has not been fully elucidated yet.

Aim: In this chapter the aim was to investigate the extent of CpG methylation at *PTPRG* locus in a series of CML patients.

Methods: Peripheral blood samples from CML patients at time of diagnosis [no tyrosine kinase inhibitors (TKIs)] (n=13) and failure to (TKIs) treatment (n=13) and healthy controls (n=6) were collected, as described in the materials and methods chapter (please refer to the corresponding section in Method chapter). DNA was extracted and treated with bisulfite treatment, followed by PCR and sequencing of 25 CpG sites in the promoter region and 26 CpG sites in intron-1region of *PTPRG*. The bisulfite-sequencing technique was employed as a high-resolution method, as described in the materials and methods chapter.

Results: CML groups (new diagnosed and failed treatment) showed significantly higher methylation levels in the promoter and intron-1 regions of *PTPRG* compared to the healthy group. There were also significant differences in methylation levels of CpG sites in the promoter and intron-1 regions amongst the groups.

Conclusion: Taken together, the results presented in this chapter provide evidence that aberrant methylation of *PTPRG* is potentially one of the possible mechanisms of *PTPRG* down-regulation detected in CML.

5.2 Results

Out of the 26 CML patients, 13 were newly diagnosed (ND) with CML and 13 failed treatment (F) (Table 5. 1). Twenty-one samples in chapter 3 (page 91) were studied again here for methylation status. Patients' age ranged from 25-60 years (mean 37.48 and SD: 9.82) with a male to female ratio of 18 (69.2%) males and 8 (30.8%) females. In addition, there were 6 healthy participants who have never had cancer (H) (Age range: 23-46 years mean: 37.17; SD: 9.58; Gender: 5 (83.3%) male and 1 (16.7%) female). Out of the 26 patients, 24 patients were in Chronic Phase (CP) (92.3%), one patient was in Accelerated Phase (AP) (3.85%) and one patient was in Blast Crisis (BC) phase.

Table 5. 1 CML patients' characteristics in Methylation experiment.
According to gender, age, clinical phase, the type, and total dose of TKIs received and response to treatments. CP; Chronic phase. AP; Accelerated phase. BC; Blast crisis phase

Patients	Gender Male (M), Female (F)	Age (years)	Clinical phase	BCR/ ABL1 (IS)	PTPRG/ ABL* 100	Treatment	Response
CML case 01.	M	45	CP	100%	0.02%	No treatment.	Newly diagnosed
CML case 02.	M	23	CP	100%	0.01%	No treatment.	Newly diagnosed
CML case 03.	M	28	CP	100%	0.01%	No treatment.	Newly diagnosed
CML case 04.	M	38	CP	100%	0.01%	No treatment.	Newly diagnosed
CML case 05.	M	43	AP	100%	0.01%	No treatment.	Newly diagnosed
CML case 06.	F	45	CP	100%	0.01%	No treatment.	Newly diagnosed
CML case 07.	M	46	CP	100%	0.02%	No treatment.	Newly diagnosed
CML case 08.	F	28	CP	100%	0.01%	No treatment.	Newly diagnosed
CML case 09.	M	40	CP	100%	0.01%	No treatment.	Newly diagnosed
CML case 10.	M	34	CP	100%	0.01%	No treatment.	Newly diagnosed
CML case 11.	M	58	CP	100%	0.01%	No treatment.	Newly diagnosed
CML case 12.	F	43	CP	100%	0.01%	No treatment.	Newly diagnosed
CML case 13.	M	32	CP	100%	0.01%	No treatment.	Newly diagnosed
CML case 14.	F	49	CP	37%	0.2%	Imatinib (400mg)	Failed treatment

						No changes in treatment	
CML case 15.	F	35	CP	86%	0.01%	Imatinib (400mg), then shift to Dasatinib (50 mg)	Failed treatment
CML case 16.	M	23	CP	35%	0.3%	Imatinib (400mg) No changes in treatment	Failed treatment
CML case 17.	M	25	CP	12%	0.3%	Imatinib (400mg) No changes in treatment	Failed treatment
CML case 18.	F	34	CP	45%	0.2%	Imatinib (400mg) No changes in treatment	Failed treatment
CML case 19.	M	31	CP	33%	0.2%	Imatinib (400mg) No changes in treatment	Failed treatment
CML case 20.	F	29	CP	25%	0.3%	Imatinib (400mg) No changes in treatment	Failed treatment
CML case 21.	F	35	CP	68%	0.1%	Imatinib (400mg) No changes in treatment	Failed treatment
CML case 22.	M	38	CP	80%	0.02%	Imatinib (400mg) No changes in treatment	Failed treatment
CML case 23.	M	38	CP	60%	0.1%	Imatinib (400mg) No changes in treatment	Failed treatment
CML case 24.	M	34	CP	55%	0.1%	Imatinib (400mg) No changes in treatment	Failed treatment
CML case 25.	F	35	CP	68%	0.1%	Nilotinib (300mg) No changes in treatment	Failed treatment
CML case 26.	M	40	BC	15%	0.3%	Dasatinib (70 mg) No changes in treatment	Failed treatment

5.2.1 Gradient Polymerase Chain reaction

Gradient PCR was performed to find the specific annealing temperature for the selected gene. Specific products 321bp and 218bp were detected at 60°C for promoter and intron-1 regions of PTPRG, respectively. Bisulfite treatment was performed followed by Sanger sequencing (Figure 5. 1).

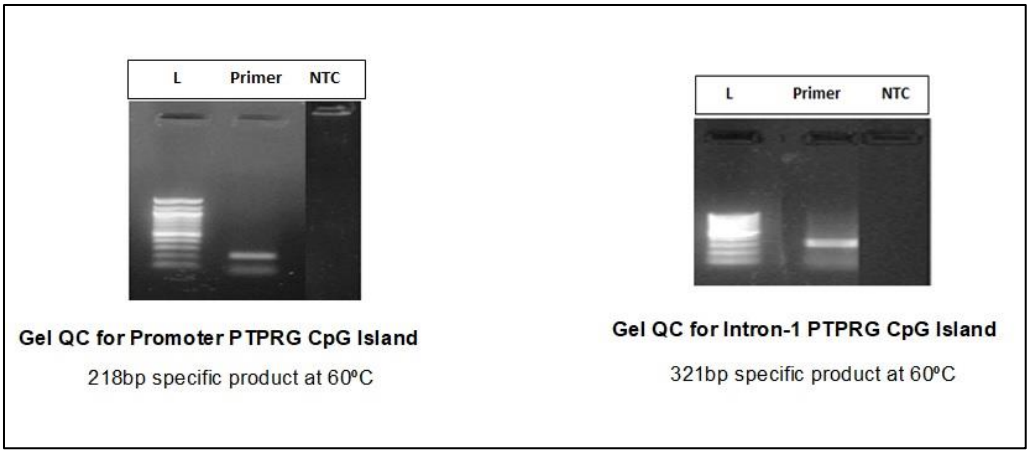

Figure 5. 1 218bp & 321 Products of PCR of Promoter and Intron-1.

5.2.2 Hypermethylation of the Promoter region of PTPRG

T-test was performed to study the methylation pattern of promoter of PTPRG in both cases and controls. The results revealed a significant difference in promoter methylation levels between CML (ND and F groups) and the healthy group ($t(30) = 5.7$, $p < 0.001$) (CML: mean=6.77, SD: 2.87; Healthy: mean=0.00, SD: 0.00). Additionally, the differences between the three groups (ND, F and H) were tested. One-way ANOVA and Bonferroni post-hoc test results indicated that the ND and F groups had significantly higher methylation compared with the H group ($p <0.001$). There was no significant difference between ND and F groups (Table 5. 2)

Table 5. 2 Descriptive analysis for methylation levels of the whole promoter region and whole intron region.

Region	Groups	N	Mean ± SD	95% Confidence Interval for Mean	
				Lower Bound	Upper Bound
Promoter	Newly Diagnosed (ND)	3	7.3 ± 3.0	5.5	9.2
	Failed (F)	3	6.1 ± 2.6	4.5	7.7
	Healthy (H)	6	0.00	.00	0.00
Intron	Newly Diagnosed (ND)	3	14.13± 3.6	11.95	16.312
	Failed (F)	13	15.11± 3.3	13.147	17.08
	Healthy (H)	6	0.00	0.00	0.00

5.2.3 Methylation patterns in the 25 CpG sites of Promoter regions of PTPRG

One-way ANOVA was performed to compare methylation status in each CpG site in the promoter region between the three groups (ND, F, and H). There were significant differences in 2 out of 25 CpG sites (13 and 143) among the groups ($F(2, 29) = 7.0$; $p = 0.003$ and $F(2, 29) = 4.35$; $p = 0.022$ respectively). Bonferroni post-hoc test results indicated that methylation in CpG 13 for the ND and the F groups was significantly higher compared to the H group ($p = 0.002$ and $p = 0.035$ respectively). Furthermore, methylation in CpG 143 for the F group was significantly higher compared to the H group ($p = 0.045$) (Figure 5. 2). No significant differences were found in the rest of the CpG sites.

5.2.4 Hypermethylation of Intron-1 region of PTPRG

T-test was performed to study the methylation pattern of intron-1 of *PTPRG* in both cases and controls. The results revealed a significant difference in intron-1 methylation levels between CML (ND and F groups) and the healthy group ($t(30) = 10.38$, $p < 0.001$) (CML: mean=14.62, SD: 3.41; Healthy: mean=0.00, SD: 0.00).

One-way ANOVA showed significant differences in methylation between the three groups (ND, F and H) for intron-1 region [$F(2, 29) = 53.590$, $p = 0.001$]. Bonferroni post-hoc test results indicated that the methylation status for the ND and the F groups was significantly higher than the H group ($p < 0.001$). There was no significant difference between the ND and the F groups (Table 5. 2).

5.2.5 Methylation patterns in 26 CpG sites of Intron-1 region of PTPRG

One-way ANOVA was also performed to compare methylation levels in each CpG sites in the intron-1 region between the three groups: ND, F, and H. The results indicated that there were significant differences in 23 out of 26 CpG sites (Figure 5. 3 and Table 5. 3).

Bonferroni post-hoc test revealed that the methylation levels were significantly higher amongst the ND and the F groups compared to the H group in most of the intron-1 CpG sites except CpG 70, CpG 94, CpG 155 and CpG 161 (in the ND group) and CpG 173

(in the F group). In addition, the F group had significantly higher methylation levels in the CpG sites 94 (p= 0.003) and 155 (p=0.01) compared to the ND group.

Finally, the genomic co-ordinates sites of promoter and intron 1 were identified for the CpG (Table 5. 4).

Table 5. 3 Methylation levels of the 23 CpG sites in the Intron region amongst F and ND groups compared to H group

Site	Groups	Mean ± SD	95% Confidence Interval Range	*P* value
CpG 59	F	17.00 ± 10.47	10.67 ± 23.32	0.013
	ND	16.07 ±13.66	7.82±24.33	0.019
CpG 70	F	21.38±24.21	6.75±36.02	0.034
	ND	15.00±5.89	11.44±18.56	0.204
CpG 77	F	8.30±5.089	5.23±11.38	0.001
	ND	8.30±3.79	6.01±10.60	0.001
CpG 86	F	5.46±3.69	3.23±7.69	0.001
	ND	4.62±1.61	3.64±5.59	0.003
CpG 88	F	2.69±2.39	1.25±4.14	0.027
	ND	2.85±1.86	1.72±3.97	0.018
CpG 91	F	1.92±3.59	-.25±4.09	0.352
	ND	1.00±1.08	0.34±1.65	1.000
CpG 94	F	11.38±6.70	7.33±15.43	0.000
	ND	4.92±2.22	3.58±6.26	0.109
CpG 111	F	2.08±6.64	-1.94±6.09	1.000
	ND	0.15±.55	-.18±.49	1.000
CpG 117	F	1.84±5.18	-1.29±4.98	0.817
	ND	0.23±.44	-.03±.50	1.000
CpG 155	F	11.30±11.78	4.19±18.43	0.016
	ND	1.77±1.48	0.87±2.66	1.000
CpG 161	F	9.46±11.23	2.68±16.25	0.041
	ND	2.69±1.75	1.63±3.75	1.000
CpG 173	F	4.00±2.97	2.204±5.80	0.169
	ND	5.85±5.59	2.46±9.22	0.021
CpG 189	F	12.38±6.51	8.45±16.32	0.042

	ND	15.07±13.44	6.95±23.20	0.011
CpG 191	F	13.85±10.97	7.22±20.47	0.002
	ND	10.92±3.33	8.91±12.93	0.016
CpG 193	F	11.38±4.37	8.74±14.02	0.000
	ND	12.70±4.73	9.83±15.55	0.000
CpG 199	F	8.00±4.14	5.50±10.50	0.000
	ND	7.85±4.02	5.42±10.27	0.001
CpG 226	F	14.62±7.10	10.32±18.90	0.000
	ND	13.62±4.23	11.06±16.17	0.000
CpG 228	F	23.62±9.82	17.68±29.55	0.000
	ND	24.46±6.92	20.28±28.65	0.000
CpG 236	F	17.62±9.22	12.05±23.18	0.000
	ND	17.62±5.58	14.25±20.98	0.000
CpG 238	F	17.54±9.47	11.81±23.26	0.000
	ND	17.62±5.55	14.26±20.97	0.000
CpG 243	F	36.23±13.23	28.24±44.23	0.000
	ND	43.23±14.76	34.21±52.15	0.000
CpG 246	F	28.54±10.71	22.07±35.01	0.000
	ND	28.54±7.48	24.02±33.06	0.000
CpG 252	F	19.77±8.05	14.90±24.64	0.000
	ND	20.23±4.21	174.70±22.77	0.000
CpG 260	F	28.00±11.23	21.21±34.79	0.000
	ND	29.69±7.03	25.45±33.94	0.000
CpG 281	F	37.23±15.54	27.84±46.62	0.000
	ND	39.69±14.37	31.01±48.38	0.000
CpG 288	F	27.31±12.60	19.70±34.92	0.000
	ND	22.77±12.50	15.21±30.33	0.001

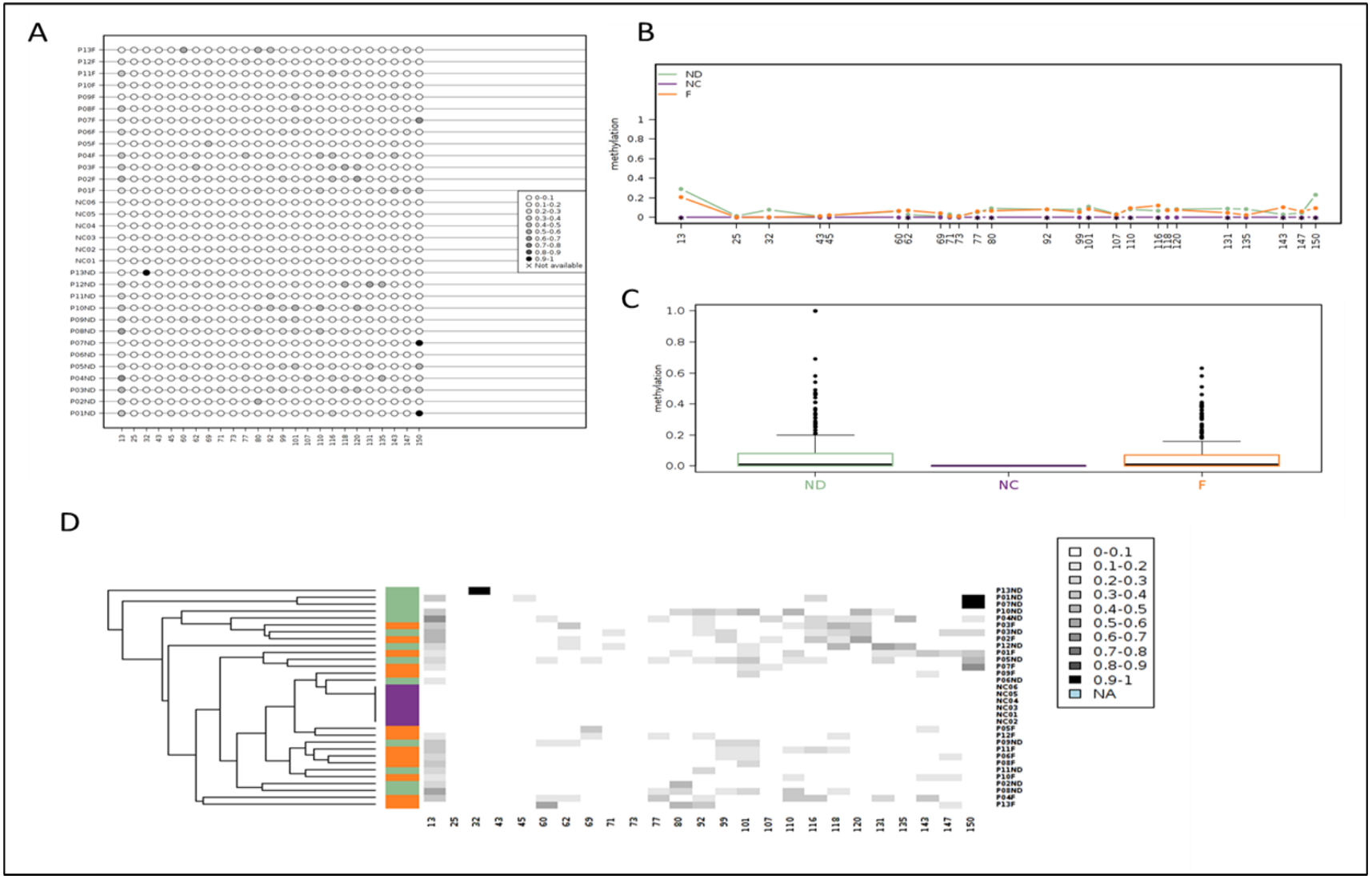

Figure 5. 2 Data visualization with Methylation plotter for 25 sites of Promoter region of PTPRG.

A lollipop-like visualization of methylation sites B, methylation profiling plot reflecting with asterisks those positions for which significant differences between groups were detected. C, boxplots for each group showing the methylation data distribution. D, unsupervised hierarchical clustering of the data; sample label colours reflect groups classification.

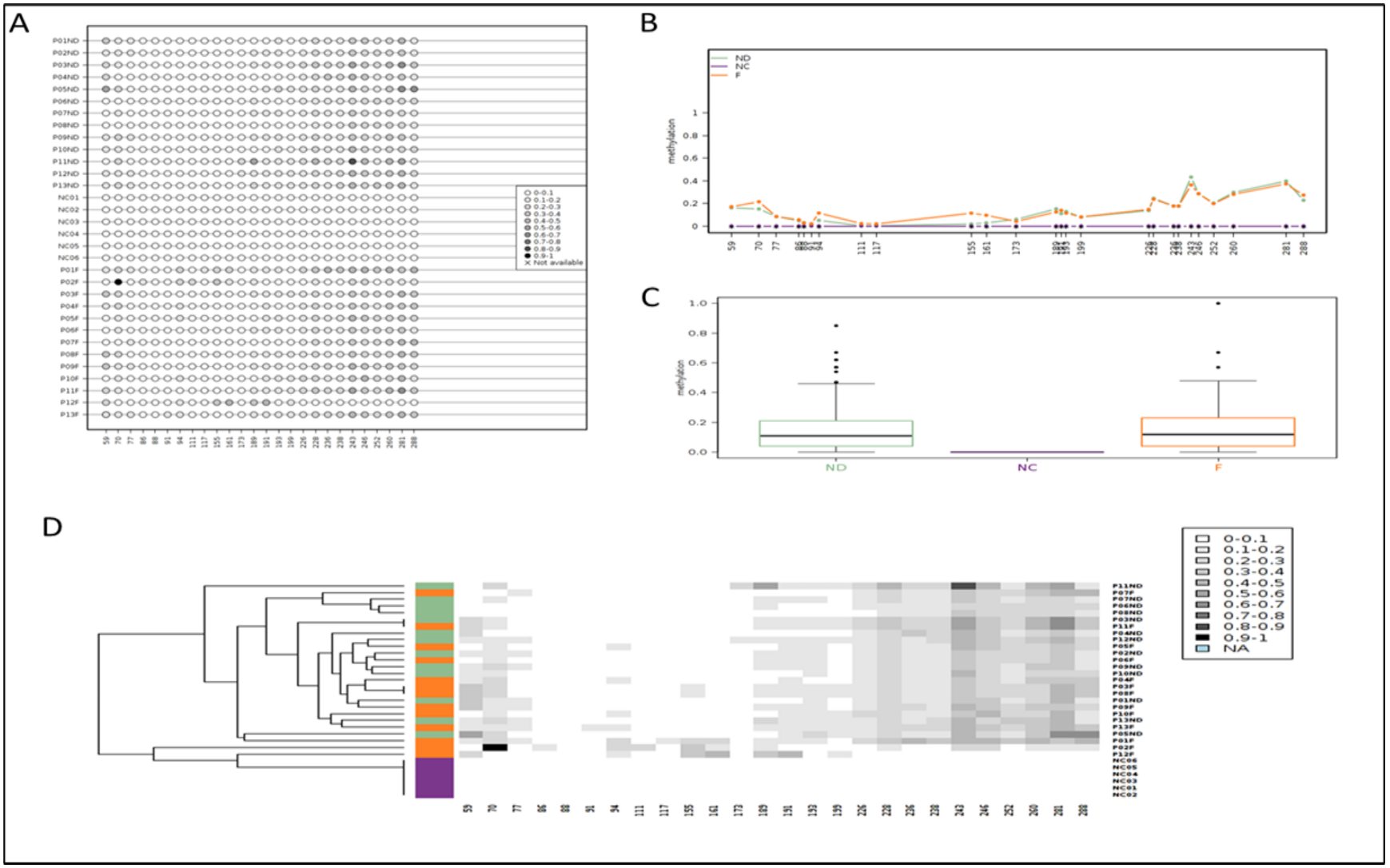

Figure 5. 3 Data visualization with Methylation plotter for 26 sites of Intron region of PTPRG.

A lollipop-like visualization of methylation sites B, methylation profiling plot reflecting with asterisks those positions for which significant differences between groups were detected. C, boxplots for each group showing the methylation data distribution. D, unsupervised hierarchical clustering of the data; sample label colours reflect the groups classification.

Table 5. 4 Genomic Co-ordinate for possible 25 CpG sites of Promoter and possible 26 CpG sites of intron-1 of PTPRG

CpG sites of Promoter	Genomic Co-ordinate
CpG 13	Chromosome 3: 61,561,400
CpG 15	Chromosome 3: 61,561,412
CpG 32	Chromosome 3: 61,561,419
CpG 43	Chromosome 3: 61,561,430
CpG 45	Chromosome 3: 61,561,432
CpG 60	Chromosome 3: 61,561,447
CpG 62	Chromosome 3: 61,561,449
CpG 69	Chromosome 3: 61,561,456
CpG 71	Chromosome 3: 61,561,458
CpG 73	Chromosome 3: 61,561,460
CpG 77	Chromosome 3: 61,561,464
CpG 80	Chromosome 3: 61,561,467
CpG 92	Chromosome 3: 61,561,479
CpG 99	Chromosome 3: 61,561,486
CpG 101	Chromosome 3: 61,561,488
CpG 107	Chromosome 3: 61,561,494
CpG 110	Chromosome 3: 61,561,497
CpG 116	Chromosome 3: 61,561,503
CpG 118	Chromosome 3: 61,561,505
CpG 120	Chromosome 3: 61,561,507
CpG 131	Chromosome 3: 61,561,518
CpG 135	Chromosome 3: 61,561,522
CpG 143	Chromosome 3: 61,561,530
CpG 147	Chromosome 3: 61,561,534
CpG 150	Chromosome 3: 61,561,537

CpG sites of Intron-1	Genomic Co-ordinate
CpG 59	Chromosome 3: 61,564.673
CpG 70	Chromosome 3: 61,564,684
CpG 77	Chromosome 3: 61,564,691
CpG 86	Chromosome 3: 61,564,700
CpG 88	Chromosome 3: 61,564,702
CpG 91	Chromosome 3: 61,564,705
CpG 94	Chromosome 3: 61,564,708
CpG 111	Chromosome 3: 61,564,725
CpG 117	Chromosome 3: 61,564,731
CpG 155	Chromosome 3: 61,564,769
CpG 161	Chromosome 3: 61,564,775
CpG 173	Chromosome 3: 61,564,787
CpG 189	Chromosome 3: 61.564,803
CpG 191	Chromosome 3: 61,564,805
CpG 193	Chromosome 3: 61,564,807
CpG 199	Chromosome 3: 61,564,812
CpG 226	Chromosome 3: 61,564,840
CpG 228	Chromosome 3: 61,564,842
CpG 236	Chromosome 3: 61,564,850
CpG 238	Chromosome 3: 61,564,852
CpG 243	Chromosome 3: 61,564,857
CpG 246	Chromosome 3: 61,564,860
CpG 252	Chromosome 3: 61,564,866
CpG 260	Chromosome 3: 61,564,874
CpG281	Chromosome 3: 61,564,895
CpG 288	Chromosome 3: 61,654,902

5.3 Discussion

This is the first prospective study to evaluate epigenetic mechanisms of *PTPRG* regulation amongst CML patient's population where the rate of IM resistances is higher than other reported parts of the world (Al-Dewik et al., 2014, Patel et al., 2017). It addresses the important role of *PTPRG* as a regulatory element in *BCR-ABL1*-mediated oncogenesis. The study provides evidence for the involvement of the epigenetic modification of *PTPRG* in the pathogenesis of CML. Indeed, *PTPRG* was found to be significantly hyper-methylated compared to the control (Figure 5. 2 and Figure 5. 3).

On the other hand, hypermethylation of CpG sites on promoter region of *PTPRG* causing loss of function are well studied in other cancers. For instance, inactive forms or loss of PTPRG protein have been described in sporadic and Lynch syndrome colorectal cancer, nasopharyngeal carcinoma, ovarian, breast, and lung cancers, gastric cancer or diseases affecting the hematopoietic compartment as Lymphoma and Leukaemia (Cheung et al., 2015, Cheung et al., 2008, Li et al., 2021, van Roon et al., 2011a).
PTPRG is known to induce a reduction of protein *BCR-ABL*-specific tyrosine phosphorylation of its direct downstream targets/substrates such as CRKL and of STAT5 (Della Peruta et al., 2010). In the current study, the methylation coverage of *PTPRG* was extended via studying two regions of its promoter: 321bp andintron-1 218bp using advanced molecular technique such as Sanger sequencing (Figure 5. 1). In the same context, Della Peruta et al., documented earlier that up-regulated *PTPRG* expression is associated with a reduction in methylation levels in 166 bp of *PTPRG* using Methylation-specific PCR technique (Della Peruta et al., 2010). More recently, in *PTPRG*-negative CML cell lines, the methylation enzyme DNA (cytosine-5)-methyl transferees 1 (DNMT1) was found to be over-expressed, bind to PTPRG promoter and be responsible for its hypermethylation, while its inhibition or down-regulation correlated with PTPRG re-expression (Ismail et al., 2020). These findings revealed that the methylation occurs more frequently in the intron-1 region compared to the promoter region in CML patients besides showing a significant increase of the methylated percentage at the CpG sites in both promoter and intron-1 regions compared to healthy individuals (Table 5. 2).

Despite the fact that the epigenetic changes are susceptible to extrinsic factors, there is a strong association between DNA methylation and aging. During ageing, the methylation patterns were found to be greater in the young people (Morgan et al., 2018). In the current study, the mean age of healthy control was similar to mean age of CML patients (mean ~ 37years). Furthermore, standard deviation of methylation patterns between the groups itself was in the same range as described in (Table 5. 2). However, further investigation using myeloid cells and the impact of age and phase of disease and the level of failure in a larger population of patients is warranted.

Interestingly, these findings indicated and confirmed that the hyper-methylated pattern of PTPRG gene in CML patients acts as an early promoter for CML formation and to be dependent on *BCR-ABL1* titters. It may therefore well contribute as a BCR-ABL1 independent resistance molecular event.

In this study, 51 CpG sites in *PTPRG* in CML and healthy control groups were analysed for methylation. Overall, the frequency of methylated CpG sites was significantly higher in CML cases compared to healthy controls, suggesting the potential involvement of CpG methylation sites in CML (Figure 5. 2and Figure 5. 3). Interestingly, two CpG sites in the intron-1 region were found to be significantly methylated amongst failed groups compared with newly diagnosed. In the newly diagnosed group, the frequency of CpG site methylation was significantly different from the healthy group, suggesting that CpG site methylation have a central role in the molecular events leading to CML. These findings support the assumption that the CML disease is not only driven by the *BCR-ABL1* translocation (Boni and Sorio, 2021). Moreover, we also observed a significantly higher methylated CpG sites in the failed group compared to the healthy group, indicating that CpG site methylation may be important for disease progression (Table 5. 4).

Several studies have documented the effect of DNA methylation pattern of regulatory genes on various cellular activities such as cell proliferation and survival, as well as cell-

signalling molecules in CML (Behzad et al., 2018). Jelinek et al 2011 studied the Methylation levels of 10 genes in CML patients and found that the frequency of methylated genes ranged from 11%to 86% as follows: ABL1 (86%), CDH13 (79%), NPM2 (74%), PGRA (66%), TFAP2E (63%), DPYS (54%), PGRB (52%),OSCP1 (30%), PDLIM4 (21%) and CDKN2B (11%), suggesting an aberrant methylation of DNA associated with the progression of the disease. Another study using a whole methylome approach in 36 CML patients, found that 31 genes were uniquely hyper methylated in CML and 42 genes that became hyper methylated with the progression of CML. Remarkably, the same group showed that utilizing DNA methylation inhibitor such as azacytidine in blastic crisis CML patients resistant to Imatinib Mesylate (IM) could reverse the aberrant hypermethylation associated with progression of CML to blast crisis and supports the use of this drug as an epigenetic therapy (Deininger et al., 2007). In another study with CML cell line K562 and its IM resistant variant (K562-R), the methylation levels were found to be significantly higher and that the gene expression levels were significantly lower for MLH1, RPRM, FEM1B, and THAP2 in K562-R cells when compared to parental K562 cells. Further, treatment of the K562-R cells with epigenetic drugs, such as 5-azacytidine (AzaC) reduced resistance to Imatinib Methylate (You et al., 2012). In another study, SOX30 methylation has been correlated with disease progression in patients with chronic myeloid leukaemia (Zhang et al., 2019).

PTPRG expression has been shown to be down-regulated by RAS activation, while its up-regulation has been observed in hypo-methylation condition in in childhood acute lymphoblastic leukaemia (ALL) (Xiao et al., 2014). Finally, PTPRG methylation has also been reported in solid cancer (Cheung et al., 2008, Wang and Dai, 2007). Eddy et al., suggested that PTPRG inton1 methylation could be a biomarker for early detection of colorectal cancer (van Roon et al., 2011b).

5.4 Summary and Conclusion

Hypermethylation of *PTPRG* locus might suggest a molecular mechanism independent of BCR-ABL1 function in CML patients. The data presented here contributes to a

deeper understanding of the crucial role of aberrant DNA methylation in CML disease initiation and progression. Potentially, *PTPRG* methylation could be a biomarker for early detection of CML. However, further studies are needed on the validation of specific aberrant methylation of *PTPRG* and its prognostic and predictive values for the response to therapy in the CML patients.

6 Cryopreservation of Chronic Myeloid Leukaemia (CML) cells in state of Qatar

This chapter will present and discuss the preliminary data of biobanking of cells from CML patients at the State of Qatar.

6.1 Introduction

Background: Cryopreservation is a procedure that preserves cells in a well-maintained property for further functional experiments by cooling the samples to very low temperatures (Liseth et al., 2005). Recent published data showed that data 20-25 % of CML patients developed kind of resistance to treatment (Baccarani et al., 2019b). Thus, cryopreserving of these precious samples is very important for further future laboratory investigations.

Aim: In this chapter, the aim was to set-up cryopreservation techniques for CML patients, which involved developing local Standard Operating Procedures (SOPs) for freezing and thawing of WBCs from CML patients and quality assurance (QA) testing.

Method: Total white blood cells were isolated from 25 CML patients at different timelines by erythrocytes Lysis buffer then cells were preserved in freezing media contain 10% DMSO, while thawing media contained DNase I. Quality checks were done for cryopreserved cells at different timeline to check the viability and functionality of the technique. The cells' viability was assessed via 7-AAD (7-amino-actinomycin D) while functionality was carried by anti-human antibodies such as CD 34, CD45, CD38 and mAb TPγ B9-2 using flow technique, as described in the materials and methods chapter.

Results: The viability of the thawed samples at diagnosis, 6 months and 27 months were 81.7%, 88.87%, and 88.2% respectively which is good indicator for further functional assay. In addition, the thawed WBCs populations (including hematopoietic stem and progenitor cells) were captured using the above-mentioned antibodies.

Conclusion: The establishment of biobanking facilities for cryopreserved cells at the state of Qatar provides an excellent opportunity for conducting further laboratory experiments and establishing national and international collaborative research on CML and these ultimately can led to a better understanding of the biology, immunology, diagnosis and the

treatment of CML patients. It should also help to resolve the dilemma of why some CML patients develop resistance to current therapeutic agents and to determine the underlying mechanisms.

6.2 Results:

6.2.1 Cryopreservation Trial 1

Flow cytometry protocol utilized to check efficacy of thawed cryovials was adopted as chapter three. Several attempts to check the viability of cryovials at different timelines (i.e. 3 months) were conducted. The rate of a live of thawed cell reached to 79%, the viability checked by flow cytometry technique. The thawed cryovials showed a good number of recovered major leukocytes populations (CD 45+) however; the CD34+ population that representing myeloid progenitors' cells were not recovered entirely (Figure 6. 1).

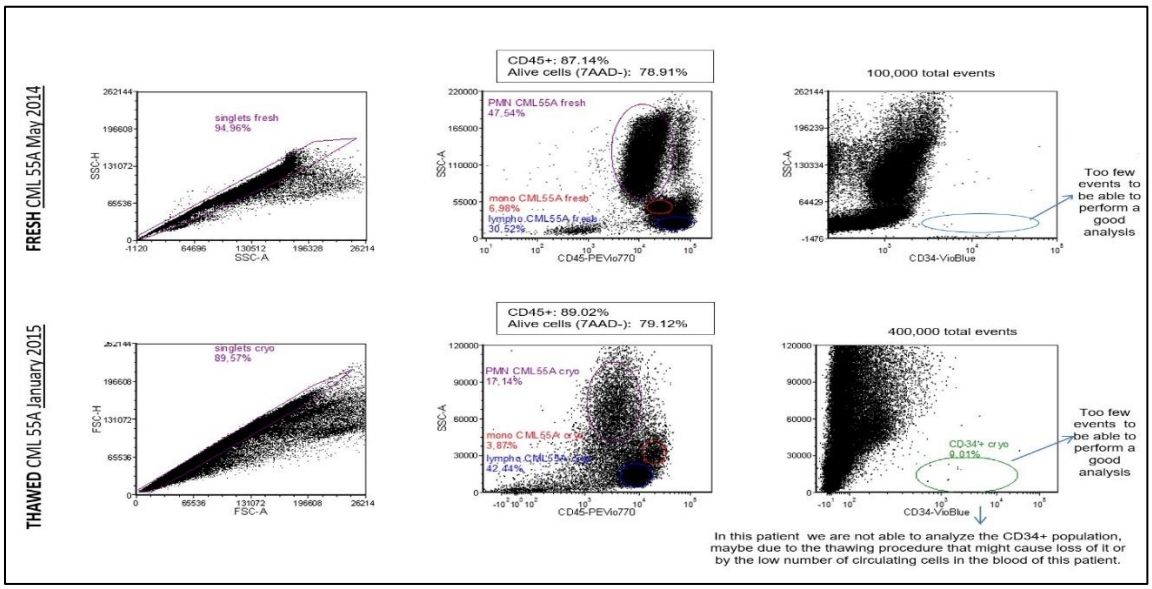

Figure 6. 1 Thawed cryovials with unsuccessful recovered progenitor cells.

Later, we run PTPRG expression by flow cytometry to compare the protein level of PTPRG of thawed cells along with fresh results. Again, in this case the analysis of PTPRG expression in major leukocytes populations was not so similar among the freshest and thawed samples (in thawed samples the PTPRG antibody was too much reactive, the MFI values were totally outside the normal ranges, even for normal

donors). The analysis of thawed cells was much more plausible but, in any case, the PTPRG positivity trend was the same (monomorphonuclear cells and polymorphonuclear leukocytes (PMN) are positive in both cases) (Figure 6. 2).

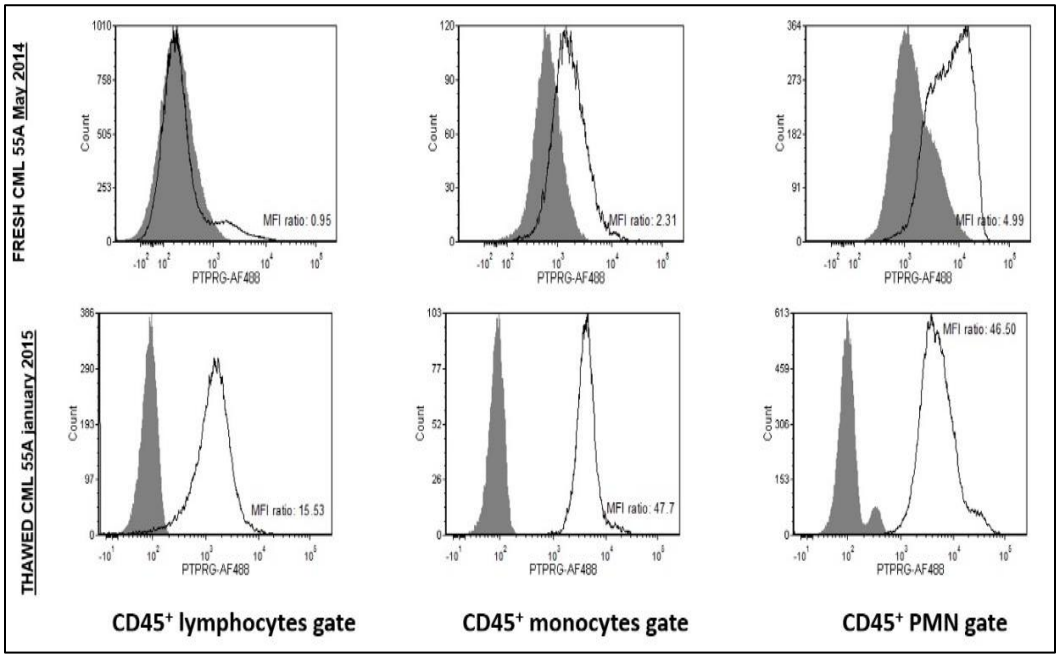

Figure 6. 2 Thawed cells showed reactive PTPRG expression to binding antibodies.

6.2.2 Cryopreservation Trial 2

The protocol of cryopreservation technique was amended. The ascending and descending speed of centrifuge was decreased from 9 to 6, in other word the centrifugation speed at 300g (Heraeurs Megafuge 16.0 r). This allowed to collect more progenitors' cells at same time maintaining the viability at the most.

6.2.2.1 Viability rate of thawed cells

Ten cryovials were thawed at different timelines and viability of thawed cells was assessed by flow cytometry technique. The rate of live thawed cells was 87% and 74% at, 6 months, and 27 months, while at diagnosis was 97% (Figure 6. 3).

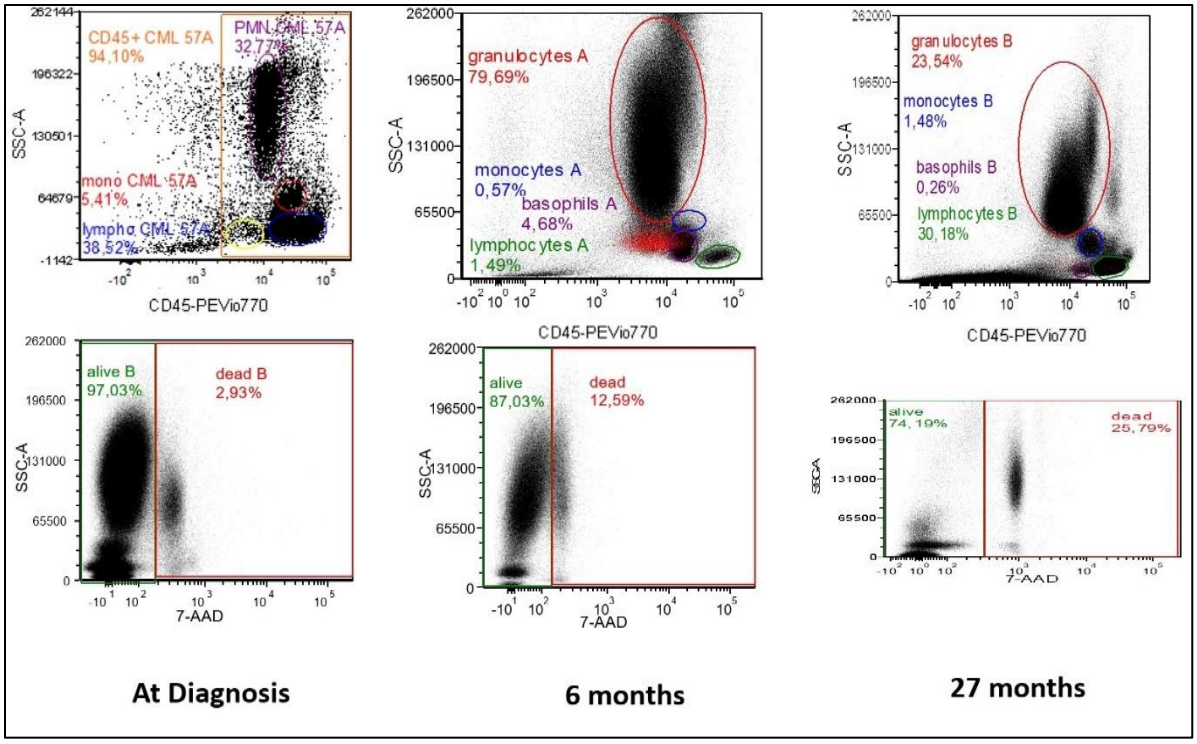

Figure 6. 3 Viability rate of thawed cells at different timelines.
The rate of a live cells of thawed cryovials was in good proportional with dead percentage.

6.2.2.2 Progenitor of thawed cells

The same thawed cryovials were also tested and successfully recovered the viable progenitor cells using CD34 and CD38 antibodies. A ratio of progenitor cells with high percentage of viability and function assay showed kind of binding with CD34 and CD38 antibodies (Figure 6. 4B).

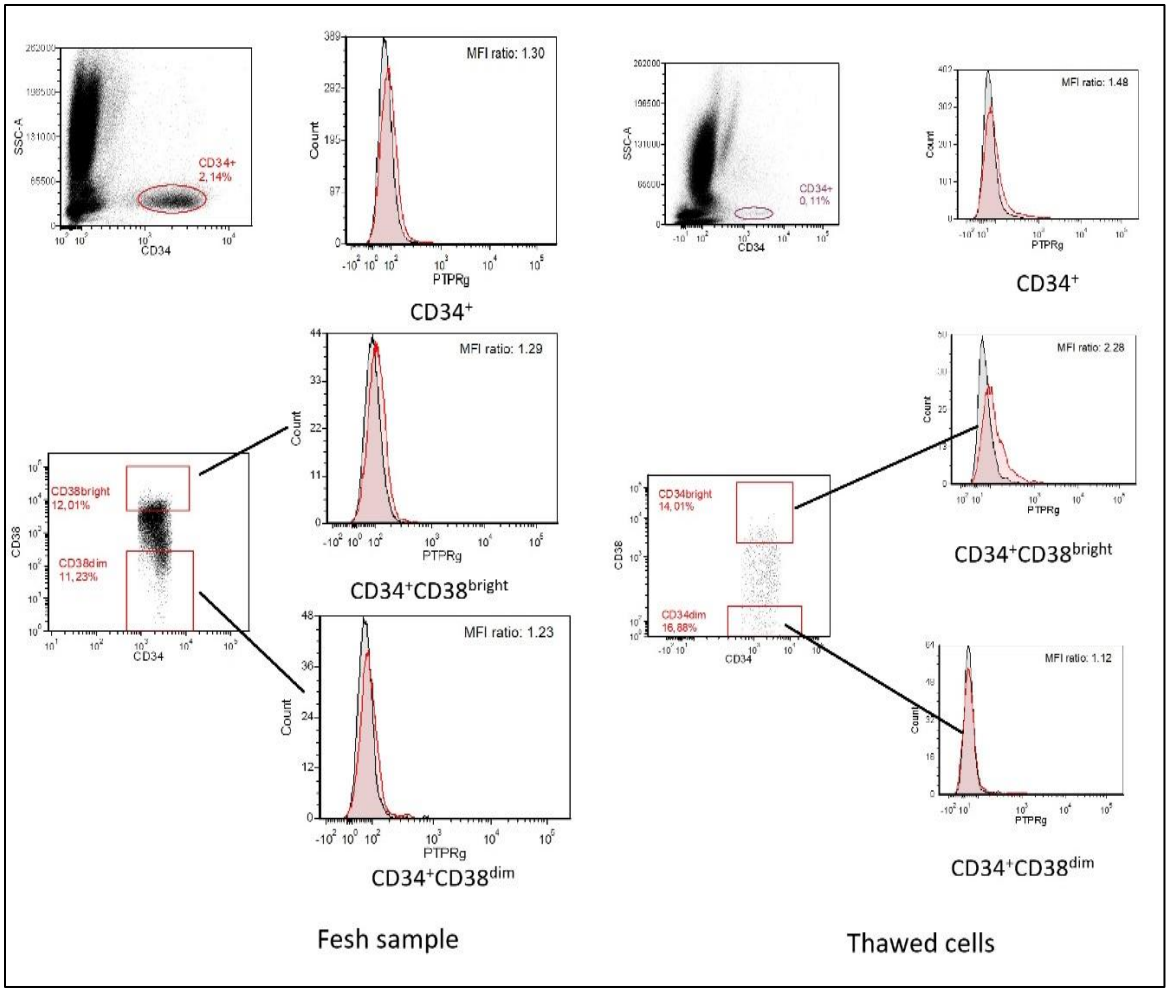

Figure 6. 4 Progenitor cells of thawed cryovials.

The thawed cell in well maintained state, there was no expression of PTPRG in the whole CD 34 population, however, subpopulations of CD34+/CD38-(Dim) and CD34+/CD38+ (bright) showed degree of PTPRG expression.

6.2.3 Function assay of thawed cells

Next, PTPRG expression was analysed in major leukocytes populations of thawed cryovials. The flow cytometry results were found to be very similar to the fresh samples (Figure 6. 5).

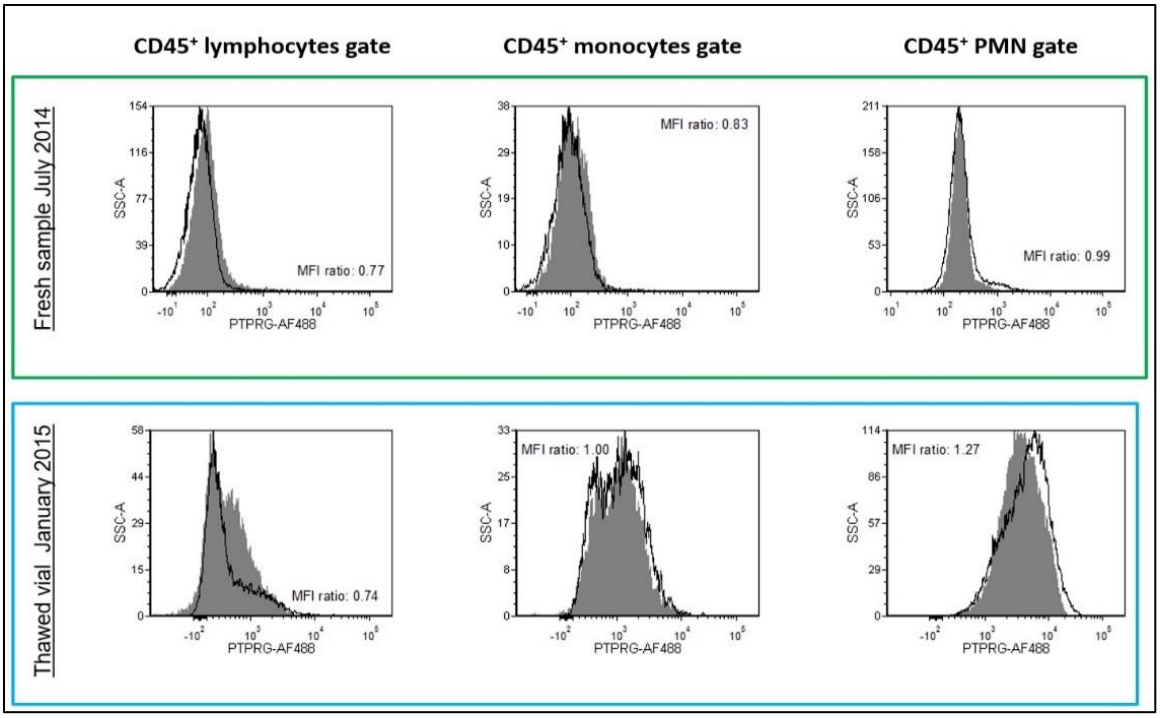

Figure 6. 5 PTPRG expression in major leukocytes populations of thawed cells.
The PTPRG expression showed very similar pattern among the fresh and thawed samples.

6.3 Discussion

Cryopreservation is a technique used to transport and preserve of peripheral blood cells in a well state feature for further function assay. The importance of cryopreservation technique is that including but not limited to clinical experiments, correlative studies for clinical trials as well as precision medicine.

Anti-leukemic drug activity on thawed CML cells is a vital tool in defining potential drug targets and selection of therapeutic agents with functional and biologic tests (Degnin et al., 2017, Kim, 2019) . This will not be possible without availability of cell lines and of cryovials of CML cells that including hematopoietic cells.

In the current study, the preliminary data showed accepted rate of live thawed cells across different timeline at 6 and 27 months, when compared to fresh samples (Figure 6. 3). The progenitor cells of CML are much delegated cells that require a unique technique during recovery process due to low count. In the current study, the thawed cryovials showed good numbers of progenitor cells in well maintained state (Figure 6. 4).

In the current study, there was a decrease in the percentage of granulocytes of thawed cells over the time while the percentage of mononuclear cells remained in acceptable range when compared to fresh samples (Figure 6. 5). On the other hand, the numbers of thawed cells were representing 20% of the original numbers of cryovials at day zero of cryopreservation process. However, further studies are still needed to increase the quality of these two factors.

At the end of PhD project, CML biobanking at Interim Translational Research Institute (iTRI) Doha-Qatar was successfully established. The establishment of such CML biobanking and further optimisation in the state of Qatar should facilitate further collaborations between scientists and clinicians both at the national and international levels in the study of CML and ultimately development of more effective therapeutic agents for CML patients and in supporting other health care research strategies.

7 General Discussion and future perspectives

In this chapter, major findings and their implications were critically discussed and summarized together with future opportunities for our better understanding of CML biology and diagnosis and developing more effective therapeutic interventions.

7.1 Summary of major findings

This prospective study is the 1st of its kind in Qatar. Chronic Myeloid Leukaemia (CML) is a haematopoietic stem cell disorder that transforms normal stem cells to hyper-proliferated abnormal stem cells (Jabbour and Kantarjian, 2020b). CML is also characterised by various types of genetic alterations including mutation, deletion, and translocation. Of these, a fusion gene termed *BCR-ABL1* has been identified in most patients with CML (Zhou et al., 2018). The expression of BCR-ABL1 oncoprotein results in the deregulated activation of its tyrosine kinase domain in patients with CML.

At present, the most common FDA approved BCR-ABL TKIs that are utilized in the clinical settings are namely Imatinib, Nilotinib and Dasatinib for the treatment of patients with CML (Cortes and Lang, 2021). However, recent studies showed there are more than 50 kinase domain mutation sites and more than 70 different *BCR-ABL1* mutations which can contribute to resistance to treatment with Imatinib, with point of mutations within the kinase domain being the most common and frequent mechanisms of resistance (Patel et al., 2017). More recently 45% of CML patients who participated in the International Randomized Study of Interferon and STI571 (IRIS) failed to continue on Imatinib therapy at the 8-year follow-up time (Deininger et al., 2009). Therefore, it is clear that not all patients with CML would gain long term benefit from therapy with TKIs and it is important to uncover the underlying mechanisms of resistance to therapy with the BCR-ABL TKIs.

In particular, it is important to study the role of tumour suppressor which has a negative regulatory effect on the phosphorylation process such as the protein tyrosine

phosphatase receptor Gamma (*PTPRG*) which is a member of receptor type protein tyrosine phosphatases (RPTPs) (Zhao et al., 2015).

The aim of this PhD project was to conduct detailed study of *PTPRG* at the molecular level and to determine its expression level and predictive value as a biomarker for the response to therapy with the small molecules tyrosine kinase inhibitors (TKIs) in CML patients in the Qatar. The results are consistent with the mainstream findings that the PTPRG has a natural inhibitory mechanism and were found to be down regulated in CML patients. In addition, using anti-PTPRG monoclonal antibody TPγ B9-2, a unique flow cytometry technique was developed and it was able to record changes in the expression level of PTPRG at diagnosis and in particular its restoration following treatment with one of the BCR/ABL TKIs. Furthermore, aberrant DNA methylation of *PTPRG* was found be one of the possible mechanisms of it's under expression in CML patients. Moreover, 10 *PTPRG* variants (7 annotated and 3 Novels) were found in this study. Of these, two variants c.841-29C>T (rs199917960) and c.1378-224A>G (rs2063204) were found to be significantly different between the TKI resistant cases compared to responders as well as healthy individuals. Finally, towards the end of project of PhD, there was successful establishment of CML biobanking at Interim Translational Research Institute (iTRI) Doha-Qatar which should open new spectrum to support health care research strategies for patients with CML. All these findings and their importance are discussed under the following headings.

7.2 Predictive value of the Tyrosine Phosphatase Receptor Gamma Protein level determined by flow cytometry for the response to treatment with TKIs in Chronic Myeloid Leukaemia patients

Earlier studies reported the down regulation of mRNA levels of *PTPRG* in Chronic Myeloid Leukaemia disease (CML) (Della Peruta et al., 2010). In this study, our results have shown that the protein levels of PTPRG is down regulated in CML patients at diagnosis and this can be restored following treatment with one of TKIs.

On the mRNA level, there was a significance difference between levels of *BCR-ABL1* and *PTPRG* at diagnosis and following introducing TKIs to treatment plan. The mRNA levels were reversed, where the peak of *BCR-ABL1* was observed at diagnosis, while the peak of *PTPRG* was observed at optimal response (Figure 3. 3 A&B). There was a significant different at *PTPRG* mRNA of optimal response group when compared to diagnosis level, while this significance was lost at failed group (Figure 3. 3 C&D). The low level of PTPRG during treatment plan could be potential indicator of treatment failure. In the same context, we analysed effect of TKIs on both genes. The resulting analysis showed a huge size effect on *BCR-ABL1* (Cohen's d = 5.05) while large size effect on *PTPRG* transcripts (Cohen's d = 0.81). The study also investigated the correlation between both genes and there was a moderate negative correlation between *BCR-ABL1* at diagnosis and *PTPRG* at follow up (rs (21) = -0.422, *p* = 0.028).

On the protein level, firstly, the study documented good expression of PTPRG on subpopulation of WBCs of healthy individuals (Figure 3. 1A), but it's down regulation in CML patients at diagnosis (Figure 3. 4C). Of note, lymphocyte was assisted as internal negative control (Figure 3. 4 B&C). Furthermore, there was a significant difference between levels of subpopulation of WBCs of CML patients at diagnosis when compared to healthy individuals (Figure 3. 4 D).

Next, the PTPRG expression level on WBCs was also re-assessed during the follow up for both optimal and failed CML groups (Figure 3. 5). The restoration levels of PTPRG on subpopulation of white blood cells were observed to level seen/ extent in healthy controls (Figure 3. 4A and Figure 3. 5). The difference in expression of PTPRG on the neutrophils at diagnosis and during the follow-up time points in the optimal response group was a statistically significant (χ^2 (2, 11) = 13.82, *p* =0.001) (Figure 3. 6 A). Same scenario was observed with monocytes subpopulation but less extent to neutrophils (χ^2 (2, 11) = 10.09, *p* =0.006) (Figure 3. 6D). Again, there was no significant differences between the follow up time-points in relation to the expression of PTPRG on the lymphocytes (χ^2 (2, 11) = 2, *p* =0.6). The study also has shown that restoration levels were greatest in optimal responders on neutrophils cells when compared to failed group

(Figure 3. 6 C). In addition, level of restoration was occurred earlier with nilotinib compared with imatinib (Table 3. 2).

Taken together, these results support that determination of PTPRG expression level by flow cytometry as a new biomarker of response to treatment with BCR-ABL1 TKIs and that it is a useful tool for studying its role in tumour progression and predicting the response to therapeutic interventions and clinical management in patients with CML and warrants further investigations in a larger group of CML patients (Ismail et al., 2021).

7.3 *PTPRG* variants may act as an indirect mechanism of resistance to treatment with the BCR-ABL1 TKIs.

As discussed earlier, mutations in *BCR-ABL1* are well studied but fail to explain 20–40% of resistant cases, suggesting the activation of alternative, BCR-ABL1-independent pathways (Braun et al., 2020). On the other hand, overexpression of PTPRG-WT was observed with nilotinib treatment however, this observation was lost with mutant PTPRG (Drube et al., 2018). In the same context, the current study reported ten variants (Table 4. 2). Seven were annotated and three were novel SNPs (c.1602_1603insC, c.85+14412delC, and c.2289-129delA). Among them, five variants were identified in 15 resistant cases. Of these, one was novel exon variant (c.1602_1603insC). The genotyping and alleles of annotated *PTPRG* variants were compared with the largest two databases, namely 1000 Genomes Project (Auton et al., 2015) and the largest database in the middle east the Qatar genome program (QGP) as references (Al Thani et al., 2019). Genotyping and alleles analysis showed that two out of seven *PTPRG* variants were significantly associated with CML disease (Table 4. 3).

The frequencies of three genotypes of rs199917960 (C/C, C/T and T/T) and rs2063204 variants (A/A, A/G and G/G) were significant different among the CML patients' group when compared to control groups [the 1000 Genomes project control and QGP] (Table 4. 3). In addition, the frequency of the major (C) and the minor (T) alleles of rs199917960 and the major (A) and the minor (G) alleles of rs2063204 variants were statistical significantly when compared to control groups (Table 4. 3).

The logistic regression analysis of rs199917960 revealed there was a significant association with CML disease in all models: co-dominant, dominant, recessive, and over dominant (Table 4. 4). On the other hand, rs2063204 was significantly associated with CML disease in the recessive and over-dominant models only (Table 4. 4). These significances were observed with the 1000 Genomes project and QGP references.

Interestingly, the current study identified two exclusive variants, c.274T>C (rs62620047) and c.1034-46C>T (rs57829866) were statistically significant with QGP but not with 1000 Genomes project. The variant rs62620047 was significantly associated with CML in the co-dominant, dominant, and over-dominant models (Table 4. 5). In contrast, rs57829866 was significantly associated with CML disease in the co-dominant model only (Table 4. 5).

Finally, the current study investigated the models for rs199917960 and rs2063204 amongst the responsive and non-responsive groups. Rs199917960 was significantly associated with non-responders in the co-dominant, dominant, and recessive models when compared to the responder's group (Table 4. 6). On the other hand, the variant rs2063204 was significantly associated with non-responsive in the recessive and over-dominant models (Table 4. 6).

Taken together, these findings suggest that *PTPRG* variants may affect the efficacy of the treatment plan of TKIs and act as an indirect resistance mechanism of *BCR-ABL1* gene and warrant further investigation in a larger cohort of CML patients (Ismail et al., 2022).

7.4 Aberrant DNA methylation of *PTPRG* as one possible mechanism of its under-expression in CML patients

Epigenetic silencing is a phenomenon whereby gene transcription is suppressed through DNA methylation resulting in decreased protein expression (Goldman, 2003b). In addition, several studies showed that aberrant DNA methylation is involved in

leukaemia and cancer pathogenesis (Jelinek et al., 2011). In the current study, gradient PCR at 60°C identified specific products of 321bp and 218bp for promoter and intron-1 regions of PTPRG (Figure 5. 1). Then we studied methylation profile of 51 CpG sites in PTPRG in CML (New diagnosis and failed groups) against healthy controls. Overall, the frequency of methylated CpG sites was significantly higher in CML cases compared to healthy controls (Table 5. 2).

Hyper methylation pattern was revealed in 2 CpG sites (13 and 143) out of 25 CpG sites of promoter regions between the three groups (ND, F, and H) (Figure 5. 2). While, hyper methylation pattern was revealed in 23 CpG sites out of 26 CpG sites of intron 1 region (Table 5. 3 & Figure 5. 3). These results suggest that aberrant DNA methylation of *PTPRG* being as one possible mechanism of its under-expression in CML patients (Ismail et al., 2020, Ismail et al., 2018).

7.5 Establishment and application of Chronic Myeloid leukaemia patients biobanking in Qatar

The current study succeeded to implement cryopreservation of samples from CML patients at Qatar. As discussed earlier, treatment with tyrosine kinase inhibitors (TKIs) produced significant improved in the lifespan of CML patients; however, there is a ratio up to 40 % failed treatment due to activation/ alteration of indirect pathways (Jabbour and Kantarjian, 2018) and in Qatar 45 % of CML patients fail imatinib treatment (Al-Dewik et al., 2015, Al-Dewik et al., 2016) and reason behind the resistance mechanism is still not fully investigated. In the current study, up to 50% of CML patients was classified as failed treatment (Table 3. 1 &Table 4. 1and Table 5. 1). Cryopreservation of samples from CML patients and further research on such samples could aid in our better understanding of CML biology, pathology, diagnosis as well as development of more effective and less toxic treatments.

The preliminary data of cryopreservation of CML patients in Qatar was promising, where the rate of live thawed cells was 87% and 74% at 6 months, and 27 months respectively, while at diagnosis was 97% (Figure 6. 3).

Another important element of thawed cells is progenitor cells; in fact that leukemic stem (LSCs) cells have a unique profile of cell surface, which is different than hematopoietic cells (Thielen et al., 2016). Furthermore, LSCs have the ability to self-renewal (Heidel et al., 2011), and a signatory high expression of a gene which independently associated with adverse response to the treatment (Andrew J. Gentles, 2010). Another recent study reported quiescent LSCs were insensitive to treatment with the TKIs (Hsieh et al., 2021). In the current study, the viable progenitor cells were successfully recovered using CD34 and CD38 antibodies. A ratio of progenitor cells with high percentage of viability and function assay showed binding with CD34 and CD38 antibodies (Figure 6. 4B). This could be prospective assay for better understanding the mechanism of LSC.

The study also tested the cryovials by running function assay. Protein expression of PTPRG by flow cytometry on thawed cells was tested and the results were compared to fresh samples. Both expression on fresh samples and thawed cells was share kind of similarly of MFI values (Figure 6. 5).

The establishment of such CML biobanking and further optimisation in the state of Qatar should facilitate further collaborations between scientists and clinicians both at the national and international levels in the study of CML and ultimately development of more effective therapeutic agents for CML patients. Taken together these studies have the potential for increasing our understanding of the biology and immunology of CML and the identification of biomarkers of diagnostic, prognostic values, and as therapeutic targets for use in the management of patients with CML.

7.6 Outstanding challenges and future considerations

There are currently several challenges when it comes to the diagnosing, monitoring, and treating of patients with the CML in the state of Qatar. Firstly, a substantial number of CML cases (~50%) are being diagnosed abroad, which leads to missed ultrasound and blood tests that are being essential to stratify the patients according to EUTOS and Sokal scores. There was inconsistency in ordering of molecular studies at diagnosis. For example, between 1-10% of cases were only studied at molecular level at diagnosis. This could be explained by utilizing GeneXpert BCR-ABL assay in diagnostic setting that was only valid for monitoring of BCR-ABL mRNA while not suitable for quantitative of BCR-ABL mRNA at diagnosis until the end of 2017.

Secondly, significant numbers of the Qatar population are expatriates. Of these, socioeconomic labour force which might leave the country due to the cost of treatments, consequences lost patient data. It is worthy to mention that cancer treatment cost was covered by 80% of the government state at Qatar, and 20% paid by cancer patient's resident, but sometimes it is still expensive for some patients. Recently 20% of treatment fee was covered by Hamad Medical Corporation to provide treatment to citizens and residents free of charge but this policy was exclusive only to National Centre for Cancer Care and Research (NCCCR). This should reduce the gap of lost CML patients at follow up.

Lastly, a timely laboratory investigation doesn't adhere to ELN timelines. The ELN timeline as stated in chapter two, the monitoring protocol was to collect peripheral blood samples at diagnosis, 3 months, 6 months, and 12 months to help the treating physician to assess the response of CML patients at the earliest. Unfortunately, this was not same to our CML cohort. A recent study documented this deficiency of adhering to ELN in the NCCCR hospital (Turkina et al., 2020).

Also, the study confirmed the high rate of resistance of CML in Qatar that reported in previous PhD study (Al-Dewik, N PhD 2006-2012). Around of 40- 50% of CML patients in this study were classified as failed treatment (Table 3. 1 &Table 4. 1and Table 5. 1).

Another area that was investigated during this project was the relationship between patient compliance and failed treatment. During the auditing process, most CML patients were found not to adhere to the treatment dose. The auditing process was done by checking pharmacy file of patients through Cerner application (cerner.com). The study observed that there was a ratio of CML patients who were in incompliance with treatment dose which could be a possible contributor to CML resistance. On the other hand, this study implemented a hospital-based database to record the results of PTPRG monitoring for CML patients in Qatar. However, due to absence of centralized CML data registry, the database is currently incomplete.

Finally, based on the results obtained in this study and future work, it would be interesting to conduct more detailed studies of the followings:

- To validate result of TPγ B9-2 antibody in a larger CML cohort.
- To establish multi centre collaboration using a larger group of patients to unravel the full potential of PTPRG protein determined by flow cytometry.
- Investigating the role of PTPRG play in other cancers such as such as Acute lymphocytic leukaemia (ALL) and breast cancer, using TPγ B9-2 antibody.
- *In-silico* and functional validations of the identified PTPRG variants and how they could affect the PTPRG structure causing protein loss of function. However, the pathogenicity of these variants in the PTPRG gene is uncertain and requires more detailed characterization for functional consequences in appropriate disease models.
- Inclusion of PTPRG as Tumour Suppressor Immune Gene Therapy in the future clinical trials.

- Utilization of cryopreservation (biobanking) of CML patients for more function assay, as there is growing evidence of body there is uncharacterized inhibitory mechanism that has ability to maintain BCR-ABL1 in active state. Yet, this mechanism still not well understood.
- More detailed studies of on Leukemic Stem Cells (LSCs). There is still argument on the surface phenotype defining this population (LSCs), more comprehensive studies on LSCs will open the spectrum of achieving a cure from disease.
- To introduce advanced molecular techniques such as NGS for the detection of *BCR-ABL* mutations.
- To improve patients' compliance to treatment as part of protocol of CML monitoring.
- To investigate the potential of monitoring PTPRG level as Quality of life indicator for CML patients.

8 Publication

8.1 Article

Mohamed. A. Ismail*+, Gheyath K. Nasrallah, Maria Monne, Ali AlSayab, Mohamed A. Yassin, Govindarajulu Varadharaj, Salma Younes, Claudio Sorio, Richard Cook, Helmout Modjtahedi and Nader I. Al-Dewik (2021) "Description of PTPRG genetic variants identified in a cohort of Chronic Myeloid Leukemia patients and their ability to influence response to Tyrosine kinase Inhibitors" Gene- Elsevier - Volume 813,2022, 146101, ISSN 0378-1119. https://doi.org/10.1016/j.gene.2021.146101. (Impact factor: 3.688). https://www.sciencedirect.com/science/article/pii/S037811192100696X

Mohamed A. Ismail*+, Vezzalini M, Morsi H, Abujaber A, Al Sayab A, Siveen K, Yassin MA, Monne M, Samara M, Cook R, Sorio C, Modjtahedi H, Al-Dewik NI (2021). Predictive value of tyrosine phosphatase receptor gamma for the response to treatment tyrosine kinase inhibitors in chronic myeloid leukemia patients. Sci Rep. 11(1):8833. doi: 10.1038/s41598-021-86875-y. PMID: 33893334; PMCID: PMC8065106 (Impact factor: 4.379). https://www.nature.com/articles/s41598-021-86875-y

Mohamed A. Ismail, Muthanna M, Al Sayab A, Alsharshani M, Yassin MA, Varadharaj G, Vezzalini M, Tomasello L, Monne M, Morsi H, Qoronfleh MW, Zayed H, Cook R, Sorio C, Modjtahedi H and Al-Dewik N (2020). Aberrant DNA methylation of PTPRG as one possible mechanism of its under-expression in CML patients in the State of Qatar. Mol Genet Genomic Med. 2020; 8: e1319 (Impact factor: 2.183). https://onlinelibrary.wiley.com/doi/full/10.1002/mgg3.131

Vezzalini M, Mafficini A, Tomasello L, Lorenzetto E, Moratti E, Fiorini Z, Holyoake TL, Pellicano F, Krampera M, Tecchio C, Yassin M, Al-Dewik N, **Ismail MA**, Al Sayab A, Monne M, Sorio C. **(2017).** A new monoclonal antibody detects downregulation of protein tyrosine phosphatase receptor type γ in chronic myeloid leukemia patients. J

Hematol Oncol. (Impact factor: 6.35). Doi: 10.1186/s13045-017-0494-z. PMID: 28637510; PMCID: PMC5479035.
https://jhoonline.biomedcentral.com/articles/10.1186/s13045-017-0494-z

8.2 Abstracts

Mohamed Ismail*, Marzia Vezzalini, Ali Al Sayab, Maria Monne, Vinod Gupta, Govundarajulu Varadharaj, Mohamed Alsharshani, Mohamed Yassin, Claudio Sorio, Helmout Modjtahedi and Nader I Al-Dewik **(2018).** "Studying Methylation Status of Protein Tyrosine Phosphatase Receptor Gamma (PTPRG) in Chronic Myeloid Leukemia Patients in the State of Qatar" Blood 132(supplment1): 5124. The 60th ASH Annual Meeting and Exposition (29/11/2018) in San Diego, CA, USA. ashpublications.org

Al-Dewik, N. I., M. Monne, **M. Araby**, A. Al Sayab, M. Vezzalini, L. Tomasello, H. Modjtahedi, C. Sorio and M. A. Yassin **(2016).** "Novel Molecular Findings in Protein Tyrosine Phosphatase Receptor Gamma (PTPRG) Among Chronic Myelocytic Leukaemia (CML) Patients Studied by Next Generation Sequencing (NGS): A Pilot Study in Patients from the State of Qatar and Italy" Blood 128(22): 5427. The 58th ASH Annual Meeting and Exposition (December 3-6, 2016) in San Diego, CA, USA. ashpublications.org.

8.3 Posters

Mohamed A. Ismail*, Mariza Vezzalini, Helmout Modjtahedi, Mohamed Yassin, Ali Alsayab, Claudio Sorio and Nader Al-Dewik: Abstract entitled **(2020)**. "Is restoring level of PTPRG drug depended in CML disease management" Annual Research Day (ARD) - Hamad Medical Corporation- Doha-Qatar.

Mohamed A. Ismail*, Mariza Vezzalini, Helmout Modjtahedi, Siveen Sivaraman, Mohamed Yassin, Ali Alsayab, Claudio Sorio and Nader Al-Dewik **(2018)**.

"Cryopreservation of Chronic myeloid leukaemia (CML) patients in state of Qatar" Annual Research Day (ARD) - Hamad Medical Corporation - Doha-Qatar.

Mohamed A. Ismail*, Mariza Vezzalini, Helmout Modjtahedi, Siveen Sivaraman, Mohamed Yassin, Ali Alsayab, Claudio Sorio and Nader Al-Dewik: Abstract entitled **(2017).** "Novel application of flow cytometry to monitor PTPRG expression in CML patients "Annual Research day (ARD) - Hamad Medical Corporation - Doha-Qatar.

*First Author

+Corresponding author

- **Acknowledgement.**

I awarded "SEC Achievement Award summer 2021" by the Kingston University for my findings and its publication in the Q1 journal.

I awarded "Completion bursary application" by Kingston University for submitting thesis before target date which was 1-11-2023.

9 Reference

ABELSON, H. T. & RABSTEIN, L. S. 1970. Lymphosarcoma: virus-induced thymic-independent disease in mice. *Cancer Res,* 30**,** 2213-22.

AKARD, L., KANTARJIAN, H. M., NICOLINI, F. E., WETZLER, M., LIPTON, J. H., BACCARANI, M., JEAN KHOURY, H., KURTIN, S., LI, E., MUNTEANU, M. & CORTES, J. 2016. Incidence and management of myelosuppression in patients with chronic- and accelerated-phase chronic myeloid leukemia treated with omacetaxine mepesuccinate. *Leuk Lymphoma,* 57**,** 654-65.

AL-BAHAR, S., PANDITA, R., AL-MUHANNAHA, A. & AL-BAHAR, E. 1994. The epidemiology of leukemia in Kuwait. *Leukemia Research,* 18**,** 251–255.

AL-DEWIK, N. I., JEWELL, A. P., YASSIN, M. A., EL-AYOUBI, H. R. & MORSI, H. M. 2014. Molecular Monitoring of patients with Chronic Myeloid Leukemia (CML) in the state of Qatar: Optimization of Techniques and Response to Imatinib. *QScience Connect,* 2014**,** 24.

AL-DEWIK, N. I., JEWELL, A. P., YASSIN, M. A. & MORSI, H. M. 2015. Studying the Impact of Presence of Alpha Acid Glycoprotein and Protein Glycoprotein in Chronic Myeloid Leukemia Patients Treated with Imatinib Mesylate in the State of Qatar. *Biomark Cancer,* 7**,** 63-7.

AL-DEWIK, N. I., MORSI, H. M., SAMARA, M. M., GHASOUB, R. S., GNANAM, C. C., BHASKARAN, S. K., NASHWAN, A. J., AL-JURF, R. M., ISMAIL, M. A., ALSHARSHANI, M. M., ALSAYAB, A. A., BEN-OMRAN, T. I., KHATIB, R. B. & YASSIN, M. A. 2016. Is Adherence to Imatinib Mesylate Treatment Among Patients with Chronic Myeloid Leukemia Associated with Better Clinical Outcomes in Qatar? *Clin Med Insights Oncol,* 10**,** 95-104.

AL THANI, A., FTHENOU, E., PAPARRODOPOULOS, S., AL MARRI, A., SHI, Z., QAFOUD, F. & AFIFI, N. 2019. Qatar Biobank Cohort Study: Study Design and First Results. *Am. J. Epidemiol.,* 188**,** 1420–1433.

ALADAG, E. & HAZNEDAROGLU, I. C. 2019. Current perspectives for the treatment of chronic myeloid leukemia. *Turk J Med Sci,* 49**,** 1-10.

ALONSO, A., SASIN, J., BOTTINI, N., FRIEDBERG, I., FRIEDBERG, I., OSTERMAN, A., GODZIK, A., HUNTER, T., DIXON, J. & MUSTELIN, T. 2004. Protein tyrosine phosphatases in the human genome. *Cell,* 117**,** 699-711.

AMIN, H. M., HOSHINO, K., YANG, H., LIN, Q., LAI, R. & GARCIA-MANERO, G. 2007. Decreased expression level of SH2 domain-containing protein tyrosine phosphatase-1 (Shp1) is associated with progression of chronic myeloid leukaemia. *J Pathol,* 212**,** 402-10.

ANDERSEN, J. N., JANSEN, P. G., ECHWALD, S. M., MORTENSEN, O. H., FUKADA, T., DEL VECCHIO, R., TONKS, N. K. & MOLLER, N. P. 2004. A genomic perspective on protein tyrosine phosphatases: gene structure, pseudogenes, and genetic disease linkage. *FASEB J,* 18**,** 8-30.

ANDERSEN, J. N., MORTENSEN, O. H., PETERS, G. H., DRAKE, P. G., IVERSEN, L. F., OLSEN, O. H., JANSEN, P. G., ANDERSEN, H. S., TONKS, N. K. & MOLLER, N. P. 2001. Structural and evolutionary relationships among protein tyrosine phosphatase domains. *Mol Cell Biol,* 21**,** 7117-36.

ANDREW J. GENTLES, P. 2010. Association of a Leukemic Stem Cell Gene Expression Signature With Clinical Outcomes in Acute Myeloid Leukemia. *JAMA,* 304**,** 2706–2715.

APPERLEY, J. F. 2007a. Part I: mechanisms of resistance to imatinib in chronic myeloid leukaemia. *Lancet Oncol,* 8**,** 1018-29.

APPERLEY, J. F. 2007b. Part II: management of resistance to imatinib in chronic myeloid leukaemia. *Lancet Oncol,* 8**,** 1116-1128.

APPERLEY, J. F. 2015. Chronic myeloid leukaemia. *Lancet,* 385**,** 1447–1459.

ARBER, D. A., ORAZI, A., HASSERJIAN, R., THIELE, J., BOROWITZ, M. J., LE BEAU, M. M., BLOOMFIELD, C. D., CAZZOLA, M. & VARDIMAN, J. W. 2016. The 2016 revision to the World Health Organization classification of myeloid neoplasms and acute leukemia. *Blood,* 127**,** 2391-405.

ARLINGHAUS, R. B. 1998. The involvement of Bcr in leukemias with the Philadelphia chromosome. *Crit Rev Oncog,* 9**,** 1-18.

AUTON, A., ABECASIS, G. R., ALTSHULER, D. M., DURBIN, R. M., ABECASIS, G. R., BENTLEY, D. R., CHAKRAVARTI, A., CLARK, A. G., DONNELLY, P., EICHLER, E. E., FLICEK, P., GABRIEL, S. B., GIBBS, R. A., GREEN, E. D., HURLES, M. E., KNOPPERS, B. M., KORBEL, J. O., LANDER, E. S., LEE, C., LEHRACH, H., MARDIS, E. R., MARTH, G. T., MCVEAN, G. A., NICKERSON, D. A., SCHMIDT, J. P., SHERRY, S. T., WANG, J., WILSON, R. K., GIBBS, R. A., BOERWINKLE, E., DODDAPANENI, H., HAN, Y., KORCHINA, V., KOVAR, C., LEE, S., MUZNY, D., REID, J. G., ZHU, Y., WANG, J., CHANG, Y., FENG, Q., FANG, X., GUO, X., JIAN, M., JIANG, H., JIN, X., LAN, T., LI, G., LI, J., LI, Y., LIU, S., LIU, X., LU, Y., MA, X., TANG, M., WANG, B., WANG, G., WU, H., WU, R., XU, X., YIN, Y., ZHANG, D., ZHANG, W., ZHAO, J., ZHAO, M., ZHENG, X., LANDER, E. S., ALTSHULER, D. M., GABRIEL, S. B., GUPTA, N., GHARANI, N., TOJI, L. H., GERRY, N. P., RESCH, A. M., FLICEK, P., BARKER, J., CLARKE, L., GIL, L., HUNT, S. E., KELMAN, G., KULESHA, E., LEINONEN, R., MCLAREN, W. M., RADHAKRISHNAN, R., ROA, A., SMIRNOV, D., SMITH, R. E., STREETER, I., THORMANN, A., TONEVA, I., VAUGHAN, B., ZHENG-BRADLEY, X., BENTLEY, D. R., GROCOCK, R., HUMPHRAY, S., JAMES, T., KINGSBURY, Z., LEHRACH, H., SUDBRAK, R., ALBRECHT, M. W., et al. 2015. A global reference for human genetic variation. *Nature,* 526**,** 68–74.

BACCARANI, M., CASTAGNETTI, F., GUGLIOTTA, G., ROSTI, G., SOVERINI, S., ALBEER, A., PFIRRMANN, M. & INTERNATIONAL, B. C. R. A. B. L. S. G. 2019a. The proportion of different BCR-ABL1 transcript types in chronic myeloid leukemia. An international overview. *Leukemia,* 33**,** 1173-1183.

BACCARANI, M., DEININGER, M. W., ROSTI, G., HOCHHAUS, A., SOVERINI, S., APPERLEY, J. F., CERVANTES, F., CLARK, R. E., CORTES, J. E., GUILHOT, F., HJORTH-HANSEN, H., HUGHES, T. P., KANTARJIAN, H. M., KIM, D. W., LARSON, R. A., LIPTON, J. H., MAHON, F. X., MARTINELLI, G., MAYER, J., MULLER, M. C., NIEDERWIESER, D., PANE, F., RADICH, J. P., ROUSSELOT, P., SAGLIO, G., SAUSSELE, S., SCHIFFER, C., SILVER, R., SIMONSSON, B., STEEGMANN, J. L., GOLDMAN, J. M. & HEHLMANN, R. 2013. European LeukemiaNet recommendations for the management of chronic myeloid leukemia: 2013. *Blood,* 122**,** 872-84.

BACCARANI, M., ROSTI, G. & SOVERINI, S. 2019b. Chronic myeloid leukemia: the concepts of resistance and persistence and the relationship with the BCR-ABL1 transcript type. *Leukemia,* 33**,** 2358-2364.

BAKHACH, J. 2009. The cryopreservation of composite tissues: Principles and recent advancement on cryopreservation of different type of tissues. *Organogenesis,* 5**,** 119-26.

BARNEA, G., SILVENNOINEN, O., SHAANAN, B., HONEGGER, A. M., CANOLL, P. D., D'EUSTACHIO, P., MORSE, B., LEVY, J. B., LAFORGIA, S., HUEBNER, K. & ET AL. 1993. Identification of a carbonic anhydrase-like domain in the extracellular region of RPTP gamma defines a new subfamily of receptor tyrosine phosphatases. *Mol Cell Biol,* 13**,** 1497-506.

BARNES, D. J. & MELO, J. V. 2002. Cytogenetic and molecular genetic aspects of chronic myeloid leukaemia. *Acta Haematol,* 108**,** 180-202.

BAUST, J. M., CORWIN, W. L., VANBUSKIRK, R. & BAUST, J. G. 2015. Biobanking: The Future of Cell Preservation Strategies. *Adv Exp Med Biol,* 864**,** 37-53.

BAWAZIR, A., AL-ZAMEL, N., AMEN, A., AKIEL, M. A., ALHAWITI, N. M. & ALSHEHRI, A. 2019. The burden of leukemia in the Kingdom of Saudi Arabia: 15 years period (1999-2013). *BMC Cancer,* 19**,** 703.

BEHZAD, M. M., SHAHRABI, S., JASEB, K., BERTACCHINI, J., KETABCHI, N. & SAKI, N. 2018. Aberrant DNA Methylation in Chronic Myeloid Leukemia: Cell Fate Control, Prognosis, and Therapeutic Response. *Biochem Genet,* 56**,** 149-175.

BHAYAT, F., DAS-GUPTA, E., SMITH, C., MCKEEVER, T. & HUBBARD, R. 2009. The incidence of and mortality from leukaemias in the UK: a general population-based study. *BMC Cancer,* 9**,** 252.

BIERNAUX, C., LOOS, M., SELS, A., HUEZ, G. & STRYCKMANS, P. 1995. Detection of major bcr-abl gene expression at a very low level in blood cells of some healthy individuals. *Blood,* 86**,** 3118-22.

BONI, C. & SORIO, C. 2021. Current Views on the Interplay between Tyrosine Kinases and Phosphatases in Chronic Myeloid Leukemia. *Cancers,* 13**,** 2311.

BONIFACIO, M. 2018. Recent Developments in Chronic Myeloid Leukemia Biology and Treatment. *Frontiers in Clinical Drug Research-Hematology,* Vol. 3**,** CHAPTER 2.

BONIFACIO, M., STAGNO, F., SCAFFIDI, L., KRAMPERA, M. & DI RAIMONDO, F. 2019. Management of Chronic Myeloid Leukemia in Advanced Phase. *Front Oncol,* 9**,** 1132.

BOSE, S., DEININGER, M., GORA-TYBOR, J., GOLDMAN, J. M. & MELO, J. V. 1998. The presence of typical and atypical BCR-ABL fusion genes in leukocytes of normal individuals: biologic significance and implications for the assessment of minimal residual disease. *Blood,* 92**,** 3362-7.

BRANFORD, S., CROSS, N. C., HOCHHAUS, A., RADICH, J., SAGLIO, G., KAEDA, J., GOLDMAN, J. & HUGHES, T. 2006. Rationale for the recommendations for harmonizing current methodology for detecting BCR-ABL transcripts in patients with chronic myeloid leukaemia. *Leukemia,* 20**,** 1925-30.

BRANFORD, S., KIM, D. D. H., APPERLEY, J. F., EIDE, C. A., MUSTJOKI, S., ONG, S. T., NTELIOPOULOS, G., ERNST, T., CHUAH, C., GAMBACORTI-PASSERINI, C., MAURO, M. J., DRUKER, B. J., KIM, D. W., MAHON, F. X., CORTES, J., RADICH, J. P., HOCHHAUS, A., HUGHES, T. P. & INTERNATIONAL, C. M. L. F. G. A. 2019. Laying the foundation for genomically-based risk assessment in chronic myeloid leukemia. *Leukemia,* 33**,** 1835-1850.

BRAUN, T. P., EIDE, C. A. & DRUKER, B. J. 2020. Response and Resistance to BCR-ABL1-Targeted Therapies. *Cancer Cell,* 37**,** 530-542.

CANCER, U. F. I. 2015. *WHO | Medicines for treatment of the following cancers – review – EML and EMLc* [Online]. World Health Organization. Available: https://www.who.int/selection_medicines/committees/expert/20/applications/cancer/en [Accessed].

CANNELL, E. 2007. Dasatinib is effective in imatinib-resistant CML. *Lancet Oncol,* 8**,** 286.

CASTAGNETTI, F., BRECCIA, M., GUGLIOTTA, G., MARTINO, B., D'ADDA, M., STAGNO, F., CARELLA, A. M., AVANZINI, P., TIRIBELLI, M., TRABACCHI, E., VISANI, G., GOBBI, M., SALVUCCI, M., LEVATO, L., BINOTTO, G., CAPALBO, S. F., BOCHICCHIO, M. T., SOVERINI, S., CAVO, M., MARTINELLI, G., ALIMENA, G., PANE, F., SAGLIO, G., ROSTI, G., BACCARANI, M. & PARTY, G. C. W. 2016. Nilotinib 300 mg twice daily: an academic single-arm study of newly diagnosed chronic phase chronic myeloid leukemia patients. *Haematologica,* 101**,** 1200-1207.

CHAITANYA, P. K., KUMAR, K. A., STALIN, B., SADASHIVUDU, G. & SRINIVAS, M. L. 2017. The Role of Mutation Testing in Patients with Chronic Myeloid Leukemia in Chronic Phase after Imatinib Failure and Their Outcomes after Treatment Modification: Single-institutional Experience Over 13 Years. *Indian Journal of Medical and Paediatric Oncology : Official Journal of Indian Society of Medical & Paediatric Oncology,* 38**,** 328.

CHANDRASEKHAR, C., KUMAR, P. S. & SARMA, P. 2019. Novel mutations in the kinase domain of BCR-ABL gene causing imatinib resistance in chronic myeloid leukemia patients. *Sci Rep,* 9**,** 2412.

CHEN, C., PARKER, M. S., BARNES, A. P., DEININGER, P. & BOBBIN, R. P. 2000. Functional expression of three P2X(2) receptor splice variants from guinea pig cochlea. *J Neurophysiol,* 83**,** 1502-9.

CHEUNG, A. K., IP, J. C., CHU, A. C., CHENG, Y., LEONG, M. M., KO, J. M., SHUEN, W. H., LUNG, H. L. & LUNG, M. L. 2015. PTPRG suppresses tumor growth and invasion via inhibition of Akt signaling in nasopharyngeal carcinoma. *Oncotarget,* 6**,** 13434-47.

CHEUNG, A. K., LUNG, H. L., HUNG, S. C., LAW, E. W., CHENG, Y., YAU, W. L., BANGARUSAMY, D. K., MILLER, L. D., LIU, E. T., SHAO, J. Y., KOU, C. W., CHUA, D., ZABAROVSKY, E. R., TSAO, S. W., STANBRIDGE, E. J. & LUNG, M. L. 2008. Functional analysis of a cell cycle-associated, tumor-suppressive gene, protein tyrosine phosphatase receptor type G, in nasopharyngeal carcinoma. *Cancer Res,* 68**,** 8137-45.

CHISSOE, S. L., BODENTEICH, A., WANG, Y. F., WANG, Y. P., BURIAN, D., CLIFTON, S. W., CRABTREE, J., FREEMAN, A., IYER, K., JIAN, L. & ET AL. 1995. Sequence and analysis of the human ABL gene, the BCR gene, and regions involved in the Philadelphia chromosomal translocation. *Genomics,* 27**,** 67-82.

CHOHAN, T. A., QAYYUM, A., REHMAN, K., TARIQ, M. & AKASH, M. S. H. 2018. An insight into the emerging role of cyclin-dependent kinase inhibitors as potential therapeutic agents for the treatment of advanced cancers. *Biomed. Pharmacother.,* 107**,** 1326–1341.

CHURCH, B. V., WILLIAMS, H. T. & MAR, J. C. 2019. Investigating skewness to understand gene expression heterogeneity in large patient cohorts. *BMC Bioinf.,* 20**,** 1–14.

CILLONI, D. & SAGLIO, G. 2009. CML: a model for targeted therapy. *Best Pract Res Clin Haematol,* 22**,** 285-94.

COHEN, G. B., REN, R. & BALTIMORE, D. 1995. Modular binding domains in signal transduction proteins. *Cell,* 80**,** 237-48.

COHEN, M. H., JOHNSON, J. R. & PAZDUR, R. 2005. U.S. Food and Drug Administration Drug Approval Summary: conversion of imatinib mesylate (STI571; Gleevec) tablets from accelerated approval to full approval. *Clin Cancer Res,* 11**,** 12-9.

CORM, S., BIGGIO, V., ROCHE-LESTIENNE, C., LAI, J. L., YAKOUB-AGHA, I., PHILIPPE, N., NICOLINI, F. E., FACON, T. & PREUDHOMME, C. 2005. Coexistence of AML1/RUNX1 and BCR-ABL point mutations in an imatinib-resistant form of CML. *Leukemia,* 19**,** 1991-2.

CORTES, J. & LANG, F. 2021. Third-line therapy for chronic myeloid leukemia: current status and future directions. *J Hematol Oncol,* 14**,** 44.

CORTES, J. E., DE SOUZA, C. A., AYALA, M., LOPEZ, J. L., BULLORSKY, E., SHAH, S., HUANG, X., BABU, K. G., ABDULKADYROV, K., DE OLIVEIRA, J. S. R., SHEN, Z.-X., SACHA, T., BENDIT, I., LIANG, Z., OWUGAH, T., SZCZUDLO, T., KHANNA, S., FELLAGUE-CHEBRA, R. & LE COUTRE, P. D. 2016. Switching to nilotinib versus imatinib dose escalation in patients with chronic myeloid leukaemia in chronic phase with suboptimal response to imatinib (LASOR): a randomised, open-label trial. *Lancet. Haematol.,* 3**,** 581–591.

CORTES, J. E., GAMBACORTI-PASSERINI, C., DEININGER, M. W., MAURO, M. J., CHUAH, C., KIM, D.-W., DYAGIL, I., GLUSHKO, N., MILOJKOVIC, D., LE COUTRE, P., GARCIA-GUTIERREZ, V., REILLY, L., JEYNES-ELLIS, A., LEIP, E., BARDY-BOUXIN, N., HOCHHAUS, A. & BRÜMMENDORF, T. H. 2018. Bosutinib Versus Imatinib for Newly Diagnosed Chronic Myeloid Leukemia: Results From the Randomized BFORE Trial. *J. Clin. Oncol.,* 36**,** 231–237.

DAI, S., ZHOU, Z., CHEN, Z., XU, G. & CHEN, Y. 2019. Fibroblast Growth Factor Receptors (FGFRs): Structures and Small Molecule Inhibitors. *Cells,* 8.

DAI, Z. & PENDERGAST, A. M. 1995. Abi-2, a novel SH3-containing protein interacts with the c-Abl tyrosine kinase and modulates c-Abl transforming activity. *Genes Dev,* 9**,** 2569-82.

DASGUPTA, S., RAY, U. K., MITRA, A. G., BHATTACHARYYA, D. M., MUKHOPADHYAY, A., DAS, P., GANGOPADHYAY, S., ROY, S. & MUKHOPADHYAY, S. 2017. Evaluation of a new flow cytometry based method for detection of BCR-ABL1 fusion protein in chronic myeloid leukemia. *Blood Res,* 52**,** 112-118.

DEGNIN, M., AGARWAL, A., TARLOCK, K., MESHINCHI, S., DRUKER, B. J. & TOGNON, C. E. 2017. Novel Method Enabling the Use of Cryopreserved Primary Acute Myeloid Leukemia Cells in Functional Drug Screens. *J Pediatr Hematol Oncol,* 39**,** e359-e366.

DEININGER, M., O'BRIEN, S. G., GUILHOT, F. O., GOLDMAN, J. M., HOCHHAUS, A., HUGHES, T. P., RADICH, J. P., HATFIELD, A. K., MONE, M., FILIAN, J., REYNOLDS, J., GATHMANN, I., LARSON, R. A. & DRUKER, B. J. 2009. International Randomized Study of Interferon Vs STI571 (IRIS) 8-Year Follow up: Sustained Survival and Low Risk for Progression or Events in Patients with Newly Diagnosed Chronic Myeloid Leukemia in Chronic Phase (CML-CP) Treated with Imatinib. *Blood,* 114**,** 1126–1126.

DEININGER, M. W., CORTES, J., PAQUETTE, R., PARK, B., HOCHHAUS, A., BACCARANI, M., STONE, R., FISCHER, T., KANTARJIAN, H., NIEDERWIESER, D., GAMBACORTI-PASSERINI, C., SO, C., GATHMANN, I., GOLDMAN, J. M., SMITH, D., DRUKER, B. J. & GUILHOT, F. 2007. The prognosis for patients with chronic myeloid leukemia who have clonal cytogenetic abnormalities in philadelphia chromosome-negative cells. *Cancer,* 110**,** 1509-19.

DEININGER, M. W., GOLDMAN, J. M. & MELO, J. V. 2000. The molecular biology of chronic myeloid leukemia. *Blood,* 96**,** 3343-56.

DEL PESO, L., GONZALEZ-GARCIA, M., PAGE, C., HERRERA, R. & NUNEZ, G. 1997. Interleukin-3-induced phosphorylation of BAD through the protein kinase Akt. *Science,* 278**,** 687-9.

DELLA PERUTA, M., MARTINELLI, G., MORATTI, E., PINTANI, D., VEZZALINI, M., MAFFICINI, A., GRAFONE, T., IACOBUCCI, I., SOVERINI, S., MURINEDDU, M., VINANTE, F., TECCHIO, C., PIRAS, G., GABBAS, A., MONNE, M. & SORIO, C. 2010. Protein tyrosine phosphatase receptor type {gamma} is a functional tumor suppressor gene specifically downregulated in chronic myeloid leukemia. *Cancer Res,* 70**,** 8896-906.

DEMIROGLU, A., STEER, E. J., HEATH, C., TAYLOR, K., BENTLEY, M., ALLEN, S. L., KODURU, P., BRODY, J. P., HAWSON, G., RODWELL, R., DOODY, M. L., CARNICERO, F., REITER, A., GOLDMAN, J. M., MELO, J. V. & CROSS, N. C. 2001. The t(8;22) in chronic myeloid leukemia fuses BCR to FGFR1: transforming activity and specific inhibition of FGFR1 fusion proteins. *Blood,* 98**,** 3778-83.

DENG, N., ZHOU, H., FAN, H. & YUAN, Y. 2017. Single nucleotide polymorphisms and cancer susceptibility. *Oncotarget,* 8**,** 110635.

DENHARDT, D. T. 1996. Signal-transducing protein phosphorylation cascades mediated by Ras/Rho proteins in the mammalian cell: the potential for multiplex signalling. *Biochem J,* 318 (Pt 3)**,** 729-47.

DIEKMANN, D., BRILL, S., GARRETT, M. D., TOTTY, N., HSUAN, J., MONFRIES, C., HALL, C., LIM, L. & HALL, A. 1991. Bcr encodes a GTPase-activating protein for p21rac. *Nature,* 351**,** 400-2.

DO, T. N., UCISIK-AKKAYA, E., DAVIS, C. F., MORRISON, B. A. & DORAK, M. T. 2010. An intronic polymorphism of IRF4 gene influences gene transcription in vitro and shows a risk association with childhood acute lymphoblastic leukemia in males. *Biochim. Biophys. Acta,* 1802**,** 292–300.

DONATO, N. J., WU, J. Y., STAPLEY, J., GALLICK, G., LIN, H., ARLINGHAUS, R. & TALPAZ, M. 2003. BCR-ABL independence and LYN kinase overexpression in chronic myelogenous leukemia cells selected for resistance to STI571. *Blood,* 101**,** 690-8.

DONG, Y., SHI, O., ZENG, Q., LU, X., WANG, W., LI, Y. & WANG, Q. 2020. Leukemia incidence trends at the global, regional, and national level between 1990 and 2017. *Exp Hematol Oncol,* 9**,** 14.

DRUBE, J., ERNST, T., PFIRRMANN, M., ALBERT, B. V., DRUBE, S., REICH, D., KRESINSKY, A., HALFTER, K., SORIO, C., FABISCH, C., HOCHHAUS, A. & BÖHMER, F.-D. 2018. PTPRG and PTPRC modulate nilotinib response in chronic myeloid leukemia cells. *Oncotarget,* 9**,** 9442.

DRUKER, B. J., GUILHOT, F., O'BRIEN, S. G., GATHMANN, I., KANTARJIAN, H., GATTERMANN, N., DEININGER, M. W. N., SILVER, R. T., GOLDMAN, J. M., STONE, R. M., CERVANTES, F., HOCHHAUS, A., POWELL, B. L., GABRILOVE, J. L., ROUSSELOT, P., REIFFERS, J., CORNELISSEN, J. J., HUGHES, T., AGIS, H., FISCHER, T., VERHOEF, G., SHEPHERD, J., SAGLIO, G., GRATWOHL, A., NIELSEN, J. L., RADICH, J. P., SIMONSSON, B., TAYLOR, K., BACCARANI, M., SO, C., LETVAK, L. & LARSON, R. A. 2006. Five-Year Follow-up of Patients Receiving Imatinib for Chronic Myeloid Leukemia. *N. Engl. J. Med.,* 355**,** 2408–2417.

DRUKER, B. J., TAMURA, S., BUCHDUNGER, E., OHNO, S., SEGAL, G. M., FANNING, S., ZIMMERMANN, J. & LYDON, N. B. 1996. Effects of a selective inhibitor of the Abl tyrosine kinase on the growth of Bcr-Abl positive cells. *Nat Med,* 2**,** 561-6.

DU, Y. & GRANDIS, J. R. 2015. Receptor-type protein tyrosine phosphatases in cancer. *Chin J Cancer,* 34**,** 61-9.

DVORAK, P., DVORAKOVA, D., DOUBEK, M., FAITOVA, J., PACHOLIKOVA, J., HAMPL, A. & MAYER, J. 2003. Increased expression of fibroblast growth factor receptor 3 in CD34+ BCR-ABL+ cells from patients with chronic myeloid leukemia. *Leukemia,* 17**,** 2418-25.

EDEN, R. E. & COVIELLO, J. M. 2019. Cancer, Chronic Myelogenous Leukemia (CML, Chronic Granulocytic Leukemia). *StatPearls.* Treasure Island (FL).

ENZYMOLOGY, I. O. 2020. *BiSearch: Primer Design and Search Tool* [Online]. Available: http://bisearch.enzim.hu [Accessed].

FADERL, S., TALPAZ, M., ESTROV, Z. & KANTARJIAN, H. M. 1999. Chronic myelogenous leukemia: biology and therapy. *Ann Intern Med,* 131**,** 207-19.

FAN, Z., LUO, H., ZHOU, J., WANG, F., ZHANG, W., WANG, J., LI, S., LAI, Q., XU, Y., WANG, G., LIANG, A. & XU, J. 2020. Checkpoint kinase‑1 inhibition and etoposide exhibit a strong synergistic anticancer effect on chronic myeloid leukemia cell line K562 by impairing homologous recombination DNA damage repair. *Oncol. Rep.,* 44**,** 2152–2164.

FLIS, S. & CHOJNACKI, T. 2019. Chronic myelogenous leukemia, a still unsolved problem: pitfalls and new therapeutic possibilities. *Drug Des Devel Ther,* 13**,** 825-843.

FOLEY, S. B., HILDENBRAND, Z. L., SOYOMBO, A. A., MAGEE, J. A., WU, Y., ORAVECZ-WILSON, K. I. & ROSS, T. S. 2013. Expression of BCR/ABL p210 from a knockin allele enhances bone marrow engraftment without inducing neoplasia. *Cell Rep,* 5**,** 51-60.

FRANKE, T. F., KAPLAN, D. R. & CANTLEY, L. C. 1997. PI3K: downstream AKTion blocks apoptosis. *Cell,* 88**,** 435-7.

GABERT, J., BEILLARD, E., VAN DER VELDEN, V. H., BI, W., GRIMWADE, D., PALLISGAARD, N., BARBANY, G., CAZZANIGA, G., CAYUELA, J. M., CAVE, H., PANE, F., AERTS, J. L., DE MICHELI, D., THIRION, X., PRADEL, V., GONZALEZ, M., VIEHMANN, S., MALEC, M., SAGLIO, G. & VAN DONGEN, J. J. 2003. Standardization and quality control studies of 'real-time' quantitative reverse transcriptase polymerase chain reaction of fusion gene transcripts for residual disease detection in leukemia - a Europe Against Cancer program. *Leukemia,* 17**,** 2318-57.

GARCIA-GUTIERREZ, V. & HERNANDEZ-BOLUDA, J. C. 2019. Tyrosine Kinase Inhibitors Available for Chronic Myeloid Leukemia: Efficacy and Safety. *Front Oncol,* 9**,** 603.

GOLDMAN, J. 2003a. Chronic myeloid leukemia--past, present, and future. *Semin Hematol,* 40**,** 1-3.

GOLDMAN, M. A. 2003b. The epigenetics of the cell. *Genome Biol,* 4**,** 309.

GÓMEZ-CASARES, M. T., GARCÍA-ALEGRIA, E., LÓPEZ-JORGE, C. E., FERRÁNDIZ, N., BLANCO, R., ALVAREZ, S., VAQUÉ, J. P., BRETONES, G., CARABALLO, J. M., SÁNCHEZ-BAILÓN, P., DELGADO, M. D., MARTÍN-PEREZ, J., CIGUDOSA, J. C. & LEÓN, J. 2013. MYC antagonizes the differentiation induced by imatinib in chronic myeloid leukemia cells through downregulation of p27KIP1. *Oncogene,* 32**,** 2239–2246.

GONFLONI, S. 2014. Defying c-Abl signaling circuits through small allosteric compounds. *Front Genet,* 5**,** 392.

GOVER-PROAKTOR, A., GRANOT, G., PASMANIK-CHOR, M., PASVOLSKY, O., SHAPIRA, S., RAZ, O., RAANANI, P. & LEADER, A. 2019. Bosutinib, dasatinib, imatinib, nilotinib, and ponatinib differentially affect the vascular molecular pathways and functionality of human endothelial cells. *Leuk Lymphoma,* 60**,** 189-199.

GRCH37. 2021. *Exons - Homo_sapiens - GRCh37 Archive browser 104* [Online]. Available: https://grch37.ensembl.org/Homo_sapiens/Transcript/Exons?db=core%3Bg=ENSG00000144724%3Br=3:61547243-62283288%3Bt=ENST00000474889 [Accessed].

GROFFEN, J., STEPHENSON, J. R., HEISTERKAMP, N., DE KLEIN, A., BARTRAM, C. R. & GROSVELD, G. 1984. Philadelphia chromosomal breakpoints are clustered within a limited region, bcr, on chromosome 22. *Cell,* 36**,** 93-9.

GUGLIOTTA, G., CASTAGNETTI, F., BRECCIA, M., LEVATO, L., D'ADDA, M., STAGNO, F., TIRIBELLI, M., SALVUCCI, M., FAVA, C., MARTINO, B., CEDRONE, M., BOCCHIA, M., TRABACCHI, E., CAVAZZINI, F., USALA, E., RUSSO ROSSI, A., BOCHICCHIO, M. T., SOVERINI, S., ALIMENA, G., CAVO, M., PANE, F., MARTINELLI, G., SAGLIO, G., BACCARANI, M. & ROSTI, G. 2015. Long-term outcome of a phase 2 trial with nilotinib 400 mg twice daily in first-line treatment of chronic myeloid leukemia. *Haematologica,* 100**,** 1146–1150.

GUO, Y.-J., PAN, W.-W., LIU, S.-B., SHEN, Z.-F., XU, Y. & HU, L.-L. 2020. ERK/MAPK signalling pathway and tumorigenesis (Review). *Experimental and Therapeutic Medicine,* 19**,** 1997–2007.

HANTSCHEL, O., NAGAR, B., GUETTLER, S., KRETZSCHMAR, J., DOREY, K., KURIYAN, J. & SUPERTI-FURGA, G. 2003. A myristoyl/phosphotyrosine switch regulates c-Abl. *Cell,* 112**,** 845-57.

HANTSCHEL, O. & SUPERTI-FURGA, G. 2004. Regulation of the c-Abl and Bcr-Abl tyrosine kinases. *Nat Rev Mol Cell Biol,* 5**,** 33-44.

HAO, T., LI-TALLEY, M., BUCK, A. & CHEN, W. 2019. An emerging trend of rapid increase of leukemia but not all cancers in the aging population in the United States. *Sci Rep,* 9**,** 12070.

HARRINGTON, P., KIZILORS, A. & DE LAVALLADE, H. 2017. The Role of Early Molecular Response in the Management of Chronic Phase CML. *Current Hematologic Malignancy Reports,* 12**,** 79.

HASFORD, J., BACCARANI, M., HOFFMANN, V., GUILHOT, J., SAUSSELE, S., ROSTI, G., GUILHOT, F., PORKKA, K., OSSENKOPPELE, G., LINDOERFER, D., SIMONSSON, B., PFIRRMANN, M. & HEHLMANN, R. 2011. Predicting complete cytogenetic response and subsequent progression-free survival in 2060 patients with CML on imatinib treatment: the EUTOS score. *Blood,* 118**,** 686-92.

HAZLEHURST, L. A., BEWRY, N. N., NAIR, R. R. & PINILLA-IBARZ, J. 2009. Signaling networks associated with BCR-ABL-dependent transformation. *Cancer Control,* 16**,** 100-7.

HEIDEL, F. H., MAR, B. G. & ARMSTRONG, S. A. 2011. Self-renewal related signaling in myeloid leukemia stem cells. *Int. J. Hematol.,* 94**,** 109–117.

HERMANS, A., HEISTERKAMP, N., VON LINDEN, M., VAN BAAL, S., MEIJER, D., VAN DER PLAS, D., WIEDEMANN, L. M., GROFFEN, J., BOOTSMA, D. & GROSVELD, G. 1987. Unique fusion of bcr and c-abl genes in Philadelphia chromosome positive acute lymphoblastic leukemia. *Cell,* 51**,** 33-40.

HERNANDEZ, H. G., TSE, M. Y., PANG, S. C., ARBOLEDA, H. & FORERO, D. A. 2013. Optimizing methodologies for PCR-based DNA methylation analysis. *Biotechniques,* 55**,** 181-97.

HOCHHAUS, A. 2006. Chronic myelogenous leukemia (CML): resistance to tyrosine kinase inhibitors. *Ann Oncol,* 17 Suppl 10**,** x274-9.

HOCHHAUS, A., SAUSSELE, S., ROSTI, G., MAHON, F. X., JANSSEN, J., HJORTH-HANSEN, H., RICHTER, J., BUSKE, C. & COMMITTEE, E. G. 2017. Chronic myeloid leukaemia: ESMO Clinical Practice Guidelines for diagnosis, treatment and follow-up. *Ann Oncol,* 28**,** iv41-iv51.

HOCHHAUS, A., YAN, X. H., WILLER, A., HEHLMANN, R., GORDON, M. Y., GOLDMAN, J. M. & MELO, J. V. 1997. Expression of interferon regulatory factor (IRF) genes and response to interferon-alpha in chronic myeloid leukaemia. *Leukemia,* 11**,** 933-9.

HOGLUND, M., SANDIN, F. & SIMONSSON, B. 2015. Epidemiology of chronic myeloid leukaemia: an update. *Ann Hematol,* 94 Suppl 2**,** S241-7.

HOUSHMAND, M., SIMONETTI, G., CIRCOSTA, P., GAIDANO, V., CIGNETTI, A., MARTINELLI, G., SAGLIO, G. & GALE, R. P. 2019. Chronic myeloid leukemia stem cells. *Leukemia,* 33**,** 1543–1556.

HOWLADER. 2016. *PDF Version - SEER Cancer Statistics Review (CSR), 1975-2016* [Online]. Available: https://seer.cancer.gov/csr/1975_2016/sections.html [Accessed].

HSIEH, Y. C., KIRSCHNER, K. & COPLAND, M. 2021. Improving outcomes in chronic myeloid leukemia through harnessing the immunological landscape. *Leukemia,* 35**,** 1229-1242.

HUANG, X., CORTES, J. & KANTARJIAN, H. 2012. Estimations of the increasing prevalence and plateau prevalence of chronic myeloid leukemia in the era of tyrosine kinase inhibitor therapy. *Cancer,* 118**,** 3123-7.

HUGHES, T. P., KAEDA, J., BRANFORD, S., RUDZKI, Z., HOCHHAUS, A., HENSLEY, M. L., GATHMANN, I., BOLTON, A. E., VAN HOOMISSEN, I. C., GOLDMAN, J. M., RADICH, J. P. & INTERNATIONAL RANDOMISED STUDY OF INTERFERON VERSUS, S. T. I. S. G. 2003. Frequency of major molecular responses to imatinib or interferon alfa plus cytarabine in newly diagnosed chronic myeloid leukemia. *N Engl J Med,* 349**,** 1423-32.

HUNT, C. J. 2019. Technical Considerations in the Freezing, Low-Temperature Storage and Thawing of Stem Cells for Cellular Therapies. *Transfus Med Hemother,* 46**,** 134-150.

ISMAIL, M., VEZZALINI, M., AL SAYAB, A., MONNE, M., GUPTA, V., VARADHARAJ, G., ALSHARSHANI, M., YASSIN, M., SORIO, C., MODJTAHEDI, H. & AL-DEWIK, N. I. 2018. Studying Methylation Status of Protein Tyrosine Phosphatase Receptor Gamma (PTPRG) in Chronic Myeloid Leukemia Patients in the State of Qatar. *Blood,* 132**,** 5124–5124.

ISMAIL, M. A., NASRALLAH, G. K., MONNE, M., ALSAYAB, A., YASSIN, M. A., VARADHARAJ, G., YOUNES, S., SORIO, C., COOK, R., MODJTAHEDI, H. & AL-DEWIK, N. I. 2022. Description of PTPRG genetic variants identified in a cohort of Chronic Myeloid Leukemia patients and their ability to influence response to Tyrosine kinase Inhibitors. *Gene,* 813**,** 146101.

ISMAIL, M. A., SAMARA, M., AL SAYAB, A., ALSHARSHANI, M., YASSIN, M. A., VARADHARAJ, G., VEZZALINI, M., TOMASELLO, L., MONNE, M., MORSI, H., QORONFLEH, M. W., ZAYED, H., COOK, R., SORIO, C., MODJTAHEDI, H. & AL-DEWIK, N. I. 2020. Aberrant DNA methylation of PTPRG as one possible mechanism of its under-expression in CML patients in the State of Qatar. *Mol. Genet. Genomic Med.,* 8**,** e1319.

ISMAIL, M. A., VEZZALINI, M., MORSI, H., ABUJABER, A., AL SAYAB, A., SIVEEN, K., YASSIN, M. A., MONNE, M., SAMARA, M., COOK, R., SORIO, C., MODJTAHEDI, H. & AL-DEWIK, N. I. 2021. Predictive value of tyrosine phosphatase receptor gamma for the response to treatment tyrosine kinase inhibitors in chronic myeloid leukemia patients. *Sci Rep,* 11**,** 8833.

ISMAIL, S. I., NAFFA, R. G., YOUSEF, A. M. & GHANIM, M. T. 2014. Incidence of bcrabl fusion transcripts in healthy individuals. *Mol Med Rep,* 9**,** 1271-6.

ITO, T., KWON, H. Y., ZIMDAHL, B., CONGDON, K. L., BLUM, J., LENTO, W. E., ZHAO, C., LAGOO, A., GERRARD, G., FORONI, L., GOLDMAN, J., GOH, H., KIM, S. H., KIM, D. W., CHUAH, C., OEHLER, V. G., RADICH, J. P., JORDAN, C. T. & REYA, T. 2010. Regulation of myeloid leukaemia by the cell-fate determinant Musashi. *Nature,* 466**,** 765-8.

JABBOUR, E. & KANTARJIAN, H. 2016. Chronic myeloid leukemia: 2016 update on diagnosis, therapy, and monitoring. *Am J Hematol,* 91**,** 252-65.

JABBOUR, E. & KANTARJIAN, H. 2018. Chronic myeloid leukemia: 2018 update on diagnosis, therapy and monitoring. *Am. J. Hematol.,* 93**,** 442–459.

JABBOUR, E. & KANTARJIAN, H. 2020a. Chronic myeloid leukemia: 2020 update on diagnosis, therapy and monitoring. *Am. J. Hematol.,* 95**,** 691–709.

JABBOUR, E. & KANTARJIAN, H. 2020b. Chronic myeloid leukemia: 2020 update on diagnosis, therapy and monitoring. *Am J Hematol,* 95**,** 691-709.

JANG, T. H., PARK, S. C., YANG, J. H., KIM, J. Y., SEOK, J. H., PARK, U. S., CHOI, C. W., LEE, S. R. & HAN, J. 2017. Cryopreservation and its clinical applications. *Integr Med Res,* 6**,** 12-18.

JELINEK, J., GHARIBYAN, V., ESTECIO, M. R. H., KONDO, K., HE, R., CHUNG, W., LU, Y., ZHANG, N., LIANG, S., KANTARJIAN, H. M., CORTES, J. E. & ISSA, J.-P. J. 2011. Aberrant DNA methylation is associated with disease progression, resistance to imatinib and shortened survival in chronic myelogenous leukemia. *PLoS One,* 6**,** e22110.

JENNINGS, B. A. & MILLS, K. I. 1998. c-myc locus amplification and the acquisition of trisomy 8 in the evolution of chronic myeloid leukaemia. *Leuk Res,* 22**,** 899-903.

JIANG, G., DEN HERTOG, J. & HUNTER, T. 2000. Receptor-like protein tyrosine phosphatase alpha homodimerizes on the cell surface. *Mol Cell Biol,* 20**,** 5917-29.

JIANG, M., ZHANG, Y., FEI, J., CHANG, X., FAN, W., QIAN, X., ZHANG, T. & LU, D. 2010. Rapid quantification of DNA methylation by measuring relative peak heights in direct bisulfite-PCR sequencing traces. *Lab Invest,* 90**,** 282-90.

JULIEN, S. G., DUBE, N., HARDY, S. & TREMBLAY, M. L. 2011. Inside the human cancer tyrosine phosphatome. *Nat Rev Cancer,* 11**,** 35-49.

KANTARJIAN, H. M., SHAH, N. P., CORTES, J. E., BACCARANI, M., AGARWAL, M. B., UNDURRAGA, M. S., WANG, J., IPIÑA, J. J. K., KIM, D.-W., OGURA, M., PAVLOVSKY, C., JUNGHANSS, C., MILONE, J. H., NICOLINI, F. E., ROBAK, T., VAN DROOGENBROECK, J., VELLENGA, E., BRADLEY-GARELIK, M. B., ZHU, C. & HOCHHAUS, A. 2012. Dasatinib or imatinib in newly diagnosed chronic-phase chronic myeloid leukemia: 2-year follow-up from a randomized phase 3 trial (DASISION). *Blood,* 119**,** 1123–1129.

KARBOWNIK, M. S., SZEMRAJ, J., WIETESKA, Ł., ANTCZAK, A., GÓRSKI, P., KOWALCZYK, E. & PIETRAS, T. 2016. Antipsychotic Drugs Differentially Affect mRNA Expression of Genes Encoding the Neuregulin 1-Downstream ErbB4-PI3K Pathway. *Pharmacology,* 98**,** 4–12.

KASTURY, K., OHTA, M., LASOTA, J., MOIR, D., DORMAN, T., LAFORGIA, S., DRUCK, T. & HUEBNER, K. 1996. Structure of the human receptor tyrosine phosphatase gamma gene (PTPRG) and relation to the familial RCC t(3;8) chromosome translocation. *Genomics,* 32**,** 225-35.

KIM, D. D. H. 2019. Are we ready to use precision medicine in chronic myeloid leukemia practice? *Haematologica,* 104**,** 2327–2329.

KIPREOS, E. T. & WANG, J. Y. 1992. Cell cycle-regulated binding of c-Abl tyrosine kinase to DNA. *Science,* 256**,** 382-5.

KNIGHTON, D. R., ZHENG, J. H., TEN EYCK, L. F., XUONG, N. H., TAYLOR, S. S. & SOWADSKI, J. M. 1991. Structure of a peptide inhibitor bound to the catalytic subunit of cyclic adenosine monophosphate-dependent protein kinase. *Science,* 253**,** 414-20.

KUJAWSKI, L. A. & TALPAZ, M. 2007. The role of interferon-alpha in the treatment of chronic myeloid leukemia. *Cytokine Growth Factor Rev.,* 18**,** 459–471.

KUMAR, D., BANSAL, G., NARANG, A., BASAK, T., ABBAS, T. & DASH, D. 2016. Integrating transcriptome and proteome profiling: Strategies and applications. *Proteomics,* 16**,** 2533–2544.

KURZROCK, R., KANTARJIAN, H. M., DRUKER, B. J. & TALPAZ, M. 2003. Philadelphia chromosome-positive leukemias: from basic mechanisms to molecular therapeutics. *Ann Intern Med,* 138**,** 819-30.

LABBE, D. P., HARDY, S. & TREMBLAY, M. L. 2012. Protein tyrosine phosphatases in cancer: friends and foes! *Prog Mol Biol Transl Sci,* 106**,** 253-306.

LAFORGIA, S., LASOTA, J., LATIF, F., BOGHOSIAN-SELL, L., KASTURY, K., OHTA, M., DRUCK, T., ATCHISON, L., CANNIZZARO, L. A., BARNEA, G. & ET AL. 1993. Detailed genetic and physical map of the 3p chromosome region surrounding the familial renal cell carcinoma chromosome translocation, t(3;8)(p14.2;q24.1). *Cancer Res,* 53**,** 3118-24.

LANEUVILLE, P. 1995. Abl tyrosine protein kinase. *Semin Immunol,* 7**,** 255-66.

LAURENT, E., TALPAZ, M., KANTARJIAN, H. & KURZROCK, R. 2001. The BCR gene and philadelphia chromosome-positive leukemogenesis. *Cancer Res,* 61**,** 2343-55.

LEE, H., YI, J. S., LAWAN, A., MIN, K. & BENNETT, A. M. 2015. Mining the function of protein tyrosine phosphatases in health and disease. *Semin Cell Dev Biol,* 37**,** 66-72.

LEUKEMIANET, E. 2015a. *Calculation of Relative Risk of CML Patients* [Online]. Available: https://www.leukemia-net.org/content/leukemias/cml/euro__and_sokal_score/index_eng.html [Accessed].

LEUKEMIANET, E. 2015b. *Online calculation of the EUTOS Score* [Online]. Available: https://www.leukemia-net.org/content/leukemias/cml/eutos_score/index_eng.html [Accessed].

LEWIN, J., SCHMITT, A. O., ADORJAN, P., HILDMANN, T. & PIEPENBROCK, C. 2004. Quantitative DNA methylation analysis based on four-dye trace data from direct sequencing of PCR amplificates. *Bioinformatics,* 20**,** 3005-12.

LI, J., MA, X., CHAKRAVARTI, D., SHALAPOUR, S. & DEPINHO, R. A. 2021. Genetic and biological hallmarks of colorectal cancer. *Genes Dev,* 35**,** 787-820.

LI, Y., YANG, L., PAN, Y., YANG, J., SHANG, Y. & LUO, J. 2014. Methylation and decreased expression of SHP-1 are related to disease progression in chronic myelogenous leukemia. *Oncol Rep,* 31**,** 2438-46.

LIPP, H.-P. & HARTMANN, J. T. 2008. Cytostatic and cytotoxic drugs. *Side Effects of Drugs Annual.* Walthm, MA, USA: Elsevier.

LISETH, K., ABRAHAMSEN, J. F., BJORSVIK, S., GROTTEBO, K. & BRUSERUD, O. 2005. The viability of cryopreserved PBPC depends on the DMSO concentration and the concentration of nucleated cells in the graft. *Cytotherapy,* 7**,** 328-33.

LIU, B., WANG, Y., ZHOU, C., WEI, H., LIN, D., LI, W., LIU, K., ZHANG, G., WEI, S., LI, Y., GONG, B., LIU, Y., GONG, X., MI, Y. & WANG, J. 2019. Nilotinib combined with multi-agent chemotherapy in newly diagnosed Philadelphia chromosome-positive acute lymphoblastic leukemia: a single-center prospective study with long-term follow-up. *Ann Hematol,* 98**,** 633-645.

LORENZETTO, E., MORATTI, E., VEZZALINI, M., HARROCH, S., SORIO, C. & BUFFELLI, M. 2014. Distribution of different isoforms of receptor protein tyrosine phosphatase gamma (Ptprg-RPTP gamma) in adult mouse brain: upregulation during neuroinflammation. *Brain Struct Funct,* 219**,** 875-90.

LUI, V. W., PEYSER, N. D., NG, P. K., HRITZ, J., ZENG, Y., LU, Y., LI, H., WANG, L., GILBERT, B. R., GENERAL, I. J., BAHAR, I., JU, Z., WANG, Z., PENDLETON, K. P., XIAO, X., DU, Y., VRIES, J. K., HAMMERMAN, P. S., GARRAWAY, L. A., MILLS, G. B., JOHNSON, D. E. & GRANDIS, J. R. 2014. Frequent mutation of receptor protein tyrosine phosphatases provides a mechanism for STAT3 hyperactivation in head and neck cancer. *Proc Natl Acad Sci U S A,* 111**,** 1114-9.

MAHON, F. X. 2015. Discontinuation of tyrosine kinase therapy in CML. *Ann Hematol,* 94 Suppl 2**,** S187-93.

MAHON, F. X., BELLOC, F., LAGARDE, V., CHOLLET, C., MOREAU-GAUDRY, F., REIFFERS, J., GOLDMAN, J. M. & MELO, J. V. 2003. MDR1 gene overexpression confers resistance to imatinib mesylate in leukemia cell line models. *Blood,* 101**,** 2368-73.

MALLONA, I., DIEZ-VILLANUEVA, A. & PEINADO, M. A. 2014. Methylation plotter: a web tool for dynamic visualization of DNA methylation data. *Source Code Biol Med,* 9**,** 11.

MARUM, J. E. & BRANFORD, S. 2016. Current developments in molecular monitoring in chronic myeloid leukemia. *Ther Adv Hematol,* 7**,** 237-251.

MAZUR, P. 1984. Freezing of living cells: mechanisms and implications. *Am J Physiol,* 247**,** C125-42.

MCWHIRTER, J. R. & WANG, J. Y. 1993. An actin-binding function contributes to transformation by the Bcr-Abl oncoprotein of Philadelphia chromosome-positive human leukemias. *EMBO J,* 12**,** 1533-46.

MEDINA, J., KANTARJIAN, H., TALPAZ, M., O'BRIEN, S., GARCIA-MANERO, G., GILES, F., RIOS, M. B., HAYES, K. & CORTES, J. 2003. Chromosomal abnormalities in Philadelphia chromosome-negative metaphases appearing during imatinib mesylate therapy in patients with Philadelphia chromosome-positive chronic myelogenous leukemia in chronic phase. *Cancer,* 98**,** 1905-11.

MEGGYESI, N., KALMAR, L., FEKETE, S., MASSZI, T., TORDAI, A. & ANDRIKOVICS, H. 2012. Characterization of ABL exon 7 deletion by molecular genetic and bioinformatic methods reveals no association with imatinib resistance in chronic myeloid leukemia. *Med Oncol,* 29**,** 2136-42.

MERYMAN 1971. Cryoprotective agents.

MINCIACCHI, V. R., KUMAR, R. & KRAUSE, D. S. 2021. Chronic Myeloid Leukemia: A Model Disease of the Past, Present and Future. *Cells,* 10.

MOJTAHEDI, H., YAZDANPANAH, N. & REZAEI, N. 2021. Chronic myeloid leukemia stem cells: targeting therapeutic implications. *Stem Cell Res Ther,* 12**,** 603.

MORADI, F., BABASHAH, S., SADEGHIZADEH, M., JALILI, A., HAJIFATHALI, A. & ROSHANDEL, H. 2019. Signaling pathways involved in chronic myeloid leukemia pathogenesis: The importance of targeting Musashi2-Numb signaling to eradicate leukemia stem cells. *Iran J Basic Med Sci,* 22**,** 581-589.

MORATTI, E., VEZZALINI, M., TOMASELLO, L., GIAVARINA, D. & SORIO, C. 2015. Identification of protein tyrosine phosphatase receptor gamma extracellular domain (sPTPRG) as a natural soluble protein in plasma. *PLoS One,* 10**,** e0119110.

MORGAN, A. E., DAVIES, T. J. & MC AULEY, M. T. 2018. The role of DNA methylation in ageing and cancer. *Proc Nutr Soc,* 77**,** 412-422.

MORRIS, C. M. & BENJES, S. M. 2008. *BCR-ABL1*, Springer, Berlin, Heidelberg.

MU, H., ZHU, X., JIA, H., ZHOU, L. & LIU, H. 2021. Combination Therapies in Chronic Myeloid Leukemia for Potential Treatment-Free Remission: Focus on Leukemia Stem Cells and Immune Modulation. *Front. Oncol.,* 11.

MUGHAL, T. I., RADICH, J. P., DEININGER, M. W., APPERLEY, J. F., HUGHES, T. P., HARRISON, C. J., GAMBACORTI-PASSERINI, C., SAGLIO, G., CORTES, J. & DALEY, G. Q. 2016. Chronic myeloid leukemia: reminiscences and dreams. *Haematologica,* 101**,** 541-58.

NAGAR, B., BORNMANN, W. G., PELLICENA, P., SCHINDLER, T., VEACH, D. R., MILLER, W. T., CLARKSON, B. & KURIYAN, J. 2002. Crystal structures of the kinase domain of c-Abl in complex with the small molecule inhibitors PD173955 and imatinib (STI-571). *Cancer Res,* 62**,** 4236-43.

NAGAR, B., HANTSCHEL, O., YOUNG, M. A., SCHEFFZEK, K., VEACH, D., BORNMANN, W., CLARKSON, B., SUPERTI-FURGA, G. & KURIYAN, J. 2003. Structural basis for the autoinhibition of c-Abl tyrosine kinase. *Cell,* 112**,** 859-71.

NAGARAJ, N., WISNIEWSKI, J. R., GEIGER, T., COX, J., KIRCHER, M., KELSO, J., PÄÄBO, S. & MANN, M. 2011. Deep proteome and transcriptome mapping of a human cancer cell line. *Mol. Syst. Biol.,* 7**,** 548.

NATARAJAN, A., THANGARAJAN, R. & KESAVAN, S. 2019. Repurposing Drugs by In Silico Methods to Target BCR Kinase Domain in Chronic Myeloid Leukemia. *Asian Pac J Cancer Prev,* 20**,** 3399-3406.

NCBI. 2020. *National Center for Biotechnology Information* [Online]. Available: https://www.ncbi.nlm.nih.gov [Accessed].

NIH, N. C. F. B. I. 2007. *Nilotinib hydrochloride monohydrate* [Online]. Available: https://pubchem.ncbi.nlm.nih.gov/compound/Nilotinib-hydrochloride-monohydrate [Accessed].

OCHI, Y., YOSHIDA, K., HUANG, Y. J., KUO, M. C., NANNYA, Y., SASAKI, K., MITANI, K., HOSOYA, N., HIRAMOTO, N., ISHIKAWA, T., BRANFORD, S., SHANMUGANATHAN, N., OHYASHIKI, K., TAKAHASHI, N., TAKAKU, T., TSUCHIYA, S., KANEMURA, N., NAKAMURA, N., UEDA, Y., YOSHIHARA, S., BERA, R., SHIOZAWA, Y., ZHAO, L., TAKEDA, J., WATATANI, Y., OKUDA, R., MAKISHIMA, H., SHIRAISHI, Y., CHIBA, K., TANAKA, H., SANADA, M., TAKAORI-KONDO, A., MIYANO, S., OGAWA, S. & SHIH, L. Y. 2021. Clonal evolution and clinical implications of genetic abnormalities in blastic transformation of chronic myeloid leukaemia. *Nat Commun,* 12**,** 2833.

ODA, T., HEANEY, C., HAGOPIAN, J. R., OKUDA, K., GRIFFIN, J. D. & DRUKER, B. J. 1994. Crkl is the major tyrosine-phosphorylated protein in neutrophils from patients with chronic myelogenous leukemia. *J Biol Chem,* 269**,** 22925-8.

OOMS, L. M., BINGE, L. C., DAVIES, E. M., RAHMAN, P., CONWAY, J. R., GURUNG, R., FERGUSON, D. T., PAPA, A., FEDELE, C. G., VIEUSSEUX, J. L., CHAI, R. C., KOENTGEN, F., PRICE, J. T., TIGANIS, T., TIMPSON, P., MCLEAN, C. A. & MITCHELL, C. A. 2015. The Inositol Polyphosphate 5-Phosphatase PIPP Regulates AKT1-Dependent Breast Cancer Growth and Metastasis. *Cancer Cell,* 28**,** 155-69.

OSTMAN, A., HELLBERG, C. & BOHMER, F. D. 2006. Protein-tyrosine phosphatases and cancer. *Nat Rev Cancer,* 6**,** 307-20.

OTTMANN, O., DOMBRET, H., MARTINELLI, G., SIMONSSON, B., GUILHOT, F., LARSON, R. A., REGE-CAMBRIN, G., RADICH, J., HOCHHAUS, A., APANOVITCH, A. M., GOLLERKERI, A. & COUTRE, S. 2007. Dasatinib induces rapid hematologic and cytogenetic responses in adult patients with Philadelphia chromosome positive acute lymphoblastic leukemia with resistance or intolerance to imatinib: interim results of a phase 2 study. *Blood,* 110**,** 2309-15.

OWEN, K. L., BROCKWELL, N. K. & PARKER, B. S. 2019. JAK-STAT Signaling: A Double-Edged Sword of Immune Regulation and Cancer Progression. *Cancers,* 11.

PAEZ, J. G., JANNE, P. A., LEE, J. C., TRACY, S., GREULICH, H., GABRIEL, S., HERMAN, P., KAYE, F. J., LINDEMAN, N., BOGGON, T. J., NAOKI, K., SASAKI, H., FUJII, Y., ECK, M. J., SELLERS, W. R., JOHNSON, B. E. & MEYERSON, M. 2004. EGFR mutations in lung cancer: correlation with clinical response to gefitinib therapy. *Science,* 304**,** 1497-500.

PATEL, A. B., O'HARE, T. & DEININGER, M. W. 2017. Mechanisms of Resistance to ABL Kinase Inhibition in Chronic Myeloid Leukemia and the Development of Next Generation ABL Kinase Inhibitors. *Hematol Oncol Clin North Am,* 31**,** 589-612.

PEGG, D. E. 2007. Principles of cryopreservation. *Methods Mol Biol,* 368**,** 39-57.

PELICCI, G., LANFRANCONE, L., SALCINI, A. E., ROMANO, A., MELE, S., GRAZIA BORRELLO, M., SEGATTO, O., DI FIORE, P. P. & PELICCI, P. G. 1995. Constitutive phosphorylation of Shc proteins in human tumors. *Oncogene,* 11**,** 899-907.

PENDERGAST, A. M., QUILLIAM, L. A., CRIPE, L. D., BASSING, C. H., DAI, Z., LI, N., BATZER, A., RABUN, K. M., DER, C. J., SCHLESSINGER, J. & ET AL. 1993. BCR-ABL-induced oncogenesis is mediated by direct interaction with the SH2 domain of the GRB-2 adaptor protein. *Cell,* 75**,** 175-85.

PERL, K., USHAKOV, K., POZNIAK, Y., YIZHAR-BARNEA, O., BHONKER, Y., SHIVATZKI, S., GEIGER, T., AVRAHAM, K. B. & SHAMIR, R. 2017. Reduced changes in protein compared to mRNA levels across non-proliferating tissues. *BMC Genomics,* 18**,** 1–14.

PRESS, R. D., LOVE, Z., TRONNES, A. A., YANG, R., TRAN, T., MONGOUE-TCHOKOTE, S., MORI, M., MAURO, M. J., DEININGER, M. W. & DRUKER, B. J. 2006. BCR-ABL mRNA levels at and after the time of a complete cytogenetic response (CCR) predict the duration of CCR in imatinib mesylate-treated patients with CML. *Blood,* 107**,** 4250-6.

PUIL, L., LIU, J., GISH, G., MBAMALU, G., BOWTELL, D., PELICCI, P. G., ARLINGHAUS, R. & PAWSON, T. 1994. Bcr-Abl oncoproteins bind directly to activators of the Ras signalling pathway. *EMBO J,* 13**,** 764-73.

QUINTAS-CARDAMA, A. & CORTES, J. 2009. Molecular biology of bcr-abl1-positive chronic myeloid leukemia. *Blood,* 113**,** 1619-30.

RADIVOYEVITCH, T., JANKOVIC, G. M., TIU, R. V., SAUNTHARARAJAH, Y., JACKSON, R. C., HLATKY, L. R., GALE, R. P. & SACHS, R. K. 2014. Sex differences in the incidence of chronic myeloid leukemia. *Radiat. Environ. Biophys.,* 53**,** 55.

RANDOLPH, T. R. 2020. 32 - Myeloproliferative neoplasms. *Rodak's Hematology (Sixth Edition)***,** 555–588.

REN, R. 2005. Mechanisms of BCR-ABL in the pathogenesis of chronic myelogenous leukaemia. *Nat Rev Cancer,* 5**,** 172-83.

RESEARCH(UK), C. 2020. *Chronic myeloid leukaemia (CML) incidence statistics* [Online]. Available: https://www.cancerresearchuk.org/health-professional/cancer-statistics/statistics-by-cancer-type/leukaemia-cml/incidence [Accessed].

REUTHER, G. W., FU, H., CRIPE, L. D., COLLIER, R. J. & PENDERGAST, A. M. 1994. Association of the protein kinases c-Bcr and Bcr-Abl with proteins of the 14-3-3 family. *Science,* 266**,** 129-33.

RON, D., ZANNINI, M., LEWIS, M., WICKNER, R. B., HUNT, L. T., GRAZIANI, G., TRONICK, S. R., AARONSON, S. A. & EVA, A. 1991. A region of proto-dbl essential for its transforming activity shows sequence similarity to a yeast cell cycle gene, CDC24, and the human breakpoint cluster gene, bcr. *New Biol,* 3**,** 372-9.

ROSKOSKI, R., JR. 2003. STI-571: an anticancer protein-tyrosine kinase inhibitor. *Biochem Biophys Res Commun,* 309**,** 709-17.

ROSS, T. S. & MGBEMENA, V. E. 2014. Re-evaluating the role of BCR/ABL in chronic myelogenous leukemia. *Mol Cell Oncol,* 1**,** e963450.

ROSSARI, F., MINUTOLO, F. & ORCIUOLO, E. 2018. Past, present, and future of Bcr-Abl inhibitors: from chemical development to clinical efficacy. *J Hematol Oncol,* 11**,** 84.

SALMEEN, A. & BARFORD, D. 2005. Functions and mechanisms of redox regulation of cysteine-based phosphatases. *Antioxid Redox Signal,* 7**,** 560-77.

SAWYERS, C. L., MCLAUGHLIN, J., GOGA, A., HAVLIK, M. & WITTE, O. 1994. The nuclear tyrosine kinase c-Abl negatively regulates cell growth. *Cell,* 77**,** 121-31.

SCHINDLER, T., BORNMANN, W., PELLICENA, P., MILLER, W. T., CLARKSON, B. & KURIYAN, J. 2000. Structural mechanism for STI-571 inhibition of abelson tyrosine kinase. *Science,* 289**,** 1938-42.

SHINTANI, T., MAEDA, N., NISHIWAKI, T. & NODA, M. 1997. Characterization of rat receptor-like protein tyrosine phosphatase gamma isoforms. *Biochem Biophys Res Commun,* 230**,** 419-25.

SHIOTSU, Y., KIYOI, H., ISHIKAWA, Y., TANIZAKI, R., SHIMIZU, M., UMEHARA, H., ISHII, K., MORI, Y., OZEKI, K., MINAMI, Y., ABE, A., MAEDA, H., AKIYAMA, T., KANDA, Y., SATO, Y., AKINAGA, S. & NAOE, T. 2009. KW-2449, a novel multikinase inhibitor, suppresses the growth of leukemia cells with FLT3 mutations or T315I-mutated BCR/ABL translocation. *Blood,* 114**,** 1607-17.

SHU, S. T., SUGIMOTO, Y., LIU, S., CHANG, H. L., YE, W., WANG, L. S., HUANG, Y. W., YAN, P. & LIN, Y. C. 2010. Function and regulatory mechanisms of the candidate tumor suppressor receptor protein tyrosine phosphatase gamma (PTPRG) in breast cancer cells. *Anticancer Res,* 30**,** 1937-46.

SIEGEL, R. L., MILLER, K. D. & JEMAL, A. 2020. Cancer statistics, 2020. *CA Cancer J Clin,* 70**,** 7-30.

SKORSKI, T., BELLACOSA, A., NIEBOROWSKA-SKORSKA, M., MAJEWSKI, M., MARTINEZ, R., CHOI, J. K., TROTTA, R., WLODARSKI, P., PERROTTI, D., CHAN, T. O., WASIK, M. A., TSICHLIS, P. N. & CALABRETTA, B. 1997. Transformation of hematopoietic cells by BCR/ABL requires activation of a PI-3k/Akt-dependent pathway. *EMBO J,* 16**,** 6151-61.

SKORSKI, T., KANAKARAJ, P., NIEBOROWSKA-SKORSKA, M., RATAJCZAK, M. Z., WEN, S. C., ZON, G., GEWIRTZ, A. M., PERUSSIA, B. & CALABRETTA, B. 1995. Phosphatidylinositol-3 kinase activity is regulated by BCR/ABL and is required for the growth of Philadelphia chromosome-positive cells. *Blood,* 86**,** 726-36.

SMITH, A. G., PAINTER, D., HOWELL, D. A., EVANS, P., SMITH, G., PATMORE, R., JACK, A. & ROMAN, E. 2014. Determinants of survival in patients with chronic myeloid leukaemia treated in the new era of oral therapy: findings from a UK population-based patient cohort. *BMJ Open,* 4.

SOKAL, J. E., COX, E. B., BACCARANI, M., TURA, S., GOMEZ, G. A., ROBERTSON, J. E., TSO, C. Y., BRAUN, T. J., CLARKSON, B. D., CERVANTES, F. & ET AL. 1984. Prognostic discrimination in "good-risk" chronic granulocytic leukemia. *Blood,* 63**,** 789-99.

SOVERINI, S., BASSAN, R. & LION, T. 2019. Treatment and monitoring of Philadelphia chromosome-positive leukemia patients: recent advances and remaining challenges. *J. Hematol. Oncol.,* 12**,** 1–14.

STRONCEK, D. F., XING, L., CHAU, Q., ZIA, N., MCKELVY, A., PRACHT, L., SABATINO, M. & JIN, P. 2011. Stability of cryopreserved white blood cells (WBCs) prepared for donor WBC infusions. *Transfusion,* 51**,** 2647-55.

TAKAHASHI, N., MIURA, I., KOBAYASHI, Y., KUME, M., YOSHIOKA, T., OTANE, W., OHTSUBO, K., TAKAHASHI, K., KITABAYASHI, A., KAWABATA, Y., HIROKAWA, M., NISHIJIMA, H., ICHINOHASAMA, R., DECOTEAU, J., MIURA, A. B. & SAWADA, K.-I. 2005. Fluorescence In Situ Hybridization Monitoring of BCR-ABL-Positive Neutrophils in Chronic-Phase Chronic Myeloid Leukemia Patients during the Primary Stage of Imatinib Mesylate Therapy. *Int. J. Hematol.,* 81**,** 235–241.

TALPAZ, M., MERCER, J. & HEHLMANN, R. 2015. The interferon-alpha revival in CML. *Ann Hematol,* 94 Suppl 2**,** S195-207.

TARTAGLIA, M., NIEMEYER, C. M., FRAGALE, A., SONG, X., BUECHNER, J., JUNG, A., HAHLEN, K., HASLE, H., LICHT, J. D. & GELB, B. D. 2003. Somatic mutations in PTPN11 in juvenile myelomonocytic leukemia, myelodysplastic syndromes and acute myeloid leukemia. *Nat Genet,* 34**,** 148-50.

THE SURVEILLANCE, E., AND END RESULTS 2019. *Chronic Myeloid Leukemia - Cancer Stat Facts* [Online]. Available: https://seer.cancer.gov/statfacts/html/cmyl.html [Accessed].

THE SURVEILLANCE, E., AND END RESULTS (SEER). 2020. *Chronic Myeloid Leukemia - Cancer Stat Facts* [Online]. Available: https://seer.cancer.gov/statfacts/html/cmyl.html [Accessed].

THIELEN, N., RICHTER, J., BALDAUF, M., BARBANY, G., FIORETOS, T., GILES, F., GJERTSEN, B.-T., HOCHHAUS, A., SCHUURHUIS, G. J., SOPPER, S., STENKE, L., THUNBERG, S., WOLF, D., OSSENKOPPELE, G., PORKKA, K., JANSSEN, J. & MUSTJOKI, S. 2016. Leukemic Stem Cell Quantification in Newly Diagnosed Patients With Chronic Myeloid Leukemia Predicts Response to Nilotinib Therapy. *Clin. Cancer Res.,* 22**,** 4030–4038.

TIM 2020. *Protein P190 - an overview | ScienceDirect Topics*.

TOKARSKI, J. S., NEWITT, J. A., CHANG, C. Y., CHENG, J. D., WITTEKIND, M., KIEFER, S. E., KISH, K., LEE, F. Y., BORZILLERRI, R., LOMBARDO, L. J., XIE, D., ZHANG, Y. & KLEI, H. E. 2006. The structure of Dasatinib (BMS-354825) bound to activated ABL kinase domain elucidates its inhibitory activity against imatinib-resistant ABL mutants. *Cancer Res,* 66**,** 5790-7.

TOMASELLO, L. 2016. Regulative Loop between β-Catenin and Protein Tyrosine Phosphatase Receptor Type γ (PTPRG) in Chronic Myeloid Leukemia. *The FASEB Journal*.

TONKS, N. K. 2006. Protein tyrosine phosphatases: from genes, to function, to disease. *Nat Rev Mol Cell Biol,* 7**,** 833-46.

TRAN, H. T. T., TAKESHIMA, Y., SURONO, A., YAGI, M., WADA, H. & MATSUO, M. 2005. A G-to-A transition at the fifth position of intron-32 of the dystrophin gene inactivates a splice-donor site both in vivo and in vitro. *Mol. Genet. Metab.,* 85**,** 213–219.

TSUKAMOTO, T., TAKAHASHI, T., UEDA, R., HIBI, K., SAITO, H. & TAKAHASHI, T. 1992. Molecular analysis of the protein tyrosine phosphatase gamma gene in human lung cancer cell lines. *Cancer Res,* 52**,** 3506-9.

TURKINA, A., WANG, J., MATHEWS, V., SAYDAM, G., JUNG, C. W., AL HASHMI, H. H., YASSIN, M., LE CLANCHE, S., MILJKOVIC, D., SLADER, C. & HUGHES, T. P. 2020. TARGET: a survey of real-world management of chronic myeloid leukaemia across 33 countries. *Br. J. Haematol.,* 190**,** 869–876.

VAN DOORN, R., ZOUTMAN, W. H., DIJKMAN, R., DE MENEZES, R. X., COMMANDEUR, S., MULDER, A. A., VAN DER VELDEN, P. A., VERMEER, M. H., WILLEMZE, R., YAN, P. S., HUANG, T. H. & TENSEN, C. P. 2005. Epigenetic profiling of cutaneous T-cell lymphoma: promoter hypermethylation of multiple tumor suppressor genes including BCL7a, PTPRG, and p73. *J Clin Oncol,* 23**,** 3886-96.

VAN ETTEN, R. A. 1999. Cycling, stressed-out and nervous: cellular functions of c-Abl. *Trends Cell Biol,* 9**,** 179-86.

VAN ROON, E. H., DE MIRANDA, N. F., VAN NIEUWENHUIZEN, M. P., DE MEIJER, E. J., VAN PUIJENBROEK, M., YAN, P. S., HUANG, T. H., VAN WEZEL, T., MORREAU, H. & BOER, J. M. 2011a. Tumour-specific methylation of PTPRG intron 1 locus in sporadic and Lynch syndrome colorectal cancer. *Eur J Hum Genet,* 19**,** 307-12.

VAN ROON, E. H. J., DE MIRANDA, N. F. C. C., VAN NIEUWENHUIZEN, M. P., DE MEIJER, E. J., VAN PUIJENBROEK, M., YAN, P. S., HUANG, T. H.-M., VAN WEZEL, T., MORREAU, H. & BOER, J. M. 2011b. Tumour-specific methylation of PTPRG intron 1 locus in sporadic and Lynch syndrome colorectal cancer. *Eur. J. Hum. Genet.,* 19**,** 307–312.

VEZZALINI, M., MAFFICINI, A., TOMASELLO, L., LORENZETTO, E., MORATTI, E., FIORINI, Z., HOLYOAKE, T. L., PELLICANO, F., KRAMPERA, M., TECCHIO, C., YASSIN, M., AL-DEWIK, N., ISMAIL, M. A., AL SAYAB, A., MONNE, M. & SORIO, C. 2017. A new monoclonal antibody detects downregulation of protein tyrosine phosphatase receptor type gamma in chronic myeloid leukemia patients. *J Hematol Oncol,* 10**,** 129.

VINHAS, R., CORDEIRO, M., PEDROSA, P., FERNANDES, A. R. & BAPTISTA, P. V. 2017. Current trends in molecular diagnostics of chronic myeloid leukemia. *Leuk. Lymphoma,* 58**,** 1791–1804.

VONCKEN, J. W., VAN SCHAICK, H., KAARTINEN, V., DEEMER, K., COATES, T., LANDING, B., PATTENGALE, P., DORSEUIL, O., BOKOCH, G. M., GROFFEN, J. & ET AL. 1995. Increased neutrophil respiratory burst in bcr-null mutants. *Cell,* 80**,** 719-28.

WANG, J. F. & DAI, D. Q. 2007. Metastatic suppressor genes inactivated by aberrant methylation in gastric cancer. *World J Gastroenterol,* 13**,** 5692-8.

WANG, J. Y. 2014. The capable ABL: what is its biological function? *Mol Cell Biol,* 34**,** 1188-97.

WANG, W., CHEN, Z., HU, Z., YIN, C. C., LI, S., BAI, S., BUESO-RAMOS, C. E., MEDEIROS, L. J. & HU, S. 2016. Clinical significance of trisomy 8 that emerges during therapy in chronic myeloid leukemia. *Blood Cancer J,* 6**,** e490.

WANG, W., CORTES, J. E., LIN, P., KHOURY, J. D., AI, D., TANG, Z., TANG, G., JORGENSEN, J. L., MEDEIROS, L. J. & HU, S. 2015. Impact of trisomy 8 on treatment response and survival of patients with chronic myelogenous leukemia in the era of tyrosine kinase inhibitors. *Leukemia,* 29**,** 2263-6.

WANG, Z., SHEN, D., PARSONS, D. W., BARDELLI, A., SAGER, J., SZABO, S., PTAK, J., SILLIMAN, N., PETERS, B. A., VAN DER HEIJDEN, M. S., PARMIGIANI, G., YAN, H., WANG, T. L., RIGGINS, G., POWELL, S. M., WILLSON, J. K., MARKOWITZ, S., KINZLER, K. W., VOGELSTEIN, B. & VELCULESCU, V. E. 2004. Mutational analysis of the tyrosine phosphatome in colorectal cancers. *Science,* 304**,** 1164-6.

WELCH, P. J. & WANG, J. Y. 1993. A C-terminal protein-binding domain in the retinoblastoma protein regulates nuclear c-Abl tyrosine kinase in the cell cycle. *Cell,* 75**,** 779-90.

WESTBROOK, C. A., HOOBERMAN, A. L., SPINO, C., DODGE, R. K., LARSON, R. A., DAVEY, F., WURSTER-HILL, D. H., SOBOL, R. E., SCHIFFER, C. & BLOOMFIELD, C. D. 1992. Clinical significance of the BCR-ABL fusion gene in adult acute lymphoblastic leukemia: a Cancer and Leukemia Group B Study (8762). *Blood,* 80**,** 2983-90.

WETZLER, M., TALPAZ, M., VAN ETTEN, R. A., HIRSH-GINSBERG, C., BERAN, M. & KURZROCK, R. 1993. Subcellular localization of Bcr, Abl, and Bcr-Abl proteins in normal and leukemic cells and correlation of expression with myeloid differentiation. *J Clin Invest,* 92**,** 1925-39.

WHITE, H. E., MATEJTSCHUK, P., RIGSBY, P., GABERT, J., LIN, F., LYNN WANG, Y., BRANFORD, S., MULLER, M. C., BEAUFILS, N., BEILLARD, E., COLOMER, D., DVORAKOVA, D., EHRENCRONA, H., GOH, H. G., EL HOUSNI, H., JONES, D., KAIRISTO, V., KAMEL-REID, S., KIM, D. W., LANGABEER, S., MA, E. S., PRESS, R. D., ROMEO, G., WANG, L., ZOI, K., HUGHES, T., SAGLIO, G., HOCHHAUS, A., GOLDMAN, J. M., METCALFE, P. & CROSS, N. C. 2010. Establishment of the first World Health Organization International Genetic Reference Panel for quantitation of BCR-ABL mRNA. *Blood,* 116**,** e111-7.

WOODRING, P. J., HUNTER, T. & WANG, J. Y. 2001. Inhibition of c-Abl tyrosine kinase activity by filamentous actin. *J Biol Chem,* 276**,** 27104-10.

WOOLTHUIS, C. M., DE JONGE, H. J. M., VOS, A. Z., MULDER, A. B., BERG, E. V. D., KLUIN, P. M., VAN DER WEIDE, K., DE BONT, E. S., HULS, G. A., VELLENGA, E. & SCHURINGA, J. J. 2010. Gene Expression Profiling In Leukemic Stem Cell-Enriched AML CD34+ Cell Fraction Identifies Target Genes That Predict Prognosis In Normal Karyotype AML. *Blood,* 116**,** 952–952.

WU, W., XU, N., ZHOU, X., LIU, L., TAN, Y., LUO, J., HUANG, J., QIN, J., WANG, J., LI, Z., YIN, C., ZHOU, L. & LIU, X. 2020. Integrative Genomic Analysis Reveals Cancer-Associated Gene Mutations in Chronic Myeloid Leukemia Patients with Resistance or Intolerance to Tyrosine Kinase Inhibitor. *Onco Targets Ther,* 13**,** 8581-8591.

XIAO, J., LEE, S. T., XIAO, Y., MA, X., HOUSEMAN, E. A., HSU, L. I., ROY, R., WRENSCH, M., DE SMITH, A. J., CHOKKALINGAM, A., BUFFLER, P., WIENCKE, J. K. & WIEMELS, J. L. 2014. PTPRG inhibition by DNA methylation and cooperation with RAS gene activation in childhood acute lymphoblastic leukemia. *Int J Cancer,* 135**,** 1101-9.

XIE, S., LIN, H., SUN, T. & ARLINGHAUS, R. B. 2002. Jak2 is involved in c-Myc induction by Bcr-Abl. *Oncogene,* 21**,** 7137-46.

YANG, J., NIE, J., MA, X., WEI, Y., PENG, Y. & WEI, X. 2019. Targeting PI3K in cancer: mechanisms and advances in clinical trials. *Mol. Cancer,* 18**,** 1–28.

YOU, R.-I., HO, C.-L., HUNG, H.-M., HSIEH, Y.-F., JU, J.-C. & CHAO, T.-Y. 2012. Identification of DNA methylation biomarkers in imatinib-resistant chronic myeloid leukemia cells. *Genomic Medicine, Biomarkers, and Health Sciences,* 4**,** 12–15.

ZHANG, C., LOPEZ, M. S., DAR, A. C., LADOW, E., FINKBEINER, S., YUN, C. H., ECK, M. J. & SHOKAT, K. M. 2013. Structure-guided inhibitor design expands the scope of analog-sensitive kinase technology. *ACS Chem Biol,* 8**,** 1931-8.

ZHANG, H., JIN, X., DIAO, Y., WANG, L., LI, N. & CHEN, M. 2019. Imatinib mesylate inhibits proliferation and promotes apoptosis of chronic myeloid leukemia cells via STAT3 pathway. *Panminerva Med*.

ZHANG, J., ADRIAN, F. J., JAHNKE, W., COWAN-JACOB, S. W., LI, A. G., IACOB, R. E., SIM, T., POWERS, J., DIERKS, C., SUN, F., GUO, G. R., DING, Q., OKRAM, B., CHOI, Y., WOJCIECHOWSKI, A., DENG, X., LIU, G., FENDRICH, G., STRAUSS, A., VAJPAI, N., GRZESIEK, S., TUNTLAND, T., LIU, Y., BURSULAYA, B., AZAM, M., MANLEY, P. W., ENGEN, J. R., DALEY, G. Q., WARMUTH, M. & GRAY, N. S. 2010. Targeting Bcr-Abl by combining allosteric with ATP-binding-site inhibitors. *Nature,* 463**,** 501-6.

ZHAO, S., SEDWICK, D. & WANG, Z. 2015. Genetic alterations of protein tyrosine phosphatases in human cancers. *Oncogene,* 34**,** 3885.

ZHOU, T., MEDEIROS, L. J. & HU, S. 2018. Chronic Myeloid Leukemia: Beyond BCR-ABL1. *Curr Hematol Malig Rep,* 13**,** 435-445.

ZUR, H. & TULLER, T. 2012. Strong association between mRNA folding strength and protein abundance in S. cerevisiae. *EMBO Rep.,* 13**,** 272–277.

Appendices removed for copyright reasons